Thesis

on

Multi Objective Optimal Power Flow Considering Wind Power Penetration

Submitted in fulfillment of the requirements

of

DOCTOR OF PHILOSOPHY

Submitted by

MANDEEP KAUR

(Registration No. 901604004)

Under the supervision of

Dr. Nitin Narang

Associate Professor, EIED

THAPAR INSTITUTE

Department of Electrical & Instrumentation Engineering

Thapar Institute of Engineering & Technology

(Deemed-to-be-University)

Patiala-147004, Punjab (India)

March, 2023

Dedicated to

My Respected Father

S. Tej Bahadur Singh

Respected Mother

Smt. Ravinderjit Kaur

and

My Beloved Husband

Er. Rajinder Singh

CERTIFICATE

Certified that the thesis entitled, "**Multi Objective Optimal Power Flow Considering Wind Power Penetration**", which is being submitted by Mandeep Kaur in fulfillment of the requirements for the award of the degree of **Doctor of Philosophy**, to the Department of Electrical and Instrumentation Engineering, Thapar Institute of Engineering & Technology, Patiala, is a bonafide records of the candidate's own work carried out by her under my supervision and guidance.

The matter contained in this thesis has not submitted, neither in part or in full to any other university or institute for the award of any degree.

Mandeep Kaur

Ms. Mandeep Kaur

Regd. No. 901604004

This is to certify that the above statement made by the candidate is correct to the best of my knowledge.

N Narang

(Dr. Nitin Narang)

Associate Professor

Department of Electrical &Instrumentation Engineering

Thapar Institute of Engineering &Technology, Patiala

Punjab, India

ACKNOWLEDGMENT

The foremost thanks to the Almighty for showering his grace and providing good health to accomplish this research work. I would like to express my deepest gratitude to my guide and mentor Dr. Nitin Narang for pioneering me all the way during this research work. He has been a continuous source of inspiration and guidance all along the way towards the completion of research work. This work would never have been realty without his kind support and guidance. I am greatly obliged to Dr. Teena Narang, wife of Dr. Nitin Narang, for being very supportive and generous during the course of this research work.

I would also like to thank my Ph.D. doctoral committee members Dr. Prasenjit Basak, Dr. Shakti Singh and Dr. Neeraj Kumar for imparting their valuable suggestions to refine my research work.

I represent the appreciation to my grandfather S. Mann Singh and parents S. Tej Bahadur Singh and Smt. Ravinderjit Kaur for their unconditional love and support that has been consistent source of inspiration for me. I am wordless to express my gratitude to my beloved husband Er. Rajinder Singh for his love, support and encouragement that kept me motivated. I am highly indebted to my brother Er. Davinder Singh and sister-in-law Er. Gagandeep Kaur for their supportive and caring attitude. I feel thankful to my parents-in-law for their motivation and support. The power of unconditional love of my daughter Savreen Kaur Hundal kept me highly encouraged for accomplishment of this research work. I am sincerely thankful to all my friends and research scholars for their timely help and cooperation.

Ms. Mandeep Kaur
Regd. No. 901604004
Thapar Institute of Engineering &
Technology, Patiala

TABLE OF CONTENTS

TABLE OF CONTENTS (Continued)

TABLE OF CONTENTS (Continued)

TABLE OF CONTENTS (Continued)

LIST OF TABLES

LIST OF TABLES (Continued)

LIST OF FIGURES

LIST OF FIGURES (Continued)

NOMENCLATURE

The main symbols and notation used in this thesis are listed below. Sometimes a symbol may have alternate meaning, but in such a case, the context is sufficient to avoid confusion.

Indices	**Description**
i	Index for wind units
j	Index for the total number of transmission lines
k	Index for PQ buses
l	Index for the cogeneration units
m	Index for the thermal generating units
n	Index for heat units
p	Index for tap changing transformers
q	Index for shunt compensators

Input data	**Description**
a_m, b_m, c_m, d_m, e_m	Coefficients of the fuel cost for the m^{th} generating unit
a_n, b_n, c_n	Fuel cost coefficients of n^{th} heat only unit
A_n, B_n	Lower and upper values of n^{th} dimension decision variable
$A_r(IT)$	Randomly selected solution from the archive A
$\alpha_l, \beta_l, \gamma_l \lambda_l, \varepsilon_l, \xi_l$	Fuel cost coefficients of l^{th} cogeneration unit
$\alpha_m, \beta_m, \gamma_m, \eta_m, \lambda_m$	Coefficients of emission for the m^{th} generating unit
c, k	Shape and scale parameters of Weibull distribution model
χ_i	Chaotic number
χ_l	Emission coefficient of l^{th} cogeneration unit
d_i, d_{ri}, d_{pi}	Cost coefficients of i^{th} wind generator for direct, overestimated and under estimated power
D	Decision variables
G_j	Conductance of j^{th} transmission line connecting k^{th} bus with l^{th} bus
G_{kl}, B_{kl}	Conductance, susceptance of transmission line between k^{th} bus and l^{th} bus
H	Intermediary parameter
H_D	Total heat demand
$H_{Cl}^{\max}, H_{Cl}^{\min}$	Upper, lower heat limits for the l^{th} cogeneration unit
$H_{hn}^{\max}, H_{hn}^{\min}$	Upper, lower heat limits for the n^{th} heat only unit
$IT^{\max}$	Maximum number of iterations
M	Number of objective functions
μ_k^*	Step size of the PPS method
ni	Number of inequality constraints
N	Total system buses except slack bus

NOMENCLATURE (Continued)

N_{BUS}, N_{TCPS}	Total number of buses and TCPS devices
N_C	Total number of cogeneration units
N_g	Total number of generating units that contains thermal units, cogeneration units and wind units
N_h	Total number of heat units
N_m	Modulation index
N_{obj}	Number of objectives
N_{PQ}	Total number of load buses
N_{PV}	Number of voltage-controlled buses
N_{TCSC}	Total number of TCSC devices
N_W	Total number of wind generators
NC	Total number of shunt compensators
NG	Total number of thermal generating units
NL	Total number of transmission lines
NP	Total population
NT	Total number of tap changing transformers
$of_k^{\max}, of_k^{\min}$	Maximum and minimum values of k^{th} objective function
ω, F	Inertia weight and scaling parameter
p_1, p_2, p_3, p_4	Penalty function parameters
$P_{Cl}^{\max}, P_{Cl}^{\min}$	Upper, lower power limits for the l^{th} cogeneration unit
P_D	System power demand
P_{Gk}, Q_{Gk}	Active and reactive power generation available at the k^{th} bus
$P_{Gm}^{\min}, P_{Gm}^{\max}$	Minimum and maximum active power limits for the m^{th} generating unit
P_{kl}, Q_{kl}	Active, reactive power flows of transmission line between k^{th} bus and l^{th} bus
P_{ks}, Q_{ks}	Active and reactive powers injected by TCPS at the k^{th} bus
P_{Lk}, Q_{Lk}	Active and reactive power demand at the k^{th} bus
P_R	Rated wind power output
$P_{Wi}^{\max}$	Maximum power of i^{th} wind generator
$\phi_{Tn}^{\min}, \phi_{Tn}^{\max}$	Minimum and maximum phase angle shift corresponding to n^{th} TCPS
ψ_i	Penalty coefficient of i^{th} inequality constraint
ψ_n	Emission coefficient of n^{th} heat only unit
$Q_{Gm}^{\min}, Q_{Gm}^{\max}$	Minimum and maximum reactive power limits of the m^{th} generating unit
$Q_q^{\min}, Q_q^{\max}$	Minimum and maximum VAR limits injected by the q^{th} shunt compensator

NOMENCLATURE (Continued)

$seed_{\max}, seed_{\min}$	Maximum and minimum number of seeds
$SD^{initial}, SD^{final}$	Initial and final value of SD
S_k^j	Search direction
$S_{Lj}^{\max}$	maximum apparent power flow of the j^{th} branch
σ_{cur}	SD of the present iteration
$t_p^{\min}, t_p^{\max}$	Minimum and maximum tap setting limits of the p^{th} transformer
v	Current wind speed
v_{IN}, v_R, v_o	Cut-in, rated and cut-out wind speed, respectively
$V_{Gm}^{\min}, V_{Gm}^{\max}$	Minimum and maximum voltage magnitudes limits for the m^{th} generating unit
V_k, V_l ,and θ_k, θ_l	Voltage magnitudes and phase angles for buses k and l, respectively
$V_{Lk}^{\min}, V_{Lk}^{\max}$	Minimum and maximum limits for the k^{th} load bus voltage
$V_{reference}$	Reference voltage magnitude in p.u.
x_k	k^{th} decision variable
$X_{Cl}^{\min}$ and $X_{Cl}^{\max}$	Minimum and maximum reactance correspond to l^{th} TCSC
X_{kl}, R_{kl}	Reactance and resistance of transmission line between k^{th} bus and l^{th} bus
$X_n^{\max}, X_n^{\min}$	Maximum and minimum values of n^{th} decision variable
Y_{kl}, δ_{kl}	Total admittance and admittance angle of the transmission line connecting the k^{th} and l^{th} bus

Decision variables	**Description**
H_{Cl}	Heat produced by l^{th} cogeneration unit
H_{hn}	Heat produced by n^{th} heat only unit
P_{Cl}	Power generated by l^{th} cogeneration unit
P_{Ck}, P_{Wk}	Active powers generated by cogeneration and wind units at the k^{th} bus
P_{Gm}	Active power generated by m^{th} generating unit
P_{Wi}	Actual power of i^{th} wind generator
ϕ_{Tn}	Phase angle shift corresponding to n^{th} TCPS
Q_q	VAR injected by the q^{th} shunt compensator
t_p	Tap setting limit of the p^{th} transformer
V_{Gm}	Voltage magnitude generated by m^{th} generating unit
X_C	The TCSC reactance located at the transmission line that connects k^{th} bus and l^{th} bus

NOMENCLATURE (Continued)

Function	Description
err	Cumulative error of all constraints violation
$E(P_{oe,i}), E(P_{ue,i})$	Expected overestimation and underestimation power of i^{th} wind generator
f, of_i	The fitness function value and objective function at i^{th} objective
f_C	Fuel cost of cogeneration units
f_H	Fuel cost of heat only units
f_T	Fuel cost of conventional thermal units
f_W	Operating cost of wind units
f_{worst} , f_{best}	The worst and best fitness in the present population
F_C, E, P_{LOSS}, VMD	The objective function for fuel cost, emission pollutant, active power loss and total voltage magnitude deviations
F_{OC}	Overall cost of system
μ_C	Cardinal priority ranking
μ_{Cbest} , μ_{Cworst}	Best and worst fitness in the present population
$\mu_1(F_C), \mu_2(E), \mu_3(P_{LOSS}), \mu_4(VMD)$	Membership value of fuel cost, emission pollutant, active power losses and total voltage magnitude deviations.
$n(X_i)$	Weed fitness
$P_{G,slack}$	Slack bus active power generation
P_L	Transmission losses
φ_i	Penalty function
Q_{Gm}	Reactive power generated by m^{th} thermal unit
S_{Lj}	Actual apparent power flow of the j^{th} branch
S_T	Scalarized objective function value
V_{Lk} V_{Lk}	Voltage magnitude of k^{th} load buses
$X_{j,l}, \overline{X}_{j,l}$	Current solution and transformed solution

GLOSSARY OF ACRONYMS

Acronym	Description
ABC	Artificial bee colony
AGSO	Adaptive group search optimization
ALC-PSO	Ageing leader and challengers-particle swarm optimization
AMTPG-JAYA	Adaptive multiple teams perturbation-guiding Jaya
BFA	Bacteria foraging algorithm
CE	Cross-entropy
CHP	Combined heat and power
CIWO-PPS	Chaotic invasive weed optimization-Powell's pattern search
CIWO-STS	Chaotic invasive weed optimization-space transformation search
DE	Differential evolution
DM	Decision maker
EP	Evolutionary Programming
ESDE	Enhanced self adaptive differential evolution
ESDE-EC	Enhanced self adaptive differential evolution-eigenvector crossover
ESDE-MC	Enhanced self-adaptive differential evolution-mixed crossover
FACTS	Flexible ac transmission systems
FOR	Feasible operation region
FIDE	Forced initialized differential evolution
GA	Genetic algorithm
GABC	Gbest guided artificial bee colony
GM	Gradient method
GPU-PSO	Graphic processing unit-particle swarm optimizer
GSA	Gravitational search algorithm
GSO	Glowworm swarm optimization
GWO	Grey wolf optimizer
ICA	Imperialist competitive algorithm
ICBO	Improved colliding bodies optimization
ICBOA	Improved colliding bodies optimization algorithm
IPM	Interior point method
IPSO	Improved particle swarm optimization
IWO	Invasive weed optimization
IWO-PPS	Invasive weed optimization-Powell's pattern search
IWO-STS	Invasive weed optimization-space transformation search
KH	Krill herd
KHA	Krill herd algorithm
LP	Linear Programming
LTCs	Load tap changers
LTLBO	Levy mutation based teaching-learning-based optimization
MFO	Moth flame optimization

GLOSSARY OF ACRONYMS (Continued)

Acronym	Description
MICA-IWO	Modified imperialist competitive algorithm-invasive weed optimization
MICA-TLA	Modified imperialist competitive algorithm-teaching learning algorithm
MO	Multi-objective
MOABC/D	Multi-objective artificial bee colony algorithm based on decomposition
MODFA	Multi-objective dimension-based firefly algorithm
MOEA/D	Multi objective evolutionary algorithm based decomposition
MO-OPF	Multi-objective optimal power flow
MPIO-COSR	Modified pigeon inspired optimization algorithm-constraint objective sorting rule
MSA	Moth swarm algorithm
MSCA	Modified sine cosine algorithm
NFE	Number of fitness evaluations
NISSO	Novel improved social spider optimization
NM	Newton method
NR	Newton Raphson
OPF	Optimal power flow
OKHA	Oppositional krill herd algorithm
ORPD	Optimal reactive power dispatch
PDF	Probability density function
PPS	Powell's pattern search
PSO	Particle swarm optimization
PSO-APO	Particle swarm optimization-artificial physics optimization
QP	Quadratic programming
RESs	Renewable energy sources
SD	Standard deviation
SF-DE	Superiority of feasibly solutions-differential evolution
SKH	Stud krill herd
SOA	Seeker optimization algorithm
SOS	Symbiotic organism search
SQP	Sequential quadratic programming
SSO	Social spider optimization
STS	Space transformation search
TCPS	Thyristor controlled phase shifter
TCSC	Thyristor controlled series capacitor
TLBO	Teaching-learning-based optimization
TSA	Tree seed algorithm
TS/SA	Tabu search and simulated annealing
VAR	Volt ampere reactive
WP	Wind power
WSM	Weighted sum method

ABSTRACT

The study of the *optimal power flow* (OPF) is an important tool, in modern-day power systems, to enhance the existing system capacities and to plan for new extensions in an efficient manner. The OPF is a large-scale, highly constrained, nonlinear, non-convex optimization problem that includes a mixture of discrete and continuous control variables. The minimization of fuel cost is mostly considered as an objective function of the OPF problem. Moreover, the increasing environmental protection concerns make it important to take emission pollutant minimization as an objective function. Furthermore, the minimization of real power loss is included in the OPF problem because transmission losses are very significant aspect of the power system planning and design. Additionally, due to the mismatch of generation and transmission capacity, the overall system voltage instability leads to disputes of network participants. This factor makes it necessary to consider the voltage magnitude deviations as one of the objectives of the OPF problem. Due to the contradictory nature of objective functions *i.e.,* fuel cost, emission pollutant, real power loss and voltage magnitude deviations, the OPF problem is considered as a *multi-objective optimal power flow* (MO-OPF) problem.

The power generation companies are facing challenges like scarcity of conventional fossil fuels, increasing energy production cost and environmental concerns. The researchers are focusing on *combined heat and power* (CHP) generation and *renewable energy sources* (RESs) for clean and efficient energy generation. The CHP generation is relatively economical and environment friendly technology to produce heat and power. The RESs are non-polluting sources to supply electricity to consumers which helps to reduce dependency on conventional fuels. *Wind power* (WP) is one of the most popular form of RESs having great prospective for the solution of aforementioned problems. However, the integration of WP and CHP units makes the OPF problem more complex.

The intent of the thesis is to formulate and solve the OPF problems for thermal generation system, wind-thermal generation system and CHP-thermal-wind generation system. An integrated optimization technique, established with the integration of the *invasive weed optimization* (IWO) and *Powell's pattern search* (PPS) method is proposed for the solution of OPF problem. The IWO algorithm has been undertaken as a global search technique and the PPS method is employed as a local search technique. The effectiveness of the proposed IWO-PPS technique is tested by applying it to the standard IEEE test systems and results are compared with the reported results by the well-established optimization techniques and found

promising. A non-interactive approach is applied to search the best non-dominated solution of MO-OPF problem. The results illustrate that the IWO-PPS technique performs better as compared to IWO technique in terms of the quality of solution and convergence characteristics. A hybrid approach integrating the IWO and space transformation search (STS) technique has also been implemented to the OPF problem to authenticate the performance of proposed IWO-PPS technique. Further, the chaotic Tent map is applied with both IWO-PPS and IWO-STS techniques to tune the algorithm parameters that accelerate the convergence speed and helps to avoid local optimal solutions. A *t*-test is performed to validate the statistical performance of the optimization technique.

CHAPTER-1
INTRODUCTION

1.1 INTRODUCTION

The modern-day power systems are designed to deliver the output in an efficient manner with taking care of the economic, environmental and system security aspects as well. The load demand is increasing at a high pace and the system network needs to be updated by utilizing modern-day tools to maintain stability and efficiency. The study of the *optimal power flow* (OPF) is an important tool to enhance the existing system capacities and to plan for new extensions. The ever-increasing load demand requires a substantial increase of power transfer capability for ensuring energy transactions. The existing transmission facilities are becoming overburdened due to practical constraints. Various technologies are being explored to keep the power system secure, while conducting large energy transactions [76]. *Flexible ac transmission systems* (FACTS) is extensively used technology that maximizes the use of the existing transmission assets by redistributing the line power flow and regulating bus voltages [2,12,75,137].

The OPF is a large-scale, highly constrained, nonlinear, non-convex optimization problem that includes a mixture of discrete and continuous control variables. The minimization of fuel cost is most frequently considered as an objective function of the OPF problem. Moreover, the increasing environmental protection concerns make it important to take emission pollutant minimization as an objective function. Furthermore, minimization of real power loss is included in the OPF problem because the transmission losses are very significant aspect of the power system planning and design. Additionally, due to the mismatch of generation and transmission capacity, the overall system voltage instability leads to disputes of network participants. This factor makes it necessary to consider the voltage magnitude deviations as one of the objectives of the OPF problem. Due to the contradictory nature of objects *i.e.,* fuel cost, emission pollutant, active power loss and voltage magnitude deviations, the power system OPF problem is considered as a *multi-objective optimal power flow* (MO-OPF) problem.

The power generation companies are facing challenges like increasing energy production cost, environmental regulations and scarcity of conventional fossil fuels. The researchers are focusing on *combined heat and power* (CHP) generation and renewable energy

generation to take care of these issues to some extent. The CHP generation is relatively economical and environment-friendly technology to produce heat and power [20,57,63,86,96]. The efficiency of fuel conversion of CHP unit is around 85-90% in comparison to the 35-40% level of thermal units and the CHP unit is more environment-friendly. The *renewable energy sources* (RESs) are non-polluting sources that reduce the dependency on conventional fuels. *Wind power* (WP) is one of the most popular forms of RESs, having great prospective for the solution of the aforementioned problems. The WP penetration has substantially increased into electric power systems in recent past due to environmental benefits and the low cost of wind generators [55,119,140,191,197,208]. However, the integration of WP and CHP units makes the OPF problem more complex.

Researchers have applied various optimization techniques to solve the OPF problem. These techniques are basically classified into two categories *i.e.,* classical and global search techniques. The application of classical optimization techniques in solving real-world optimization problems always involves few assumptions due to non-differentiable and discontinuous objective functions and constraints. Therefore, these techniques lack in finding the global best solution. The global optimization techniques are employed to solve non-differential and discontinuous OPF optimization problems. For global optimization techniques, algorithm parameter tuning is an important aspect since convergence characteristics and solution quality get influenced by parameter setting. Thangaraj *et al.* [190] have proposed the chaos maps for selecting the control parameters of the algorithm. The chaotic maps are widely used by various researchers to tune the algorithm parameters. Chaotic Tent map has been used by various researchers that accelerates the convergence speed and helps to avoid local optimal solutions. The global search techniques have better exploration capability; however, these techniques lack in exploitation capability and have high computational complexity. Hence, researchers have proposed hybrid optimization techniques with the integration of the different optimization techniques in a systematic manner for solving complex optimization problems.

One of the natural characteristics linked with complex real-world decision-making problems is their *multi-objective* (MO) nature. For MO problems, there is no unique solution for all objectives; however, there is a group of solutions that cannot be dominated by any other solution in the search space. Researchers have proposed a number of classical and intelligent optimization algorithms for getting a trade-off solution to the problems. The classical methods transform the MO problem to a single objective problem. The classical methods require pre-determining the significant degree of each objective employing priori method or establish it by utilizing an interactive method during the search process. The execution of classical methods is

easy and these are frequently useful to solve convex type optimization problems. The intelligent optimization algorithms have an exclusive feature to search and maintain multiple solutions in a single simulation run. Intelligent optimization algorithms are capable to solve the non-convex optimization problems without coupling the different objectives while maintaining individual features of all the objectives [146]. However, these techniques are less efficient and sometimes face difficulties in dealing with the problems arising during simultaneous convergence and distribution of the optimization technique [99,172]. The choice of a particular method depends upon the type of information available, the user's preferences and the solution requirements.

1.2 OPTIMIZATION TECHNIQUES

Optimization is the process of searching the optimum solution for a particular problem. Optimization problems may be continuous or combinatorial, constrained or unconstrained and static or dynamic problems. The mathematical representation of the constrained optimization problem is given as

Minimize $of(U,X)$ (1.1)

Subject to: $g(U,X)=0$ (1.2)

$h(U,X)\le 0$ (1.3)

where *of* is the objective function to be minimized; *g(U,X)* and *h(U,X)* are the set of equality and inequality constraints, respectively; *U* and *X* are the vectors of dependent and decision variables, respectively.

The decision variables are bounded to be within the minimum and maximum limits as follows:

$X_j^{\min} \le X_j \le X_j^{\max} \ (j=1,2,3,...,N)$ (1.4)

where *N* is the number of decision variables.

The optimization technique is a useful tool for modern research to solve complex optimization problems. The researchers are continuously working to develop various optimization techniques for the solution of real-world optimization problems. These techniques are basically classified into two types *i.e.*, classical and global search techniques.

1.2.1 Classical Optimization Techniques

Researchers have applied various classical optimization techniques for solving real-world optimization problems. The classical optimization techniques are easy to understand and use.

The classical or local search methods are classified into two categories *i.e.*, gradient and direct search methods. The gradient search methods *i.e.*, Steepest descent method, *Newton method* (NM), Quasi-Newton method *etc.* utilize the derivative information for guiding the search process. These methods are not suitable for problems having discrete or discontinuous objective functions or constraints.

The direct search methods *i.e.*, simplex method, univariate method, Pattern search method *etc*. do not require derivative information of the objective function to obtain the optimum solution [45]. The direct search method can be applied for discontinuous and non-differential optimization problems. The simplex method searches the basic feasible solution by sifting through the set of basic feasible solutions. The univariate method searches the minimum point along the parallel directions to the coordinate axes. This method is easy to implement; however, it finds difficult to converge in some cases and even the convergence process is very slow near the optimum point [150,158]. In an alternative approach, the search direction is preceded in a specific direction, namely the pattern directions, instead of retaining parallel to the coordinate axes. The Hooke Jeeves and *Powell's pattern search* (PPS) method use pattern directions to update the decision variables. The main disadvantage of direct search techniques is that several trials with different initial conditions need to be conducted to ascertain that the global optimum is truly found. The direct search methods involve more computations than the gradient search methods.

Some particular class of problems is solved by using linear, non-linear, quadratic programming. The linear programming method obtains quick results however, the accuracy is not guaranteed and the selection of improper gradient step size affects the solution. The non-linear programming is robust and capable of solving large-scale problems with good accuracy. However, it involves high algorithm complexity and has poor convergence behaviors.

Classical optimization techniques involve high computational process while solving complex optimization problems. Moreover, the classical method may converge prematurely for non-linear optimization problems. In order to overcome the limitations of classical optimization techniques, the researchers have explored the global optimization techniques.

1.2.2 Global Optimization Techniques

In recent years, various global optimization techniques are introduced by the researchers to solve the real-world optimization problems [7,15,73,88,138]. The global search techniques have various advantages *i.e.*, robust and reliable performance, global search capability, require

less information, easy implementation, parallelism, no need of continuous and differentiable objective function. The global optimization techniques are classified on the basis of source of inspiration like evolution and natures *i.e.,* swarm intelligence, physics-inspired algorithms and bio-inspired algorithms.

The swarm based algorithms take inspiration from the collective behavior of a social group. The swarm participants cooperate for searching the food and defending from other attacking agents [58,77,212]. Researchers have proposed various global optimization techniques to solve complex optimization problems. Kennedy and Eberhart [87] have introduced *particle swarm optimization* (PSO) that takes inspiration from the natural concept of bird flocking. Krishnanand and Ghose [90] have introduced *Glowworm Swarm Optimization* (GSO) algorithm that is nature-inspired swarm based optimization algorithm. Yang [211] has introduced swarm based bat algorithm and it takes inspiration from the capability of micro-bats to distinguish different types of insects in darkness. Bansal *et al.* [21] have introduced swarm based spider monkey optimization algorithm. Mirjalili [109] has introduced nature-inspired *moth flame optimization* (MFO) algorithm based on the transverse orientation type navigation used by moths. The researchers have introduced various other swarm based nature-inspired algorithms like the *grey wolf optimizer* (GWO) algorithm [112,162,183], ant lion optimizer [110], whale optimization algorithm [111] for solving the optimization problems.

The Physics laws also inspire the researchers while designing the optimization algorithms. Tamura and Yasuda *et al.* [186] have introduced a spiral dynamic algorithm, inspired from the spiral phenomenon in nature. Hatamlou *et al.* [67] have introduced the ions-motion algorithm based on the motion of ions in nature. Tayarani and Akbarzadeh [187] have introduced magnetic optimization algorithm that takes inspiration from the theory of magnetic field. Rashedi *et al.* [152] have introduced gravitational search algorithm inspired of the law of gravity and mass interactions.

The bio-inspired algorithms are evolutionary type algorithms. Dai *et al.* [42] have introduced seeker optimization algorithm that takes inspiration from the egotistic, altruistic and pro-active behavior of the seeker. Civicioglu [39] has introduced artificial cooperative search algorithm, in line with the biological interaction and migration of two artificial super organisms to achieve the global minimum value. Civicioglu [40] has proposed bio-inspired backtracking search optimization algorithm, which is based on the concept of visit of a group of living creatures repeatedly to hunting areas that had been prolific previously for getting nourishment.

Mehrabian and Lucas [105] have proposed bio-inspired evolutionary type optimization technique named as *invasive weed optimization* (IWO). It is inspired of the invasive behavior

of weeds in their natural growth. The weeds spread over the cropping field and take up the prospective spaces. The weeds with better environmental adoption capability exhibits better growth and result in the production of more seeds. The IWO algorithm exhibits high explorative power over the bound-constrained search space and requires less number of parameters to solve complex real-world problems [9,84,163]. Researchers have successfully applied IWO algorithm to solve complex optimization problems [59,78,124,129,157].

Despite the various advantages of global search techniques, these optimization techniques involve higher computational complexity and the solution depends upon algorithm parameters, which sometimes make it difficult to converge on the global best optimal solution in every attempt. In order to achieve the global best solution with least computational efforts, researchers have proposed various hybrid optimization techniques.

1.2.3 Hybrid Optimization Technique

The hybrid techniques integrate two or more optimization techniques and these are operated collectively to solve the optimization problems. The common searching features of the optimization technique are *i.e.*, diversification and intensification [109].The hybrid optimization technique has the advantage of maintaining the proper balance between diversification and intensification. Harman and McMinn [66] have conducted a large empirical study and suggested that a hybrid global-local search is suitable to solve the real-world optimization problems. Noman and Iba [134] have introduced a crossover based adaptive local search operation to improve the performance of the standard *differential evolution* (DE) algorithm. Narang *et al.* [127-128] have successfully applied the local PPS method integrated with predator-prey optimization technique to solve the optimum generation schedule for the hydrothermal system. Singh *et al.* [175] have applied the PPS method with chaotic DE to solve the thermal power load dispatch problem. Anand *et al.* [13] have employed hybrid optimization technique integrating binary successive approach with civilized swarm optimization for the solution of the unit commitment problem taking dual-mode CHP units. Hmida *et al.* [70] have successfully applied hybrid technique that embeds modified Imperialist competitive algorithm and the *sequential quadratic programming* (SQP) for the solution of OPF problem. Researchers have also explored various hybrid techniques that integrate the global-global optimization techniques to search the optimum solution. Gilvaei *et al.* [62] have applied hybrid optimization technique that embeds firefly algorithm and adaptive particularly tunable fuzzy PSO for the solution of *optimal reactive power dispatch* (ORPD) problem. Li *et al.* [93] have

integrated the chaotic artificial bee colony and DE techniques to solve the ORPD problem.

The hybridization of different optimization techniques is a complex task since every technique has some pros and cons [205]. Cui *et al.* [41] have discussed in detail the advantages and disadvantages of optimization techniques used for solving real-world complex optimization problems. The researchers have been proposing various hybrid optimization techniques *i.e.*, global-global, global-local techniques to solve complex optimization problems.

1.3 MULTI-OBJECTIVEOPTIMIZATION

The real-world problems involve simultaneous optimization of non-commensurable, conflicting and competing objectives. MO optimization problems with conflicting objectives give a set of optimal solutions instead of single optimal solution because no solution can be better than any other with respect to all objective functions. These optimal solutions are termed as Pareto optimal solutions. The MO optimization problem having a number of objectives with several equality and inequality constraints is formulated as under:

Minimize $of_i(U,X)\ i=1,2,...,N_{obj}$ (1.5)

Subject to
$$\begin{cases} g_l(U,X)=0 & (l=1,2,3,...,L) \\ h_k(U,X)\le 0 & (k=1,2,3,...,K) \\ X_j^{\min}\le X_j\le X_j^{\max} & (j=1,2,3,...,N) \end{cases} \quad (1.6)$$

where of_i is the i^{th} objective function, N_{obj} is the number of objectives, L and K denotes equality and inequality constraints. N is the number of decision variables. U and X are the vectors of dependent and decision variables, respectively.

There is a number of factors that need the simultaneous management of multiple, contrary and incommensurable objectives. The different real-world optimization problems have been formulated in MO optimization framework. For MO optimization problems, the best non-dominated solution is searched that satisfies each of the objectives up to a certain level of satisfaction. The researchers have employed different MO optimization techniques for solving the MO problems [19,41,44,53,177].The solution methods of MO optimization problems are generally categorized in two ways. Firstly, the kind of information available to the *decision maker* (DM) like, trade-offs. Secondly, the process employed to get Pareto optimal solutions and the ways to act together with the DM. Researchers have applied various classical and intelligent optimization algorithms to get a trade-off solution to the problems. The classical methods transformed the MO problems into single-objective problems. The classical methods need to pre-determine the significant degree of each objective using the priori method or

determine it by employing an interactive method during the search process [125,210]. Several priori methods are reported in literature like *weighted sum method* (WSM), the ε-constraint method, the dictionary ordering method, the objective programming method. The classical methods are easy to execute; however, they are frequently useful for the convex type of optimization problems. The interactive methods vigorously use the knowledge of DM and these methods provide useful results for non-convex optimization problems [85]. The unique feature of intelligent optimization algorithms is to search and maintain multiple solutions in one simulation run. Intelligent optimization algorithms, like dynamic artificial bee multi-colony algorithm [209], self-adaptive multi-objective teaching-learning based optimization method [213], multi-objective genetic algorithm [170], multi-objective harmony search algorithm [26], multi-objective manta ray foraging optimizer [83] *etc*. are commonly utilized for achieving the Pareto front of the MO optimization problem. Although having the edge on classical methods from the viewpoint of convergence, diversity, robustness and flexibility, the intelligent optimization techniques sometimes suffer the time-consuming computation process and are relatively less efficient [99]. To search the most suitable Pareto optimal solution of the non-convex optimization problem, recently, Singh *et al.* [174] have implemented a non-interactive approach for solving the multi-objective thermal power load dispatch problem, where either DM is not concerned or prior preference information is available.

As discussed above, both the approaches for the solution of the MO optimization problems have their pros and cons. Researchers are continuously working on MO optimization techniques to solve complex MO problems.

1.4 OPTIMAL POWER FLOW PROBLEMS

The power system network is a complex network that interconnects various types of power generation and transmission sources of electric power. The OPF is an important aspect of power system operation, introduced by Carpentier about 60 years ago. The OPF is a non-linear highly constrained optimization problem. It is basically divided into two main parts: optimal active power dispatch and optimal reactive power dispatch problem. In this research work, OPF problem of thermal generation, wind-thermal generation and CHP-thermal-wind generation systems have been undertaken.

1.4.1 Optimal Power Flow of a Thermal Generation System

Power system planners and researchers have employed different optimization techniques to

solve the OPF problem. Different classical techniques like *gradient method* (GM) [92,192], NM [71], *Linear programming* (LP) [56], interior point method [64,149] and *quadratic programming* (QP) [153] *etc.* are employed for the solution of OPF problems. The GM technique lacks in convergence rate with the steepest descent direction and the researchers have proposed NM technique to overcome this shortcoming of GM technique [71]. The NM technique is very sensitive to the initial presumption and may result in convergence failure because of the improper selection of initial conditions [185]. The LP method suffers to provide solution if the improper gradient step size is selected [56]. The shortcomings of LP method are addressed with QP method [153].

In order to overcome the limitations of classical optimization techniques, the power system researchers have explored the global optimization techniques to solve the OPF problem. Abou El Ela *et al.* [4] have solved ORPD problem by employing DE algorithm. The performance comparison of three population-based algorithms *i.e.*, PSO, *evolutionary programming* (EP) and *genetic algorithm* (GA) has been carried out by Kahourzade *et al.* [82] to solve the ORPD problem and they found that EP method outperformed GA and PSO. Vaisakh *et al.* [195] have solved the OPF problem having non-convex and non-smooth generator cost characteristics employing an evolving ant direction PSO algorithm. To solve the ORPD problem, the improved Pseudo-gradient search PSO technique has been employed by Polprasert *et al.* [141]. Shaw *et al.* [168] have solved the ORPD problem using an opposition-based *gravitational search algorithm* (GSA). Mukherjee and Mukherjee [121] have applied the *krill herd algorithm* (KHA) and *oppositional KHA* (OKHA) to solve the OPF problem. Mukherjee and Mukherjee [122] have solved the ORPD problem for real power loss minimization and improvement of voltage profiles using the chaotic krill herd algorithm. Warid *et al.* [203] have formulated the OPF problem with the distribution generation effect and solved it employing the Jaya algorithm. Jadhav and Bamane [74] have implemented the g-best guided *artificial bee colony* (ABC) algorithm to solve OPF problem. To solve the ORPD problem for the transmission loss minimization and voltage stability enhancement, the ABC algorithm has been applied by Ettappan *et al.* [54]. Abaci and Yamacli [1] have applied differential search algorithm to solve the ORPD problem. Mohamed *et al.* [114] have solved the constrained OPF problem using *moth swarm algorithm* (MSA). To solve the OPF problem, a sine-cosine algorithm has been proposed [17]. Taher *et al.* [184] have proposed the modified grasshopper optimization algorithm for the solution of the OPF problem. Srilakshmi *et al.* [179] have solved the OPF problem using the most valuable player algorithm. El-Sattar *et al.* [51] have proposed improved salp swarm algorithm to solve the OPF problem. Shaheen *et al.*

[165] have proposed improved heap optimization algorithm to solve the OPF problem. Basu [24] has presented the modeling of FACTS devices *i.e.*, thyristor controlled series capacitor, thyristor controlled phase shifter and solved the OPF problem including FACTS devices using DE technique. In order to solve the OPF problem with FACTS devices, various optimization techniques, *i.e.*, Bacteria foraging optimization [194], PSO with ageing leader and challengers [176], *symbiotic organism search* (SOS) [142], *imperialist competitive algorithm* (ICA) [81], OKHA [121], cumulative gravitational search algorithm [136] and partitioned ant lion optimizer [100] have been applied.

The researchers have applied various hybrid optimization techniques to solve the OPF problems. To solve the transient stability constraint OPF problem, a hybrid algorithm integrating the DE and SOS algorithms has been proposed by Saha *et al.* [159]. For the solution of OPF problem, a hybrid algorithm merging Salp and PSO algorithms has been implemented by El-Sehiemy *et al.* [52]. To solve security constrained OPF problems, a hybrid algorithm embedding DE with PSO has been proposed [102]. A hybrid algorithm combining the self-adaptive PSO and DE has been proposed to solve the OPF problem [123]. Pulluri *et al.* [143] have applied a bio-inspired stud KHA for the solution of the OPF problem. A hybrid optimization algorithm combining ICA and teaching-learning algorithm has been proposed to solve ORPD problems [60]. Khorsandi *et al.* [89] have applied a hybrid optimization technique based on the integration of shuffled frog leaping technique and Nelder-Mead simplex method to solve the ORPD problem. Rajan and Malakar [148] have solved the ORPD problem by combining FA and Nelder-Mead simplex method. An enhanced evolutionary algorithm based on OKHA has been proposed for obtaining the optimal steady-state performance of power networks [47].

To solve the OPF problem of conventional thermal generation system, various optimization techniques have been applied by researchers. The scarcity of fossil fuels, high cost component and increasing environmental concerns are making it mandatory to look for increased share of RESs. Researchers are exploring various techniques for the efficient and secure integration of renewable generation sources in the conventional power system networks.

1.4.2 Optimal Power Flow of a Wind-Thermal Energy Generation System

The WP is one of the widely utilized forms of RESs in electrical power systems. However, the random and intermittent nature of WP has brought new challenges to system planners. Researchers have solved the OPF problem of a wind-thermal generation system. A stochastic

model of WP in the OPF dispatching problem has been presented by Jabr and Pal [72]. Attarha *et al.* [16] have proposed an adaptive robust optimization model, integrated with WP generators, for solving the OPF problem. Zhang *et al.* [216] have formulated the OPF problem by including the intermittent WP availability. To solve the wind integrated power system OPF problem, the modified bacteria foraging algorithm has been implemented by Panda and Tripathy [139]. Mohseni-Bonab *et al.* [115] has formulated the multi-objective ORPD problem for the wind integrated power system having the focus on the uncertainty of load and WP generation. For the solution of stochastic OPF problem of the system including RESs, the DE algorithm has been applied by Awad *et al.* [18]. Shilaja and Arunprasath [169] have solved the OPF problem incorporating WP generators using hybrid approach that combines the MSA and GSA technique. Hmida *et al.* [70] have formulated and solved constrained OPF problem containing RESs by employing hybrid algorithm integrating modified ICA and SQP. Souza *et al.* [178] have applied the gradient-based approach to solve the stochastic OPF problem including WP units. Sulaiman and Mustaffa [180] have solved the OPF problem including renewable energy generators using recent metaheuristic techniques.

Researchers have solved the OPF problem of a wind-thermal generation system using various optimization techniques. The researchers are exploring the solution for the optimal power system network problem integrating CHP units with conventional thermal system in order to meet high power demand in an efficient and optimal manner.

1.4.3 Optimal Power Flow of a CHP-Thermal-Wind Energy Generation System

Integration of CHP in the power network is also in rising trend for having efficient and clean energy generation. CHP generation is a very economical and environment-friendly power and heat delivery method. The overall efficiency of thermal units is less as the large share of energy is wasted in the form of heat [96]. CHP utilizes this heat to achieve the energy conversion efficiency of up to 85% [155]. It reduces the cost of generation in the range of 10 to 40% [131-132].

Recently, the researchers have applied different optimization techniques to solve the OPF problems of power system networks including CHP units [91]. Adhvaryyu *et al.* [6] have formulated and solved the dynamic OPF problem incorporating CHP using KHA technique. Adhvaryyu and Adhvaryyu [5] have formulated static load flow problem of the power system considering the valve point effect and prohibited operating zones incorporating cogeneration units.

1.4.4 Multi-objective Optimal Power Flow

The aim of OPF problem solution is to optimize various objectives *i.e.,* fuel cost, pollutant emission, active power transmission losses and total voltage magnitude deviations simultaneously. Due to the conflicting nature of these objectives, the OPF problem has been treated as MO problem. The MO-OPF is a large-scale, nonlinear, multi-modal optimization problem. Researchers have applied classical and intelligent optimization techniques to solve MO-OPF problems [173,201,206]. The classical methods *i.e.*, price penalty factor, WSM, Ɛ-constraint method *etc*. convert the MO-OPF problem into a single-objective problem and provide the single solution from the set of Pareto solutions. An OPF problem, considering both cost and emission simultaneously, is transformed into a single objective optimization problem with price penalty factor and solved by using DE technique [24].To solve MO-OPF problem, the enhanced FA technique has been applied along with weighing factors and fuzzy membership function is used to select the best compromise solution [95].Prasad and Mukherjee [142] have solved the MO-OPF problem using the SOS algorithm with price penalty factor approach. To solve the combined economic and environmental problem, OKHA technique with price penalty factor approach is used [121]. Daryani *et al.* [43] have applied an *adaptive group search optimization* (AGSO) algorithm with WSM approach to solve MO-OPF problem and the fuzzy decision making approach is utilized to extract the best compromising solution out of all the non-dominated solutions. Biswas *et al.* [28] have employed DE technique with WSM approach to solve the MO-OPF problem. The MO-OPF problem having objective functions as minimization of active power transmission losses and voltage stability index is solved with Ɛ-constraint method and fuzzy satisfying approach [116]. Sakr *et al.* [161] have solved the optimal reactive power management problem having the objectives of minimization of transmission network losses and voltage deviation using weighting factors and modified DE algorithm. Shojaei *et al.* [171] have applied the Ɛ-constraint method to solve multi-objective reactive power planning problem, including the uncertainties of load demand and WP generation. In order to select the best compromising solution, the fuzzy decision-making and min-max approaches are jointly employed. The classical methods are easy to execute and these are useful for convex type optimization problems. However, these methods involve larger computational time and find difficulties for solving non-convex and non-differentiable type optimization problems.

To overcome the disadvantages of classical methods, researchers have employed various intelligent optimization techniques. Zhihuan *et al.* [219] have employed a non-

dominated sorting genetic algorithm-II for minimizing the real power transmission losses and voltage deviations. A multi-objective reactive power market clearing optimization problem has been solved using a hybrid fuzzy multi-objective evolutionary algorithm [160]. Rao and Vaisakh *et al.* [195] have solved the MO-OPF problem using a multi-objective adaptive colonel selection algorithm. This algorithm utilizes a non-dominated sorting and crowding distance to search and manage the Pareto optimal front. Pulluri *et al.* [144] have proposed enhanced self adaptive DE with mixed crossover that is a combination of eigenvector and binomial crossover to solve the MO-OPF problem. Man-Im *et al.* [101] have solved the MO-OPF problem including WP cost functions by employing enhanced PSO including chaotic mutation and stochastic weight trade-off features. For the solution of the MO-OPF problem, multi-objective evolutionary algorithm is applied and the fuzzy decision-making approach is employed to obtain the best compromising solution [29,215].

The intelligent optimization algorithms have an exclusive feature to search and maintain multiple solutions in a single simulation run. However, these techniques are less efficient and sometimes face difficulties to deal with the problems arising during simultaneous convergence and distribution of the optimization technique [172]. Marler and Arora [103] have presented a survey of MO optimization concepts consolidating the seemingly different terminology and methods. Researchers are continuously working to propose multi-objective optimization techniques to find the best non-dominated solution of MO-OPF problem.

1.5 RESEARCH GAP

The OPF is very important aspect in the field of operation and control of modern power system networks. Researchers have solved the conventional OPF problems by various optimization techniques. Different energy sources are being integrated in the conventional power system networks to cope up with the increasing electricity demand and environmental concerns. The contribution of CHP units is increasing in the power system networks to meet high power demand in an efficient and optimal manner. In today's electricity networks, the WP is one of the potential sources of renewable energy generation. The rise of WP penetration has posed new challenges for the system operators and planners due to its intermittent nature. The solution of OPF problem for a network that includes CHP and wind units along with thermal units is a challenging task due to the interdependence of power and heat generation in the process of cogeneration and intermittent nature of wind energy sources. As per best of the author's knowledge, no significant work related to the optimal solution of power system

network problem involving combined thermal, CHP and wind generation system has been carried out.

According to “no free lunch” theorem, no optimization technique can search the best results of all optimization problems, which encourages the researchers to propose an optimization technique that can be applied to solve all types of optimization problems and able to search optimal results in minimum computational efforts. Researchers have proposed various conventional and global optimization techniques to solve OPF problems. However, for better exploration and exploitation capability, a hybrid optimization technique can be proposed to search optimal solution of OPF problem. In OPF problem normally, fuel cost, emission pollutant, active power losses and total voltage magnitude deviations objectives are minimized. Due to contradictory nature of these objectives OPF problem considers as MO-OPF problem. Various classical and intelligent techniques are applied to search the best Pareto optimal solution. However, each classical and intelligent technique has its own limitations, which motivates the researchers to propose new interactive or non-interactive approaches to search the best Pareto optimal solution.

1.6 SCOPE OF THE WORK

The modern-day power systems are facing various challenges related to generation-demand imbalance and environmental regulations. The advanced technologies and equipments are being integrated to the system for the optimal utilization of existing generation and transmission resources. The OPF is an important tool to enhance the existing system capacities and to plan for new extensions. The exhaustion of the conventional energy sources, their increasing prices worldwide and the modern-day environmental concerns have increased the contribution of RESs for meeting the energy demand. The WP is one of the foremost sources of renewable energy generation. The rise of WP penetration has posed new challenges for the system operators and planners due to its intermittent nature.

The system planners are trying to improve the conversion efficiency of conventional thermal generation system to provide secure electricity at the competitive prices. The CHP generation is very effective in improving the conversion efficiency of conventional fuels along with effective reduction of pollutant emission. The integration of CHP units along with wind units makes the existing system quite complicated due to the interdependence of power and heat generation in the process of cogeneration and intermittent nature of wind energy source. The OPF problem is a non-convex, nonlinear and complex optimization problem subject to a

number of constraints. The classical techniques face difficulties in solving this type of complex optimization problem. The global search techniques address most of the limitations of the classical techniques and exhibits admirable exploration capability. The global search techniques lack in exploitation capability and have high computational complexity. Hence, there is a need to propose an integrated optimization technique to find the global optimum of OPF problem with least computational efforts. The objectives of the OPF problem are minimization of fuel cost, emission pollutant, active transmission loss and total voltage magnitude deviations. The objectives of the OPF problem under consideration are of contradictory nature and hence the problem is framed as a MO optimization problem. A multi-objective solution approach is required to find the best non-dominated solution of MO optimization problem. The MO-OPF problem has a great future scope for economical, secure, stable and environment-friendly operations of an integrated modern-day power system.

1.7 OBJECTIVES OF THE RESEARCH

The intent of thesis work is to solve the OPF problem withconventional thermal unit system, thermal and wind unit system and CHP, thermal-wind generation system by proposing a hybrid optimization technique. The research work includes the fuel cost, pollutant emission, system transmission losses and total voltage magnitude deviation as objective functions.

The objectives of the research work are as follows:

1) To solve optimal power flow problem including FACT devices.
2) To formulate optimal power flow problem incorporating wind energy source.
3) To propose a hybrid optimization technique to solve optimal power flow problem considering wind power penetration.
4) Apply proposed hybrid optimization technique in multi-objective framework for optimal power flow problem.

1.8 OUTLINE OF THE THESIS

In this research work, OPF problem is formulated for conventional thermal unit system, thermal and wind unit system and CHP, thermal-wind generation system. The OPF problem is a mixed integer, highly constrained and complex optimization problem. The integrated optimization technique embedding the IWO technique with the PPS method is proposed to solve the OPF problem. Another hybrid optimization technique that embeds IWO and *space transformation search* (STS) techniques is implemented to solve the OPF problem. Further, a

chaotic Tent-map based hybrid IWO-PPS technique is proposed to solve OPF problem incorporating wind and CHP units. The chaotic Tent-map increases the convergence speed and helps to avoid local optimal solutions. The impact of CHP and wind units is analyzed on standard IEEE test systems. A non-interactive approach is applied to search the best non-dominated solution of the MO-OPF problem, where either DM is not concerned or prior preference information is available. The thesis work is organized into seven chapters. A brief description of all the chapters is as under:

Chapter 1: This chapter describes the OPF problem of power system incorporating thermal units, thermal-wind units and CHP-thermal-wind units. The introduction of different optimization techniques is carried out for solving the OPF problem. Being an OPF problem with contradictory objectives, the multi-objective optimization techniques are also discussed for the solution of the OPF problem. The relevant literature is given for various types of OPF problems and optimization techniques.

Chapter 2 presents the integrated IWO-PPS optimization technique for the solution of the OPF problem including FACTS devices. The IWO algorithm is applied as a global search technique, which is inspired from the specific ecological behavior of weeds and has the ability to adapt to the changing environment. The PPS method is employed as a local search method and is based upon a conjugate-based search. This method exhibits excellent exploitation search capability that helps to improve the solution obtained from the IWO technique. The equality constraints are satisfied by static load flow equations and inequality constraints are satisfied by exterior penalty method. The efficacy of the proposed IWO-PPS technique is tested on four test systems of OPF problem by undertaking fuel cost, pollutant emission and transmission loss objectives, sequentially. The attained results have been compared with the results stated in the literature. Further, *t*-test is performed to validate the statistical performance of the IWO-PPS technique.

In chapter-3, the OPF problem is framed as the MO-OPF problem due to the conflicting nature of objective functions. A satisficing function is offered to take care of the conflict among non-commensurable objectives and the MO problem is reformulated as a scalar optimization problem. The integrated IWO-PPS technique is applied to obtain the satisficing solutions. A non-interactive approach is employed to find the best non-dominated solution of MO-OPF problem. In this approach, the DM has access to prior information about preferences; however DM is not involved in the selection process of the best non-dominated solution. This approach reduces the computation work involved for generating the Pareto front and for selecting the best satisficing solution. The proposed solution approach has been tested on three

MO-OPF problems with FACTS devices and the comparison is carried out with the well-established algorithms. Further, *t*-test confirms the robustness of the proposed solution approach.

Chapter 4 describes the implementation of a hybrid IWO-STS optimization technique to solve the OPF problem. The IWO technique is a population-based stochastic algorithm inspired by nature while the STS is an evolutionary technique inspired by opposition-based learning. The STS technique compares a solution with its opposition to obtain a better solution which reduces the computational efforts and search direction moves toward the promising region to conquer the premature convergence problem. To obtain the best non-dominated solution for MO-OPF problem, non-interactive approach is used. The performance of the IWO-STS technique is verified on three IEEE test systems and the achieved results are compared with recently published results.

In chapter 5, the OPF problem is formulated by including the WP units in the system by considering the power uncertainty of WP units as a cost factor. Integration of wind units into OPF problem imposes various challenges due to intermittent nature of WP availability. The IWO, IWO-STS and IWO-PPS techniques are applied for the solution of the OPF problem including wind units. The impact of WP units is analyzed on two standard IEEE test systems. The attained results are compared with the results stated in the literature.

In chapter-6, the OPF problem has been formulated by incorporating wind and CHP units. The operation of the CHP unit is restricted by the feasible operation region of heat and power, which further restrict the search space for decision variables. A chaotic Tent map-based hybrid optimization technique that embeds the IWO technique with the PPS method (CIWO-PPS) is proposed for the solution of OPF problem including WP and CHP units. The chaotic Tent map has been applied to tune the algorithm parameters, which accelerates the convergence speed and helps to evade local optimal solutions. The CIWO-PPS technique is tested on standard IEEE test systems and it outperforms the other well-established state of art techniques. The statistical *t*-test is executed to authenticate the robustness of the CIWO-PPS technique.

Finally, chapter 7 concludes the contribution of this research work. The scope of future research work in the field of OPF problem and optimization techniques is also presented.

CHAPTER-2

OPTIMAL POWER FLOW SOLUTION USING AN INTEGRATED OPTIMIZATION TECHNIQUE

2.1 INTRODUCTION

The *optimal power flow* (OPF) is a non-linear, non-differentiable and multimodal optimization problem with a mixture of discrete and continuous variables. In order to solve the OPF problem, various optimization techniques have been applied by the researchers [25,36,68,94,120]. Despite the various advantages of global search techniques, these optimization techniques involve higher computational complexity and the solution depends upon algorithm parameters. To attain the global best solution, researchers are vigorously working to propose hybrid optimization techniques to solve OPF problems with the least computational efforts.

In this chapter, an integrated optimization technique that integrates the IWO technique with the PPS method (IWO-PPS) is proposed to solve the OPF problem of the thermal generation system. In this integrated technique, the IWO technique is applied for exploring the search area and the PPS method exploits the promising search area. The efficacy of the IWO-PPS technique is tested on four test systems of OPF problem by undertaking fuel cost, pollutant emission and transmission loss objectives sequentially. The FACTS devices, namely, *thyristor controlled series capacitor* (TCSC) and *thyristor controlled phase shifter* (TCPS) have also been undertaken in the OPF problem formulation.

2.2 MATHEMATICAL MODELLING OF FACTS DEVICES

The modeling of two types of FACTS devices *i.e.*, TCSC and TCPS are taken from ref. [24] and presented below:

Modeling of TCSC

The network model for TCSC is represented by Figure 2.1. This model represents the TCSC with a variable capacitive reactance incorporated in the respective transmission line. The line flow equations for the transmission line are given as follows [24]:

$$P_{kl} = V_k^2 G_{kl} - V_k V_l G_{kl} \cos(\theta_k - \theta_l) - V_k V_l B_{kl} \sin(\theta_k - \theta_l) \quad (2.1)$$

$$Q_{kl} = -V_k^2 B_{kl} - V_k V_l G_{kl} \sin(\theta_k - \theta_l) + V_k V_l B_{kl} \cos(\theta_k - \theta_l) \quad (2.2)$$

$$P_{lk} = V_l^2 G_{kl} - V_k V_l G_{kl} \cos(\theta_k - \theta_l) + V_k V_l B_{kl} \sin(\theta_k - \theta_l) \quad (2.3)$$

$$Q_{lk} = -V_l^2 B_{kl} + V_l V_l G_{kl} \sin(\theta_k - \theta_l) + V_k V_l B_{kl} \cos(\theta_k - \theta_l) \quad (2.4)$$

where P_{kl}, Q_{kl} are the active, reactive power flows of transmission line between k^{th} bus and l^{th} bus, respectively; V_k, θ_k and V_l, θ_l are voltage magnitudes, voltage phase angles corresponding to k^{th} bus and l^{th} bus, respectively; G_{kl}, B_{kl} are the conductance, susceptance of transmission line between k^{th} bus and l^{th} bus, respectively.

The transmission line conductance and susceptance are given by Eqs. (2.5) and (2.6).

$$G_{kl} = \frac{R_{kl}}{R_{kl}^2 + (X_{kl} - X_C)^2} \quad (2.5)$$

$$B_{kl} = \frac{X_{kl} - X_C}{R_{kl}^2 + (X_{kl} - X_C)^2} \quad (2.6)$$

where X_{kl} and R_{kl} are the reactance and resistance of transmission line between k^{th} bus and l^{th} bus, respectively; X_C is the TCSC reactance located at the transmission line that connects k^{th} bus and l^{th} bus, respectively.

The limits for the TCSC reactance are defined as under:

$$X_{Cl}^{\min} \le X_{Cl} \le X_{Cl}^{\max} \ (l = 1,2,..., N_{TCSC}) \quad (2.7)$$

where $X_{Cl}^{\min}$ and $X_{Cl}^{\max}$ represent the minimum and maximum reactance correspond to l^{th} TCSC, respectively; N_{TCSC} is the total number of TCSC devices connected in the system.

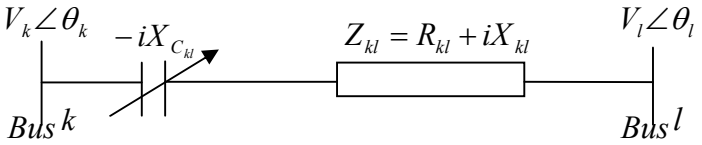

Figure 2.1: TCSC circuit model

Modeling of TCPS

TCPS is represented as a phase controlling transformer having control parameter ϕ. Figure 2.2 shows the TCPS circuit model of the network. The line flow equations for the transmission line are given as follows [24].

$$P_{kl} = \frac{V_k^2 G_{kl}}{\cos^2 \phi} - \frac{V_k V_l}{\cos \phi} [G_{kl} \cos(\theta_k - \theta_l + \phi) + B_{kl} \sin(\theta_k - \theta_l + \phi)] \quad (2.8)$$

$$Q_{kl} = -\frac{V_k^2 B_{kl}}{\cos^2\phi} - \frac{V_k V_l}{\cos\phi}\left[G_{kl}\sin(\theta_k - \theta_l + \phi) - B_{kl}\cos(\theta_k - \theta_l + \phi)\right] \quad (2.9)$$

$$P_{lk} = V_l^2 G_{kl} - \frac{V_k V_l}{\cos\phi}\left[G_{kl}\cos(\theta_k - \theta_l + \phi) - B_{kl}\sin(\theta_k - \theta_l + \phi)\right] \quad (2.10)$$

$$Q_{lk} = -V_l^2 B_{kl} + \frac{V_k V_l}{\cos\phi}\left[G_{kl}\sin(\theta_k - \theta_l + \phi) + B_{kl}\cos(\theta_k - \theta_l + \phi)\right] \quad (2.11)$$

Figure 2.3 illustrates the TCPS power injected model. The TCPS supplies active and reactive powers at bus *k* and bus *l* as under:

$$P_{ks} = -G_{kl}V_k^2\tan^2\phi - V_k V_l\tan\phi\left[G_{kl}\sin(\theta_k - \theta_l) - B_{kl}\cos(\theta_k - \theta_l)\right] \quad (2.12)$$

$$Q_{ks} = B_{kl}V_k^2\tan^2\phi + V_k V_l\tan\phi\left[G_{kl}\cos(\theta_k - \theta_l) + B_{kl}\sin(\theta_k - \theta_l)\right] \quad (2.13)$$

$$P_{ls} = -V_k V_l\tan\phi\left[G_{kl}\sin(\theta_k - \theta_l) + B_{kl}\cos(\theta_k - \theta_l)\right] \quad (2.14)$$

$$Q_{ls} = -V_k V_l\tan\phi\left[G_{kl}\cos(\theta_k - \theta_l) - B_{kl}\sin(\theta_k - \theta_l)\right] \quad (2.15)$$

The Phase shift contribution from the TCPS should lie within limits as under:

$$\phi_{Tn}^{\min} \le \phi_{Tn} \le \phi_{Tn}^{\max} \ (n = 1,2,...,N_{TCPS}) \quad (2.16)$$

where $\phi_{Tn}^{\min}$ and $\phi_{Tn}^{\max}$ represent the minimum and maximum phase angle shift of n^{th} TCPS, respectively.

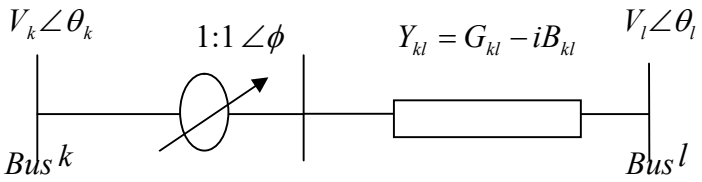

Figure 2.2: TCPS Circuit model

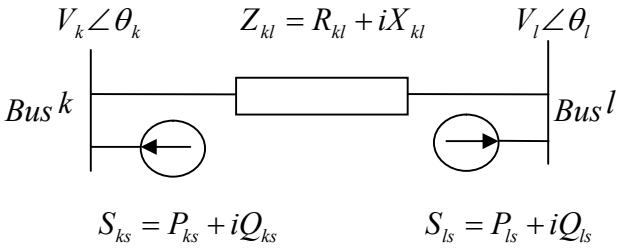

Figure 2.3: TCPS Power injected model

2.3 OPTIMAL POWER FLOW PROBLEM WITH FACTS DEVICES

The main aim of the OPF problem is to optimize various objectives *i.e.*, fuel cost of thermal

generators, emission pollutant and active power losses, sequentially, while satisfying all the constraints. It is a non-linear constrained optimization problem. In power system network, there are four types of buses *i.e.*, slack bus, load bus, generator bus and voltage-controlled bus. Each bus is characterized by four variables *i.e.*, voltage magnitude, voltage angle, real power and reactive power, from which two are specified and the other two need to be found. The variables are specified depending on what kind of devices is connected to that bus. The specified variables are considered as independent variables and unspecified variables are considered as dependent variables. The specified variables for the slack bus are voltage magnitude and voltage angle. The real and reactive powers, real power and voltage magnitude are the specified variables for load bus, generator bus, respectively. The specified variables for voltage-controlled buses are real power, reactive power and voltage magnitude. The active power output of generators except slack bus, voltages of generators, transformers tap settings and reactive powers injected by shunt *volt ampere reactive* (VAR) compensators are independent variables or decision variables. The OPF problem consists of dependent variables *i.e.*, generator active power output at slack bus, load bus voltages, reactive power outputs of generators and line flows of the system. The transformer tap settings and shunt VAR compensators are discrete type of decision variables.

2.3.1 Objective Functions

The mathematical model of each objective function is presented as under:

***Total fuel cost*:** The total fuel cost of the thermal generators with valve point loading effect is represented as [24]:

$$F_C = \sum_{m=1}^{NG} a_m + b_m P_{Gm} + c_m P_{Gm}^2 + \left| d_m \sin\left(e_m \left(P_{Gm}^{\min} - P_{Gm}\right)\right)\right| \tag{2.17}$$

where a_m, b_m, c_m, d_m and e_m represent the coefficients of the fuel cost for the m^{th} generating unit; P_{Gm} represents the active power output of the m^{th} generating unit; and *NG* denotes the total number of thermal generating units.

***Emission pollutant*:** Thermal generators have a major share in environmental emission pollution. The total pollutant emission released by thermal generators is represented as [24]:

$$E = \sum_{m=1}^{NG} \left(\alpha_m + \beta_m P_{Gm} + \gamma_m P_{Gm}^2 + \eta_m \exp\left(\lambda_m P_{Gm}\right)\right) \tag{2.18}$$

where $\alpha_m, \beta_m, \gamma_m, \eta_m$ and λ_m represent the coefficients of emission for the m^{th} generating unit.

***Active power loss*:** The total active power losses of transmission lines are expressed as follows [24]:

$$P_{LOSS} = \sum_{j=1}^{NL} G_j \left[V_k^2 + V_l^2 - 2|V_k||V_l|\cos(\theta_k - \theta_l) \right] \tag{2.19}$$

where G_j represents the conductance of j^{th} transmission line connecting k^{th} bus with l^{th} bus; V_k, V_l and θ_k, θ_l represent the voltage magnitudes and phase angles for buses k and l, respectively; *NL* represents the total number of transmission lines.

2.3.2 System Constraints

The system must satisfy the various system constraints that are listed as under [24]:

***Equality constraints*:** The following load flow equations represent the active and reactive power equality constraints:

$$\sum_{k=1}^{N_{BUS}} (P_{Gk} - P_{Lk}) + \sum_{k=1}^{N_{TCPS}} P_{ks} = \sum_{k=1}^{N_{BUS}} \sum_{l=1}^{N_{BUS}} |V_k||V_l||Y_{kl}|\cos(\delta_{kl} + \theta_k - \theta_l) \tag{2.20}$$

$$\sum_{k=1}^{N_{BUS}} (Q_{Gk} - Q_{Lk}) + \sum_{k=1}^{N_{TCPS}} Q_{ks} = -\sum_{k=1}^{N_{BUS}} \sum_{l=1}^{N_{BUS}} |V_k||V_l||Y_{kl}|\sin(\delta_{kl} + \theta_k - \theta_l) \tag{2.21}$$

where P_{Gk}, Q_{Gk} represent the active and reactive power generation available at the k^{th} bus, respectively; P_{Lk}, Q_{Lk} are the active and reactive power demand at the k^{th} bus, respectively; P_{ks}, Q_{ks} are the active and reactive powers injected by TCPS at the k^{th} bus, respectively; Y_{kl} and δ_{kl} represent the total admittance and admittance angle of the transmission line, which connect the k^{th} and l^{th} bus; N_{BUS}, N_{TCPS} are the total number of buses and TCPS devices, respectively.

***Inequality constraints*:** The OPF problem is subjected to various inequality constraints, which are given as:

(i) Generator constraints: The active and reactive power generation for each generator should be within specified limits and are given as:

$$P_{Gm}^{\min} \le P_{Gm} \le P_{Gm}^{\max} \quad (m = 1,2,...,NG) \tag{2.22}$$

$$Q_{Gm}^{\min} \le Q_{Gm} \le Q_{Gm}^{\max} \quad (m = 1,2,...,NG) \tag{2.23}$$

$$V_{Gm}^{\min} \le V_{Gm} \le V_{Gm}^{\max} \quad (m = 1,2,...,NG) \tag{2.24}$$

where $P_{Gm}^{\min}$ and $P_{Gm}^{\max}$ represent the minimum and maximum active power limits for the m^{th} generating unit, respectively; $Q_{Gm}^{\min}$ and $Q_{Gm}^{\max}$ are the minimum and maximum reactive power limits of the m^{th} generating unit, respectively.

(ii) Load Bus voltage constraint: The load bus voltage magnitude should lie in the bounds and is stated as:

$$V_{Lk}^{\min} \le V_{Lk} \le V_{Lk}^{\max} \ (k = 1,2,..., N_{PQ}) \tag{2.25}$$

where N_{PQ} represents the total number of load buses; $V_{Lk}^{\min}$ and $V_{Lk}^{\max}$ denote the minimum and maximum limits for the k^{th} load bus voltage, respectively.

(iii) Transformer tap ratio: The transformer tap ratio should be within specified limits and is represented as:

$$t_p^{\min} \le t_p \le t_p^{\max} \ (p = 1,2,..., NT) \tag{2.26}$$

where *NT* represents the total number of tap changing transformers; $t_p^{\min}$ and $t_p^{\max}$ denote the minimum and maximum tap setting limits of the p^{th} transformer, respectively.

(iv) Shunt VAR compensator constraints: The VAR compensation contribution from the shunt compensator is bounded as per the following limits:

$$Q_q^{\min} \le Q_q \le Q_q^{\max} \ (q = 1,2,..., NC) \tag{2.27}$$

where *NC* represents the total number of shunt compensators; $Q_q^{\min}$ and $Q_q^{\max}$ represent the minimum and maximum VAR limits injected by the q^{th} shunt compensator, respectively.

(v) Transmission lines loading: The line flow corresponding to each transmission line is restricted as per its maximum line capacity and is represented as under:

$$S_{Lj} \le S_{Lj}^{\max} \ (j = 1,2,..., NL) \tag{2.28}$$

where S_{Lj} and $S_{Lj}^{\max}$ represent the actual and maximum apparent power flow of the j^{th} branch, respectively.

2.3.3 Fitness Function Formulation

The load flow solution method "*Newton Raphson* (NR)" takes care of equality constraints, which are given by Eqs. (2.20) and (2.21). This method is executed for obtaining the values of the slack active power, voltage magnitudes of load buses, reactive powers generated by all thermal generator units and line flows of the system. The fitness function is formulated with the inclusion of the penalty term for penalizing the inequality constraint violation. The fitness function is given as:

$$f = of_i + p_1\left(P_{G,slack} - P_{G,slack}^{\lim}\right)^2 + \sum_{k=1}^{N_{PQ}} p_2 (V_{Lk} - V_{Lk}^{\lim})^2 + \sum_{m=1}^{NG} p_3 (Q_{Gm} - Q_{Gm}^{\lim})^2 + \sum_{j=1}^{NL} p_4 \left(|S_{Lj}| - S_{Lj}^{\max}\right)^2 \ (i = 1,2,..., N_{obj}) \tag{2.29}$$

The model equation of the slack bus active power is given as [22]:

$$P_{G,slack} = \sum_{i=1}^{N_{PV}} P_{Gi} - \left(P_D + P_L\right) \tag{2.30}$$

In Eq. (2.29), f represents the fitness function; of_i represents objective function at i^{th} objective; $P_{G,slack}$ is slack bus active power generation; N_{obj} is the number of objectives; p_1, p_2, $p_3$and p_4 are the penalty function parameters corresponding to slack bus active power generation, voltage magnitude at load buses, reactive power generation and apparent line flow limit violations respectively; N_{PV} represents the voltage-controlled buses; P_D is the system power demand; and P_L is the transmission losses.

2.4 INVASIVE WEED OPTIMIZATION TECHNIQUE

The IWO algorithm is the colonization phenomenon of invasive weeds in nature [105]. The weeds spread into the cropping system and take up prospective spaces along the crops. The flowering weeds fitness value decides the count of new weed production. The weeds having a better environmental adoption and captivating on unutilized resources exhibit better growth and lead to further production of seeds. The number of seeds produced by each weed is derived by considering best and worst fitness values and is given as:

$$N_{SEED} = \frac{f - f_{worst}}{f_{best} - f_{worst}}\left(seed_{\max} - seed_{\min}\right) + seed_{\min} \tag{2.31}$$

where f represents the weed fitness; f_{worst} and f_{best} are the worst and best fitness in the present population, respectively; $seed^{\max}$ and $seed^{\min}$ are the maximum and minimum number of seeds, respectively.

The seeds produced from the parent weed normally spread around the parent weed and having zero mean and dynamic *standard deviation* (SD). The SD decreases from the initial value to the final value with the iteration, which helps to move from exploration to exploitation phase, and is given as:

$$\sigma_{cur} = \frac{(IT^{\max} - IT)^{N_m}}{(IT^{\max})^{N_m}}\left(\sigma^{init} - \sigma^{final}\right) + \sigma^{final} \tag{2.32}$$

where $IT^{\max}$ represents the maximum number of iterations; σ_{cur} denotes the SD of the present iteration; σ^{init} and σ^{final} represent the initial and final value of SD, respectively; N^m represents the modulation index.

Each weed acquires the unutilized resources from the cropping field and transforms it into the flowering weed and further, new weeds are produced out of it. This process continues

till the population number of seeds and weeds in the colony reaches to the maximum size of the population. Consequently, the collective arrangement of the seeds along with their parent weeds is carried out to select the best population-based on fitness evaluation. This aggressive competition among the weeds leads them to develop well-adapted and superior weeds over time.

2.5 POWELL'S PATTERN SEARCH METHOD

Powell's pattern search method is the conjugate based direct search method. It can be applied for non-differential and discontinuous optimization problems. In the PPS method, the search is performed by direct and pattern search [150]. The initial move is performed by exploiting the direct search direction for each decision variable and decision variables are updated as follows:

$$x_k = x_k + \mu_k^* S_k^j \ \left(k = 1,2,...,D\right) \tag{2.33}$$

$$S_k^j = \begin{cases} 1; \ k = j \\ 0; \ k \neq j \end{cases} \left(k = 1,2,...,D; j = 1,2,...,D\right) \tag{2.34}$$

where x_k represents the k^{th} decision variable; μ_k^* represents the step size of the PPS method; S_k^j is the search direction; D represents the number of decision variables.

After the execution of the direct search for all the decision variables, the search is directed towards the pattern search direction. The pattern search direction is obtained by computing the discrepancy between updated positions and corresponding previous positions and one of the direct search directions is replaced by the corresponding pattern search direction. This process continues till all the direct search directions are discarded.

2.6 PROPOSED OPTIMIZATION TECHNIQUE

The proposed integrated optimization technique integrates the IWO technique and PPS method. The IWO technique is used for exploration purpose and the PPS method is applied to exploit the promising search area. The best value obtained from the IWO technique is further improved by applying the PPS method, which avoids any stagnation of the solution to the local best solution and also improves the convergence characteristics. The algorithm of the proposed optimization technique is given as:

Algorithm 1: Proposed Optimization Technique

Step 1: Read the algorithm parameters and decision variables bounds.

Step 2: Generate random values for each weed within the decision variable bounds.

Step 3: Evaluate the fitness function value as Eq. (2.29).

Step 4: Asses the number of seeds produced out of each weed pertaining to the best and worst fitness function value as per Eq. (2.31).

Step 5: Disperse the produced seeds over the search area by normally distributed random numbers having zero mean value and varying SD as per Eq. (2.32).

Step 6: Compute the fitness function value and sort the population of seed and weed based on the fitness function value.

Step 7: The best performing weed is selected based on fitness function evaluation.

Step 8: If the solution does not converge to the set number of iterations (k=10), then apply the PPS method using Eq. (2.33) for further improvement of the best solution obtained by the IWO technique thus far.

Step 9: The maximum *number of fitness evaluations* (NFE) is set to terminate the iterative procedure, if the termination criteria satisfy, then go to step 10.

Else continue with step 3

Step 10: Optimum solution is obtained.

2.7 IMPLEMENTATION OF PROPOSED OPTIMIZATION TECHNIQUE

The decision variables for the OPF problem include active power generation of all the units except slack bus active power, the voltage magnitude of generators, tap changing transformer ratios, the number of shunt devices, and reactance and phase shifts of FACTS devices. The tap position transformer ratios and the number of shunt devices are discrete variables and the remaining are continuous decision variables. The tap position of the transformer determines the tap ratio and shunt outputs are decided by the number of switched shunts.

The [X] represents the array of decision variables as under:

$$X=\begin{matrix} P_{1,1} & \cdots & P_{1,N_{PV}}, V_{1,1} & \cdots & V_{1,NG}, t_{1,1} & \cdots & t_{1,NT}, Q_{1,1} & \cdots & Q_{1,NC}, X_{1,1} & \cdots & X_{1,N_{TCSC}}, \phi_{1,1} & \cdots & \phi_{1,N_{TCPS}} \\ \vdots & \vdots & \vdots & \vdots & \vdots & \vdots & \vdots & \vdots & \vdots & \vdots & \vdots & \vdots & \vdots \\ P_{G,1} & \cdots & P_{G,N_{PV}}, V_{G,1} & \cdots & V_{G,NG}, t_{p,1} & \cdots & t_{p,NT}, Q_{q,1} & \cdots & Q_{q,NC}, X_{C,1} & \cdots & X_{C,N_{TCSC}}, \phi_{T,1} & \cdots & \phi_{T,N_{TCPS}} \end{matrix} \tag{2.35}$$

where t_p denotes the tap position number; Q_q denotes the number of switched shunt devices.

The implementation of an integrated IWO-PPS optimization technique for the solution of the OPF problem is described in the following steps:

Step 1: *Initialization*: The initial values of continuous decision variables are randomly

generated within specified limits and given as:

$$X_{i,k} = X_k^{\min} + ran[0,1] \times \left(X_k^{\max} - X_k^{\min} \right) (i = 1,2,...,N_P; k = 1,2,...,D) \tag{2.36}$$

For discrete decision variables, initialization is performed by using Eq. (2.36) and then it is rounded off to the nearest integer as under

$$X_{i,k} = \begin{cases} INT(X_{i,k} + 0.5); & x_{i,k} > 0 \\ INT(X_{i,k} - 0.5); & else \end{cases} \tag{2.37}$$

Step 2: *Fitness function Evaluation:* After initialization, the NR method is applied to solve the OPF problem and the fitness function value is computed as per Eq. (2.29).

Step 3: *Reproduction and Dispersion of Seed*: Each weed produces the number of seeds based on the best and worst fitness function value as per Eq. (2.31) and those are dispersed as given by Eq. (2.32).

Step 4: If IWO does not converge up to a certain level of expected result for the set iterations, then the PPS method is applied. The NR method is applied to the solution upgraded by the PPS method to compute the fitness function value.

Step 5: *Selection of population*: The selection of population for the next cycle is done by the collective arrangement of the seeds along with parent weeds based on the fitness function value.

Step 6: If a termination criterion is not met, continue with step 2.

Step 7: The decision variables of the global best solution represent the final solution.

The Figure 2.4 illustrates the implementation of the proposed IWO-PPS technique to solve the OPF problem.

2.8 TEST SYSTEMS AND RESULTS

The integrated IWO-PPS optimization technique has been applied to solve four test systems of the OPF problem. The test system-I and test system-II are the standard IEEE 30-bus and IEEE 57-bus systems without FACTS devices. The test system-III and IV are modified IEEE 30-bus and modified IEEE 57-bus systems, including FACT devices. The IWO-PPS technique has been applied to solve three cases of the OPF problem, sequentially *i.e.*, minimum fuel cost (case-I), pollutant emission (case-II), active power loss (case-III).

Test system-I

The test system-I includes 6-generating units, 4-tap changing transformers and 2-shunt capacitors with 41 transmission lines [196]. The total active power demand of the system is 2.834p.u. at 100MVA base. The constraint limit for voltage of all buses is considered to be

0.95p.u.-1.1p.u. For all the tap-controlled transformers, the tap setting limit is considered to be 0.9p.u.-1.1p.u., with a step change of 0.01. The compensation capacitor banks range is considered to be 0 to 30MVAr with the discrete steps of 1MVAr.

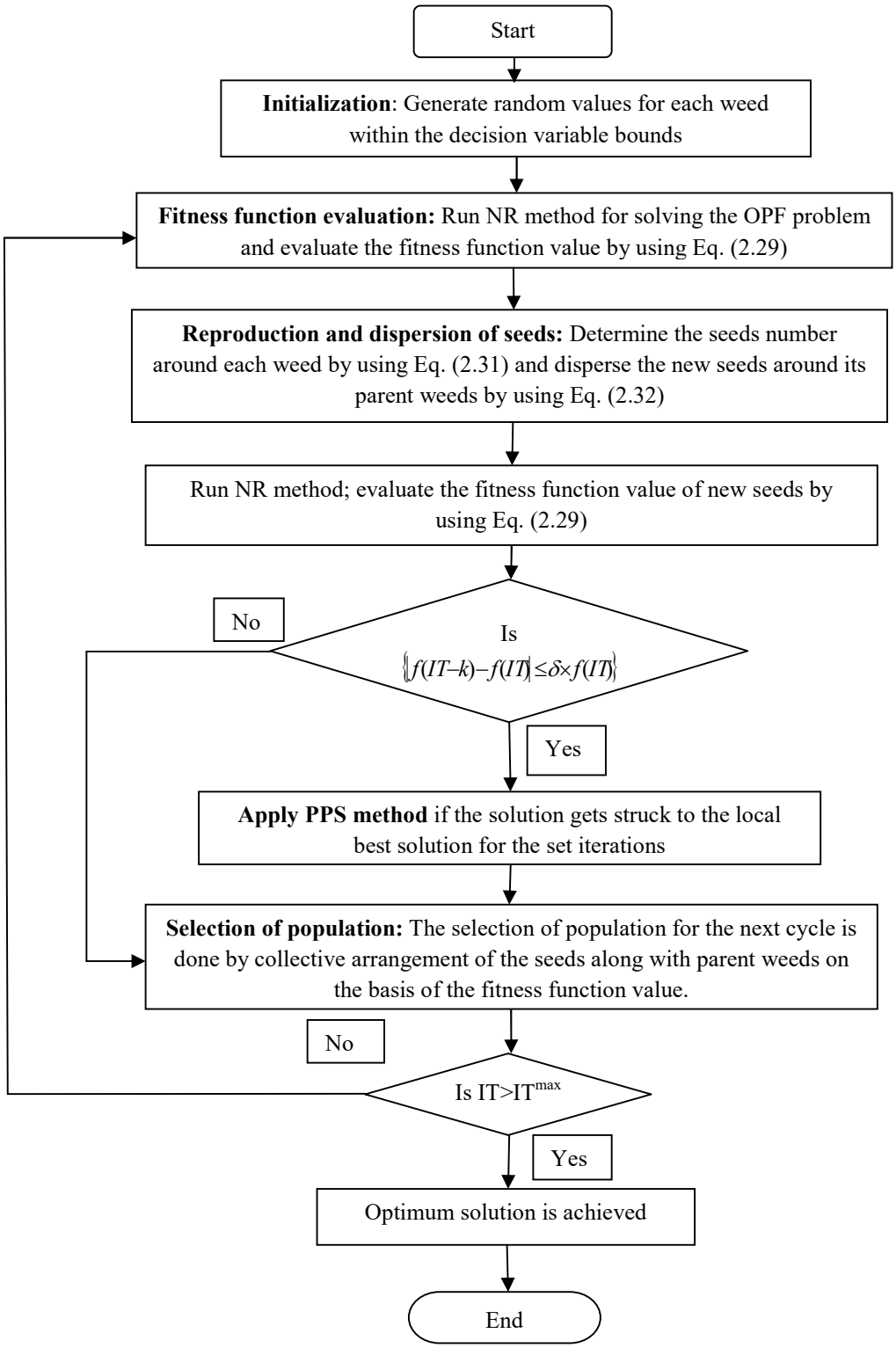

Figure 2.4: Flow chart of the implementation of proposed IWO-PPS technique

The single-line diagram of test system-I is shown in Figure A.1.1 under Appendix-A. The generating limits of thermal units, operating cost and emission coefficients of thermal units, load and transmission lines data are given in Tables A.1.1, A.1.2, A.1.3 and A.1.4, respectively, under Appendix-A.

Test system-II

In this test system, 7-generating units and 3-shunt capacitors with 80 transmission lines have been undertaken. The total active power demand is 12.508p.u. at 100MVA base. The compensation capacitor banks range is considered to be 0 to 30MVAr with the discrete steps of 1MVAr. The constraint limit for the voltage of all the buses is considered to be 0.94 p.u.-1.06 p.u. for the fuel cost objective [33]. The constraint limit for generator bus voltages and load bus voltages is considered to be 0.94p.u.-1.06p.u. and 0.95p.u.-1.1p.u., respectively, for the objectives pollutant emission and active power losses [106]. The single-line diagram of test system-II is shown in Figure A.1.2 under Appendix-A. The thermal generating units, load and transmission lines data are given in Tables A.1.5, A.1.6 and A.1.7, respectively, under Appendix-A.

Test system-III

The test system-III consists of 6-generating units and 24-load buses interconnected with 41-transmission lines [24,121]. The four line branches have transformers with a tap changer facility and nine line branches are equipped with shunt capacitors. The total demand of the system is 2.834p.u. at 100MVA base. The voltage range of all buses is considered to be 0.95p.u.-1.1p.u. Two branches are equipped with TCSCs and two branches are having TCPSs. The generating limits of thermal units, load data, transmission lines data and generator cost and emission coefficient are given in Tables A.1.1, A.1.3, A.1.4 and A.1.8, respectively, under Appendix-A.

Test system-IV

The test system-IV consists of 7-generating units, including 50-load busses, interconnected with 80-transmission line branches. Seventeen transformers are equipped with the load tap settings and three shunt capacitors are installed [24,121]. The active power demand of the system is 12.508p.u. at 100 MVA base. The constraint limitation for a voltage of generator buses and load buses are considered to be 0.95p.u.-1.1p.u. and 0.93p.u.-1.1p.u., respectively. Five line branches are equipped with TCSCs and five line branches are having TCPSs. The load, transmission lines and the generating units data are given in Tables A.1.6, A.1.7 and A.1.9, respectively, under Appendix-A.

2.8.1 Parameter Tuning

For any global search technique, algorithm parameters affect the quality of solution and convergence characteristics. In the IWO-PPS technique, the algorithm parameters *i.e.*, initial SD, final SD, modulation index and step size of the PPS method need to be adjusted. A high preliminary SD and low final SD are preferred to preserve the composure between exploration and exploitation capability. It has been revealed that the performance of the IWO technique is greatly influenced by the value of the nonlinear modulation index [105]. The step size of the PPS method affects the exploitation capability of the algorithm. The number of trials has been given with different parameters to set the best parameter values. The suitable values of algorithm parameters are given in Table 2.1.The sensitivity analysis has been confirmed by perturbed parameters around the original parameter values for the test system-I for finding the minimum value of cost (case-1). The best, average and the worst value of objective function is achieved by giving thirty one trial runs. The perturbation (Δ) is ±20% of the suitable parameter. The effect of the parameters' perturbations is given in Table 2.2.

Table 2.1: Suitable values of algorithm parameters

Parameter	**Values**
Initial size of population	20
Max. number of seeds	4
Min. number of seeds	0
Initial SD	10-20
Final SD	1
Modulation index	4-5
Step Size (PPS)	0.01
k	10
δ	0.01

Table 2.2: Achieved result considering perturbing parameter for minimization of fuel cost (Test system-I)

Parameter	Down (suitable parameter-Δ)			UP (suitable parameter+Δ)		
	Best	Average	Worst	Best	Average	Worst
Initial size of population	805.15 (0.528%)	806.86 (0.742%)	807.67 (0.843%)	807.45 (0.815%)	808.85 (0.990%)	809.63 (1.087%)
Max. number of seeds	804.25 (0.415%)	806.01 (0.635%)	807.14 (0.777%)	808.62 (0.961%)	809.76 (1.104%)	810.56 (1.203%)
Min. number of seeds	806.89 (0.745%)	807.83 (0.863%)	808.56 (0.953%)	802.65 (0.216%)	803.39 (0.308%)	803.79 (0.358%)
Initial SD	805.34 (0.551%)	806.79 (0.733%)	807.83 (0.863%)	804.61 (0.461%)	804.97 (0.506%)	805.21 (0.536%)
Final SD	802.56 (0.205%)	806.29 (0.670%)	806.78 (0.732%)	801.92 (0.125%)	802.49 (0.196%)	802.99 (0.258%)
Modulation index	806.67 (0.718%)	807.95 (0.878%)	809.45 (1.065%)	804.55 (0.453%)	805.72 (0.599%)	806.68 (0.719%)
Step Size (PPS)	801.98 (0.132%)	802.99 (0.258%)	803.62 (0.337%)	803.78 (0.357%)	804.68 (0.469%)	805.23 (0.538%)
k	802.04 (0.139%)	802.87 (0.243%)	803.56 (0.329%)	801.76 (0.105%)	802.09 (0.146%)	802.95 (0.253%)
δ	804.65 (0.465%)	804.98 (0.507%)	805.43 (0.563%)	803.76 (0.354%)	804.34 (0.427%)	805.12 (0.524%)

2.8.2 Test System-I

The best, average, and worst results and the SD of results for 31 trial runs are compared with established techniques and are represented in Table2.3. It is evident from Table 2.3 that the minimum fuel cost obtained from the IWO-PPS technique outperforms the results reported for TS/SA [135], PSO [133], IPSO [133], AGSO [43], PSO-APO [189] and MICA-TLA [60] techniques.

In order to investigate the impact of the PPS method of integrated IWO-PPS optimization technique, results are also compared with the IWO technique. The minimum fuel cost (case-I) obtained by the IWO-PPS technique is at least 0.016% less than the other published results. The average fuel cost obtained by the IWO-PPS technique is less than the cost obtained by MICA-TLA [60] and IWO techniques. However, the worst fuel cost and SD of the results reported for the MICA-TLA technique are better than the IWO-PPS technique. The scarcity of fossil fuels and rise in fuel prices poses financial constraints to the system operators. The fuel cost optimization increases the efficiency of the system and hence makes the system economically more viable.

Table 2.3: Comparison of results: Test system-I

Algorithms/ indexes	Best	Worst	Average	SD	Average NFE
Test system-I					
Case-I: Fuel cost($/hr)					
TS/SA [135]	804.784	-	-	-	-
PSO [133]	802.205	-	-	-	-
IPSO [133]	801.98	-	-	-	-
AGSO [43]	801.75	-	-	-	-
PSO-APO [189]	801.708	-	-	-	-
MICA-TLA [60]	801.048	801.0493	801.049	0.0006	-
IWO	807.47	813.554	809.24	1.6624	48000
IWO-PPS	800.92	801.106	801.024	0.0457	48000
Case-II: Pollutant emission(ton/hr)					
PSO [133]	0.2063	-	-	-	-
IPSO [133]	0.206	-	-	-	-
AGSO [43]	0.2059	-	-	-	-
IWO	0.20558	0.205632	0.2056	0.0000133	48000
IWO-PPS	0.205203	0.20528	0.20522	0.0000132	48000
Case-III: Active power loss (MW)					
PSO [198]	5.092	-	-	-	-
DE [196]	5.011	-	-	-	-
ICA [59]	4.944	5.118	4.9735	0.08428	-
MICA-IWO [59]	4.917	4.9202	4.9197	0.0008725	-
IWO	4.988	5.126	5.0042	0.0278	48000
IWO-PPS	3.732	3.863	3.845	0.0214	48000

TS/SA: Hybrid Tabu search and simulated annealing; PSO: Particle swarm optimization; IPSO: Improved particle swarm optimization; AGSO: Adaptive group search optimization; PSO-APO: Hybrid particle swarm optimization-artificial physics optimization; MICA-TLA: Modified imperialist competitive algorithm and teaching-learning algorithm; DE: Differential optimization; ICA: Imperialist competitive algorithm; MICA-IWO: Modified imperialist competitive algorithm-invasive weed optimization

For case-II, the minimum pollutant emission obtained by the IWO-PPS technique is 0.2052 ton/hr, which is less as compared to the results reported for PSO [133], IPSO [133], AGSO [43] and IWO techniques. The average and worst pollutant emission values and SD of the results obtained by the IWO-PPS technique are less than the results obtained by the IWO technique, which validates the exploitation capability of the PPS method. The increasing environmental concerns are causing new standards of emission reduction. The optimization of pollutant emission enables the system operator to cope with the present-day environmental standards of pollutant emission. For loss minimization, the results obtained from the IWO-PPS technique have been compared with the results of other state-of-art techniques, *i.e.*, PSO[198], DE[196], ICA[59], MICA-IWO [59].The minimum active power loss obtained by the IWO-PPS technique is 3.732MW, which is less as compared to the best result reported in the literature, *i.e.*, MICA-IWO technique [59].The average and worst active power loss obtained from the IWO-PPS technique is less as compared to active power loss attained by ICA [59], MICA-IWO [59] and IWO techniques. The optimum values of decision variables obtained from the IWO technique and IWO-PPS technique for all the cases are represented in Table 2.4. The optimization of transmission line losses increases the transmission capacity of the existing network and hence reduces the cost portion of system extension. It also reduces the energy cost and hence makes the system more economically viable.

Table 2.4: Optimal value of decision variables: Test system-I

Decision variables	**Limits**		**Case-I Fuel cost ($/hr)**		**Case-II Pollutant emission (ton/hr)**		**Case-III Active power loss (MW)**	
	min	max	IWO	IWO-PPS	IWO	IWO-PPS	IWO	IWO-PPS
P_{G1} *(MW)*	50	200	170.996	165.62	62.502	61.206	98.389	62.912
P_{G2} *(MW)*	20	80	50.822	50.82	71.383	71.383	80.00	79.664
P_{G5} *(MW)*	15	50	23.707	21.215	50.00	50.00	50.00	44.383
P_{G8} *(MW)*	10	35	17.127	30.081	35.00	35.00	20.00	35.00
P_{G11}*(MW)*	10	30	12.6	11.674	30.00	30.00	20.00	30.00
P_{G13}*(MW)*	12	40	18.226	12	40.00	40.00	20.00	35.193
V_{G1} *(p.u.)*	0.95	1.1	1.066726	1.1	1.096134	1.096134	1.1	1.0975
V_{G2} *(p.u.)*	0.95	1.1	1.027057	1.08963	1.078458	1.088458	1.09	1.0965
V_{G5} *(p.u.)*	0.95	1.1	0.987316	1.06467	1.1	1.1	1.08257	1.09501
V_{G8} *(p.u.)*	0.95	1.1	0.992765	1.07385	1.1	1.1	1.077885	1.095
V_{G11}*(p.u.)*	0.95	1.1	0.969506	1.1	1.1	1.0981	1.055645	1.07301
V_{G13}*(p.u.)*	0.95	1.1	0.983353	1.1	1.1	1.0892	1.07205	1.0956
Q_{10}*(MVAr)*	0	30	26	26	23	23	13	10
Q_{24}*(MVAr)*	0	30	10	10	30	30	18	05
t_{11}	0.9	1.1	0.93	0.93	1.1	1.1	1.04	1.1
t_{12}	0.9	1.1	1.03	1.03	1.1	1.1	0.92	1.1
t_{15}	0.9	1.1	1.03	1.01	1.08	1.08	1.0	1.07
t_{36}	0.9	1.1	1.06	0.96	1.1	1.1	1.08	1.06
Cost ($/hr)	-	-	**807.474**	**800.92**	956.463	953.268	1042.17	931.556
Emission (ton/hr)	-	-	0.3481	0.33744	**0.20558**	**0.20521**	0.23271	0.21062
P_{LOSS} *(MW)*	-	-	10.078	8.017	5.487	4.189	**4.989**	**3.732**

Note: Highlighted text represents the best results.

2.8.3 Test System-II

The best, average, and worst results along with the SD values obtained by the IWO-PPS technique with 31 trial runs, are presented in Table 2.5 and are compared with published results. In test system-II, case-I either shunt capacitor or *load tap changers* (LTCs) has been considered in the system. It is evident from Table 2.5 that for case-I (with shunt capacitor), the minimum fuel cost obtained by the IWO-PPS technique is 0.035% and 0.086% less than the fuel cost obtained by the *cross-entropy* (CE) method [33] and IWO technique, respectively. Further, it is observed that the IWO-PPS technique is able to produce better results in terms of the best, worst and SD as compared to its counterpart. For case-I with LTCs, it is evident from Table 2.5 that the results obtained by IWO-PPS technique are superior as compared with the results of the binomial distribution [33], Gaussian distribution [33] and IWO technique. The IWO-PPS technique is able to search the better results in terms of the best, worst, and average cost and SD. Further, a comparison of NFE is done and it is found that the mean NFE required by the IWO-PPS technique is 48000, which is less as compared to NFE required by CE, binomial and Gaussian distribution methods.

Table 2.5: Comparison of results: Test system-II

Algorithms/ indexes	Best	Worst	Average	SD	Average NFE
Test system-II					
Case-I: Fuel cost($/hr) with shunt capacitor optimization					
CE [33]	41848.78	41850.63	41849.38	0.58	50000
IWO	41869.37	41998.7	41927.23	37.224	48000
IWO-PPS	41833.95	41835.98	41835.01	0.57	48000
Case-I: Fuel cost($/hr) with LTCs					
Binomial [33]	41786.01	41834.18	41804.02	12.01	50000
Gaussian [33]	41772.26	41796.72	41781.69	6.72	50000
IWO	41804.87	41898.35	41836.59	29.065	48000
IWO-PPS	41768.49	41787.22	41771.86	5.485	48000
Case-II: Pollutant emission(ton/hr)					
GSO [43]	0.8358	-	-	-	-
AGSO [43]	0.8222	-	-	-	-
IWO	0.8355	0.9050	0.85548	0.01995	48000
IWO-PPS	0.7980	0.8196	0.8048	0.00614	48000
Case-III: Active power loss (MW)					
SOA [35]	24.265	-	-	-	-
GWO [181]	24.752	-	-	-	-
ICA [59]	24.479	25.548	25.387	0.80561	-
MICA-IWO [59]	24.257	24.284	24.276	0.023361	-
MFO [106]	24.253	-	-	-	-
IWO	24.49	25.813	24.753	0.32246	48000
IWO-PPS	24.19	24.27	24.202	0.0147	48000

Note: CE: Cross entropy; GSO: Group search optimization; AGSO: Adaptive group search optimization; SOA: Seeker optimization algorithm; GWO: Grey wolf optimizer; ICA: Imperialist competitive algorithm; MICA-IWO: Modified imperialist competitive algorithm-invasive weed optimization; MFO: Moth flame optimization

For case-II, the minimum pollutant emission obtained by the IWO-PPS technique is

0.798ton/hr, which is less than the results reported for GSO [43], AGSO [43] and IWO techniques. The average and worst emission values and SD of the results obtained by the IWO-PPS technique are less than the results obtained by the IWO technique. For case-III, the minimum, average and the worst active power loss obtained by the IWO-PPS technique is less than the results reported for various other state-of-art techniques *i.e.*, SOA [35], GWO [181], ICA [59], MICA-IWO [59], MFO [106], IWO techniques. The SD index authenticates that the IWO-PPS technique is able to search the high quality solution repeatedly. The optimum values of decision variables obtained by the IWO-PPS technique and IWO technique are given in Tables 2.6 and 2.7 for case-I and in Tables 2.8 and 2.9 for case-II and III, respectively.

Table 2.6: Optimal value of decision variables: Test system-II, case-I (with shunt capacitor)

Decision variables	Limits		IWO	IWO-PPS
	min	max		
P_{G1} *(MW)*	0	575.88	156.86	156.06
P_{G2} *(MW)*	0	150	96.039	96.039
P_{G3} *(MW)*	42	140	43.140	43.140
P_{G6} *(MW)*	0	150	69.280	69.280
P_{G8} *(MW)*	165	550	420.165	420.165
P_{G9} *(MW)*	0	150	92.483	92.483
P_{G12} *(MW)*	123	410	388.328	388.328
V_{G1} *(p.u.)*	0.94	1.06	0.970755	1.0101
V_{G2} *(p.u.)*	0.94	1.06	1.012472	1.00941
V_{G3} *(p.u.)*	0.94	1.06	0.997108	1.011
V_{G6} *(p.u.)*	0.94	1.06	1.055683	1.0243
V_{G8} *(p.u.)*	0.94	1.06	1.00839	1.0109
V_{G9} *(p.u.)*	0.94	1.06	0.99979	1.0010
V_{G12} *(p.u.)*	0.94	1.06	0.98332	1.01001
Q_{18}*(MVAr)*	0	30	20	20
Q_{25}*(MVAr)*	0	30	11.8	11.8
Q_{53}*(MVAr)*	0	30	12.6	12.6
Cost ($/h)	-	-	**41869.37**	**41833.949**
P_{LOSS} *(MW)*	-	-	15.46	14.66

Note: Highlighted text represents the best results.

2.8.4 Test System-III

The IWO-PPS and IWO techniques have been executed 31 times to achieve the best results. The best, average and worst results along with the SD have been presented in Table 2.10. The comparison of results for test system-III is carried out with global search optimization techniques such as DE [24], ALC-PSO [176] and OKHA [121]. It is evident from Table 2.10 that the results obtained by the IWO-PPS technique are superior as compared to other compared technique results. The minimum value of fuel cost, pollutant emission and active power loss attained by the IWO-PPS technique is 823.473$/hr, 0.20471ton/hr, 2.69MW, respectively. The minimum value of results attained by the IWO-PPS technique is better than the previous best result reported for the OKHA technique [121] by 0.075% for case-I, 0.021%

for case-II and 0.332% for case-III. The average and worst values and SD of the results achieved by the IWO-PPS technique are less than the results achieved by the IWO technique.

Table 2.7: Optimal value of decision variables: Test system-II, case-I (with LTCs)

Decision Variables	Limits		IWO	IWO-PPS	Decision Variables	Limits		IWO	IWO-PPS
	min	max				min	max		
P_{G1} *(MW)*	0	575.88	146.457	132.432	t_{20}	0.9	1.1	0.99	0.99
P_{G2} *(MW)*	0	150	95.948	98.908	t_{31}	0.9	1.1	0.99	0.99
P_{G3} *(MW)*	42	140	47.968	43.758	t_{35}	0.9	1.1	0.95	0.95
P_{G6} *(MW)*	0	150	72.644	67.072	t_{36}	0.9	1.1	0.92	0.92
P_{G8} *(MW)*	165	550	464.175	456.87	t_{37}	0.9	1.1	0.95	0.95
P_{G9} *(MW)*	0	150	95.397	67.88	t_{41}	0.9	1.1	0.99	0.99
P_{G12} *(MW)*	123	410	346.67	398.36	t_{46}	0.9	1.1	0.97	0.97
V_{G1} *(p.u.)*	0.94	1.06	1.003409	1.048565	t_{54}	0.9	1.1	0.93	0.93
V_{G2} *(p.u.)*	0.94	1.06	1.011382	1.052680	t_{58}	0.9	1.1	1.01	1.01
V_{G3} *(p.u.)*	0.94	1.06	1.029527	1.035885	t_{59}	0.9	1.1	0.99	0.99
V_{G6} *(p.u.)*	0.94	1.06	1.041157	1.046020	t_{65}	0.9	1.1	0.99	0.99
V_{G8} *(p.u.)*	0.94	1.06	0.998349	1.049765	t_{66}	0.9	1.1	0.96	0.96
V_{G9} *(p.u.)*	0.94	1.06	1.004768	1.038473	t_{71}	0.9	1.1	0.97	0.97
V_{G12} *(p.u.)*	0.94	1.06	0.996293	1.033193	t_{73}	0.9	1.1	0.96	0.96
Q_{18}*(MVAr)*	0	30	20	20	t_{76}	0.9	1.1	0.94	0.94
Q_{25}*(MVAr)*	0	30	11.8	11.8	t_{80}	0.9	1.1	0.99	0.99
Q_{53}*(MVAr)*	0	30	12.6	12.6	*Cost($/hr)*	-	-	**41804.87**	**41768.49**
t_{19}	0.9	1.1	1.01	1.01	P_{LOSS}*(MW)*	-	-	18.46	14.48

Note: Highlighted text represents the best results.

Table 2.8: Optimal value of decision variables: Test system-II, case-II

Decision variables	Limits		IWO	IWO-PPS	Decision variables	Limits		IWO	IWO-PPS
	min	max				min	max		
P_{G1} *(MW)*	0	575.88	239.02	224.118	t_{19}	0.9	1.1	1.01	1.01
P_{G2} *(MW)*	0	150	99.948	99.948	t_{20}	0.9	1.1	0.99	0.99
P_{G3} *(MW)*	42	140	99.968	129.644	t_{31}	0.9	1.1	0.99	0.99
P_{G6} *(MW)*	0	150	99.644	99.968	t_{37}	0.9	1.1	0.95	0.95
P_{G8} *(MW)*	165	550	314.175	306.175	t_{41}	0.9	1.1	0.99	0.99
P_{G9} *(MW)*	0	150	99.397	99.397	t_{46}	0.9	1.1	0.97	0.97
P_{G12} *(MW)*	123	410	316.67	309.671	t_{54}	0.9	1.1	0.93	0.93
V_{G1} *(p.u.)*	0.94	1.06	1.003409	1.003409	t_{58}	0.9	1.1	1.01	1.01
V_{G2} *(p.u.)*	0.94	1.06	1.011382	1.011382	t_{59}	0.9	1.1	0.99	0.99
V_{G3} *(p.u.)*	0.94	1.06	1.029527	1.029527	t_{65}	0.9	1.1	0.99	0.99
V_{G6} *(p.u.)*	0.94	1.06	1.041157	1.041157	t_{66}	0.9	1.1	0.96	0.96
V_{G8} *(p.u.)*	0.94	1.06	0.998349	0.998349	t_{71}	0.9	1.1	0.97	0.97
V_{G9} *(p.u.)*	0.94	1.06	1.004768	1.004768	t_{73}	0.9	1.1	0.96	0.96
V_{G12} *(p.u.)*	0.94	1.06	0.996293	0.996293	t_{76}	0.9	1.1	0.94	0.94
Q_{18}*(MVAr)*	0	30	30	30	t_{80}	0.9	1.1	0.99	0.99
Q_{25}*(MVAr)*	0	30	30	30	*Emission(ton/hr)*	-	-	**0.8355**	**0.798**
Q_{53}*(MVAr)*	0	30	30	30					

Note: Highlighted text represents the best results.

The Figures 2.5, 2.6 and 2.7 represent the comparative convergence characteristics of IWO and IWO-PPS techniques for case-I, II and III, respectively. It can be accomplished from the convergence characteristics that integration of the PPS method with the IWO technique improves the convergence behavior of the proposed IWO-PPS technique. The optimal value of the decision variables obtained by IWO and IWO-PPS techniques for all the cases is presented

in Table 2.11.

Table 2.9: Optimal value of decision variables: Test system-II, case-III

Decision variables	Limits		IWO	IWO-PPS
	min	max		
V_{G1} *(p.u.)*	0.94	1.06	1.06	1.06
V_{G2} *(p.u.)*	0.94	1.06	1.06	1.06
V_{G3} *(p.u.)*	0.94	1.06	1.06	1.051602
V_{G6} *(p.u.)*	0.94	1.06	1.06	1.048586
V_{G8} *(p.u.)*	0.94	1.06	1.06	1.06
V_{G9} *(p.u.)*	0.94	1.06	1.06	1.06
V_{G12} *(p.u.)*	0.94	1.06	1.06	1.045251
Q_{18}*(MVAr)*	0	30	10	10
Q_{25}*(MVAr)*	0	30	5.9	5.9
Q_{53}*(MVAr)*	0	30	6.3	6.3
t_{19}	0.9	1.1	0.92	0.92
t_{20}	0.9	1.1	0.98	0.98
t_{31}	0.9	1.1	0.95	0.95
t_{37}	0.9	1.1	0.93	0.93
t_{41}	0.9	1.1	0.95	0.95
t_{46}	0.9	1.1	0.92	0.92
t_{54}	0.9	1.1	0.94	0.94
t_{58}	0.9	1.1	0.98	0.98
t_{59}	0.9	1.1	0.98	0.98
t_{65}	0.9	1.1	1.0	1.0
t_{66}	0.9	1.1	0.93	0.93
t_{71}	0.9	1.1	0.95	0.95
t_{73}	0.9	1.1	0.92	0.92
t_{76}	0.9	1.1	0.95	0.95
t_{80}	0.9	1.1	0.95	0.95
P_{LOSS} *(MW)*	-	-	**24.49**	**24.19**

Note: Highlighted text represents the best results.

Table 2.10: Comparison of results: Test system-III

Algorithms/ indexes	**Best**	**Worst**	**Average**	**SD**	**Average NFE**
Test system-III					
Case-I: Fuel cost($/hr)					
DE [24]	826.54	-	-	-	-
ALC-PSO [176]	825.89	-	-	-	-
OKHA [121]	824.09	-	-	-	-
IWO	839.257	842.478	840.36	0.9506	48000
IWO-PPS	823.473	824.561	823.846	0.3072	48000
Case-II: Pollutant emission(ton/hr)					
DE [24]	0.2048	-	-	-	-
ALC-PSO [176]	0.20476	-	-	-	-
OKHA [121]	0.204754	-	-	-	-
IWO	0.20492	0.20508	0.204954	0.000088	48000
IWO-PPS	0.20471	0.20479	0.20473	0.000022	48000
Case-III: Active power loss (MW)					
DE [24]	2.74	-	-	-	-
ALC-PSO [176]	2.73	-	-	-	-
OKHA [121]	2.708	-	-	-	-
IWO	2.826	3.33	3.059	0.20477	48000
IWO-PPS	2.699	2.7245	2.707	0.0081	48000

Note: DE: Differential evolution; ALC-PSO: Ageing leader and challengers–particle swarm optimization; OKHA: Oppositional krill herd algorithm

Table 2.11: Optimal value of decision variables: Test system-III

Decision variables	Limits		**Case-I Fuel cost ($/hr)**		**Case-II Pollutant emission (ton/hr)**		**Case-III Active power loss (MW)**	
	min	max	IWO	IWO-PPS	IWO	IWO-PPS	IWO	IWO-PPS
P_{G1} *(MW)*	50	200	199.844	199.928	63.955	63.27	51.302	51.099
P_{G2} *(MW)*	20	80	44.76	38.58	68.27	68.27	80.00	80.00
P_{G5} *(MW)*	15	50	17.83	21.09	50.00	50.00	50.00	50.00
P_{G8} *(MW)*	10	35	10.30	10.00	35.00	35.00	35.00	35.00
P_{G11}*(MW)*	10	30	10.16	10.00	30.00	30.00	30.00	30.00
P_{G13}*(MW)*	12	40	13.15	12.00	40.00	40.00	40.00	40.00
V_{G1} *(p.u.)*	0.95	1.1	1.02993	1.1	1.08610	1.1	1.1	1.1
V_{G2} *(p.u.)*	0.95	1.1	1.00655	1.08173	1.08046	1.0917	1.1	1.09823
V_{G5} *(p.u.)*	0.95	1.1	1.03491	1.05035	1.1	1.07539	1.08038	1.08138
V_{G8} *(p.u.)*	0.95	1.1	0.97267	1.06002	1.1	1.1	1.08931	1.08931
V_{G11}*(p.u.)*	0.95	1.1	0.96246	1.09111	1.1	1.1	1.1	1.1
V_{G13}*(p.u.)*	0.95	1.1	1.00751	1.1	1.1	1.1	1.1	1.1
Q_{10}*(MVAr)*	0	5	5	5	5	5	5	5
Q_{12}*(MVAr)*	0	5	5	5	5	5	5	5
Q_{15}*(MVAr)*	0	5	5	5	5	5	5	5
Q_{17}*(MVAr)*	0	5	5	5	4	4	5	5
Q_{20}*(MVAr)*	0	5	5	5	5	5	5	5
Q_{21}*(MVAr)*	0	5	4	4	5	5	5	5
Q_{23}*(MVAr)*	0	5	5	5	5	5	5	5
Q_{24}*(MVAr)*	0	5	5	5	5	5	5	5
Q_{29}*(MVAr)*	0	5	5	5	5	5	3	3
t_{11}	0.9	1.1	0.92	1.0	1.04	1.04	1.0	1.0
t_{12}	0.9	1.1	0.95	0.91	0.99	0.99	0.94	0.94
t_{15}	0.9	1.1	0.94	1.01	1.01	1.01	0.99	0.99
t_{36}	0.9	1.1	0.98	0.96	0.98	0.98	0.99	0.99
$\phi_{T5\text{-}7}(°)$	-5	5	0.3587	0.8102	-0.4996	-0.4996	0.5435	0.5435
$\phi_{T10\text{-}22}(°)$	-5	5	0.8102	-0.1984	0.0394	0.0394	-0.3533	-0.3533
$X_{T3\text{-}4}$ *(p.u.)*	0.0	0.1	0.0164	0.03	0.035	0.035	0.02	0.02
$X_{T19\text{-}20}$ *(p.u.)*	0.0	0.1	0.0296	0.035	0.035	0.035	0.02919	0.02919
Cost ($/hr)	-	-	**839.257**	**823.473**	1017.95	1015.85	1026.814	1026.195
Emission (ton/hr)	-	-	0.4418	0.44209	**0.20492**	**0.20471**	0.20713	0.20710
P_{LOSS} *(MW)*	-	-	12.44	8.198	3.706	3.12	**2.902**	**2.699**

Note: Highlighted text represents the best results.

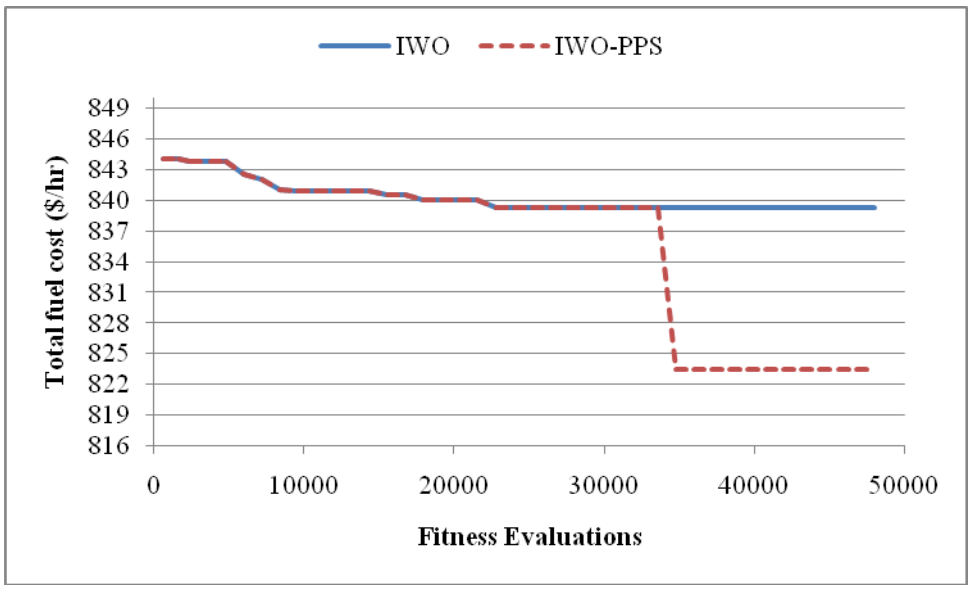

Figure 2.5: Comparative convergence of fuel cost of test system-III

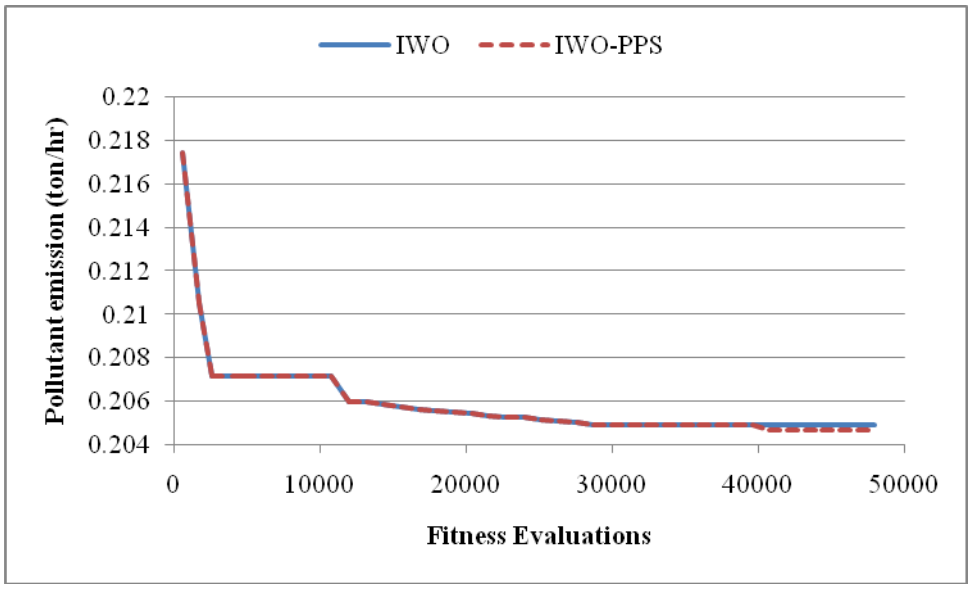

Figure 2.6: Comparative convergence of pollutant emission of test system-III

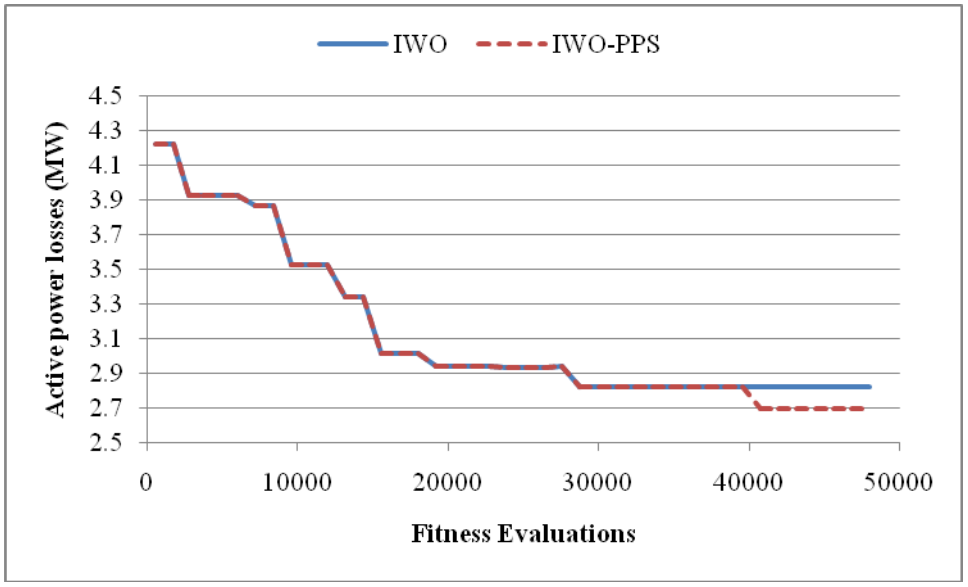

Figure 2.7: Comparative convergence of active power loss of test system-III

2.8.5 Test System-IV

For test system-IV, the comparison of results is carried out with state-of-art techniques *i.e.*, DE [24], ALC-PSO [176] and OKHA [121] and is presented in Table 2.12. The IWO-PPS and IWO techniques have been executed 31 times, and the best, average, and worst results along with SD are given in Table 2.12. It has been evident from Table 2.12 that the IWO-PPS technique is able to attain better results as compared to other techniques. It has been observed that the minimum fuel cost with the IWO-PPS technique is 7996.98$/hr, which is reduced by 0.407% as compared to the previous best results reported for the OKHA technique [121]. The

IWO-PPS technique is able to improve the results of minimum emission and active power loss by 4.028% and 0.342%, respectively, as compared to the OKHA technique results [121]. The optimum value of decision variables obtained from the IWO technique and IWO-PPS technique for all the cases are presented in Table 2.13. Figures 2.8, 2.9 and 2.10 show the comparative convergence characteristics attained by the IWO technique and the IWO-PPS technique for all the cases.

Table 2.12: Comparison of results: Test system-IV

Algorithms/ indexes	Best	Worst	Average	SD	Average NFE
Test system-IV					
Case-I: Fuel cost($/hr)					
DE [24]	8309.27	-	-	-	-
ALC-PSO [176]	8103.18	-	-	-	-
OKHA [121]	8029.64	-	-	-	-
IWO	8071.64	8073.78	8072.73	0.59051	48000
IWO-PPS	7996.98	7997.32	7997.11	0.1158	48000
Case-II: Pollutant emission(ton/hr)					
DE [24]	1.858705	-	-	-	-
ALC-PSO [176]	1.8387	-	-	-	-
OKHA [121]	1.834913	-	-	-	-
IWO	1.765	1.7712	1.76657	0.00129	48000
IWO-PPS	1.761	1.76202	1.7616	0.0003	48000
Case-III: Active power loss (MW)					
DE [24]	16.36	-	-	-	-
ALC-PSO [176]	16.353	-	-	-	-
OKHA [121]	16.346	-	-	-	-
IWO	17.78	27.453	22.307	3.164	48000
IWO-PPS	16.29	17.115	16.615	0.2012	48000

Note: DE: Differential evolution; ALC-PSO: Ageing leader and challengers–particle swarm optimization; OKHA: Oppositional krill herd algorithm

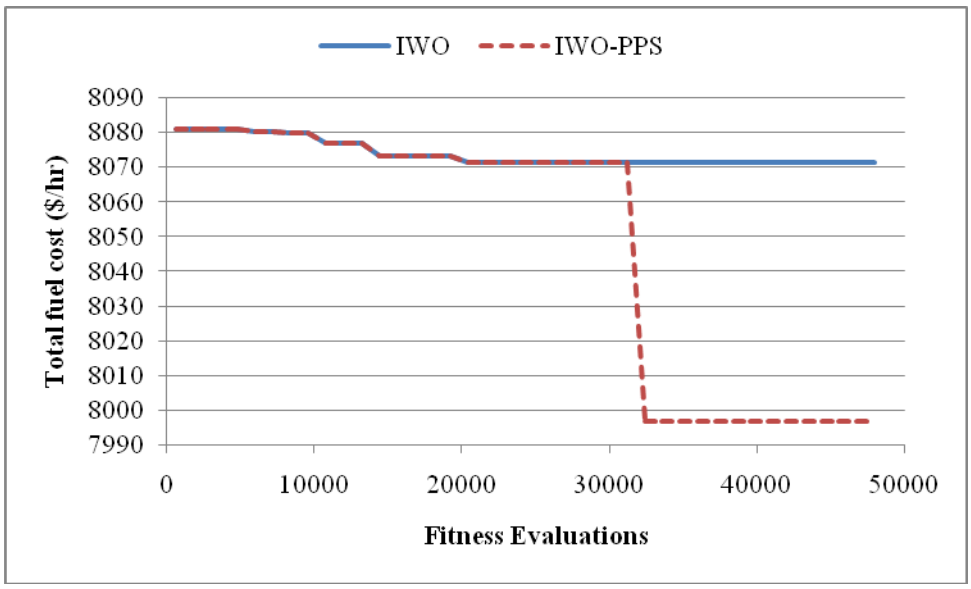

Figure 2.8: Comparative convergence of fuel cost of test system-IV

It has been observed from these figures that the IWO-PPS technique shows superior convergence characteristics as compared to the IWO technique and is able to avoid any

stagnation into the local best solutions. Therefore, it is concluded that the integration of PPS with the IWO technique improves the quality of solution and convergence behavior.

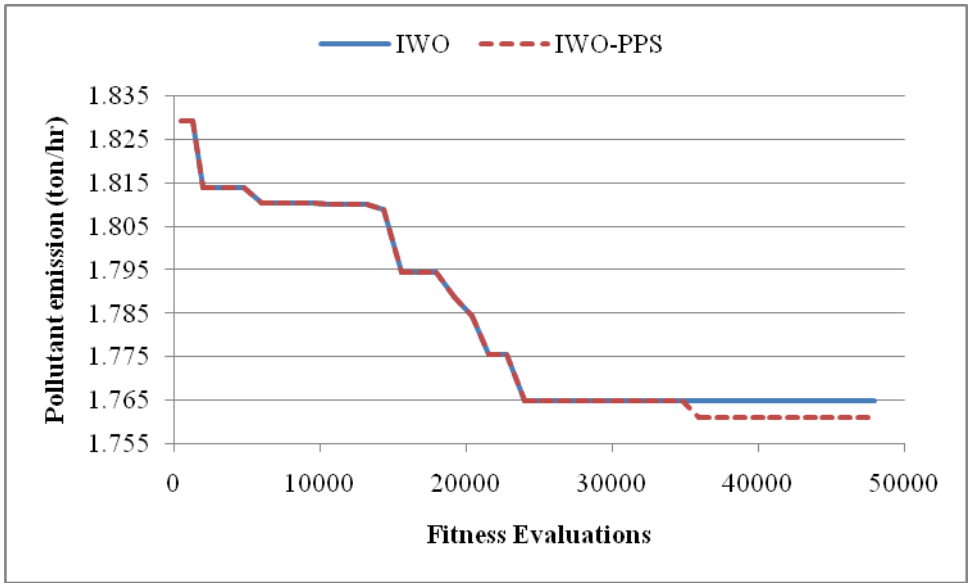

Figure 2.9: Comparative convergence of pollutant emission of test system-IV

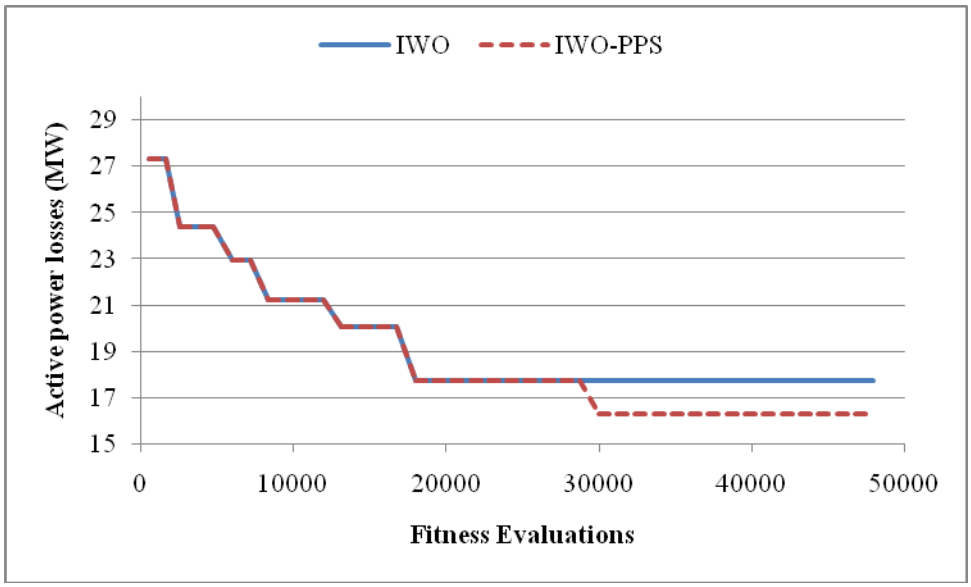

Figure 2.10: Comparative convergence of active power loss of test system-IV

2.8.6 Statistical Analysis

The success rate of an optimization algorithm is analyzed by its robustness. In this work, two sample *t*-test (two tails) has been performed at a significant level of 5% to investigate the robustness of the IWO-PPS technique. Table 2.14 shows the *t*-test results for all the four considered IEEE test systems. It has been found from *t*-test results that for all test systems, the *p* value is less than 0.05, which shows that the IWO-PPS technique is able to achieve better results as compared to its counterparts. Hence, it can be summarized that the IWO-PPS

technique demonstrates better robustness than the other state-of-art techniques reported in the literature.

Table 2.13: Optimal value of decision variables: Test system-IV

Decision Variables	**Limits**		**Case-I Fuel cost ($/hr)**		**Case-II Pollutant emission (ton/hr)**		**Case-III Active power loss (MW)**	
	min	max	IWO	IWO-PPS	IWO	IWO-PPS	IWO	IWO-PPS
P_{G1} *(MW)*	0	600	511.705	526.978	170.459	166.567	309.68	308.19
P_{G2} *(MW)*	0	500	0	0	0	0	0	0
P_{G3} *(MW)*	0	500	134.357	130.682	436.922	435.577	61.54	61.54
P_{G6} *(MW)*	0	500	0	0	0	0	0	0
P_{G8} *(MW)*	0	650	152.338	150.313	369.344	369.34	401.31	401.31
P_{G9} *(MW)*	0	500	0	0	0	0	0	0
P_{G12} *(MW)*	0	500	490.00	480.807	301.563	306.563	496.05	496.05
V_{G1} *(p.u.)*	0.95	1.1	1.099984	1.1	1.043020	1.043020	1.1	1.097548
V_{G2} *(p.u.)*	0.95	1.1	1.1	1.0989	1.068473	1.068473	1.1	1.091366
V_{G3} *(p.u.)*	0.95	1.1	1.057678	1.0655	1.081077	1.081077	1.044636	1.051472
V_{G6} *(p.u.)*	0.95	1.1	1.073861	1.0676	1.080166	1.080166	1.003022	1.034437
V_{G8} *(p.u.)*	0.95	1.1	0.985073	0.99177	1.035233	1.035233	1.029904	1.041014
V_{G9} *(p.u.)*	0.95	1.1	1.061875	1.05767	1.014005	1.014005	1.1	1.091386
V_{G12} *(p.u.)*	0.95	1.1	1.1	1.0993	1.040469	1.040469	1.070408	1.070488
Q_{18}*(MVAr)*	0	30	8	8	4	4	4	4
Q_{25}*(MVAr)*	0	30	2	2	8	8	4	4
Q_{53}*(MVAr)*	0	30	1	1	1	1	7	7
t_{19}	0.9	1.1	0.92	0.92	0.92	0.92	0.96	0.96
t_{20}	0.9	1.1	0.99	0.99	0.99	0.99	0.96	0.96
t_{31}	0.9	1.1	0.94	0.94	0.96	0.96	0.99	0.99
t_{35}	0.9	1.1	0.93	0.93	0.92	0.92	0.95	0.95
t_{36}	0.9	1.1	0.98	0.98	0.93	0.93	0.97	0.97
t_{37}	0.9	1.1	0.93	0.93	0.99	0.99	1.01	1.01
t_{41}	0.9	1.1	0.95	0.95	0.94	0.94	1.01	1.01
t_{46}	0.9	1.1	0.91	0.91	0.99	0.99	0.92	0.92
t_{54}	0.9	1.1	0.98	0.98	0.94	0.94	0.98	0.98
t_{58}	0.9	1.1	0.98	0.98	0.94	0.94	0.96	0.96
t_{59}	0.9	1.1	0.92	0.92	0.99	0.99	0.92	0.98
t_{65}	0.9	1.1	0.97	0.97	0.97	0.97	0.94	0.94
t_{66}	0.9	1.1	0.98	0.98	0.96	0.96	0.98	0.98
t_{71}	0.9	1.1	0.94	0.94	0.96	0.96	0.99	0.99
t_{73}	0.9	1.1	0.95	0.95	0.99	0.99	0.92	0.92
t_{76}	0.9	1.1	0.97	0.97	0.95	0.95	0.92	0.92
t_{80}	0.9	1.1	0.93	0.93	0.92	0.92	0.97	0.97
$\phi_{T4\text{-}5}(°)$	-5	5	0.25623	-0.8103	0.2562	0.2562	0.8103	0.8103
$\phi_{T5\text{-}6}(°)$	-5	5	0.3341	0.1822	0.6779	0.6779	-0.4438	-0.4438
$\phi_{T26\text{-}27}(°)$	-5	5	-0.2807	0.1145	-0.3623	-0.3623	0.5124	0.5124
$\phi_{T41\text{-}43}(°)$	-5	5	0.8102	0.1403	0.1146	0.1146	1.0249	1.0249
$\phi_{T53\text{-}54}(°)$	-5	5	0.2562	-0.5403	-0.8101	-0.8101	1.3558	1.3558
$X_{T18\text{-}19}$ *(p.u.)*	0.0	0.1	0.02135	0.02135	0.0526	0.0526	0.0195	0.0195
$X_{T31\text{-}32}$ *(p.u.)*	0.0	0.1	0.02914	0.02914	0.0529	0.0529	0.0115	0.0115
$X_{T34\text{-}32}$ *(p.u.)*	0.0	0.1	0.00112	0.00112	0.0846	0.0846	0.0056	0.0056
$X_{T40\text{-}56}$ *(p.u.)*	0.0	0.1	0.02040	0.02040	0.0829	0.0829	0.0045	0.0045
$X_{T39\text{-}57}$ *(p.u.)*	0.0	0.1	0.03154	0.03154	0.0451	0.0451	0.0038	0.0038
Cost ($/hr)	-	-	**8071.64**	**7996.98**	17199.65	17198.16	15422.12	15416.11
Emission(ton/hr)	-	-	2.394	2.456	**1.765**	**1.761**	1.919	1.914
P_{LOSS} *(MW)*	-	-	37.60	37.98	27.48	27.24	**17.78**	**16.29**

Note: Highlighted text represents the best results.

Table 2.14: Results of two sample *t*-test at 95% confidence level

	p-value	Action	Is significant difference?
Test system-I			
Case-I			
IWO-PPS vs. MICA-TLA	3.490536E-03	Reject	Yes
IWO-PPS vs. IWO	00E+00	Reject	Yes
Case-II			
IWO-PPS vs. IWO	00E+00	Reject	Yes
Case-III			
IWO-PPS vs. ICA	00E+00	Reject	Yes
IWO-PPS vs. MICA-IWO	00E+00	Reject	Yes
IWO-PPS vs. IWO	00E+00	Reject	Yes
Test system-II			
Case-I, with shunt capacitor			
IWO-PPS vs. CE	00E+00	Reject	Yes
IWO-PPS vs. IWO	2.9047E-20	Reject	Yes
Case-I, with LTCs			
IWO-PPS vs. Binomial	6.26793E-20	Reject	Yes
IWO-PPS vs. Gaussian	3.71431E-08	Reject	Yes
IWO-PPS vs. IWO	7.16619E-18	Reject	Yes
Case-II			
IWO-PPS vs. IWO	2.86134E-19	Reject	Yes
Case-III			
IWO-PPS vs. ICA	4.9479E-11	Reject	Yes
IWO-PPS vs. MICA-IWO	3.3835E-21	Reject	Yes
IWO-PPS vs. IWO	3.5334E-13	Reject	Yes
Test system-III			
Case-I			
IWO-PPS vs. IWO	00E+00	Reject	Yes
Case-II			
IWO-PPS vs. IWO	3.3493E-20	Reject	Yes
Case-III			
IWO-PPS vs. IWO	1.1262E-13	Reject	Yes
Test system-IV			
Case-I			
IWO-PPS vs. IWO	00E+00	Reject	Yes
Case-II			
IWO-PPS vs. IWO	00E+00	Reject	Yes
Case-III			
IWO-PPS vs. IWO	2.1690E-14	Reject	Yes

2.9 CONCLUSIONS

In this chapter, an integrated optimization technique based on the integration of IWO and PPS technique is proposed. The IWO technique is taken as a global search technique and the PPS method has been explored as a local search technique. The PPS method is applied to exploit the best result obtained by the IWO technique. The proposed IWO-PPS technique is applied to solve the OPF problem of power system incorporating the FACTS devices. Three objectives, fuel cost, pollutant emission and active power loss have been minimized sequentially. For observing the effectiveness of the IWO-PPS integrated technique, it is tested on IEEE 30-bus,

IEEE 57-bus, modified IEEE 30-bus and modified IEEE 57-bus power systems including TCPS and TCSC FACTS devices connected at fixed locations. The results obtained by the IWO-PPS technique are compared with the results reported in the literature. It is observed that the IWO-PPS technique improves the fuel cost, pollutant emission and active power loss results by 0.016%, 0.335% and 31.75%, respectively, as compared to the previous best results for test system-I. For test system-II, the fuel cost obtained by the IWO-PPS technique is reduced by 0.035%, 0.042% and 0.009% as compared to the CE method, binomial method and Gaussian method, respectively. Further, pollutant emission and active power loss are reduced by 0.029% as compared to AGSO technique and 0.259% as compared to the MFO technique, respectively. For test system-III, the fuel cost, pollutant emission and active power loss are reduced by 0.075%, 0.021% and 0.332%, respectively, by applying the IWO-PPS technique as compared to OKHA technique. The similar trends of results have been observed in test system-IV. Further, the comparative convergence characteristics illustrate that IWO-PPS technique is able to search high quality solution with same NFE. The *t*-test results demonstrate that the IWO-PPS technique is more robust as compared to MICA-TLA, ICA, MICA-IWO and IWO techniques for test system-I. The statistical test results indicate that the IWO-PPS technique is able to generate optimal results with high precision as compared to CE, binomial, Gaussian, ICA and MICA-IWO techniques for test system-II. The statistical results of test system-III and IV confirm that there is a significant difference between the performance of IWO-PPS and IWO techniques and justify the integration of PPS method with IWO technique.

CHAPTER-3

MULTI-OBJECTIVE OPTIMAL POWER FLOW SOLUTION USING AN INTEGRATED OPTIMIZATION TECHNIQUE

3.1 INTRODUCTION

The conflicting nature of fuel cost, pollutant emission and active power loss objectives make the OPF problem to be considered as a *multi-objective optimal power flow* (MO-OPF) problem. The MO-OPF is a large-scale, nonlinear, multimodal optimization problem. A non-interactive approach is applied by various researchers to search the best non-dominated solution of the MO problem. In the non-interactive approach, the *decision maker* (DM) has access to prior information about preferences, but DM is not involved in the selection process of the best non-dominated solution. A non-interactive approach is employed to formulate a scalarized objective function that combines the different objectives of the problem. This approach is competent to select the satisficing solution with less computational work involved for generating the Pareto front. The fuzzy membership function is used due to the vague nature of different objectives.

In this chapter, the integrated IWO-PPS optimization technique is applied to solve the MO-OPF problem for searching the global best optimal solution. To search the best non-dominated solution of MO-OPF problem, non-interactive approach has been explored, in which DM is not concerned or prior preference information is available. The proposed solution approach has been tested on three MO-OPF problems with FACT devices.

3.2 MULTI-OBJECTIVE OPTIMAL POWER FLOW PROBLEM FORMULATION

The MO-OPF is a non-linear, highly constrained optimization problem. The foremost aim of this research work is the minimization of fuel cost, pollutant emission and system transmission loss simultaneously by applying integrated IWO-PPS optimization technique.The mathematical model of each objective function is discussed in detail in sub-section 2.3.1 under Chapter 2. Mathematically, the MO-OPF problem is represented as below

Minimize $\left[F_C, E, P_{LOSS}\right]^T$ (3.1)

Subject to the various equality and inequality constraints as discussed in detail in subsection 2.3.2 in Chapter 2.

3.3 NON-INTERACTIVE MULTI-OBJECTIVE APPROACH

The MO-OPF problem has partially comparable objectives, which make it practically impossible to have a single non-dominated solution. The best non-dominated solution should satisfy all the objectives up to a certain compromising level. In this work, a non-interactive method is used, in which a scaled objective function is formed to obtain the satisficing solution. The satisficing function undertakes the information of the satisfaction level of an objective with reference to other objectives in a quantitative way and is given as [174]:

$$S_T = \frac{1}{M(M-1)}\left(\sum_{i}^{M}\sum_{\substack{j=1 \\ j\neq i}}^{M}\frac{\mu(of_i)}{\mu(of_j)}\right) \tag{3.2}$$

In Eq. (3.2), the fuzzy membership function is used due to vague nature of different objectives and is given as:

$$\mu(of_k) = \begin{cases} 0; & of_k > of_k^{\max} \\ \dfrac{of_k^{\max} - of_k}{of_k^{\max} - of_k^{\min}}; & of_k^{\min} \le of_k \le of_k^{\max} \quad (k = 1,2,...,M) \\ 1; & of_k < of_k^{\min} \end{cases} \tag{3.3}$$

where $of_k^{\max}, of_k^{\min}$ are the values of k^{th} objective function and M is the number of objective functions.

In order to achieve the highest satisfaction for all the objectives, the cardinal priority ranking, μ_c needs to maximize and is given as:

$$\mu_c = \max\left(\min(\mu_1(of_1), \mu_2(of_2), \mu_3(of_3))\right) \tag{3.4}$$

Finally, based on scalarized objective function value S_T, the cardinal priority ranking is obtained as [174]:

$$\mu_C = \begin{cases} \mu_c S_T; & S_T \le 1 \\ \mu_c S_T^{-1}; & S_T > 1 \end{cases} \tag{3.5}$$

The maximum cardinal priority ranking value μ_C provides the most suitable non-dominated solution.

3.4 PROPOSED SOLUTION APPROACH

The integrated IWO-PPS optimization technique is applied to solve the MO-OPF problem. The

IWO technique explores the search space and the PPS method enhances the exploitation ability of the search algorithm. The non-interactive approach is employed to search the best non-dominated solution of the MO problem. The algorithm of the proposed solution approach is given as:

Algorithm 1: Proposed Solution Approach

Step 1: Read the algorithm parameters and decision variables bounds.

Step 2: Generate random values for each weed within the decision variable bounds.

Step 3: Apply NR method to solve the OPF problem corresponding to each weed in the population.

Step 4: compute the membership value for MO problem by considering the minimum and the maximum (unacceptable) values of function for each objective function as per Eq. (3.3).

Step 5: Compute the satisfaction level for one objective with respect to others as per Eq. (3.2) and cardinal priority ranking as per Eq. (3.4).

Step 6: Compute the cardinal priority ranking based on scalarized objective function value as per Eq. (3.5).

Step 7: Arrange the weeds starting from the best to the worst cardinal priority ranking. The maximum cardinal priority ranking value provides the most suitable non-dominated solution.

Step 8: Evaluate the count of new seeds according to the best and the worst cardinal priority ranking by using Eq. (3.6) and disperse the new seeds by using Eq. (2.32) under Chapter 2.

$$n(X_i) = \frac{\mu_C(X_i) - \mu_{C\,worst}}{\mu_{C\,best} - \mu_{C\,worst}} \left(seeds_{\max} - seeds_{\min}\right) + seeds_{\min} \tag{3.6}$$

where $\mu_C(X_i)$ represents the weed fitness; $\mu_{C\,worst}$ and $\mu_{C\,best}$ are the worst and best fitness in the present population, respectively; $seed_{\max}$ and $seed_{\min}$ are the maximum and minimum number of seeds, respectively.

Step 9: If the solution gets struck to a local best solution for defined number of iterations during the search process, then the solution is transferred to the PPS method for further up-gradation.

Step 10: Select the next cycle population by the combined arrangement of seeds and parent weeds on the basis of cardinal priority ranking.

Step 11: The maximum *number of fitness evaluations* (NFE) is set to terminate the iterative procedure, If the terminate criteria satisfy, then go to step 10.

Else

Continue with step 3

Step 12: Optimum solution is achieved.

3.5 IMPLEMENTATION OF PROPOSED SOLUTION APPROACH

The decision variables of the MO-OPF problem incorporating FACTS devices are active power generations of the generators except for the slack bus, the generators voltages magnitude, transformer tap ratios, shunt *volt ampere reactive* (VARs), phase shifters and reactance. Transformer tap ratios and the shunt outputs are discrete type variables and the rest are the continuous type variables. The transformer tap setting governs the tap ratio and the number of actively connected shunts decides the shunt VARs. The decision variables array is represented as per Eq. (2.35) under Chapter 2.

The procedure to implement the proposed solution approach is explained as below:

Step 1: *Initialization*: The continuous and discrete decision variables are randomly initialized within the defined limits as per Eq. (2.36) and Eq. (2.37), respectively under Chapter 2.

Step 2: During the search process, the equality constraints are handled by the NR method as per Eq. (2.20) and (2.21) under Chapter 2. Inequality constraints are handled by an exterior penalty method. This method computes the error for each violation of inequality constraints as

$$err = \left(p_1\left(P_{G,slack} - P_{G,slack}^{\lim}\right)^2 + \sum_{k=1}^{N_{PQ}} p_2 (V_{Lk} - V_{Lk}^{\lim})^2 + \sum_{m=1}^{NG} p_3 (Q_{Gm} - Q_{Gm}^{\lim})^2 + \sum_{j=1}^{NL} p_4 (\left|S_{Lj}\right| - S_{Lj}^{\max})^2 \right) \quad (3.7)$$

where *err* represents the cumulative error of all constraint violations; $P_{G,slack}$ is slack bus active power generation; N_{PQ} , *NG, NL* are the number of load buses, active power generators and transmission lines, respectively; V_{Lk} is voltage magnitude of k^{th} load buses; Q_{Gm} is reactive power generated by m^{th} thermal unit; S_{Lj} is line flow at j^{th} transmission line; p_1, p_2, $p_3$and p_4 are the penalty function parameters corresponding to slack bus active power generation, voltage magnitude at load buses, reactive power generation and apparent line flow limit violations respectively.

In order to restrict the solutions into a feasible operating region, the cumulative error of all constraint violations is incorporated as a penalty in Eq. (3.4) as under.

$$\mu_c = \left\{\max\left(\min\left(\mu_1(of_1), \mu_2(of_2), \mu_3(of_3)\right) - err\right)\right\} \quad (3.8)$$

Step 3: *Objective Function Evaluation:* Subsequent to the initialization, the power flow problem is solved for each weed by using the NR method and objective functions are computed by using Eqs. (2.17)-(2.19) under Chapter 2. The membership value of each objective function is computed by Eq. (3.3).The satisfaction level of an objective with reference to other

objectives is computed by Eq. (3.2). The cardinal priority ranking is computed using Eqs. (3.5) and (3.8).

Step 4: *Reproduction and Dispersion of Seed*: Reproduction and dispersion of seeds depend upon the best and the worst values of cardinal priority ranking.

Step 5: *Exploitation by Powell's Method:* The PPS method helps to enhance the exploitation ability of the search algorithm. If the solution gets struck to a local best solution for a defined number of iterations during the search process, then the solution is transferred to the PPS method for further up-gradation.

Step 6: *Population selection*: The next cycle population is selected by the combined arrangement of seeds and parent weeds on the basis of the value of cardinal priority ranking.

Step 7: If the termination criterion is not reached, continue with step 3.

Step 8: The optimum solution is obtained.

3.6 TEST SYSTEMS AND RESULTS

The proposed solution approach is applied to the optimal solution for the MO-OPF problem. The efficacy of the proposed solution methodology is demonstrated by implementing it on three systems *i.e.*, test system-III, test system-IV, test system-V. The test system-III and IV are modified IEEE 30-bus and modified IEEE 57-bus system, both include FACTS devices and the details are discussed in section 2.8 under Chapter 2.Test system-V is the standard IEEE 30-bus system without FACTS devices. Test system-V has 41 transmission lines and a total load demand of 283.4 MW. The system contains 24 control variables that include 5-active powers of thermal generators, 6-voltage magnitude of the generators, 4-transformers with tap changers and 9-shunt VARs [92]. The data of generating limits of thermal units, operating cost and emission coefficients of thermal units, load and transmission lines are given in Tables A.1.1, A.1.2, A.1.3 and A.1.4, respectively under Appendix-A.

3.6.1 Algorithm Parameter Setting

The selection of algorithm parameters is an important aspect of the global search technique as it has a great impact on the solution quality and convergence characteristics. To work out the best parameter value, a number of trials are taken by the IWO technique for each parameter. For the PPS method, the step size consideration is an important task as it affects the exploitation ability of the algorithm; therefore, the necessary trails runs are to be taken to select the finest step size. The appropriate parameter values for the IWO-PPS technique are listed in

Table 3.1.

Table 3.1: Algorithm parameters of IWO-PPS technique

Parameter	**Values**
Initial size of population	20
Max. number of seeds	5
Min. number of seeds	0
Initial SD	10
Final SD	1
Modulation index	2-5
Step Size (PPS)	0.01

3.6.2 Results and Discussion

The proposed solution approach is employed for solving the MO-OPF problem in the command line of FORTRAN-90. The thirty one trials runs are carried out to attain the global best results. The best, mean, worst results and SD of results are also computed. The usefulness and performance of the proposed solution approach for solving MO-OPF problems is carried out by undertaking four cases of all the test systems.

Case-I: Simultaneous minimization of the total fuel cost and emission pollutant.

Case-II: Simultaneous minimization of the total fuel cost and active power losses.

Case-III: Simultaneous minimization of emission pollutant and active power losses.

Case-IV: Simultaneous minimization of the total fuel cost, emission pollutant and active power losses.

3.6.2.1 Test System-III

In this work, a non-interactive method is applied to deal with the MO-OPF problem. In MO problems, due to the conflicting nature of objectives, the optimization of one objective leads to the degradation of other objectives. For test system-III, the minimum values attained by the IWO-PPS technique for fuel cost, emission pollutant and active power losses are 823.473$/hr, 0.20471ton/hr and 2.69MW, respectively as discussed in detail under subsection 2.5.3, Chapter 2 and corresponding undesired values of other objectives are computed and are given in Table 3.2.

Table 3.2: Comparison of results: Test system-III

Technique	Min. F_C ($/hr)		Min. E (ton/hr)		Min. P_{LOSS}(MW)	
	IWO	IWO-PPS	IWO	IWO-PPS	IWO	IWO-PPS
Cost ($/hr)	839.257	823.473	1017.95	1015.85	**1026.814**	**1026.195**
Emission (ton/hr)	**0.4418**	**0.44209**	0.20492	0.20471	0.20713	0.20710
P_L *(MW)*	**12.44**	**8.198**	3.706	3.12	2.902	2.699

Note: Highlighted text represents the maximum value of objective functions

For MO, the attained results for test system-III, case-I are compared with its counterpart techniques *i.e.*, DE [24], ALC-PSO [176], KHA [121], OKHA [121] and are given in Table 3.3. For MO-OPF, case-I, the fuel cost and pollutant emission attained by the IWO-PPS technique are 873.18$/hr and 0.2678ton/hr. The MO results are compared on the basis of cardinal priority ranking. A higher cardinal priority ranking value indicates more satisfied non-dominated solution for all the objectives. As per Table 3.3, the cardinal priority ranking attained with the IWO-PPS technique is 0.73377 for case-I and that is highest in comparison to its counterparts.

Table 3.3: Comparison of multi-objective results: Test system-III

Case-I				
Technique	F_C($/hr)	E(ton/hr)		μ_C
DE [24]	922.36	0.2364		0.44874
ALC-PSO [176]	907.17	0.2430		0.55168
KHA [121]	897.41	0.2491		0.61643
OKHA[121]	897.51	0.2490		0.61576
IWO	887.97	0.2579		0.67618
IWO-PPS	**873.18**	**0.2678**		**0.73377**
Case-II				
Technique	F_C ($/hr)	P_{LOSS} (MW)		μ_C
IWO	920.75	5.599		0.47047
IWO-PPS	**912.177**	**4.7100**		**0.55839**
Case-III				
Technique	E(ton/hr)	P_{LOSS} (MW)		μ_C
IWO	0.20645	3.010		0.94222
IWO-PPS	**0.20644**	**2.98**		**0.94793**
Case-IV				
Technique	F_C ($/hr)	E(ton/hr)	P_{LOSS}(MW)	μ_C
IWO	885.057	0.26122	7.053	0.13036
IWO-PPS	**927.716**	**0.23368**	**4.505**	**0.44576**

Note: Highlighted text represents the best results.
DE: differential evolution; ALC-PSO: ageing leader and challengers-PSO; KHA: krill herd algorithm; OKHA: oppositional krill herd algorithm.

For the remaining three cases, no results have been reported in the literature as per the best of the Author's knowledge; hence the results are compared with the IWO technique. The cardinal priority ranking achieved by the IWO-PPS technique is 0.55839, 0.94793 and 0.44576 for case-II, III and IV, respectively, which is better than the IWO technique. It is clear from Table 3.3 that the IWO-PPS technique has the capability to search a better solution with respect to all the objectives. The optimum values of the decision variables obtained by the IWO-PPS technique for the MO-OPF problem including FACTS devices are tabulated in Table 3.4.

3.6.2.2 Test system-IV

The minimum values obtained by the IWO-PPS technique for cost, emission pollutant and

active power losses are 7996.98 $/hr, 1.761 ton/hr and 16.29 MW, respectively as discussed in detail under subsection 2.5.4, Chapter 2, and corresponding undesired values of other objectives are computed and are given in Table 3.5. For MO-OPF, case-I, the attained results have been compared with published results *i.e.*, DE [24], ALC-PSO [176], KHA [121], OKHA [121] and are given in Table 3.6.

Table 3.4: Optimal decision variables for MO-OPF problem: Test system-III

Control variables	**Limits**		**Case-I**	**Case-II**	**Case-III**	**Case-IV**
	min	max				
P_{G1} *(MW)*	50	200	132.295	115.332	53.271	98.444
P_{G2} *(MW)*	20	80	57.86	58.349	78.109	76.156
P_{G5} *(MW)*	15	50	25.08	36.882	50	21.437
P_{G8} *(MW)*	10	35	25.52	21.720	35	22.608
P_{G11} *(MW)*	10	30	25.06	16.161	30	29.754
P_{G13} *(MW)*	12	40	25.815	39.666	40	39.506
$\phi_{T5\text{-}7}$ *(°)*	-5	5	0.5404	0.5443	0.5387	0.5387
$\phi_{T10\text{-}22}$ *(°)*	-5	5	0.2459	0.2388	0.2422	0.2422
$X_{C3\text{-}4}$ *(p.u.)*	0.0	0.1	0.0348	0.01416	0.035	0.00703
$X_{C19\text{-}20}$ *(p.u.)*	0.0	0.1	0.0296	0.00764	0.035	0.01275
V_{G1} *(p.u.)*	0.95	1.1	1.056077	1.089457	1.099961	1.096563
V_{G2} *(p.u.)*	0.95	1.1	1.076241	1.086125	1.0975	1.096641
V_{G5} *(p.u.)*	0.95	1.1	0.950857	1.081261	1.083179	1.09
V_{G8} *(p.u.)*	0.95	1.1	1.016044	1.07343	1.085449	1.09
V_{G11} *(p.u.)*	0.95	1.1	1.025901	1.065402	1.083736	1.1
V_{G13} *(p.u.)*	0.95	1.1	0.97963	1.098726	1.08	1.1
t_{11}	0.9	1.1	1.01	0.97	1.1	1.0
t_{12}	0.9	1.1	0.99	1.07	1.1	0.97
t_{15}	0.9	1.1	1.08	1.04	1.1	1.0
t_{36}	0.9	1.1	0.99	0.94	1.1	0.95
Q_{10} *(MVAr)*	0	5	1	2	1	3
Q_{12} *(MVAr)*	0	5	2	4	5	3
Q_{15} *(MVAr)*	0	5	5	4	5	5
Q_{17} *(MVAr)*	0	5	0	0	5	5
Q_{20} *(MVAr)*	0	5	5	2	5	1
Q_{21} *(MVAr)*	0	5	4	0	5	3
Q_{23} *(MVAr)*	0	5	2	5	5	0
Q_{24} *(MVAr)*	0	5	4	1	5	2
Q_{29} *(MVAr)*	0	5	1	1	5	2
Cost ($/hr)	-	-	**873.182**	**912.177**	1025.006	**927.716**
Emission (ton/hr)	-	-	**0.26784**	0.24469	**0.20644**	**0.23368**
P_L *(MW)*	-	-	8.23	**4.71**	**2.98**	**4.505**

Note: Highlighted text represents the best results.

Table 3.5: Comparison of results: Test system-IV

Technique	Min. F_C ($/hr)		Min. E (ton/hr)		Min. P_{LOSS} (MW)	
	IWO	IWO-PPS	IWO	IWO-PPS	IWO	IWO-PPS
Cost ($/hr)	8071.64	7996.98	**17199.65**	**17198.16**	15422.12	15416.11
Emission (ton/hr)	**2.394**	**2.456**	1.765	1.761	1.919	1.914
P_L *(MW)*	**37.60**	**37.98**	27.48	27.24	17.78	16.29

Note: Highlighted text represents the maximum value of objective functions

For MO-OPF, case-I, the fuel cost and pollutant emission attained by the IWO-PPS technique are 10047.96$/hr and 1.914ton/hr, respectively and the cardinal priority ranking value is 0.77709, that is better than the other reported results. The values of cardinal priority

ranking achieved by the IWO-PPS technique for case-II, III and IV are 0.77712, 0.78897 and 0.57047, respectively, which indicate that the IWO-PPS technique is able to search more acceptable results for all the four cases. The optimum values of decision variables obtained by the IWO-PPS technique for MO-OPF problem incorporating FACTS devices are reported in Table 3.7. The convergence characteristics obtained with IWO and IWO-PPS techniques for case-I, II, III and IV are presented in Figures 3.1, 3.2, 3.3 and 3.4, respectively. It is illustrated from the figures that the IWO-PPS technique has superior convergence criteria.

Table 3.6: Comparison of multi-objective results: Test system-IV

Case-I				
Technique	F_C(\$/hr)	E(ton/hr)		μ_C
DE [24]	10408.49	2.2116		0.27313
ALC-PSO [176]	10237.79	2.2274		0.24049
KHA [121]	9898.54	2.196		0.28864
OKHA [121]	9895.01	2.194		0.29218
IWO	10322.88	2.08		0.51397
IWO-PPS	**10047.96**	**1.914**		**0.77709**
Case-II				
Technique	F_C(\$/hr)	P_{LOSS}(MW)		μ_C
IWO	9653.518	22.935		0.68404
IWO-PPS	**10046.81**	**20.852**		**0.77712**
Case-III				
Technique	E(ton/hr)	P_{LOSS}(MW)		μ_C
IWO	1.791	21.786		0.72421
IWO-PPS	**1.786**	**20.578**		**0.78897**
Case-IV				
Technique	F_C(\$/hr)	E(ton/hr)	P_{LOSS}(MW)	μ_C
IWO	9854.41	1.837	27.11	0.44749
IWO-PPS	**10469.93**	**1.762**	**24.813**	**0.57047**

Note: Highlighted text represents the best results

DE: differential evolution; ALC-PSO: aging leader and challengers-PSO; KHA: krill herd algorithm; OKHA: oppositional krill herd algorithm.

3.6.2.3 Test system-V

The minimum values obtained by the IWO-PPS technique for fuel cost, emission pollutant and active power losses are 798.84\$/hr, 0.2047ton/hr and 2.887MW, respectively and corresponding undesired values of other objectives are computed and are given in Table 3.8. The comparisons of MO results are given in Table 3.9. It is clear from Table 3.9 that for case-I, the cardinal priority ranking obtained by ESDE-MC technique [144], IWO technique and IWO-PPS technique is 0.72916, 0.75165 and 0.75584, respectively. Hence, it is summarized that the IWO-PPS technique searches for better satisfying results.

A similar trend has been observed in all other cases, in which the IWO-PPS technique outperforms the IWO technique. The optimum decision variables for the MO-OPF problem are given in Table 3.10.

Table 3.7: Optimal decision variables for MO-OPF problem: Test system-IV

Decision variables	**Limits**		**Case-I**	**Case-II**	**Case-III**	**Case-IV**
	min	max				
P_{G1} *(MW)*	0	600	409.58	338.092	376.448	383.691
P_{G2} *(MW)*	0	500	0	0	0	0
P_{G3} *(MW)*	0	500	148.06	201.9	187.92	227.635
P_{G6} *(MW)*	0	500	0	0	0	0
P_{G8} *(MW)*	0	650	253.67	231.66	371.41	258.839
P_{G9} *(MW)*	0	500	0	0	0	0
P_{G12}*(MW)*	0	500	463.59	500	335.60	405.448
$\phi_{T4\text{-}5}$ *(°)*	-5	5	0.5436	0.5544	0.5467	0.5487
$\phi_{T5\text{-}6}$ *(°)*	-5	5	-0.4481	-0.4488	-0.4334	-0.4444
$\phi_{T26\text{-}27}$ *(°)*	-5	5	0.5405	0.5445	0.5434	0.5445
$\phi_{T41\text{-}43}$*(°)*	-5	5	-0.6264	-0.6226	-0.6259	-0.6226
$\phi_{T53\text{-}54}$ *(°)*	-5	5	0.7302	0.7332	0.7289	0.7229
$X_{C18\text{-}19}$ *(p.u.)*	0.0	0.1	0.00143	0.05	0.02929	0.01880
$X_{C31\text{-}32}$ *(p.u.)*	0.0	0.1	0.00304	0.05	0.04299	0.04423
$X_{C34\text{-}32}$ *(p.u.)*	0.0	0.1	0.02014	0.05	0.02636	0.03557
$X_{C40\text{-}56}$ *(p.u.)*	0.0	0.1	0.02596	0.05	0.07794	0.00275
$X_{C39\text{-}57}$ *(p.u.)*	0.0	0.1	0.02638	0.05	0.03007	0.04980
V_{G1} *(p.u.)*	0.95	1.1	1.1	1.1	1.070266	1.079518
V_{G2} *(p.u.)*	0.95	1.1	1.1	1.1	1.072209	1.067986
V_{G3} *(p.u.)*	0.95	1.1	1.1	1.1	1.073332	1.065747
V_{G6} *(p.u.)*	0.95	1.1	1.1	1.055023	1.090714	1.081106
V_{G8} *(p.u.)*	0.95	1.1	1.1	1.033283	1.06008	1.069612
V_{G9} *(p.u.)*	0.95	1.1	1.04761	1.1	1.064078	1.056174
V_{G12} *(p.u.)*	0.95	1.1	1.1	1.1	1.056070	1.079291
t_{19}	0.9	1.1	0.99	0.99	0.99	0.94
t_{20}	0.9	1.1	0.97	0.98	0.98	0.97
t_{31}	0.9	1.1	0.94	0.99	0.98	1.0
t_{35}	0.9	1.1	0.97	0.99	0.96	0.98
t_{36}	0.9	1.1	0.98	0.98	0.92	0.93
t_{37}	0.9	1.1	0.94	1.01	0.92	0.97
t_{41}	0.9	1.1	0.97	0.99	0.95	0.93
t_{46}	0.9	1.1	0.95	0.98	0.96	0.97
t_{54}	0.9	1.1	0.93	0.99	0.96	0.91
t_{58}	0.9	1.1	0.97	0.98	0.98	0.98
t_{59}	0.9	1.1	0.98	0.98	0.96	0.92
t_{65}	0.9	1.1	0.97	0.99	1.0	0.95
t_{66}	0.9	1.1	0.92	0.98	0.98	0.99
t_{71}	0.9	1.1	0.99	0.99	0.96	0.98
t_{73}	0.9	1.1	0.96	0.98	0.92	0.91
t_{76}	0.9	1.1	0.96	0.99	0.96	1.0
t_{80}	0.9	1.1	0.94	0.99	0.95	0.97
Q_{18}*(MVAr)*	0	30	3	7	9	3
Q_{25}*(MVAr)*	0	30	8	1	9	8
Q_{53}*(MVAr)*	0	30	3	6	5	2
Cost ($/hr)	-	-	**10047.96**	**10046.81**	13802.26	**10469.93**
Emission (ton/hr)	-	-	**1.914**	1.741	**1.786**	**1.763**
P_L*(MW)*	-	-	24.10	**20.852**	**20.578**	**24.813**

Note: Highlighted text represents the best results.

Table 3.8: Comparison of results: Test System-V

Technique	Min. F_C ($/hr)		Min. E (ton/hr)		Min. P_{LOSS}(MW)	
	IWO	IWO-PPS	IWO	IWO-PPS	IWO	IWO-PPS
Cost ($/hr)	816.61	798.84	944.521	944.076	**963.253**	**967.154**
Emission (ton/hr)	**0.32624**	**0.36792**	0.2048	0.2047	0.20771	0.20713
P_L *(MW)*	**10.51**	**8.601**	3.47	3.29	3.17	2.887

Note: Highlighted text represents the maximum value of objective functions

Table 3.9: Comparison of multi-objective results: Test System-V

Case-I			
Technique	F_C($/hr)	E(ton/hr)	μ_C
ESDE-MC [144]	830.71	0.2483	0.72916
IWO	836.463	0.24246	0.75165
IWO-PPS	**835.121**	**0.24447**	**0.75584**
Case-II			
Technique	F_C($/hr)	P_{LOSS}(MW)	μ_C
IWO	870.307	6.55	0.32238
IWO-PPS	**855.921**	**4.67**	**0.66033**
Case-III			
Technique	E(ton/hr)	P_{LOSS}(MW)	μ_C
IWO	0.20574	3.12	0.95863
IWO-PPS	**0.20564**	**2.889**	**0.99422**

Case-IV				
Technique	F_C($/hr)	E(ton/hr)	P_{LOSS}(MW)	μ_C
IWO	899.25	0.21161	4.195	0.33265
IWO-PPS	**875.426**	**0.2181**	**4.645**	**0.50968**

Note: Highlighted text represents the best results
ESDE-MC: Enhanced self-adaptive DE-mixed crossover

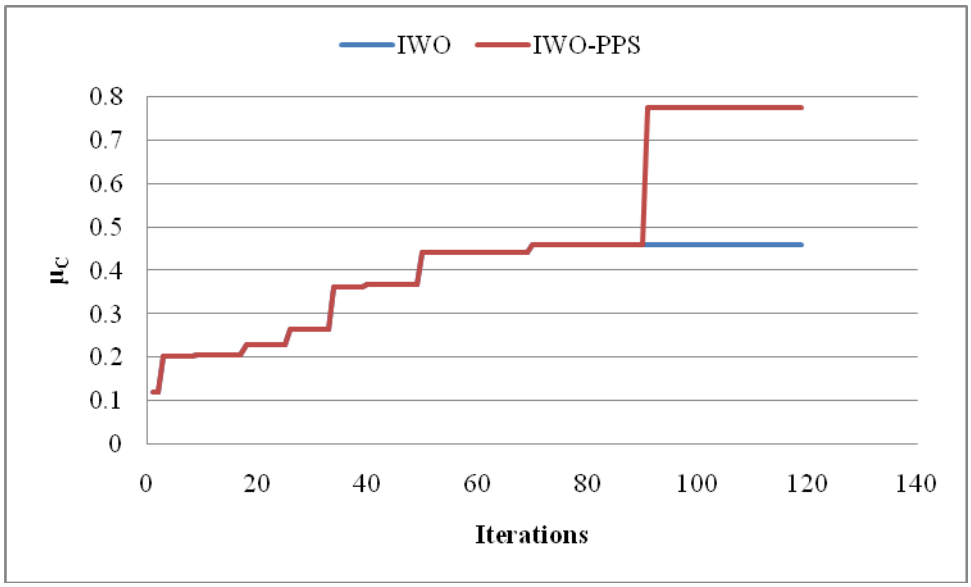

Figure 3.1: Convergence characteristics: Test system-IV, case-I.

3.6.3 Statistical Analysis

The robustness of the IWO-PPS technique has been examined by executing it for thirty one trial runs for test system-IV, case-I. Table 3.11 shows the minimum, mean and the worst results and SD of the results attained by the IWO-PPS technique and IWO technique. It is confirmed that the IWO-PPS technique exhibits more robustness in comparison to the IWO technique. Further, *t*-test (two sample, two tails) is carried out to ascertain the robustness. The significant difference of 5% is set for the test. It is observed from Table 3.12 that the statistical output *t-calculated* is higher than the critical value. Therefore, the null hypothesis is rejected. This

confirms that there is a significant difference between two population means at the 5% level of significance.

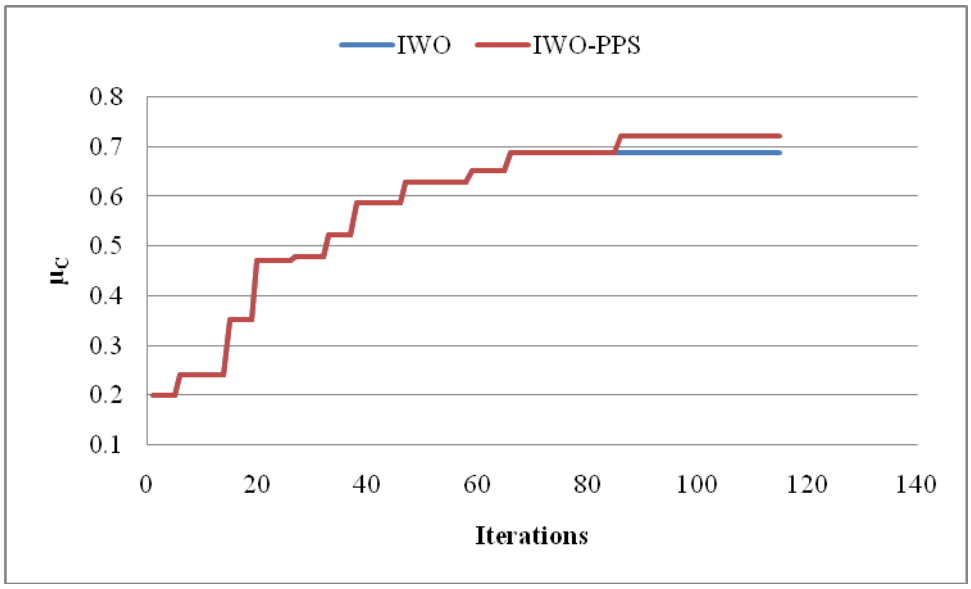

Figure 3.2: Convergence characteristics: Test system-IV, case-II.

Table 3.10: Optimal control variables for MO-OPF problem: Test system-V

Decision variables	Limits		Case-I	Case-II	Case-III	Case-IV
	min	max				
P_{G1} *(MW)*	50	200	114.09	106.83	72.201	89.378
P_{G2} *(MW)*	20	80	60.917	70.159	59.088	61.99
P_{G5} *(MW)*	15	50	24.378	37.587	50	31.787
P_{G8} *(MW)*	10	35	34.799	22.843	35	34.89
P_{G11} *(MW)*	10	30	27.154	18.919	30	30
P_{G13} *(MW)*	12	40	27.629	31.7306	40	40
V_{G1} *(p.u.)*	0.95	1.1	1.1	1.1	1.087288	1.1
V_{G2} *(p.u.)*	0.95	1.1	1.0914	1.0936	1.078176	1.1
V_{G5} *(p.u.)*	0.95	1.1	1.0655	1.064534	1.084644	1.081125
V_{G8} *(p.u.)*	0.95	1.1	1.0899	1.051373	1.097097	1.1
V_{G11} *(p.u.)*	0.95	1.1	1.0526	1.044599	1.080905	1.1
V_{G13} *(p.u.)*	0.95	1.1	1.0227	1.070466	1.081021	1.1
t_{11}	0.9	1.1	1.01	0.99	1.0	1.1
t_{12}	0.9	1.1	1.04	1.05	0.98	1.07
t_{15}	0.9	1.1	1.04	0.95	0.99	0.94
t_{36}	0.9	1.1	1.07	0.95	0.93	1.0
Q_{10} *(MVAr)*	0	5	1	1	4	5
Q_{12} *(MVAr)*	0	5	3	4	2	4
Q_{15} *(MVAr)*	0	5	3	1	2	1
Q_{17} *(MVAr)*	0	5	4	5	3	1
Q_{20} *(MVAr)*	0	5	1	4	4	5
Q_{21} *(MVAr)*	0	5	1	0	3	5
Q_{23} *(MVAr)*	0	5	2	4	0	5
Q_{24} *(MVAr)*	0	5	4	3	1	3
Q_{29} *(MVAr)*	0	5	1	4	5	5
Cost($/hr)	-	-	**835.121**	**855.921**	931.171	**875.426**
Emission (ton/hr)	-	-	**0.24447**	0.23927	**0.20564**	**0.21810**
P_L*(MW)*	-	-	5.567	**4.67**	**2.889**	**4.645**

Note: Highlighted text represents the best results.

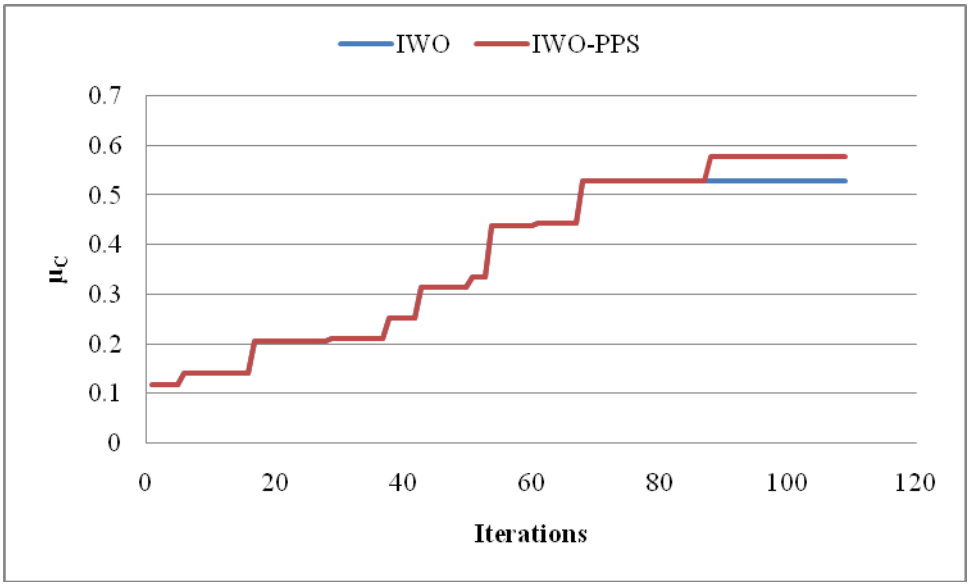

Figure 3.3: Convergence characteristics: Test system-IV, case-III.

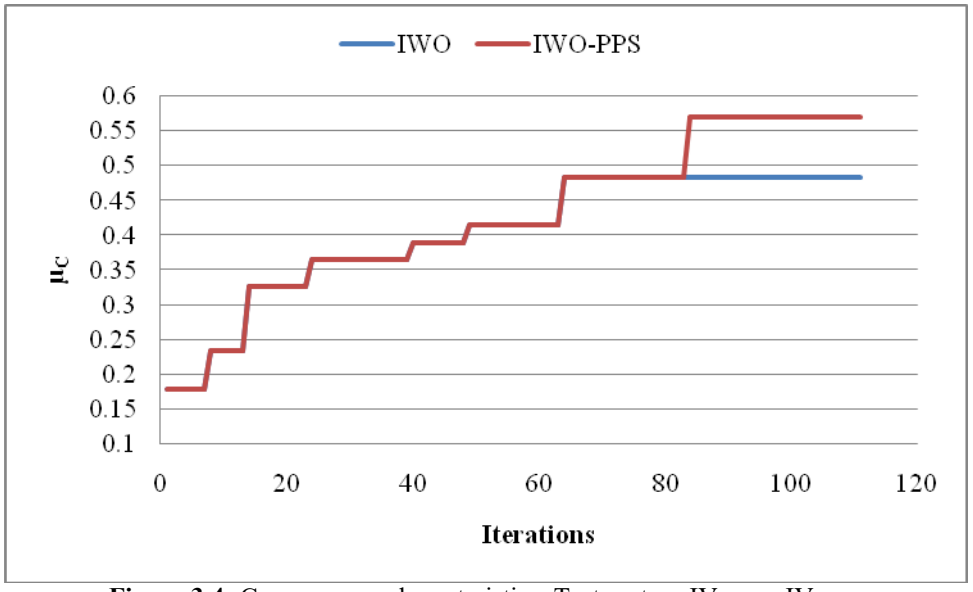

Figure 3.4: Convergence characteristics: Test system-IV, case-IV

Table 3.11: Descriptive statistics: Test system-IV, case-1

Technique	Worst (μ_C)	Mean (μ_C)	Best (μ_C)	SD	Observations
IWO	0.32387	0.39718	0.46108	0.0346	31
IWO-PPS	0.634	0.68886	0.77709	0.0333	31

Table 3.12: *t*-test (two sample, two tail) results for IWO-PPS technique versus IWO technique at α=0.05

Statistics	Test system-IV, case-I
t-calculated	33.818
t-critical	2

3.7 CONCLUSIONS

In this chapter, a non-interactive approach is successfully implemented to solve the MO-OPF problem. Being indistinct, the conflicting objectives have been characterized by their

membership functions employing fuzzy theory and these are further utilized for the implementation of the satisficing function. In order to search the high quality satisficing solutions, the IWO technique is integrated with the PPS method. The PPS method exploits the solution attained by the IWO technique. The effectiveness of the IWO-PPS technique is confirmed by testing it on three test systems and each system having four cases. In test system-III, the cardinal priority ranking attained by the IWO-PPS technique for case-I is 0.73377 and that is better than the other state of art techniques, *i.e.*, DE, ALC-PSO, KHA and OKHA. For cases II, III and IV, the cardinal priority ranking attained by the IWO-PPS technique is compared with the IWO technique. The cardinal priority ranking attained by the IWO-PPS technique is 0.55839, 0.94793 and 0.44576 for case-II, III, IV, respectively which shows that the IWO-PPS technique outperforms the IWO technique. Similar trends of results have been observed in test system-IV and V. Hence, it is concluded that the IWO-PPS technique has the capability to search the global best solution. Further, the ability of the IWO-PPS technique to search high-quality solution is confirmed by the comparative convergence characteristics. The robustness of the IWO-PPS technique is also examined by applying the *t*-test and found satisfactory.

CHAPTER-4

OPTIMAL POWER FLOW SOLUTION USING HYBRID INVASIVE WEED OPTIMIZATION AND SPACE TRANSFORMATION SEARCH TECHNIQUE

4.1 INTRODUCTION

In order to solve the complex optimization problems, various hybrid optimization techniques have been applied by the researchers [13,66,70]. The hybridization of different optimization techniques is a complex task since every technique has some pros and cons [205]. Hence, the researchers have explored various hybrid optimization techniques to search the optimum solution. Naidu and Ojha [126] have hybridized the *invasive weed optimization* (IWO) technique with space transformation search (STS) technique to solve various complex optimization problems. The STS is an evolutionary technique introduced by Wang *et al.* [199]. It takes inspiration from the opposition-based learning [193]. The STS technique transforms the current search space into a transformed search space and computes the new solutions in both the current and transformed search space simultaneously. This technique basically selects the best one from a solution and its opposite solution that reduces the computational time and the search direction is attained in the promising regions of the search space. Thus the STS technique enhances the probability to obtain the solutions that are closer to the global optimum solutions.

In this chapter, a hybrid optimization technique (IWO-STS) has been undertaken to solve OPF problem of a thermal generation system. In the IWO-STS technique, the IWO technique explores the search area and then the STS method exploits the promising search area. The effectiveness of the IWO-STS technique is tested on three IEEE test systems of OPF problem by considering fuel cost, pollutant emission, active power losses and total voltage magnitude deviations objectives sequentially and simultaneously. For obtaining the best non-dominated solution of MO-OPF problem, a non-interactive approach is used.

4.2 PROBLEM FORMULATION

The *multi-objective optimal power flow* (MO-OPF) problem is formulated with the aim to

optimize the objectives, *i.e.*, the fuel cost of thermal generator units, emission pollutant, active power losses and voltage magnitude deviations, simultaneously while satisfying the system constraints. The mathematical models of objective functions *i.e.*, fuel cost, emission pollutant, active power losses are discussed in detail in subsection 2.3.1 under Chapter 2. The fourth objective function *i.e.*, total voltage magnitude deviation with respect to 1 p.u. reference for all the load buses, is represented as under [214].

$$VMD = \sum_{k=1}^{N_{PQ}} \left| V_{Lk} - V_{reference} \right| \tag{4.1}$$

where V_{Lk} represents magnitude of voltage at load bus k; $V_{reference}$ represents the reference voltage magnitude in p.u. and N_{PQ} represents the number of buses.

Mathematically MO-OPF problem is stated as under:

Minimize $\left[F_C, E, P_{LOSS}, VMD\right]^T$ (4.2)

subjected to various equality and inequality constraints, which are given as:

Equality constraints: The following load flow equations represent the active and reactive power equality constraints [214]:

$$\sum_{k=1}^{N_{BUS}} \left(P_{Gk} - P_{Lk}\right) = \sum_{k=1}^{N_{BUS}} \sum_{l=1}^{N_{BUS}} \left|V_k\right| \left|V_l\right| \left|Y_{kl}\right| \cos\left(\delta_{kl} + \theta_k - \theta_l\right) \tag{4.3}$$

$$\sum_{k=1}^{N_{BUS}} \left(Q_{Gk} - Q_{Lk}\right) = -\sum_{k=1}^{N_{BUS}} \sum_{l=1}^{N_{BUS}} \left|V_k\right| \left|V_l\right| \left|Y_{kl}\right| \sin\left(\delta_{kl} + \theta_k - \theta_l\right) \tag{4.4}$$

where P_{Gk}, Q_{Gk} represent the active and reactive power generation available at the k^{th} bus, respectively; P_{Lk}, Q_{Lk} are the active and reactive power demand at the k^{th} bus, respectively; Y_{kl} and δ_{kl} represent the total admittance and admittance angle of the transmission line, which connect the k^{th} and l^{th} bus; N_{BUS} is the total number of buses.

Inequality constraints: The OPF problem is subjected to various inequality constraints that are discussed in detail in sub-section 2.3.2 under Chapter 2.

4.3 SPACE TRANSFORMATION SEARCH

The STS technique is presented by Wang *et al.* [199]. This is an evolutionary type technique, motivated from the opposition-based learning. The STS prohibits premature convergence and enhances the chances of finding the solutions nearer to the global optimum solution [200,204]. The STS transforms the current search area and solutions are simultaneously searched in the

current and transformed search area.

Let the current search area S has the solution $X \forall [A, B]$, and the new solution, $\overline{X}$ is generated in the transformed search area $\overline{S}$.For D-dimensional space, the new solution is generated as:

$$\overline{X}_{i,n} = \Delta - X_{i,n} \left(i = 1,2,..., NP; n = 1,2,..., D\right) \tag{4.5}$$

With

$$\Delta = k(A_n + B_n)\ ;\ k = ran[0,1] \tag{4.6}$$

where D is the number of decision variables; NP is the total population; A_n , B_n are the lower and upper values of n^{th} dimension decision variable, respectively.

If $\overline{X}_{i,n}$ violates its limits, then $\overline{X}_{i,n}$ is randomly initialized within limits $[A_n, B_n]$.

The solution is updated as follows:

$$X_{i,n} = \begin{cases} \overline{X}_{i,n}; & f\left(\overline{X}_{i,n}\right) > f\left(X_{i,n}\right) \\ X_{i,n}; & else \end{cases} (i = 1,2,..., NP; n = 1,2,..., D) \tag{4.7}$$

4.4 SOLUTION METHODOLOGY

For the OPF problem, decision variables are active power generated from thermal units, the magnitude of voltage for thermal units, transformer tap ratios and shunt compensator VAR values. The continuous type variables are the active power and the voltage magnitude of thermal units. The transformers tap ratios and the shunt compensator device output constitute discrete variables. The array of decision variables is given as [X] in Eq. (4.8)

$$X = \begin{matrix} P_{1,1} & \cdots & P_{1,NG-1}, & V_{1,1} & \cdots & V_{1,NG}, & Q_{1,1} & \cdots & Q_{1,NC}, & t_{1,1} & \cdots & t_{1,NT} \\ \vdots & & \vdots & \vdots & & \vdots & \vdots & & \vdots & \vdots & & \vdots \\ P_{G,1} & \cdots & P_{G,NG-1}, & V_{G,1} & \cdots & V_{G,NG}, & Q_{q,1} & \cdots & Q_{q,NC}, & t_{p,1} & \cdots & t_{p,NT} \end{matrix} \tag{4.8}$$

where P_G is power generated by thermal generators; V_G is voltage magnitude for all generating units; Q_q is the output of shunt devices and t_p is transformer tap ratio.

The following steps describe the implementation procedure of the IWO-STS technique for the OPF problem.

Step 1: The weeds are randomly initialized within the defined limits as per Eq. (2.36) and Eq. (2.37), respectively under Chapter 2.

Step 2: After initialization, the NR method is employed for the solution of the OPF problem corresponding to each weed in the population. The fitness function value is computed as per

Eq. (2.29) under Chapter 2.

Step 3: Weeds are arranged according to the best to the worst fitness function value and the new seeds are generated in current search space by using Eq. (2.32) under Chapter 2.

Step 4: The STS technique is applied to direct the current solution obtained by the IWO technique to transformed search space and the new solution is obtained for all the new seeds by using Eq. (4.5).

Step 5: The fitness function value is computed for the current solution and new solution in transformed search space simultaneously in each population and the solution is updated in the next cycle population, if required, by using Eq. (4.7).

Step 6: The next cycle population is arranged from the combination of the current population and transformed population according to the fitness function value.

Step 7: The step 2 continues until the termination criterion reaches.

For the MO-OPF problem, a non-interactive approach is applied to obtain the best non-dominated solution as discussed under section 3.3, Chapter 3. The membership value is computed by considering the minimum and the maximum (unacceptable) values of function corresponding to each objective function as per Eq. (3.3) under Chapter 3. The satisfaction level corresponding to one objective is computed with respect to others as per Eq. (3.2) under Chapter 3.

In order to achieve the highest satisfaction for all the objectives, the cardinal priority ranking, μ_c needs to maximize and is given as [174]:

$$\mu_c = \max(\min(\mu_1(F_C), \mu_2(E), \mu_3(P_{LOSS}), \mu_4(VMD))) \tag{4.9}$$

In order to restrict the solutions into a feasible operating region, the cumulative error of all constraint violations is figured out as per Eq. (3.7) under Chapter 3 is incorporated as a penalty in Eq. (4.9) as under.

$$\mu_c = \{\max(\min(\mu_1(F_C), \mu_2(E), \mu_3(P_{LOSS}), \mu_4(VMD)) - err)\} \tag{4.10}$$

Finally, by using Eq. (4.10), the cardinal priority ranking is computed as per Eq. (3.5) under Chapter 3.The procedure of implementation of the IWO-STS technique to solve the MO-OPF problem is represented with the flowchart as per Figure 4.1.

4.5 TEST SYSTEMS AND RESULTS

The effectiveness of the hybrid IWO-STS optimization technique is checked on three test systems, *i.e.,* test system-VI, test system-VII and test system-VIII. The test system-VI, test

system-VII and test system-VIII are IEEE 30-bus system, IEEE 57-bus and IEEE 118-bus system, respectively.

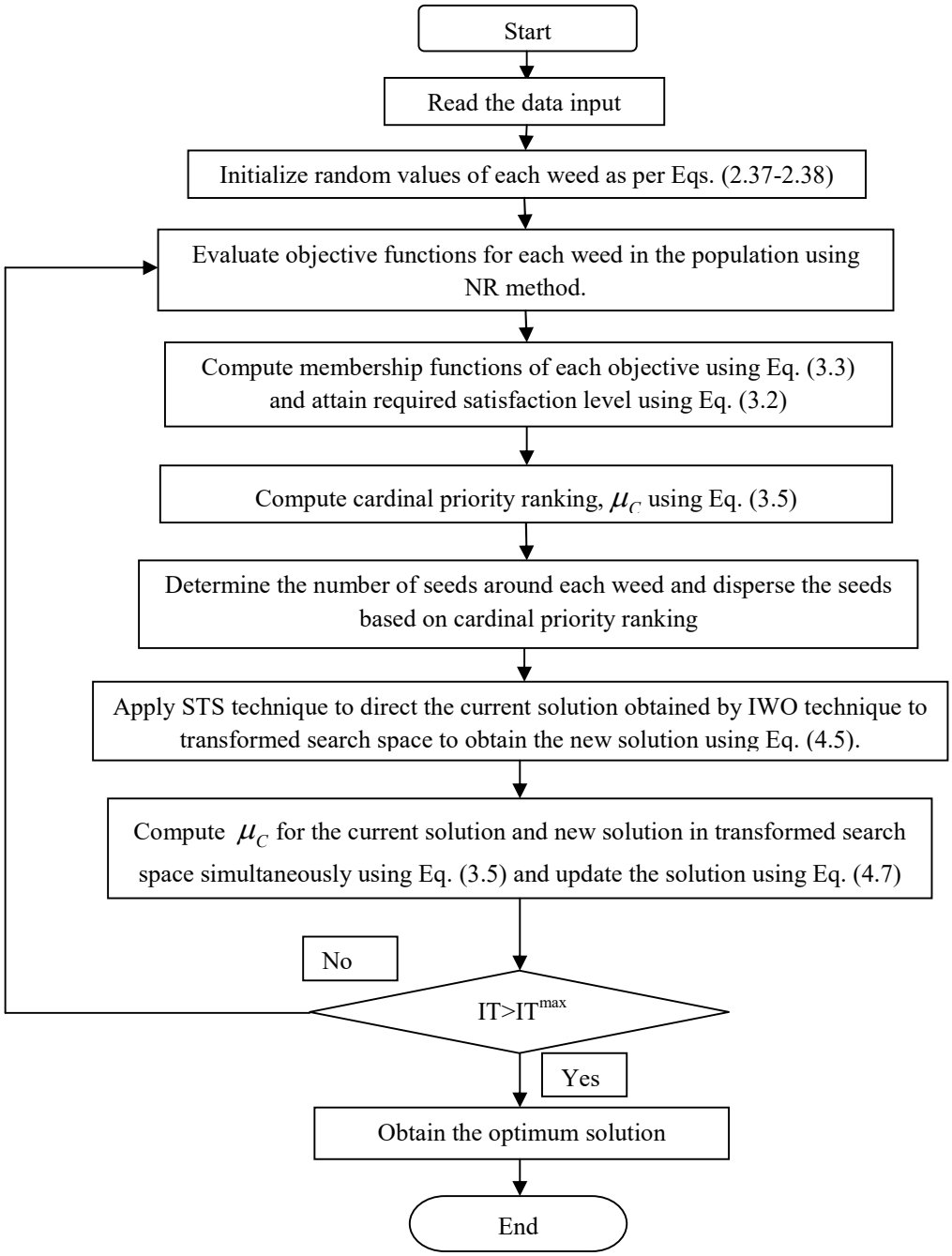

Figure 4.1: Flowchart of the implementation of IWO-STS technique for solving the MO-OPF problem

Test system-VI comprises of 41 transmission lines with 283.4 MW of total load demand. The system includes 5-active power thermal generator units, 41-transmission line branches, 24-load buses, 4-transformers tap position settings and 9-shunt compensators. Test system-VII includes 7-thermal generator units, 80-transmission line branches, 50-load buses,

17-transformer tap position settings, 3-shunt compensators and having 1250.8 MW of total load demand [144]. The generating limits of thermal units, operating cost and emission coefficients of thermal units, load data and transmission lines data for test system-VI are given in Tables A.1.1, A.1.2, A.1.3 and A.1.4, respectively under Appendix-A. The generating units, load and transmission lines data for test system-VII are given in Tables A.1.5, A.1.6 and A.1.7, respectively under Appendix-A. The test system-VIII includes 54-thermal generator units, 186-transmission line branches, 64-load buses, 9-transformer tap position settings, 12-shunt compensators and having 4242.0 MW of total load demand [202].The single-line diagram of test system-VIII is shown in Figure A.1.3 under Appendix-A. The generating units, load and transmission lines data for test system-VIII are provided in Tables A.1.10, A.1.11 and A.1.12, respectively under Appendix-A.

4.5.1 Parameter Tuning

The algorithm parameter selection affects the convergence characteristics and solution quality. The best values of IWO-STS parameters *i.e.,* modulation index, Initial SD, final SD, scaling parameter and inertia weight are set by executing the program multiple times. The high initial and small final SD values are required to sustain the balance between diversification and intensification capability of the IWO technique. The non-linear modulation index significantly influences the performance and inertia weight and scaling parameters enhance the solution quality of the IWO technique [126].The best parameter values of the IWO-STS technique are presented by Table 4.1.

Table 4.1: Best parameters values of IWO-STS technique

Parameter	**Values**
Population size (Initial)	20
SD (initial)	5-20
SD (final)	1
Seeds (maximum)	3
Seeds (minimum)	0
Non-linear modulation index	3-5
Scaling parameter	0.001-0.005
Inertia weight	0.8-1

4.5.2 Results and Discussion

The IWO-STS technique is applied in the FORTRAN-90 command line for the solution of the MO-OPF problem. Thirty-one trial runs have been taken for searching global best solution. The mean, worst results and the SD of results are evaluated to judge the robustness of the

IWO-STS technique. The IWO-STS technique is employed to solve single-objective OPF problem and seven cases of MO-OPF problems. The details of undertaken objectives in different cases are given as:

Case-I: Simultaneous minimization of the total fuel cost and emission pollutant.

Case-II: Simultaneous minimization of the emission pollutant and active power losses.

Case-III: Simultaneous minimization of the total fuel cost and active power losses.

Case-IV: Simultaneous minimization of the total fuel cost and total voltage magnitude deviations.

Case-V: Simultaneous minimization of the emission pollutant and total voltage magnitude deviations.

Case-VI: Simultaneous minimization of the active power losses and total voltage magnitude deviations.

Case-VII: Simultaneous minimization of the total fuel cost, emission pollutant, active power losses and total voltage magnitude deviations.

4.5.2.1 Test system-VI

The IWO-STS approach is employed to minimize total fuel cost, emission pollutant, active power losses and total voltage magnitude deviations, sequentially as well as simultaneously. The best, mean, worst results and the SD of results for the single objective output results of the IWO-STS technique are compared with results of established techniques and are given in Table 4.2. The effect of the STS technique is also investigated by comparing the results obtained by the IWO technique with the IWO-STS technique. Table 4.2 shows that the value of minimum quadratic fuel cost obtained by the IWO-STS technique is 799.73 $/hr that is better than the results reported by PSO [133], IPSO [133], JAYA [203], AGSO [43], SF-DE [28], AMTPG-JAYA [202] and IWO techniques. The best, mean and worst fuel cost attained with the IWO-STS technique is less in comparison to the cost attained with SF-DE [28], AMTPG-JAYA [202] and IWO techniques. The SD of results obtained by the IWO-STS technique is 0.0059, which is better than AMTPG-JAYA [202] and IWO results. However, the SD for the results provided by SF-DE [28] technique is better in comparison to the IWO-STS technique. To compare the computational cost of the optimization techniques, NFE has been computed, as CPU time depends on the hardware configuration of the machine, operating system *etc*. The NFE for IWO-STS is compared and found that the IWO-STS technique requires 7.41% less NFE in comparison to the IWO technique.

The minimum value of emission pollutant attained with the IWO-STS technique is 0.2047 ton/hr, that is better in comparison to the results reported by TLBO [117], LTLBO [117], SF-DE [28], NISSO [130] and IWO techniques. The mean and the worst values of the emission pollutant attained with the IWO-STS technique are superior in comparison to their counterparts. Further, the SD and NFE of the IWO-STS technique are better than the IWO technique. For minimization of active power losses, the results of IWO-STS are compared to that of its counterpart techniques *i.e.*, GA [82], PSO [82], EP [82], SF-DE [28] and AMTPG-JAYA [202]. The active power loss obtained by the IWO-STS technique is 3.33% less in comparison to the best reported result by AMTPG-JAYA technique [202]. The best, mean, and worst active power losses values attained with the IWO-STS technique are less as compared to SF-DE [28], AMTPG-JAYA [202] and IWO techniques.

Table 4.2: Statistical comparison of single-objective results: Test system-VI.

Techniques applied/indexes	Best	Mean	Worst	SD	NFE
F_C**($/hr)**					
PSO [133]	802.205	-	-	-	-
IPSO [133]	801.98	-	-	-	-
JAYA [203]	800.479	-	-	-	-
AGSO [43]	801.75	-	-	-	-
SF-DE [28]	800.413	800.415	800.419	0.0015	-
AMTPG-JAYA [202]	800.195	800.224	800.343	0.0063	-
IWO	816.61	816.67	817.13	0.1201	30160
IWO-STS	799.73	799.755	799.77	0.0059	28080
E**(ton/hr)**					
TLBO [117]	0.2124	0.2141	0.2156	-	-
LTLBO [117]	0.2047	0.2065	0.2104	-	-
SF-DE[28]	0.20482	0.20482	0.20482	0	-
NISSO [130]	0.20479	-	-	-	
IWO	0.20487	0.20493	0.20529	0.0001	31200
IWO-STS	0.2047	0.20476	0.20481	0.000046	29520
P_{LOSS}**(MW)**					
PSO [82]	3.43	-	-	-	-
EP [82]	3.335	-	-	-	-
GA [82]	3.37	-	-	-	-
SF-DE[28]	3.0844	3.0849	3.0857	0.0003	-
AMTPG-JAYA [202]	3.0802	3.0836	3.0937	0.0027	-
IWO	3.17	3.184	3.254	0.0144	34320
IWO-STS	2.981	2.987	2.991	0.00259	33120
VMD**(p.u.)**					
MSCA [17]	0.1030	-	-	-	-
IWO	0.1243	0.12876	0.12997	0.00196	31800
IWO-STS	0.1019	0.10222	0.1094	0.00135	31080

PSO: particle swarm optimization; IPSO: improved PSO; TLBO: teaching-learning-based optimization; AGSO: adaptive group search optimization; LTLBO: levy mutation based TLBO; SF-DE: superiority of feasibly solutions-DE; MSCA: modified sine cosine algorithm; GA: genetic algorithm; EP: evolutionary programming; AMTPG-JAYA: adaptive multiple teams perturbation-guiding Jaya; NISSO: novel improved social spider optimization

The total voltage magnitude deviations obtained by IWO-STS technique is 0.1019 p.u., which is 1.08% less in comparison to the best result provided by MSCA technique [17]. The

mean and the worst values of voltage magnitude deviations and the SD of results attained with the IWO-STS technique are better in comparison to the IWO technique. The optimum decision variable values provided by the IWO-STS technique for minimum fuel cost, emission pollutant, active power losses and voltage magnitude deviations are presented in Table 4.3.

Table 4.3: Optimum decision variables values: Test system-VI.

Decision variables (p.u.)	Limits		F_C (\$/h)	E (ton/h)	P_{LOSS} (MW)	VMD(p.u.)
	min	max				
P_{G1}	0.50	2.00	1.74113	0.6434	0.53192	1.7557
P_{G2}	0.20	0.80	0.50977	0.67292	0.79644	0.48698
P_{G5}	0.15	0.50	0.21065	0.49993	0.49383	0.22001
P_{G8}	0.10	0.35	0.22221	0.3499	0.3499	0.22723
P_{G11}	0.10	0.30	0.11645	0.2999	0.2998	0.12122
P_{G13}	0.12	0.40	0.12021	0.39991	0.39193	0.12012
V_{G1}	0.95	1.1	1.0998	1.0989	1.09889	1.0384
V_{G2}	0.95	1.1	1.08983	1.095785	1.09852	1.0209
V_{G5}	0.95	1.1	1.06655	1.094288	1.08124	1.00401
V_{G8}	0.95	1.1	1.07765	1.097330	1.09126	1.00308
V_{G11}	0.95	1.1	1.0999	1.097605	1.09975	1.03431
V_{G13}	0.95	1.1	1.0688	1.058517	1.098042	1.00101
Q_{10}	0.00	0.05	0.05	0.05	0.05	0.05
Q_{12}	0.00	0.05	0.05	0.05	0.02	0.01
Q_{15}	0.00	0.05	0.05	0.05	0.04	0.05
Q_{17}	0.00	0.05	0.05	0.05	0.02	0.00
Q_{20}	0.00	0.05	0.05	0.05	0.02	0.05
Q_{21}	0.00	0.05	0.05	0.05	0.02	0.05
Q_{23}	0.00	0.05	0.05	0.05	0.05	0.05
Q_{24}	0.00	0.05	0.05	0.03	0.02	0.05
Q_{29}	0.00	0.05	0.05	0.05	0.05	0.03
t_{11}	0.9	1.1	1.01	1.03	1.03	1.05
t_{12}	0.9	1.1	1.02	1.09	0.90	0.90
t_{15}	0.9	1.1	0.94	1.09	0.99	0.96
t_{36}	0.9	1.1	0.99	1.03	0.98	0.97
Cost (\$/hr)	-	-	**799.73**	943.738	961.120	803.557
Emission (ton/hr)	-	-	0.35866	**0.2047**	0.20734	0.36175
P_{LOSS}(MW)	-	-	8.6421	3.25	**2.981**	9.7285
Voltage deviation(p.u.)	-	-	1.65739	1.16274	1.96594	**0.1019**

Note: Highlighted text represents the best results.

This work employs a non-interactive approach for dealing with the MO-OPF problem. The cardinal priority ranking is computed for MOEA/D [214], ESDE-EC [144], ESDE-MC [144], MOABC/D [104], MPIO-COSR [38], IWO, IWO-STS techniques and the MO results are compared on the basis of cardinal priority ranking. The higher satisfaction level of the non-dominated solution is indicated by the higher value of cardinal priority ranking. Table 4.4 indicates that the cardinal priority ranking obtained with the IWO-STS technique for case-I, case-III and case-IV is 0.754611, 0.714265 and 0.85909, respectively which is better in comparison to its counterparts and IWO technique. For the remaining four cases, no results have been reported in the literature to the best of the author's information; therefore, the results for these four cases have been compared with the IWO technique. The cardinal priority ranking

achieved by the IWO-STS approach for case-II, case-V, case-VI and case-VII is 0.986692, 0.833095, 0.603169 and 0.53372, respectively, that is superior to IWO technique results. Hence, it is summarized that the IWO-STS technique provides better satisfying results for all the scenarios.

Further, Table 4.4 indicates that the NFE required by the IWO-STS technique is less in comparison to the IWO technique. The optimal decision variables obtained from the IWO-STS technique for the MO-OPF problem are given in Table 4.5.

Table 4.4: Comparison of results (multi-objective): Test system-VI

Case-I						
Technique	F_C(\$/hr)	E(ton/hr)	μ_C			NFE
MOEA/D [214]	833.72	0.2438	0.750104			-
ESDE-EC [144]	831.094	0.251	0.69898			-
ESDE-MC [144]	830.71	0.2483	0.717869			-
IWO	850.12	0.23196	0.676338			31790
IWO-STS	**837.872**	**0.24323**	**0.754611**			**29410**
Case-II						
Technique	E(ton/hr)	P_{LOSS}(MW)	μ_C			NFE
IWO	0.20534	3.27	0.956413			35400
IWO-STS	**0.20676**	**2.9161**	**0.986692**			**33760**
Case-III						
Technique	F_C(\$/hr)	P_{LOSS}(MW)	μ_C			NFE
MOEA/D [214]	835.36	4.9099	0.711399			-
ESDE-EC [144]	827.948	5.4524	0.612246			-
ESDE-MC [144]	827.159	5.227	0.651494			-
MOABC/D [104]	827.636	5.2451	0.64881			30000
MPIO-COSR [38]	831.557	5.1085	0.676094			-
IWO	866.092	4.999	0.579981			35180
IWO-STS	**845.808**	**4.784**	**0.714265**			**29920**
Case-IV						
Technique	F_C(\$/hr)	VMD(p.u.)	μ_C			NFE
MOEA/D [214]	799.99	0.354	0.856199			-
IWO	802.463	0.56574	0.725357			31800
IWO-STS	**802.589**	**0.3523**	**0.85909**			**30160**
Case-V						
Technique	E(ton/hr)	VMD(p.u.)	μ_C			NFE
IWO	0.29475	0.13991	0.312333			34080
IWO-STS	**0.23085**	**0.36403**	**0.833095**			**33180**
Case-VI						
Technique	P_{LOSS}(MW)	VMD(p.u.)	μ_C			NFE
IWO	5.31	0.79315	0.598664			33120
IWO-STS	**4.76**	**0.82276**	**0.603169**			**31200**
Case-VII						
Technique	F_C (\$/hr)	E (ton/hr)	P_{LOSS} (MW)	VMD (p.u.)	μ_C	NFE
IWO	874.07	0.21961	5.048	0.82742	0.513811	33180
IWO-STS	**870.98**	**0.22034**	**4.861**	**0.85153**	**0.53372**	**31800**

MOEA/D: multi objective evolutionary algorithm based decomposition; ESDE-EC: enhanced self adaptive DE-eigenvector crossover; ESDE-MC: enhanced self adaptive DE-mixed crossover; MOABC/D: multi-objective artificial bee colony algorithm based on decomposition; MPIO-COSR; modified pigeon inspired optimization algorithm-constraint objective sorting rule

4.5.2.2 Test system-VII

For test system-VII, the best, mean, worst results and the SD of results attained by the IWO-STS technique are compared with the state of the art techniques and are given in Table 4.6. The minimum total fuel cost attained by the IWO-STS technique is 41670.772 $/hr, which is less in comparison to the results reported by GABC [74], KH [143], SKH [143], ESDE-EC [144], ESDE-MC [144], FIDE [164], TSA [50] and IWO techniques. It is evident from operating cost results that IWO-STS technique is able to achieve better values of mean and worst results and superior SD in comparison to its counterpart techniques.

Table 4.5: Optimum decision variables for MO-OPF problem: Test system-VI

Decision variables (p.u.)	Limits		Case-I	Case-II	Case-III	Case-IV	Case-V	Case-VI	Case-VII
	min	max							
P_{G1}	0.50	2.00	1.1293	0.52435	1.1066	1.78895	1.03621	0.91004	0.90457
P_{G2}	0.20	0.80	0.61734	0.7898	0.5782	0.48982	0.59153	0.64981	0.64968
P_{G5}	0.15	0.50	0.26336	0.49955	0.3671	0.21215	0.28441	0.28132	0.29975
P_{G8}	0.10	0.35	0.34856	0.34981	0.3413	0.20081	0.33446	0.34979	0.34971
P_{G11}	0.10	0.30	0.27687	0.29974	0.2863	0.11974	0.25493	0.29982	0.29592
P_{G13}	0.12	0.40	0.25817	0.39991	0.2023	0.12001	0.39175	0.39175	0.38217
V_{G1}	0.95	1.1	1.088658	1.09929	1.099	1.0989	1.049402	1.099848	1.090218
V_{G2}	0.95	1.1	1.067475	1.09830	1.092478	1.0613	1.041428	1.099698	1.099486
V_{G5}	0.95	1.1	1.026480	1.08567	1.073135	1.03567	1.068947	1.062644	1.099105
V_{G8}	0.95	1.1	1.092281	1.08885	1.090815	1.05385	1.022715	1.099346	1.099096
V_{G11}	0.95	1.1	1.061569	1.09890	1.091536	1.0389	1.024563	1.099381	1.093201
V_{G13}	0.95	1.1	1.010694	1.09980	1.093103	1.0298	1.094847	1.094847	1.088857
Q_{10}	0.00	0.05	0.05	0.05	0.03	0.03	0.02	0.05	0.05
Q_{12}	0.00	0.05	0.02	0.05	0.03	0.05	0.03	0.05	0.05
Q_{15}	0.00	0.05	0.04	0.04	0.03	0.04	0.05	0.05	0.05
Q_{17}	0.00	0.05	0.02	0.05	0.04	0.03	0.04	0.05	0.05
Q_{20}	0.00	0.05	0.00	0.05	0.03	0.05	0.01	0.05	0.05
Q_{21}	0.00	0.05	0.01	0.05	0.01	0.05	0.04	0.05	0.05
Q_{23}	0.00	0.05	0.02	0.05	0.01	0.05	0.01	0.05	0.05
Q_{24}	0.00	0.05	0.00	0.05	0.03	0.05	0.03	0.05	0.05
Q_{29}	0.00	0.05	0.03	0.04	0.03	0.02	0.03	0.05	0.05
t_{11}	0.9	1.1	1.03	1.06	1.04	1.09	0.96	1.1	1.1
t_{12}	0.9	1.1	0.99	0.93	0.92	0.98	1.01	1.1	1.1
t_{15}	0.9	1.1	1.06	0.95	0.98	1.06	1.09	1.1	1.1
t_{36}	0.9	1.1	1.07	0.98	0.97	1.01	0.94	1.1	1.1
Cost($/hr)	-	-	**837.872**	964.667	**845.808**	**802.589**	857.905	870.47	**870.98**
Emission (ton/hr)	-	-	**0.24323**	**0.20676**	0.23941	0.37128	**0.23085**	0.22094	**0.22034**
P_{LOSS}(MW)	-	-	6.057	**2.9161**	**4.784**	9.749	5.8364	**4.76**	**4.861**
Voltage deviation (p.u.)	-	-	0.60623	2.07993	1.7717	**0.3523**	**0.36403**	**0.82276**	**0.85153**

Note: Highlighted text represents the best results.

For the second objective, the minimum value of emission pollutant achieved by the IWO-STS technique is 0.994 ton/hr, which is better by 8.53% in comparison to the previous

best reported result obtained by ESDE-MC [144] technique. The statistical results reveal that the mean, worst result values and SD of results attained by the ST-IWO technique is better in comparison to its counterpart techniques *i.e.,* KH [143], SKH [143], ESDE-EC [144], ESDE-MC [144].

Table 4.6: Statistical comparison of single-objective results: Test system-VII

Techniques applied/indexes	Best	Mean	Worst	SD	NFE
F_C(\$/hr)					
GABC [74]	41684.201	41686.729	41689.57	1.5814	-
FIDE [164]	41683	-	-	-	-
KH [143]	41681.352	41687.154	41700.592	4.6814	-
SKH [143]	41676.91	41679.044	41689.208	3.6486	-
ESDE-EC [144]	41677.754	41684.58	41697.41	6.0162	-
ESDE-MC [144]	41671.143	41674.17	41686.45	3.5790	-
TSA [50]	41685.01	41687.09	41689.05	1.169	-
IWO	41697.22	41700.15	41709.34	3.0534	45760
IWO-STS	41670.772	41671.383	41676.22	1.0112	38400
E(ton/hr)					
KH [143]	1.0811	1.0825	1.0868	0.0015	-
SKH [143]	1.0800	1.0810	1.0835	0.0011	-
ESDE-EC [144]	1.0807	1.0821	1.0844	0.0017	-
ESDE-MC [144]	1.0788	1.0800	1.0821	0.0010	-
SSO[130]	1.07024	-	-	-	-
NISSO [130]	1.03927	-	-	-	-
IWO	0.996	0.9988	1.0173	0.0039	50400
IWO-STS	0.994	0.9954	0.9963	0.0007	48720
P_{LOSS}(MW)					
FIDE [164]	10.687	-	-	-	-
KH [143]	11.216	12.027	13.528	0.636	-
SKH [143]	10.687	11.111	12.002	0.475	-
TSA [50]	12.473	12.54	12.60	0.037	-
IWO	12.51	12.67	12.96	0.1184	50160
IWO-STS	10.680	10.702	10.838	0.0311	48600
VMD(p.u.)					
TSA [50]	0.717	0.715	0.719	0.003	-
IWO	0.7158	0.7189	0.7351	0.0049	44000
IWO-STS	0.6882	0.6902	0.6985	0.0028	43680

GABC: guided artificial bee colony; FIDE: forced initialized DE; KH; krill herd; SKH: stud krill herd; ESDE-EC: enhanced self adaptive DE-eigenvector crossover; ESDE-MC: enhanced self adaptive DE-mixed crossover; TSA: tree seed algorithm; SSO: social spider optimization; NISSO: novel improved social spider optimization

Table 4.6 shows that the IWO-STS approach reduces the active power losses by 0.0655% in comparison to the best reported result attained by the SKH technique [143]. The IWO-STS technique provides better results with regard to the best, mean, and worst values of active power losses and better SD of results as compared to results attained by KH [143], SKH [143], TSA [50] and IWO techniques. For the forth objective function, "total voltage deviations", the IWO-STS results are better in comparison to TSA [50] and IWO techniques for best, mean and worst values along with SD and NFE. The optimum values of decision variables attained by the IWO-STS technique for fuel cost, emission pollutant, active power

losses and voltage magnitude deviations are presented in Table 4.7.

Table 4.7: Optimum decision variables values: Test system-VII

Decision variables (p.u.)	Limits		F_C ($/hr)	E (ton/hr)	P_{LOSS} (MW)	VMD(p.u.)
	min	max				
P_{G1}	0.00	5.7588	1.4133	2.28272	1.65571	3.17375
P_{G2}	0.00	1.50	0.8823	0.99948	0.31441	0.99908
P_{G3}	0.42	1.40	0.4556	1.29644	1.38644	0.84181
P_{G6}	0.00	1.50	0.7518	0.99968	0.99987	0.32064
P_{G8}	1.65	5.50	4.5742	3.04175	3.18175	3.63864
P_{G9}	0.00	1.50	0.9879	0.99397	0.99997	0.99224
P_{G12}	1.23	4.10	3.59209	3.07671	4.07671	2.7699
V_{G1}	0.95	1.1	1.03511	1.08340	1.05820	1.0239
V_{G2}	0.95	1.1	1.04612	1.07337	1.05040	1.0121
V_{G3}	0.95	1.1	1.04299	1.03952	1.05527	1.0092
V_{G6}	0.95	1.1	1.06056	1.06821	1.05208	1.0147
V_{G8}	0.95	1.1	1.07999	1.04983	1.04983	1.02343
V_{G9}	0.95	1.1	1.08521	1.01388	1.07381	1.01176
V_{G12}	0.95	1.1	1.04604	0.99363	1.05936	1.01399
Q_{18}	0.00	0.30	0.20	0.20	0.11	0.01
Q_{25}	0.00	0.30	0.13	0.20	0.15	0.05
Q_{53}	0.00	0.30	0.15	0.30	0.20	0.06
t_{19}	0.9	1.1	1.06	1.02	1.09	0.93
t_{20}	0.9	1.1	0.98	1.02	0.93	1.03
t_{31}	0.9	1.1	1.03	0.98	0.99	0.97
t_{35}	0.9	1.1	1.09	1.01	0.96	0.98
t_{36}	0.9	1.1	0.92	0.99	1.09	0.94
t_{37}	0.9	1.1	1.03	0.95	1.01	1.03
t_{41}	0.9	1.1	1.01	1.01	0.99	0.96
t_{46}	0.9	1.1	0.95	0.99	0.96	0.92
t_{54}	0.9	1.1	0.91	0.94	0.92	0.90
t_{58}	0.9	1.1	0.97	0.99	0.98	0.92
t_{59}	0.9	1.1	0.96	0.98	0.97	0.98
t_{65}	0.9	1.1	0.99	0.99	0.98	1.01
t_{66}	0.9	1.1	0.93	0.97	0.96	0.90
t_{71}	0.9	1.1	0.98	0.98	0.99	0.94
t_{73}	0.9	1.1	0.99	0.96	0.97	1.04
t_{76}	0.9	1.1	0.97	1.02	0.97	0.90
t_{80}	0.9	1.1	1.01	0.98	0.99	0.98
Cost ($/hr)	-	-	**41670.772**	45020.452	44611.18	45307.649
Emission (ton/hr)	-	-	1.341	**0.994**	1.107	1.320
P_{LOSS}(MW)	-	-	14.948	18.27	**10.68**	22.816
Voltage deviation (p.u.)	-	-	1.49305	1.42755	1.56173	**0.6882**

Note: Highlighted text represents the best results.

The MO-OPF simulation results of IWO-STS technique is compared with the well-established techniques and is presented in Table 4.8. For case-I, the obtained results are compared with ESDE [144], ESDE-EC [144], ESDE-MC [144], MODFA [37], MPIO-COSR [38] and IWO techniques. The cardinal priority ranking obtained by IWO-STS technique is 0.543791, which is better in comparison to its counterparts. It shows that IWO-STS technique is capable of achieving the most satisfied result with respect to both of the objectives. For case-III, the IWO-STS technique is able to achieve the cardinal priority ranking as high as 0.905131,

which indicates that IWO-STS technique is capable of searching the best non-dominated solution in comparison to FIDE [164], ESDE [144], ESDE-EC [144], ESDE-MC [144] and IWO techniques results.

Table 4.8: Comparison of results (multi-objective): Test system-VII

Case-I					
Technique	F_C(\$/hr)	E(ton/hr)	μ_C		NFE
ESDE [144]	42863.32	1.2662	0.125378		-
ESDE-EC [144]	42863.21	1.2387	0.216896		-
ESDE-MC [144]	42857.49	1.2191	0.288043		-
MODFA [37]	43174.57	1.2679	0.134039		-
MPIO-COSR [38]	43131.274	1.2314	0.260771		-
IWO	43169.96	1.031	0.539782		51040
IWO-STS	**43156.63**	**1.030**	**0.543791**		**47040**
Case-II					
Technique	E(ton/hr)	P_{LOSS}(MW)	μ_C		NFE
IWO	1.183	12.35	0.376		52000
IWO-STS	**1.123**	**13.771**	**0.619182**		**49280**
Case-III					
Technique	F_C(\$/hr)	P_{LOSS}(MW)	μ_C		NFE
FIDE [164]	42006.14	12.367	0.859788		-
ESDE [144]	42020.74	12.215	0.873011		-
ESDE-EC [144]	42013.34	11.967	0.893874		-
ESDE-MC [144]	41998.36	11.841	0.904317		-
IWO	42065.46	11.88	0.891424		46920
IWO-STS	**42015.6**	**11.71**	**0.905131**		**38440**
Case-IV					
Technique	F_C(\$/hr)	*VMD* (p.u.)	μ_C		NFE
IWO	42217.71	1.2624	0.237737		45080
IWO-STS	**42714.54**	**0.814354**	**0.70132**		**44280**
Case-V					
Technique	E(ton/hr)	*VMD* (p.u.)	μ_C		NFE
IWO	1.189	1.25869	0.337688		45760
IWO-STS	**1.125**	**0.97166**	**0.620404**		**44280**
Case-VI					
Technique	P_{LOSS}(MW)	*VMD*(p.u.)	μ_C		NFE
IWO	11.988	1.23765	0.263053		42840
IWO-STS	**13.362**	**1.13606**	**0.438187**		**38440**
Case-VII					
Technique	F_C (\$/hr)	E (ton/hr)	P_{LOSS} (MW)	*VMD* (p.u.)	μ_C	NFE
IWO	42107.14	1.225	11.634	1.2586	0.24921	48520
IWO-STS	**42747.77**	**1.109**	**14.07**	**0.84659**	**0.663658**	**46920**

Note: Highlighted text represents the best results.

ESDE: enhanced self adaptive DE; ESDE-EC: enhanced self adaptive DE-eigenvector crossover; ESDE-MC: enhanced self adaptive DE-mixed crossover; MODFA: multi-objective dimension-based firefly algorithm; FIDE: forced initialized DE; MPIO-COSR: modified pigeon inspired optimization algorithm-constraint objective sorting rule

For remaining cases, as per the best of author's information, no results are reported in literature. Therefore, the results obtained by IWO-STS and IWO techniques are compared and it has been found that IWO-STS technique is able to outperform the IWO technique in each

scenario in terms of solution quality and computational efforts. The optimum decision variables attained by IWO-STS technique for MO-OPF problem are given in Table 4.9.

Table 4.9: Optimum decision variables for MO-OPF problem: Test system-VII

Decision variables (p.u.)	Limits		Case-I	Case-II	Case-III	Case-IV	Case-V	Case-VI	Case-VII
	min	max							
P_{G1}	0.00	5.758	1.92975	1.10549	1.41307	1.24678	1.10069	1.92958	1.1642
P_{G2}	0.00	1.50	0.95447	0.98023	0.6602	0.97841	0.98865	0.95447	0.98865
P_{G3}	0.42	1.40	0.98864	0.98905	0.67904	0.97837	0.99858	0.98864	0.98852
P_{G6}	0.00	1.50	0.99086	0.9881	0.90161	0.96362	0.97896	0.99086	0.98806
P_{G8}	1.65	5.50	3.25238	3.82843	3.91846	3.73342	3.83434	3.25238	3.75434
P_{G9}	0.00	1.50	0.99897	0.98904	0.9895	0.99342	0.99045	0.99898	0.99045
P_{G12}	1.23	4.10	3.52672	3.76534	4.0633	3.75806	3.76706	3.52672	3.77453
V_{G1}	0.95	1.1	1.05020	1.01937	1.05942	1.035806	1.02907	1.05021	1.01937
V_{G2}	0.95	1.1	1.05630	1.01616	1.06268	1.021183	1.02696	1.05630	1.01609
V_{G3}	0.95	1.1	1.05024	1.02124	1.05126	0.998102	0.99622	1.05025	1.02124
V_{G6}	0.95	1.1	1.05998	1.01655	1.05916	1.011630	1.02116	1.05373	1.01656
V_{G8}	0.95	1.1	1.08035	1.03915	1.06925	1.029055	1.03915	1.04035	1.02915
V_{G9}	0.95	1.1	1.04981	1.01958	1.05548	1.012842	1.00512	1.03772	1.01958
V_{G12}	0.95	1.1	1.04936	1.02252	1.05202	1.012340	1.02252	1.04935	1.02252
Q_{18}	0.00	0.30	0.06	0.03	0.06	0.03	0.04	0.05	0.03
Q_{25}	0.00	0.30	0.12	0.12	0.12	0.09	0.08	0.12	0.12
Q_{53}	0.00	0.30	0.05	0.05	0.17	0.04	0.04	0.05	0.05
t_{19}	0.9	1.1	0.95	0.93	0.95	0.93	0.94	0.96	0.94
t_{20}	0.9	1.1	1.03	1.03	1.08	1.03	1.02	1.03	1.03
t_{31}	0.9	1.1	1.06	0.98	1.05	0.97	0.98	1.05	0.99
t_{35}	0.9	1.1	0.96	1.01	1.03	1.01	1.02	0.97	1.01
t_{36}	0.9	1.1	1.09	0.93	1.05	0.94	0.94	1.09	0.93
t_{37}	0.9	1.1	1.03	1.01	1.07	1.02	1.02	1.03	1.02
t_{41}	0.9	1.1	0.99	0.98	1.02	0.97	0.96	0.98	0.98
t_{46}	0.9	1.1	0.92	0.95	0.93	0.93	0.94	0.92	0.94
t_{54}	0.9	1.1	0.91	0.93	0.94	0.91	0.92	0.92	0.93
t_{58}	0.9	1.1	0.98	0.94	0.98	0.92	0.92	0.98	0.95
t_{59}	0.9	1.1	0.97	0.99	0.97	0.98	0.99	0.97	0.99
t_{65}	0.9	1.1	1.02	1.02	1.01	1.02	1.03	1.03	1.02
t_{66}	0.9	1.1	0.95	0.93	0.96	0.92	0.93	0.95	0.94
t_{71}	0.9	1.1	0.99	0.94	0.99	0.95	0.95	0.99	0.94
t_{73}	0.9	1.1	0.95	1.03	1.03	1.04	1.04	0.95	1.03
t_{76}	0.9	1.1	0.95	0.93	0.99	0.92	0.92	0.95	0.93
t_{80}	0.9	1.1	1.01	0.98	1.02	0.99	0.98	1.02	0.99
Cost ($/hr)	-	-	**43156.63**	42721.85	**42015.60**	**42714.53**	42802.86	43155.8	**42747.77**
Emission (ton/hr)	-	-	**1.030**	**1.123**	1.227	1.105	**1.125**	1.030	**1.109**
P_{LOSS}(MW)	-	-	13.38	**13.77**	**11.71**	14.41	15.073	**13.36**	**14.07**
Voltage deviation (p.u.)	-	-	1.334805	0.838516	1.28601	**0.814354**	**0.971663**	**1.13606**	**0.84659**

Note: Highlighted text represents the best results.

4.5.2.3 Test system-VIII

For test system-VIII, the best, mean, worst results and the SD of results obtained by IWO-STS technique is compared to its counterpart techniques and are presented in Table 4.10. The minimum total fuel cost attained by the IWO-STS technique is 128431.03 $/hr, that is less in

comparison to the results reported by TLBO [30], GPU-PSO [154], ICBO [31], MSA [114], IPM [80], GSA [27], SSO [130], NISSO [130], AMTPG-JAYA [202] and IWO techniques. The results indicate that the IWO-STS technique is competent to attain better values of mean and worst results and superior SD in comparison to the IWO technique.

Table 4.10: Statistical comparison of single-objective results: Test system-VIII

Techniques applied/indexes	Best	Mean	Worst	SD	NFE
F_C(\$/hr)					
TLBO [30]	129682.844	-	-	-	-
GPU-PSO [154]	129627.03	-	-	-	-
ICBO [31]	135121.57	-	-	-	-
MSA [114]	129640.72	-	-	-	-
IPM [80]	129720.70	-	-	-	-
GSA [27]	129565	-	-	-	-
SSO [130]	132080.41	-	-	-	-
NISSO [130]	129879.45	-	-	-	-
AMTPG-JAYA [202]	129428.703	-	-	-	-
IWO	128621.02	129017.21	129198.89	132.138	140800
IWO-STS	128431.03	128514.88	128581.03	48.008	120120
E(ton/hr)					
IWO	5.824	5.8898	5.967	0.0341	138880
IWO-STS	5.367	5.3935	5.421	0.0173	113520
P_{LOSS}(MW)					
IWO	78.383	80.80	83.87	1.935	156160
IWO-STS	73.048	74.905	76.691	0.9877	126720
VMD (p.u.)					
IWO	1.1241	1.14426	1.16544	0.01096	141120
IWO-STS	1.001795	1.00264	1.00498	0.00088	130640

TLBO: teaching learning based optimization; GPU-PSO; graphic processing unit- particle swarm optimizer;ICBO:improved colliding bodies optimization; MSA: moth swarm algorithm; IPM: interior point method; GSA; gravitational search algorithm; SSO: social spider optimization; NISSO: novel improved social spider optimization; AMTPG-JAYA: adaptive multiple teams perturbation-guiding Jaya

For the second objective, the minimum emission pollutant value attained by the IWO-STS technique is 5.367 ton/hr, which is less than by 8.515% in comparison to the IWO technique. The statistical results reveal that the mean, worst result values and SD of results attained by the IWO-STS technique are better as compared to the IWO technique. Table 4.10 shows that the IWO-STS approach reduces the active power losses by 7.303% and total voltage deviations by 12.21% in comparison to the IWO technique. The IWO-STS technique provides better results with regard to the best, mean, and worst values along with SD and NFE for the objectives “active power losses and total voltage deviations.”The optimum values of decision variables attained by the IWO-STS technique for fuel cost, emission pollutant, active power losses and voltage magnitude deviations are presented in Table 4.11. The comparative convergence characteristics of IWO-STS and IWO techniques are presented in Figures 4.2-4.5 for fuel cost, emission pollutant, active power loss and voltage magnitude deviation, respectively. Hence, this is established that the IWO-STS technique exhibits superior

convergence characteristics and avoids the stagnation to the local best solutions.

Table 4.11: Optimum decision variables values: Test system-VIII

Decision variables (p.u.)	Limits		F_C ($/hr)	E(ton/hr)	P_{LOSS} (MW)	VMD (p.u.)
	min	max				
P_{G1}	0.0	1.00	0.26037	0.28665	0.33337	0.28572
P_{G4}	0.0	1.00	0.00014	0.29876	0.26669	0.26734
P_{G6}	0.0	1.00	0.000121	0.21224	0.23622	0.24745
P_{G8}	0.0	1.00	0.000032	0.26673	0.23343	0.23452
P_{G10}	1.65	5.50	3.99193	3.45664	3.75562	3.41345
P_{G12}	0.555	1.85	0.87829	0.71123	0.87334	0.62223
P_{G15}	0.0	1.00	0.20012	0.24556	0.24729	0.20034
P_{G18}	0.0	1.00	0.10003	0.23223	0.19777	0.23455
P_{G19}	0.0	1.00	0.20933	0.11127	0.13333	0.11676
P_{G24}	0.0	1.00	0.00011	0.25668	0.24664	0.26455
P_{G25}	0.96	3.20	1.94176	1.79975	1.82334	1.73344
P_{G26}	1.242	4.14	2.80821	2.25445	2.21477	2.21237
P_{G27}	0.0	1.00	0.10036	0.25556	0.22113	0.27786
P_{G31}	0.0	1.07	0.081004	0.26673	0.25439	0.25676
P_{G32}	0.0	1.00	0.17243	0.25567	0.22254	0.28873
P_{G34}	0.0	1.00	0.000024	0.17866	0.16662	0.19982
P_{G36}	0.0	1.00	0.090132	0.19788	0.18871	0.18534
P_{G40}	0.0	1.00	0.45023	0.41233	0.41165	0.34544
P_{G42}	0.0	1.00	0.40083	0.25668	0.32281	0.20345
P_{G46}	0.0	1.19	0.187	0.14564	0.14225	0.18778
P_{G49}	0.912	3.04	1.96383	2.25445	2.38871	2.44332
P_{G54}	0.0	1.48	0.49654	0.31234	0.49966	0.29734
P_{G55}	0.0	1.00	0.29041	0.22566	0.26996	0.20063
P_{G56}	0.0	1.00	0.30006	0.26456	0.33869	0.24343
P_{G59}	0.765	2.55	1.52336	1.55676	1.72337	1.52334
P_{G61}	0.78	2.60	1.47572	1.75778	1.77681	1.75677
P_{G62}	0.0	1.00	0.000108	0.13345	0.11134	0.14563
P_{G65}	1.473	4.91	3.58642	3.32347	3.40044	3.18766
P_{G66}	1.476	4.92	3.49242	3.49766	3.44492	3.41134
P_{G69}	0.0	8.052	4.36241	3.08622	2.117403	3.55411
P_{G70}	0.0	1.00	0.000106	0.33454	0.36776	0.26679
P_{G72}	0.0	1.00	0.000012	0.26567	0.19402	0.28785
P_{G73}	0.0	1.00	0.000031	0.14567	0.15295	0.15673
P_{G74}	0.0	1.00	0.16008	0.17885	0.21998	0.12456
P_{G76}	0.0	1.00	0.24	0.23342	0.26887	0.21342
P_{G77}	0.0	1.00	0.00011	0.19566	0.17768	0.16783
P_{G80}	1.731	5.77	4.38959	4.28877	4.22113	4.23454
P_{G85}	0.0	1.00	0.000081	0.15545	0.11982	0.15673
P_{G87}	0.0	1.04	0.03125	0.17556	0.12233	0.17222
P_{G89}	2.121	7.07	5.04955	4.11233	4.07766	4.19974
P_{G90}	0.0	1.00	0.000403	0.13323	0.11991	0.14567
P_{G91}	0.0	1.00	0.000201	0.12234	0.16643	0.11633
P_{G92}	0.0	1.00	0.080122	0.12347	0.12274	0.13567
P_{G99}	0.0	1.00	0.000207	0.17341	0.12776	0.19998
P_{G100}	1.056	3.52	2.33124	2.15565	2.14492	2.25677
P_{G103}	0.0	1.40	0.41005	0.42346	0.43376	0.42244
P_{G104}	0.0	1.00	0.000008	0.12445	0.02944	0.14439
P_{G105}	0.0	1.00	0.030932	0.09445	0.12653	0.14364
P_{G107}	0.0	1.00	0.267413	0.20073	0.25665	0.217008
P_{G110}	0.0	1.00	0.07534	0.08776	0.098443	0.05556
P_{G111}	0.0	1.36	0.34442	0.41224	0.45644	0.4345

Table 4.11: Optimum decision variables values: Test system-VIII (Continued)

Decision variables (p.u.)	Limits		F_C ($/hr)	E(ton/hr)	P_{LOSS} (MW)	VMD (p.u.)
	min	max				
P_{G112}	0.0	1.00	0.37161	0.30366	0.33458	0.26784
P_{G113}	0.0	1.00	0.092123	0.11123	0.11199	0.10986
P_{G116}	0.0	1.00	0.000002	0.12223	0.13522	0.06654
V_{G1}	0.95	1.1	0.98771	0.99986	0.98933	0.99766
V_{G4}	0.95	1.1	1.01513	1.014887	1.0177	1.01356
V_{G6}	0.95	1.1	1.0108	1.01887	1.01321	1.01751
V_{G8}	0.95	1.1	1.0378	1.02192	1.0276	1.02333
V_{G10}	0.95	1.1	1.0514	1.04001	1.0413	1.04112
V_{G12}	0.95	1.1	1.0012	1.01127	1.0142	1.01456
V_{G15}	0.95	1.1	0.9998	0.987853	0.98737	0.98788
V_{G18}	0.95	1.1	0.9991	0.99988	0.99773	0.99453
V_{G19}	0.95	1.1	0.9996	0.977665	0.97332	0.97456
V_{G24}	0.95	1.1	1.0112	1.01965	1.0296	1.01833
V_{G25}	0.95	1.1	1.02898	1.01773	1.02211	1.01567
V_{G26}	0.95	1.1	1.06914	1.04223	1.04265	1.0411
V_{G27}	0.95	1.1	1.00415	1.00111	1.00188	1.0011
V_{G31}	0.95	1.1	0.9982	0.98577	0.97775	0.99991
V_{G32}	0.95	1.1	1.0035	1.01445	1.0143	1.01411
V_{G34}	0.95	1.1	1.0111	1.01866	1.0233	1.01593
V_{G36}	0.95	1.1	1.0106	1.02334	1.0118	1.01934
V_{G40}	0.95	1.1	1.00011	1.01244	1.01132	1.01212
V_{G42}	0.95	1.1	1.0083	1.01324	1.01822	1.01554
V_{G46}	0.95	1.1	1.0326	1.01655	1.0172	1.01564
V_{G49}	0.95	1.1	1.0422	1.02866	1.0311	1.02665
V_{G54}	0.95	1.1	1.0207	1.01554	1.01945	1.01344
V_{G55}	0.95	1.1	1.0205	1.02551	1.0244	1.02123
V_{G56}	0.95	1.1	1.0195	1.01334	1.0124	1.0132
V_{G59}	0.95	1.1	1.0397	1.0222	1.0233	1.02121
V_{G61}	0.95	1.1	1.0482	1.04675	1.04313	1.04113
V_{G62}	0.95	1.1	1.0442	1.02456	1.0304	1.02766
V_{G65}	0.95	1.1	1.0622	1.04998	1.0513	1.0438
V_{G66}	0.95	1.1	1.0583	1.04345	1.0411	1.04344
V_{G69}	0.95	1.1	1.0399	1.05656	1.06131	1.0468
V_{G70}	0.95	1.1	1.0205	1.01236	1.0253	1.01672
V_{G72}	0.95	1.1	1.0201	1.01445	1.00202	1.01356
V_{G73}	0.95	1.1	1.0224	1.02123	1.0326	1.02122
V_{G74}	0.95	1.1	1.0057	1.00156	1.00291	1.00111
V_{G76}	0.95	1.1	0.9888	0.98874	0.98766	0.98244
V_{G77}	0.95	1.1	1.0103	1.02924	1.0333	1.03455
V_{G80}	0.95	1.1	1.0208	1.0153	1.01121	1.01633
V_{G85}	0.95	1.1	1.0272	1.0223	1.0212	1.02335
V_{G87}	0.95	1.1	1.0433	1.0267	1.02877	1.02887
V_{G89}	0.95	1.1	1.0284	1.01123	1.01212	1.01112
V_{G90}	0.95	1.1	1.00592	1.03872	1.0302	1.0353
V_{G91}	0.95	1.1	1.00694	1.0522	1.0502	1.0534
V_{G92}	0.95	1.1	1.0103	1.0145	1.0214	1.01452
V_{G99}	0.95	1.1	1.0182	1.0245	1.0223	1.02009
V_{G100}	0.95	1.1	1.0187	1.0183	1.0122	1.01609
V_{G103}	0.95	1.1	1.0106	1.00544	1.0022	1.005045
V_{G104}	0.95	1.1	1.00687	1.00109	1.00187	1.002087
V_{G105}	0.95	1.1	1.00593	1.0224	1.0226	1.02998
V_{G107}	0.95	1.1	0.9973	0.99448	0.98889	0.98676
V_{G110}	0.95	1.1	1.01397	1.02112	1.01226	1.02335
V_{G111}	0.95	1.1	1.0249	1.04997	1.01616	1.02433

Table 4.11: Optimum decision variables values: Test system-VIII (Continued)

Decision variables (p.u.)	Limits		F_C ($/hr)	E(ton/hr)	P_{LOSS} (MW)	VMD (p.u.)
	min	max				
V_{G112}	0.95	1.1	1.00456	1.0188	1.0214	1.01499
V_{G113}	0.95	1.1	1.00567	1.00122	1.00211	1.00433
V_{G116}	0.95	1.1	1.0582	1.0287	1.0399	1.04112
Q_{34}	0.0	0.30	0.02	0.12	0.11	0.13
Q_{44}	0.0	0.30	0.06	0.14	0.15	0.12
Q_{45}	0.0	0.30	0.22	0.15	0.20	0.17
Q_{46}	0.0	0.30	0.11	0.13	0.10	0.14
Q_{48}	0.0	0.30	0.05	0.16	0.19	0.13
Q_{74}	0.0	0.30	0.24	0.15	0.21	0.13
Q_{79}	0.0	0.30	0.24	0.15	0.15	0.14
Q_{82}	0.0	0.30	0.23	0.16	0.19	0.16
Q_{83}	0.0	0.30	0.20	0.14	0.14	0.14
Q_{105}	0.0	0.30	0.13	0.12	0.19	0.14
Q_{107}	0.0	0.30	0.02	0.18	0.16	0.20
Q_{110}	0.0	0.30	0.18	0.18	0.17	0.14
t_8	0.9	1.1	1.01	0.97	0.99	0.98
t_{32}	0.9	1.1	1.09	1.01	1.01	1.02
t_{36}	0.9	1.1	1.03	0.99	0.97	0.98
t_{51}	0.9	1.1	1.02	1.02	1.02	1.02
t_{93}	0.9	1.1	0.99	1.02	1.01	1.01
t_{95}	0.9	1.1	1.01	1.01	1.02	1.01
t_{102}	0.9	1.1	0.98	0.98	0.98	0.99
t_{107}	0.9	1.1	0.97	1.02	1.01	1.02
t_{127}	0.9	1.1	1.02	1.01	1.02	1.01
Cost ($/hr)	-	-	**128431.035**	129773.837	130244.576	129652.64
Emission (ton/hr)	-	-	7.388	**5.367**	5.415	5.4473
P_{LOSS}(MW)	-	-	81.87	76.769	**73.048**	78.692
Voltage deviation (p.u.)	-	-	1.15539	1.056668	1.113395	**1.001795**

Note: Highlighted text represents the best results.

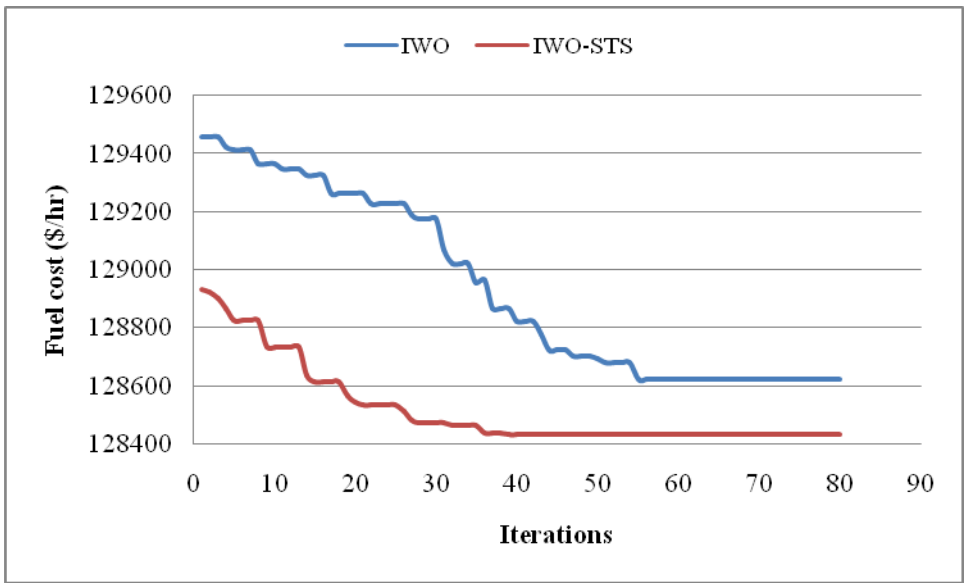

Figure 4.2: Convergence characteristics for fuel cost: Test system-VIII

Table 4.12 shows that the cardinal priority ranking obtained by the IWO-STS technique is 0.643297 for case-I, which is better in comparison to the IWO technique. It demonstrated

that the IWO-STS technique is competent to attain the most satisfied result corresponding to both of the objectives.

Table 4.12: Comparison of results (multi-objective): Test system-VIII

Case-I					
Technique	F_C($/hr)	E(ton/hr)	μ_C		NFE
IWO	128509.69	6.144	0.560195		143360
IWO-STS	**128681.78**	**6.044**	**0.643297**		**110880**
Case-II					
Technique	E(ton/hr)	P_{LOSS}(MW)	μ_C		NFE
IWO	5.683	77.762	0.394006		136640
IWO-STS	**5.456**	**74.391**	**0.841688**		**116160**
Case-III					
Technique	F_C($/hr)	P_{LOSS}(MW)	μ_C		NFE
IWO	128578.98	81.055	0.018399		153720
IWO-STS	**129620.66**	**78.198**	**0.337881**		**129600**
Case-IV					
Technique	F_C($/hr)	VMD(p.u.)	μ_C		NFE
IWO	128734.14	1.17855	0.190212		146160
IWO-STS	**129103.67**	**1.14216**	**0.367604**		**133480**
Case-V					
Technique	E(ton/hr)	VMD(p.u.)	μ_C		NFE
IWO	5.804	1.140621	0.023243		145600
IWO-STS	**6.144**	**1.10923**	**0.236973**		**116160**
Case-VI					
Technique	P_{LOSS}(MW)	VMD(p.u.)	μ_C		NFE
IWO	74.843	1.09548	0.308121		153720
IWO-STS	**75.127**	**1.06975**	**0.530939**		**129600**
Case-VII					
Technique	F_C($/hr)	E(ton/hr)	P_{LOSS}(MW)	VMD(p.u.)	μ_C	NFE
IWO	129865.7	5.405	79.632	1.12299	0.125539	143640
IWO-STS	**129779.3**	**5.39**	**77.499**	**1.02797**	**0.182163**	**133480**

Note: Highlighted text represents the best results.

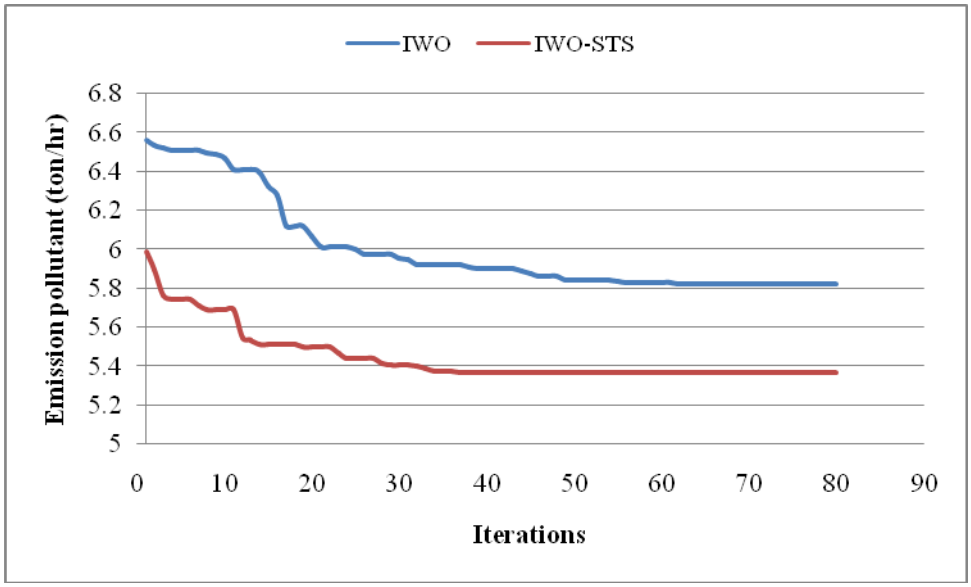

Figure 4.3: Convergence characteristics for emission pollutant: Test system-VIII

It is also clear from Table 4.12 that the IWO-STS technique has better performance

than the IWO technique for cases II-VII with respect to the solution quality and computational efforts. Hence, it is concluded that opposition-based learning of the STS technique improves the convergence process of the search algorithm. The optimum values of decision variables attained by IWO-STS techniques are presented in Table 4.13.

Figure 4.4: Convergence characteristics for active power losses: Test system-VIII

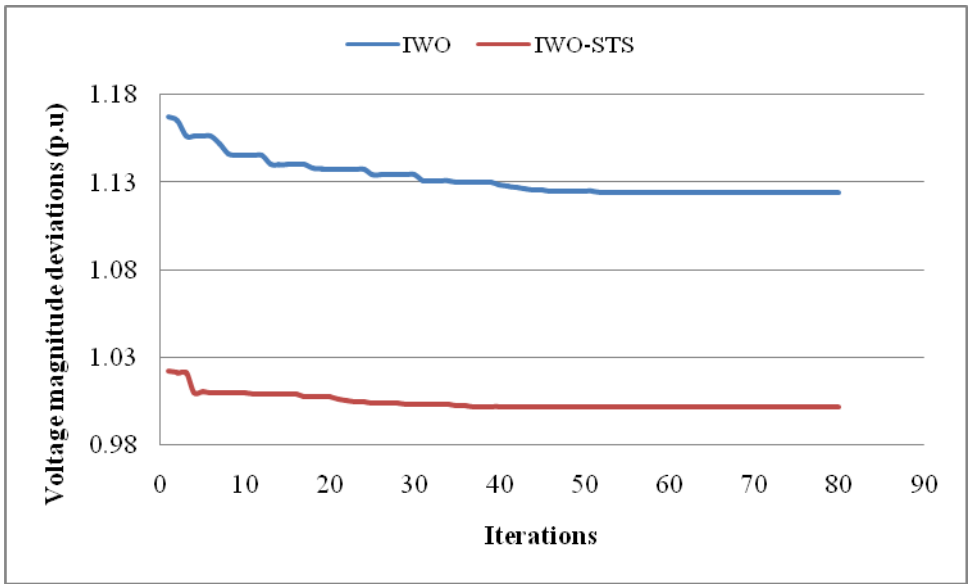

Figure 4.5: Convergence characteristics for voltage magnitude deviations: Test system-VIII

Table 4.13: Optimum decision variables for MO-OPF problem: Test system-VIII

Decision variables (p.u.)	Limits		Case-I	Case-II	Case-III	Case-IV	Case-V	Case-VI	Case-VII
	min	max							
P_{G1}	0.0	1.00	0.34166	0.38887	0.29551	0.31612	0.37211	0.22766	0.30456
P_{G4}	0.0	1.00	0.16533	0.29999	0.25221	0.19777	0.14345	0.25593	0.25569
P_{G6}	0.0	1.00	0.15144	0.21266	0.24457	0.19466	0.11511	0.24553	0.25556
P_{G8}	0.0	1.00	0.10346	0.25343	0.27782	0.16766	0.032444	0.26545	0.26558

Table 4.13: Optimum decision variables for MO-OPF problem: Test system-VIII (Continued)

Decision variables (p.u.)	Limits		Case-I	Case-II	Case-III	Case-IV	Case-V	Case-VI	Case-VII
	min	max							
P_{G10}	1.65	5.50	3.90244	3.77336	3.45673	3.85444	3.92312	3.56543	3.42123
P_{G12}	0.555	1.85	0.87544	0.85773	0.65577	0.87521	0.85175	0.81224	0.67455
P_{G15}	0.0	1.00	0.18566	0.24881	0.22541	0.21677	0.192345	0.24255	0.21223
P_{G18}	0.0	1.00	0.019388	0.19937	0.21562	0.11984	0.010733	0.23347	0.21226
P_{G19}	0.0	1.00	0.16555	0.13555	0.11126	0.17885	0.17435	0.12736	0.10097
P_{G24}	0.0	1.00	0.18455	0.21444	0.25566	0.19995	0.13604	0.25754	0.28657
P_{G25}	0.96	3.20	1.97853	1.86332	1.76453	1.97443	1.90655	1.72234	1.78766
P_{G26}	1.242	4.14	2.70733	2.23554	2.23565	2.34533	2.72637	2.27765	2.21234
P_{G27}	0.0	1.00	0.19331	0.19112	0.26776	0.16791	0.19938	0.21223	0.28986
P_{G31}	0.0	1.07	0.21062	0.254338	0.26567	0.21125	0.21656	0.29123	0.27646
P_{G32}	0.0	1.00	0.21724	0.23349	0.29655	0.26524	0.21852	0.27883	0.28897
P_{G34}	0.0	1.00	0.038664	0.15442	0.18543	0.03234	0.033466	0.18998	0.18665
P_{G36}	0.0	1.00	0.11266	0.16333	0.18995	0.16545	0.118466	0.19874	0.19654
P_{G40}	0.0	1.00	0.49344	0.43366	0.36766	0.478844	0.48554	0.41112	0.38976
P_{G42}	0.0	1.00	0.35744	0.32337	0.21228	0.366441	0.34527	0.29346	0.22338
P_{G46}	0.0	1.19	0.183305	0.14338	0.16455	0.183405	0.18334	0.15933	0.17665
P_{G49}	0.912	3.04	2.19239	2.42331	2.29877	2.43398	2.19033	2.24729	2.28664
P_{G54}	0.0	1.48	0.52676	0.47665	0.29987	0.53336	0.51596	0.41116	0.30003
P_{G55}	0.0	1.00	0.24575	0.28876	0.21226	0.25566	0.25165	0.23433	0.20096
P_{G56}	0.0	1.00	0.31533	0.33996	0.22643	0.34333	0.32553	0.31348	0.22346
P_{G59}	0.765	2.55	1.64566	1.69377	1.58031	1.67966	1.61515	1.63344	1.51445
P_{G61}	0.78	2.60	1.67321	1.76528	1.71232	1.68821	1.68133	1.71238	1.78671
P_{G62}	0.0	1.00	0.00428	0.12334	0.15477	0.02488	0.00401	0.10365	0.13577
P_{G65}	1.473	4.91	3.40633	3.42644	3.24569	3.55963	3.42266	3.32344	3.26554
P_{G66}	1.476	4.92	3.40155	3.40009	3.43334	3.45155	3.41341	3.53326	3.41223
P_{G69}	0.0	8.052	3.63074	2.66164	3.44032	3.01254	4.29323	2.52117	3.16198
P_{G70}	0.0	1.00	0.33558	0.37769	0.26669	0.34866	0.23556	0.38465	0.31776
P_{G72}	0.0	1.00	0.04563	0.19442	0.26345	0.16773	0.003363	0.29984	0.26754
P_{G73}	0.0	1.00	0.05627	0.12125	0.13998	0.05637	0.039442	0.17577	0.13237
P_{G74}	0.0	1.00	0.21187	0.21222	0.14323	0.21087	0.19184	0.19274	0.15443
P_{G76}	0.0	1.00	0.24553	0.24336	0.20092	0.24053	0.24453	0.23349	0.22342
P_{G77}	0.0	1.00	0.009467	0.01938	0.19644	0.009667	0.005944	0.19988	0.19504
P_{G80}	1.731	5.77	4.27677	4.19973	4.36564	4.22776	4.21556	4.19987	4.27344
P_{G85}	0.0	1.00	0.00224	0.11999	0.14565	0.00211	0.001714	0.16558	0.16785
P_{G87}	0.0	1.04	0.041166	0.12292	0.17233	0.066612	0.044331	0.16532	0.17644
P_{G89}	2.121	7.07	4.37366	4.00766	4.15668	4.35564	4.32533	4.17668	4.19873
P_{G90}	0.0	1.00	0.007652	0.01891	0.11136	0.007352	0.003562	0.10001	0.13387
P_{G91}	0.0	1.00	0.007654	0.15773	0.12336	0.009631	0.009924	0.17399	0.12003
P_{G92}	0.0	1.00	0.015365	0.11974	0.14573	0.015465	0.013365	0.13987	0.16554
P_{G99}	0.0	1.00	0.032215	0.03677	0.17545	0.03005	0.001215	0.13675	0.17665
P_{G100}	1.056	3.52	2.19445	2.1669	2.2123	2.11442	2.11844	2.16542	2.24444
P_{G103}	0.0	1.40	0.46083	0.44876	0.41264	0.48883	0.47083	0.41211	0.40676
P_{G104}	0.0	1.00	0.01561	0.02988	0.14567	0.01861	0.00567	0.12464	0.14334
P_{G105}	0.0	1.00	0.03875	0.03265	0.11364	0.03953	0.03917	0.09445	0.11234
P_{G107}	0.0	1.00	0.25148	0.25593	0.21677	0.2418	0.24644	0.25982	0.20122
P_{G110}	0.0	1.00	0.095554	0.095587	0.05673	0.090477	0.093554	0.09788	0.086329
P_{G111}	0.0	1.36	0.45787	0.44456	0.40345	0.44447	0.44783	0.41234	0.40345
P_{G112}	0.0	1.00	0.31235	0.32655	0.31564	0.30544	0.31343	0.30983	0.36434
P_{G113}	0.0	1.00	0.08888	0.10099	0.12455	0.08788	0.089419	0.12339	0.12347
P_{G116}	0.0	1.00	0.03292	0.13115	0.04934	0.12226	0.00122	0.12563	0.10093
V_{G1}	0.95	1.1	0.98553	0.98129	0.99763	0.97355	0.98645	0.99985	0.997655
V_{G4}	0.95	1.1	1.00215	1.0184	1.01489	1.00217	1.00235	1.0165	1.014332
V_{G6}	0.95	1.1	1.01712	1.01133	1.01745	1.0189	1.01801	1.0164	1.01766

Table 4.13: Optimum decision variables for MO-OPF problem: Test system-VIII (Continued)

Decision variables (p.u.)	Limits		Case-I	Case-II	Case-III	Case-IV	Case-V	Case-VI	Case-VII
	min	max							
V_{G8}	0.95	1.1	1.02522	1.0298	1.02123	1.02412	1.02622	1.0221	1.02276
V_{G10}	0.95	1.1	1.05113	1.0455	1.04004	1.0593	1.05001	1.0419	1.04144
V_{G12}	0.95	1.1	1.01126	1.0134	1.01561	1.01105	1.01132	1.01199	1.01745
V_{G15}	0.95	1.1	0.99247	0.98773	0.98887	0.997765	0.995034	0.976653	0.98745
V_{G18}	0.95	1.1	0.95698	0.99986	0.99676	0.96866	0.95998	0.97553	0.99006
V_{G19}	0.95	1.1	0.98922	0.98773	0.97675	0.98255	0.98925	0.96476	0.97875
V_{G24}	0.95	1.1	1.01114	1.02022	1.01865	1.0245	1.01204	1.0219	1.01856
V_{G25}	0.95	1.1	1.02945	1.02112	1.01653	1.02566	1.03084	1.0196	1.01656
V_{G26}	0.95	1.1	1.04942	1.04112	1.0423	1.04665	1.05042	1.0409	1.04344
V_{G27}	0.95	1.1	1.0124	1.00199	1.00165	1.0104	1.0022	1.00193	1.00176
V_{G31}	0.95	1.1	0.99163	0.97885	0.98773	0.98963	0.998656	0.99872	0.98598
V_{G32}	0.95	1.1	1.01943	1.0174	1.01477	1.01902	1.020474	1.0106	1.01435
V_{G34}	0.95	1.1	1.0137	1.02522	1.01678	1.016	1.0101	1.0216	1.01655
V_{G36}	0.95	1.1	1.0135	1.0109	1.0198	1.0125	1.014163	1.0231	1.0204
V_{G40}	0.95	1.1	1.01932	1.01533	1.01234	1.01882	1.00213	1.0108	1.01196
V_{G42}	0.95	1.1	1.02055	1.01998	1.01544	1.0212	1.02125	1.01665	1.01465
V_{G46}	0.95	1.1	1.0213	1.01665	1.01544	1.0207	1.0203	1.01676	1.01622
V_{G49}	0.95	1.1	1.0386	1.0329	1.0268	1.0377	1.0395	1.0299	1.02865
V_{G54}	0.95	1.1	1.0103	1.01994	1.0136	1.0113	1.0123	1.01666	1.01423
V_{G55}	0.95	1.1	1.0216	1.0276	1.02396	1.0201	1.0232	1.0211	1.02166
V_{G56}	0.95	1.1	1.0115	1.0121	1.0133	1.0119	1.0109	1.0144	1.01223
V_{G59}	0.95	1.1	1.0412	1.0276	1.0231	1.0422	1.0433	1.0222	1.0211
V_{G61}	0.95	1.1	1.03744	1.04433	1.0424	1.04704	1.03754	1.04665	1.04522
V_{G62}	0.95	1.1	1.03468	1.0319	1.02345	1.03438	1.03466	1.0279	1.02611
V_{G65}	0.95	1.1	1.0527	1.05003	1.04433	1.0522	1.05437	1.05006	1.04854
V_{G66}	0.95	1.1	1.05022	1.0408	1.04482	1.0477	1.05172	1.0417	1.04012
V_{G69}	0.95	1.1	1.04952	1.05943	1.03998	1.0542	1.04761	1.05993	1.05656
V_{G70}	0.95	1.1	1.01503	1.0259	1.01332	1.01532	1.01513	1.02112	1.0143
V_{G72}	0.95	1.1	1.0198	1.00222	1.0137	1.0155	1.0214	1.0112	1.01387
V_{G73}	0.95	1.1	1.0311	1.0336	1.02043	1.0321	1.0316	1.0253	1.0202
V_{G74}	0.95	1.1	1.00215	1.00303	1.00121	1.00285	1.00288	1.0021	1.00145
V_{G76}	0.95	1.1	0.98873	0.98792	0.98422	0.98773	0.98773	0.97888	0.98465
V_{G77}	0.95	1.1	1.0217	1.0311	1.02456	1.0317	1.0255	1.0362	1.02876
V_{G80}	0.95	1.1	1.0145	1.01191	1.01645	1.0125	1.0147	1.0101	1.01496
V_{G85}	0.95	1.1	1.0231	1.02002	1.0243	1.0211	1.0311	1.0206	1.02334
V_{G87}	0.95	1.1	1.0285	1.02887	1.0219	1.0245	1.02805	1.02009	1.0255
V_{G89}	0.95	1.1	1.01926	1.01265	1.01024	1.01961	1.01946	1.01129	1.01034
V_{G90}	0.95	1.1	1.05557	1.0399	1.0345	1.0537	1.05751	1.0388	1.03754
V_{G91}	0.95	1.1	1.05029	1.0512	1.0534	1.05129	1.052262	1.0509	1.0511
V_{G92}	0.95	1.1	1.0266	1.0204	1.01445	1.0255	1.0207	1.0186	1.01556
V_{G99}	0.95	1.1	1.0286	1.0253	1.0214	1.0266	1.0282	1.0201	1.02421
V_{G100}	0.95	1.1	1.0108	1.0138	1.0174	1.0144	1.0101	1.01962	1.0176
V_{G103}	0.95	1.1	1.00638	1.00377	1.00512	1.0064	1.00838	1.00196	1.00532
V_{G104}	0.95	1.1	1.00288	1.00188	1.00231	1.00266	1.00289	1.00129	1.00232
V_{G105}	0.95	1.1	1.01183	1.01256	1.0216	1.01083	1.01083	1.0276	1.0212
V_{G107}	0.95	1.1	0.98618	0.97899	0.98456	0.98486	0.99018	0.97976	0.98665
V_{G110}	0.95	1.1	1.01343	1.01223	1.02534	1.01032	1.01463	1.0212	1.02234
V_{G111}	0.95	1.1	1.02033	1.01664	1.0756	1.01934	1.02042	1.0572	1.07112
V_{G112}	0.95	1.1	1.0199	1.0211	1.01345	1.0166	1.0151	1.0199	1.0199
V_{G113}	0.95	1.1	1.00312	1.00233	1.00132	1.00309	1.00393	1.00154	1.00129
V_{G116}	0.95	1.1	1.04199	1.03733	1.0281	1.03999	1.04241	1.02987	1.0232
Q_{34}	0.0	0.30	0.14	0.13	0.12	0.12	0.11	0.16	0.13
Q_{44}	0.0	0.30	0.19	0.13	0.13	0.18	0.19	0.12	0.12

Table 4.13: Optimum decision variables for MO-OPF problem: Test system-VIII (Continued)

Decision variables (p.u.)	Limits		Case-I	Case-II	Case-III	Case-IV	Case-V	Case-VI	Case-VII
	min	max							
Q_{45}	0.0	0.30	0.21	0.21	0.18	0.20	0.21	0.21	0.17
Q_{46}	0.0	0.30	0.09	0.09	0.14	0.09	0.09	0.12	0.15
Q_{48}	0.0	0.30	0.12	0.19	0.14	0.11	0.13	0.17	0.13
Q_{74}	0.0	0.30	0.21	0.23	0.15	0.20	0.22	0.20	0.13
Q_{79}	0.0	0.30	0.17	0.17	0.13	0.16	0.19	0.15	0.14
Q_{82}	0.0	0.30	0.20	0.20	0.17	0.19	0.24	0.18	0.15
Q_{83}	0.0	0.30	0.21	0.15	0.14	0.18	0.21	0.15	0.17
Q_{105}	0.0	0.30	0.16	0.21	0.15	0.15	0.14	0.18	0.14
Q_{107}	0.0	0.30	0.19	0.14	0.21	0.18	0.18	0.18	0.20
Q_{110}	0.0	0.30	0.15	0.12	0.12	0.14	0.12	0.24	0.19
t_8	0.9	1.1	0.98	0.98	0.97	0.99	0.97	0.98	0.98
t_{32}	0.9	1.1	1.02	1.02	1.01	1.01	1.03	1.01	1.02
t_{36}	0.9	1.1	0.98	0.98	0.99	0.99	0.99	0.97	0.98
t_{51}	0.9	1.1	1.01	1.03	1.01	1.01	1.02	1.02	1.02
t_{93}	0.9	1.1	1.01	1.02	1.02	1.02	1.02	1.01	1.01
t_{95}	0.9	1.1	1.02	1.02	1.01	1.01	1.01	1.02	1.01
t_{102}	0.9	1.1	0.99	0.99	0.99	0.98	0.98	0.98	0.99
t_{107}	0.9	1.1	1.02	1.01	1.01	1.01	1.02	1.02	1.02
t_{127}	0.9	1.1	1.01	1.01	1.01	1.02	1.01	1.01	1.02
Cost ($/hr)	-	-	**128681.7**	129765.6	**129620.6**	**129103.6**	128509.6	129952.4	**129779.2**
Emission (ton/hr)	-	-	**6.044**	**5.456**	5.43994	5.917	**6.144**	5.368	**5.390**
P_{LOSS} (MW)	-	-	82.157	**74.391**	**78.198**	77.709	84.005	**75.127**	**77.499**
Voltage deviation (p.u.)	-	-	1.11994	1.106505	1.02396	**1.14216**	**1.109227**	**1.06975**	**1.027969**

Note: Highlighted text represents the best results.

4.5.3 Statistical Analysis

The success rate of the IWO-STS technique is confirmed by its robustness. The two sample *t*-test is performed with 5% significant level to confirm the robustness of the IWO-STS technique. Table 4.14 presents the *t*-test results for test system-VI, test system-VII and test system-VIII with single objective functions. It is evident from Table 4.14 that the IWO-STS technique has better performance in comparison to the SF-DE [28], AMTPG-JAYA [202] and IWO techniques for test system-VI for all the objectives. The robustness of the IWO-STS technique for test system-VII is analyzed as compared to KH [143], SKH [143], ESDE-EC [144], ESDE-MC [144], GABC [74], TSA [50] techniques and the robustness for test system-VIII is analyzed in comparison to IWO technique. The results of the *t*-test for all the objectives show that the *p* value is less than 0.05 which confirms the superiority of the IWO-STS technique over other techniques. The statistical results confirm that there is a significant difference between the performance of the IWO-STS technique and its counterpart techniques.

Table 4.14: Two sample *t*-test results at α=0.05

	p value	Null hypothesis	Is statistical significant difference?
Test system-VI			
Fuel cost ($/hr)			
IWO-STS vs. SF-DE	3.6656E-147	Reject	Yes
IWO-STS vs. AMTPG-JAYA	3.5368E-123	Reject	Yes
IWO-STS vs. IWO	5.1695E-122	Reject	Yes
Emission pollutant (ton/hr)			
IWO-STS vs. SF-DE	2.34493E-10	Reject	Y es
IWO-STS vs. IWO	4.69283E-12	Reject	Yes
Active power losses (MW)			
IWO-STS vs. SF-DE	3.0885E-110	Reject	Yes
IWO-STS vs. AMTPG-JAYA	2.46108E-97	Reject	Yes
IWO-STS vs. IWO	5.3358E-61	Reject	Yes
Voltage magnitude deviations (p.u.)			
IWO-STS vs. IWO	3.7726E-56	Reject	Yes
Test system-VII			
Fuel cost ($/hr)			
IWO-STS vs. GABC	3.11053E-48	Reject	Yes
IWO-STS vs. KH	2.81993E-26	Reject	Yes
IWO-STS vs. SKH	1.9034E-16	Reject	Yes
IWO-STS vs. ESDE-EC	1.16631E-17	Reject	Yes
IWO-STS vs. ESDE-MC	9.7232E-05	Reject	Yes
IWO-STS vs. TSA	8.97802E-54	Reject	Yes
IWO-STS vs. IWO	1.63992E-50	Reject	Yes
Emission pollutant (ton/hr)			
IWO-STS vs. KH	2.17376E-96	Reject	Yes
IWO-STS vs. SKH	3.75E-102	Reject	Yes
IWO-STS vs. ESDE-EC	1.54862E-93	Reject	Yes
IWO-STS vs. ESDE-MC	1.4553E-103	Reject	Yes
IWO-STS vs. IWO	1.18501E-05	Reject	Yes
Active power losses (MW)			
IWO-STS vs. KH	6.07319E-17	Reject	Yes
IWO-STS vs. SKH	1.15847E-05	Reject	Yes
IWO-STS vs. TSA	6.19757E-88	Reject	Yes
IWO-STS vs. IWO	1.40594E-65	Reject	Yes
Voltage magnitude deviations (p.u.)			
IWO-STS vs. TSA	1.19115E-40	Reject	Yes
IWO-STS vs. IWO	2.04147E-36	Reject	Yes
Test system-VIII			
Fuel cost ($/hr)			
IWO-STS vs. IWO	4.19697E-28	Reject	Yes
Emission pollutant (ton/hr)			
IWO-STS vs. IWO	4.70938E-60	Reject	Yes
Active power losses (MW)			
IWO-STS vs. IWO	4.08732E-22	Reject	Yes
Voltage magnitude deviations (p.u.)			
IWO-STS vs. IWO	7.4291E-60	Reject	Yes

4.6 CONCLUSIONS

In this chapter, a hybrid optimization technique that integrates the IWO and STS techniques (IWO-STS) is applied to solve the MO-OPF problem. The IWO-STS technique simultaneously

evaluates the solution in the current and transformed search area. This feature enhances the possibility of finding the solutions nearer to the global optimum and accelerates the convergence speed. This IWO-STS approach reduces the computational complexity and evades premature convergence. In this chapter, the four OPF objective functions *i.e.*, total fuel cost, emission pollutant, active power losses, total voltage magnitude deviations, are minimized sequentially as well as simultaneously. The non-interactive approach is utilized to reduce the computation difficulties during the Pareto front generation and to search the best non-dominated solution. The IWO-STS technique is tested on three test systems *i.e.,* test system-VI, test system-VII, and test system-VIII. For test system-VI, the IWO-STS technique achieves minimum fuel cost and pollutant emission values as 799.73 $/hr and 0.2047 ton/hr, respectively showing improvement over the best reported results. The active power losses and total voltage magnitude deviations are reduced by 3.33% and 1.08% in comparison to AMTPG-JAYA technique and MSCA technique, respectively. For test system-VII, the IWO-STS technique achieves minimum total fuel cost as 41670.772 $/hr, that is less than the results reported by well-established techniques. The minimum emission pollutant achieved by the IWO-STS technique is reduced by 8.53% in comparison to ESDE-MC technique. The results of the IWO-STS technique are superior for active power losses and total voltage magnitude deviations in comparison to its counterpart techniques. For test system-VIII, the minimum total fuel cost attained by the IWO-STS technique is 128431.03 $/hr, that is less than the results reported by its counterpart techniques. Further, the results of the IWO-STS technique are superior for emission pollutant, active power losses and total voltage magnitude deviations in comparison to IWO techniques. The comparison of multi-objective results is carried out with the other counterpart techniques *i.e.*, MOEA/D, ESDE-EC, ESDE-MC, FIDE, MODFA, DE-CH, MPIO-COSR and AMTPG-JAYA. The simulation results show the ability of the IWO-STS approach to provide better cardinal priority ranking value for all seven cases of three test systems. The comparative convergence characteristics show that the IWO-STS technique is capable of searching better quality solution. The robustness of the IWO-STS technique is validated by using the *t*-test. The *t*-test results reveal the significant difference between the performance of the IWO-STS technique and its counterpart techniques. In view of the above, this is concluded that the IWO-STS technique is capable of searching the global best result with the least computational efforts and the non-interactive approach has the ability to obtain the best non-dominated solution.

CHAPTER-5

OPTIMAL POWER FLOW SOLUTION INCORPORATING WIND UNITS USING INTEGRATED OPTIMIZATION TECHNIQUE

5.1 INTRODUCTION

In today's electricity networks, the *wind power* (WP) is one of the foremost sources of renewable energy generation. The accurate forecasting of WP generation is very difficult due to the wind speed uncertainty. This necessitates a factor that compensates the effect of the underestimation and overestimation of WP over its real availability [8,10,61,108]. The extensive study of the *optimal power flow* (OPF) problem has been carried out considering the conventional fuel based generators in the system [3,11,32,65,118,207]. Further, the studies have been conducted for the systems having wind-thermal coordination, but predominately, the deterministic approach is employed considering the ideal forecast conditions [14,34,46,98]. However, the intermittent nature of WP necessitates adding the uncertainty factor while formulating the optimization problem [145,147,156,166-167].

The cost of conventional fuel is a major portion of utility expenditure. The presence of WP uncertainty in the system needs a cost factor to be included while formulating the system model. The overall cost minimization of the wind-thermal system is the foremost objective considered for the OPF problem. The increasing environmental concerns necessitate including the emission pollutant minimization model in the OPF problem. Moreover, the minimization of active power loss is a significant objective to include in the OPF problem. Furthermore, the presence of WP sources opens up new challenges regarding the mismatch of generation and load and instability of system voltage. These uncertainties need to add an objective to the OPF problem regarding the voltage magnitude deviations.

In this chapter, the OPF problem is formulated incorporating WP generation sources in the system by considering the power uncertainty of wind units as a cost factor. The IWO, IWO-STS and IWO-PPS techniques are applied to solve the OPF problem under consideration. The two test systems, *i.e.*, modified IEEE 30-bus system and modified IEEE 118-bus system, are considered for testing the OPF problem.

5.2 MODELING OF WIND SPEED VARIABILITY

The two-parameter Weibull *probability density function* (PDF) method expresses a convincing accuracy level for the modeling of wind speed variation [69]. The assumed Weibull PDF for wind speed is converted to wind power distribution.

The Weibull PDF $f_V(v)$ for the wind speed v m/s is represented as under:

$$f_V(v) = \frac{k}{c} \times \left[\left(\frac{v}{c} \right)^{k-1} \times \exp\left\{ -\left(\frac{v}{c} \right)^{k} \right\} \right] \tag{5.1}$$

where c is scale parameter and k is shape parameter of Weibull distribution model.

Based on this, the equivalent cumulative distribution function, $F_V(v)$ has been obtained as under.

$$F_V(v) = 1 - \exp\left[-\left(\frac{v}{c} \right)^{k} \right] \tag{5.2}$$

As per the PDF, the n^{th} order moment for the wind speed variable is given as:

$$E(v^n) = \int_0^\infty v^n f_V(v) dv = c^n \Gamma(1 + nk^{-1}) \ (n = 1,2,3,...) \tag{5.3}$$

here $\Gamma(.)$ represents the incomplete gamma function, defined as under:

$$\Gamma(\beta) = \int_0^\infty y^{\beta-1} \exp(-y) dy \tag{5.4}$$

The probability formulation for the WP distribution is obtained from the distribution function of wind speed. The output power corresponding to a WP generator for a given input wind speed, ignoring non-linear characteristics, is represented as in Eq. (5.5).

$$P_W = \begin{cases} 0; & 0 < v < v_{IN} \\ p_R \{ (v - v_{IN}) / (v_R - v_{IN}) \}; & v_{IN} \le v \le v_R \\ p_R; & v_R \le v \le v_0 \\ 0; & v > v_0 \end{cases} \tag{5.5}$$

where v represents the current speed of wind; v_R, v_0 and v_{IN} represent the rated, cut-out and cut-in speed, respectively; p_R represents the rated WP output; P_W is a mixed random variable; P_W is continuous for the range [0, p_R], and discrete at 0 and p_R.

As per the theory of distribution for random variable function [97], the Weibull PDF corresponding to the wind generator power output random variable in continuous range ($v_{IN} \le v \le v_R$) is

$$f_W(p)=\frac{khv_{IN}}{p_R c}\left[\left(1+\frac{hp}{p_R}\right)v_{IN}/c\right]^{(k-1)}\times\exp\left\{-\left[\left(1+\frac{hp}{p_R}\right)v_{IN}/c\right]^{k}\right\}\ 0<p<p_R \tag{5.6}$$

where $h=(v_R/v_{IN})-1$ represents the intermediary parameter.

As per Eq. (5.5), the output variable WP has two probabilities in the discrete range *i.e.,* probability of the event $P_W=0$ is

$$f_W(P_W=0)=f_W(v<v_{IN})+f_W(v>v_0)$$

$$=1-\exp\left[-\left(\frac{v_{IN}}{c}\right)^{k}\right]+\exp\left[-\left(\frac{v_0}{c}\right)^{k}\right] \tag{5.7}$$

and at $P_W=p_R$

$$f_W(P_W=p_R)=f_W(v_R\le v\le v_0)$$

$$=\exp\left[-\left(\frac{v_R}{v_c}\right)\right]^{k}-\exp\left[-\left(\frac{v_0}{c}\right)^{k}\right] \tag{5.8}$$

It is evident from Eqs. (5.6) - (5.8), that the Weibull PDF corresponding to the output of wind turbine has higher complexity than the wind speed. It comprises both the continuous and discrete power output.

5.3 PROBLEM FORMULATION

The OPF problem incorporating WP generators is formulated with different objectives *i.e.*, overall cost of the wind-thermal system, emission pollutants, active power losses and voltage magnitude deviations, with satisfying the system constraints. The objective functions are given as under:

5.3.1 Objective Functions

The mathematical model of each objective function is presented as under:

Overall cost of system: The overall cost of the system includes fuel cost of thermal generators and total operating cost of available WP and is represented as:

$$F_{OC}=f_T+f_W \tag{5.9}$$

where f_T, and f_W represent the fuel cost of conventional thermal units and the operating cost of wind units, respectively.

Fuel cost of conventional thermal units: The fuel cost of the conventional thermal units is expressed as [6]:

$$f_T = \sum_{m=1}^{NG} a_m + b_m P_{Gm} + c_m P_{Gm}^2 + \left| d_m \sin\left(e_m \left(P_{Gm}^{\min} - P_{Gm}\right)\right)\right| \tag{5.10}$$

where a_m, b_m, c_m, d_m and e_m represent the coefficients of the fuel cost for the m^{th} generating unit; P_{Gm} represents the active power output of the m^{th} generating unit; and *NG* denotes the total number of thermal generating units.

The operating cost of wind power: Due to the intermittent availability of WP, an additional cost component is being added to the system operating cost. The cost of a wind system is segregated into three components: overestimation cost, underestimation cost and direct cost. Therefore, the total operating cost of WP generator is expressed as under [79]:

$$f_W = \sum_{i=1}^{N_W} \left\{ d_{ri} \times E\left(P_{oe,i}\right) + d_{pi} \times E\left(P_{ue,i}\right) + \left(d_i \times P_{Wi}\right)\right\} \tag{5.11}$$

where d_i, d_{ri}, d_{pi} are the cost coefficients of i^{th} wind generator for direct, overestimated and underestimated power, respectively; P_{Wi} is actual power of i^{th} wind generator; $E(P_{oe,i})$ and $E(P_{ue,i})$ represent the expected overestimation and underestimation power of i^{th} wind generator, respectively and N_W denotes the total number of WP generators.

Overestimation cost: If the available WP is less than the scheduled WP, it requires the purchase of active power from the common pool. The cost component equivalent to this cost of uncertain power purchase is taken as an overestimation cost. Expected overestimated WP corresponding to the i^{th} wind generator is given as in Eq. (5.12)

$$\begin{aligned} E\left(P_{oe,i}\right) &= P_{Wi} \times \left[1 - \exp\left(-\left(v_{IN,i}/c_i\right)^{k_i}\right) + \exp\left(-\left(v_{0,i}/c_i\right)^{k_i}\right)\right] + \left(p_{R,i} v_{IN,i} / \left(v_{R,i} - v_{IN,i}\right) + P_{Wi}\right) \\ &\times \left[\exp\left(-\left(v_{IN,i}/c_i\right)^{k_i}\right) - \exp\left(-\left(v_{1,i}/c_i\right)^{k_i}\right)\right] + \left(p_{R,i} c_i / \left(v_{R,i} - v_{IN,i}\right)\right) \\ &\times \left\{\Gamma\left[1 + 1/k_i, \left(v_{1,i}/c_i\right)^{k_i}\right] - \Gamma\left[1 + 1/k_i, \left(v_{IN,i}/c_i\right)^{k_i}\right]\right\} \end{aligned} \tag{5.12}$$

where

$$v_{1,i} = v_{IN,i} + \frac{P_{Wi} \times \left(v_{R,i} - v_{IN,i}\right)}{p_{R,i}} \tag{5.13}$$

where c_i is scale parameter and k_i is shape parameter of Weibull distribution model for i^{th} wind generator; $E(P_{oe,i})$ represent the expected overestimation power of i^{th} wind generator; $v_{R,i}$, $v_{0,i}$ and $v_{IN,i}$ represent the rated, cut-out and cut-in speed of i^{th} wind generator, respectively; $p_{R,i}$ represents the rated wind power output; P_{Wi} is actual power of i^{th} wind generator.

Underestimation cost: In the other way, if the available WP is more than the scheduled WP, it requires the operator to compensate the WP supplier against the unutilized power. This component of WP cost is taken as an underestimation cost. Expected underestimated WP

corresponding to the i^{th} wind generator is given in Eq. (5.14).

$$\begin{aligned} E(P_{ue,i}) &= (p_{R,i} - P_{Wi}) \times \left[\exp\left(-\left(v_{R,i}/c_i\right)^{k_i}\right) - \exp\left(-\left(v_{0,i}/c_i\right)^{k_i}\right)\right] \\ &+ \left(p_{R,i} v_{IN,i} / \left(v_{R,i} - v_{IN,i}\right) + P_{Wi}\right) \times \left[\exp\left(-\left(v_{R,i}/c_i\right)^{k_i}\right) - \exp\left(-\left(v_{1,i}/c_i\right)^{k_i}\right)\right] \\ &+ \left(p_{R,i} c_i / \left(v_{R,i} - v_{IN,i}\right)\right) \times \left\{\Gamma\left[1 + 1/k_i, \left(v_{1,i}/c_i\right)^{k_i}\right] - \Gamma\left[1 + 1/k_i, \left(v_{R,i}/c_i\right)^{k_i}\right]\right\} \end{aligned} \quad (5.14)$$

where c_i is scale parameter and k_i is shape parameter of Weibull distribution model for i^{th} wind generator; $E(P_{ue,i})$ represent the expected underestimation power of i^{th} wind generator; $v_{R,i}$, $v_{0,i}$ and $v_{IN,i}$ represent the rated, cut-out and cut-in speed of i^{th} wind generator, respectively; $p_{R,i}$ represents the rated WP output; P_{Wi} is actual power of i^{th} wind generator.

Direct cost: The direct cost for WP is the cost of actual WP transferred to the system by the WP generator. This cost is given as $(d_i \times P_{Wi})$.

Emission pollutant: The mathematical model for the release of pollutant emission quantum by thermal units is represented by Eq. (2.18) in subsection 2.3.1 under Chapter 2

Active power loss: The mathematical model for transmission line active power losses is represented by Eq. (2.19) in subsection 2.3.1 under Chapter 2.

Total voltage magnitude deviations: The total voltage magnitude deviation of all the load buses with respect to $V_{reference}$ is given in subsection 4.2.1 under Chapter 4.

5.3.2 System Constraints

The following system constraints are taken for the OPF problem incorporating thermal and wind generating units.

Equality constraints: Equality constraints are represented by the static power flow equations as below:

Static power flow equations:

$$P_{Gk} + P_{Wk} - P_{Lk} = |V_k| \sum_{l=1}^{N_{BUS}} |V_l| |Y_{kl}| \cos\left(\delta_{kl} + \theta_k - \theta_l\right) (k = 1,2,..., N) \quad (5.15)$$

$$Q_{gk} - Q_{Lk} = -|V_k| \sum_{l=1}^{N_{BUS}} |V_l| |Y_{kl}| \sin\left(\delta_{kl} + \theta_k - \theta_l\right) (k = 1,2,..., N_{PQ}) \quad (5.16)$$

where P_{Gk}, Q_{Gk} represent the active and reactive power generation available at the k^{th} bus, respectively; P_{Lk}, Q_{Lk} are the active and reactive power demand at the k^{th} bus, respectively; P_{Wk} is the active power generated by wind units at the k^{th} bus; Y_{kl} and δ_{kl} represent the total admittance and admittance angle of the transmission line, which connect the k^{th} and l^{th} bus;

N_{BUS} , N and N_{PQ} are the total number of buses, total system buses except slack bus and the total number of load buses, respectively.

Inequality constraints: The different inequality constraints for the system under consideration are listed as below [182]:

Generating Unit constraints: The lower and upper limits for generating units are given as:

$$P_{Gm}^{\min} \le P_{Gm} \le P_{Gm}^{\max} \ (m = 1,2,...,NG) \tag{5.17}$$

$$Q_{gl}^{\min} \le Q_{gl} \le Q_{gl}^{\max} \ (l = 1,2,...,Ng) \tag{5.18}$$

$$0 \le P_{Wi} \le P_{Wi}^{\max} \ (i = 1,2,...,N_W) \tag{5.19}$$

where $P_{Gm}^{\min}$ and $P_{Gm}^{\max}$ represent the minimum and maximum active power limits for the m^{th} thermal generating unit, respectively; $Q_{gl}^{\min}$ and $Q_{gl}^{\max}$ are the minimum and maximum reactive power limits of the l^{th} generating unit including wind units, respectively; NG represents the number of thermal units; N_g denotes total number of generating units including wind units; $P_{Wi}, P_{Wi}^{\max}$ represent the actual and maximum power of i^{th} wind generator, respectively; N_W denotes the total number of wind units.

The other system constraints *i.e.*, transformer tap setting, shunt compensator and security constraints, are discussed in detail in subsection 2.3.2 under Chapter 2.

5.4 SOLUTION METHODOLOGY

For OPF problem including wind units, decision variables are power generated from thermal and wind generators, the magnitude of voltage for all generator units, transformer tap ratios and shunt compensator VAR values. The continuous type variables are the active power of thermal and wind generators and the voltage magnitude for all the power units. The transformer tap ratios and the shunt compensator device output are discrete variables. The decision variables array is given as [X] in Eq. (5.20):

$$X = \begin{matrix} P_{1,1} & \cdots & P_{1,N_G-1}, & P_{1,1} & \cdots & P_{1,N_W-1}, & V_{1,1} & \cdots & V_{1,N_g}, & Q_{1,1} & \cdots & Q_{1,NC}, & t_{1,1} & \cdots & t_{1,N_T} \\ \vdots & \vdots & \vdots & \vdots & \vdots & \vdots & \vdots & \vdots & \vdots & \vdots & \vdots & \vdots & \vdots & \vdots & \vdots \\ P_{G,1} & \cdots & P_{G,N_G-1}, & P_{W,1} & \cdots & P_{W,N_W-1}, & V_{G,1} & \cdots & V_{G,N_g}, & Q_{q,1} & \cdots & Q_{q,NC}, & t_{p,1} & \cdots & t_{p,N_T} \end{matrix} \tag{5.20}$$

where P_G is power generated by thermal generators; P_W is power generated by wind generators; V_G is voltage magnitude for all generating units; Q_q is the output of shunt devices and t_p is transformer tap ratio.

The implementation of the IWO-PPS technique to solve the OPF problem incorporating WP sources is explained in the following steps.

Step 1: The weeds are randomly initialized within the defined limits as per Eq. (2.36) and Eq. (2.37), respectively, under Chapter 2.

Step 2: The NR method is employed for solving the OPF problem including wind sources for each weed. During the search process, the equality constraints (Eqs.(5.15)-(5.16)) are handled by the load flow solution. The NR method is executed to satisfy active and reactive power load flow. To satisfy the inequality constraints *i.e.*, slack real power output, voltage magnitudes of load buses, reactive powers generated by all generator units and line flows of the system, exterior penalty method approach is applied. In this approach, a penalty function φ_i is introduced to penalize the overall objective function by incorporating the cumulative error of all constraint violations and is given as [84]:

$$f = of_i + \sum_{i=1}^{ni} \varphi_i \ \ (i = 1,2,..., N_{obj}) \tag{5.21}$$

with

$$\varphi_i = \begin{cases} \psi_i \times \left(x_i - x_i^{\lim}\right)^2; & violated \\ 0; & else \end{cases} \tag{5.22}$$

where f represents overall objective function; of_i represents i^{th} objective function; ni denotes the number of inequality constraints; N_{obj} are the number of objectives; φ_i represents penalty function and ψ_i represents the penalty coefficient of i^{th} inequality constraint.

Step 3: The error corresponding to each inequality constraint is figured out as per Eq. (5.22) and the overall objective function is computed from Eq. (5.21).

Step 4: The weeds are arranged from the best to the worst value based on overall objective function evaluation.

Step 5: The count of new seeds is evaluated according to the best and the worst value of overall objective function and the new seeds are generated in current search space as discussed in section 2.4 under Chapter 2.

Step 6: If IWO does not converge up to a certain level of expected result for the set iterations (IT), then the PPS method is applied. The NR method is applied to the solution obtained from the PPS method to compute the overall objective function value.

Step 7: The weed population is updated on the basis of overall objective function values using Eq. (5.23).

$$X_{j,l} = \begin{cases} \overline{X}_{j,l}; & f\left(\overline{X}_{j,l}\right) < f\left(X_{j,l}\right) \\ X_{j,l}; & else \end{cases} \left(j = 1,2,...,NP; l = 1,2,...,D\right) \quad (5.23)$$

Step 8: Step 2 is repeated until the termination criterion is met.

5.5 TEST SYSTEMS AND RESULTS

In this work, two test systems are considered. The test system-IX and test system-X are modified IEEE 30-bus and modified IEEE 118-bus systems, respectively. The test system-IX includes 3-thermal units, 3-wind units, 41-transmission line branches, 24-load buses, 4-transformers tap position settings, 9-shunt compensators. The total demand of power is 283.4 MW. The three thermal units are connected at buses 1, 2 and 8. Three wind units are connected at buses 5, 11 and 13 [101].The single-line diagram of test system-IX is shown in Figure A.2.1 under Appendix-A. The load, transmission lines and generating thermal units data for test system-IX are given in Tables A.1.3, A.1.4 and A.2.1, respectively, under Appendix-A. The data of wind units of test system-IX is presented in Table A.2.2 under Appendix-A. The test system-X includes 52-thermal units, 2-wind units, 186-transmission line branches, 64-load buses, 9-transformer tap position settings, 14-shunt compensators. The power demand of the system is 4242.001 MW. The wind units are connected at buses 36 and 49 [48]. The single-line diagram of test system-X is shown in Figure A.2.2 under Appendix-A. The data of wind units of test system-X is presented in Table A.2.2 under Appendix-A. The data of generating units, load and transmission lines for test system-X are given in Tables A.1.10, A.1.11 and A.1.12, respectively, under Appendix-A.

5.5.1 Results and Discussion

The IWO, IWO-STS and IWO-PPS techniques are applied to solve the OPF problem with the wind system in FORTRAN-90 command line. Thirty one trial runs have been taken to obtain the statistical results.

5.5.1.1 Test system-IX

For test system-IX, the results obtained by IWO, IWO-STS and IWO-PPS techniques are compared with the results of its counterpart techniques *i.e.*, BFA [113] and GABC [156]. The comparison of results is presented in Table 5.1 and it is observed that the IWO-PPS technique attains the minimum overall cost as 885.05 $/hr, that is 0.09% less than the GABC technique

[156].The reported result of fuel cost for a conventional thermal system is 800.195 $/hr[202]. The inclusion of WP generators increases the overall cost of the system due to the overestimation and underestimation cost factors because of the intermittent nature of WP availability.

Table 5.1: Comparison of results for test system-IX

Techniques	Best	Worst	Average	SD	NFE
F_{OC}**($/hr)**					
BFA[113]	947.5	-	-	-	-
GABC [156]*	819.293	-	-	-	-
IWO	898.258	905.45	900.98	2.0435	31360
IWO-STS	888.541	892.332	890.417	1.0798	28880
IWO-PPS	885.05	886.92	886.07	0.48395	21840
***E*(ton/hr)**					
IWO	0.09646	0.09949	0.09695	0.00065	30680
IWO-STS	0.09448	0.09599	0.09499	0.00037	29520
IWO-PPS	0.09438	0.095001	0.094644	0.0002	25600
P_{LOSS}**(MW)**					
IWO	2.89	3.12	3.00	0.06832	33280
IWO-STS	2.709	2.895	2.7987	0.05737	32400
IWO-PPS	1.952	2.012	1.9791	0.01442	27600
***VMD* (p.u.)**					
IWO	0.211803	0.22345	0.21789	0.0038	30240
IWO-STS	0.19473	0.20556	0.19964	0.00307	28800
IWO-PPS	0.162436	0.170016	0.165319	0.00254	23400

BFA: Bacteria foraging algorithm; GABC: Gbest guided artificial bee colony

***** Actual cost is 885.847

The results obtained by the IWO-PPS technique are also compared with the results of IWO and IWO-STS techniques. The overall cost obtained by the IWO-PPS technique is 1.492% and 0.394% less than IWO and IWO-STS, respectively. The IWO-PPS technique is able to attain better average and the worst cost as compared to the IWO and IWO-STS techniques. The IWO-PPS technique also achieved better SD of results than of IWO and IWO-STS techniques. The NFE for the IWO-PPS technique is 21840 that is less in comparison to IWO and IWO-STS techniques. The value of minimum emission pollutant achieved with the IWO-PPS technique is 0.09438 ton/hr that is 2.204%, 0.1059% less as compared to the IWO and IWO-STS techniques, respectively. The average and the worst values for emission pollutants achieved with the IWO-PPS technique are better than IWO and IWO-STS techniques. Further, the SD of results and NFE required by the IWO-PPS technique are superior to IWO and IWO-STS techniques. The wind energy source impact is analyzed by the comparison of obtained results with conventional OPF system emission results. The reported result of pollutant emission for the conventional thermal system is 0.2047ton/hr [117]. The pollutant emission attained by the IWO-PPS technique is reduced by 0.11032 ton/hr over the

reported result of a conventional thermal system. Hence, it is concluded that the inclusion of wind farms reduces pollutant emissions.

For the third objective, minimization of active power loss, the losses attained by the IWO-PPS technique is 1.952 MW that is less than that of the result obtained by the IWO and IWO-STS techniques. The reported result for active power losses of the conventional thermal system is 3.0802MW [202].The active power losses attained with the inclusion of WP generation is reduced by 1.1282 MW over the reported result of a conventional thermal system. Further, the value of minimum voltage deviations achieved by the IWO-PPS technique is 0.16243 p.u. with the inclusion of WP sources. The minimum voltage deviation is increased with the penetration of WP sources due to the intermittent nature of WP availability. The value of minimum voltage deviations achieved with the IWO-PPS technique is compared with the result obtained by the IWO and IWO-STS techniques and found satisfactory. The values of average and worst active power losses and voltage deviations obtained by the IWO-PPS technique are better in comparison to IWO and IWO-STS techniques. The SD and NFE for the IWO-PPS technique are better than the IWO and IWO-STS techniques. The optimum values of decision variables corresponding to the IWO-PPS technique for all the objectives are given in Table 5.2.

5.5.1.2 *Test system-X*

The results obtained by the IWO-PPS technique is compared with the results achieved by IWO and IWO-STS techniques because, as per the best of the author's knowledge, no published literature related to the OPF problem incorporating wind units is available. The results obtained by the IWO, IWO-STS and IWO-PPS techniques are presented in Table 5.3. It is observed from Table 5.3 that for all the four objectives *i.e.*, the overall cost of the system, emission pollutant value, active power loss and magnitude of voltage deviations, results obtained by the IWO-PPS technique are 0.0935%, 1.194%, 3.794% and 7.892% less as compared to results attained by IWO-STS technique, respectively. The reported result of fuel cost for the conventional thermal system is 129428.703$/hr [202]. The overall cost attained by the IWO-PPS technique for the system including WP sources, is 119416.747 $/hr that is less by 8.384% than the reported result of the conventional thermal system. Further, it is evident from Table 5.3 that the IWO-PPS technique is capable of attaining superior results with respect to the average value, worst value, SD and NFE as compared to the IWO and IWO-STS techniques for all the objective functions.

Table 5.2: Optimum value of decision variables for test system-IX

Decision variables (p.u.)	Limits		F_{OC} ($/hr)	E(ton/hr)	P_{LOSS} (MW)	VMD (p.u.)
	min	max				
P_{T1}	0.50	2.00	0.5057	0.5478	0.50049	0.68538
P_{T2}	0.20	0.80	0.20001	0.27142	0.27599	0.79152
P_{T8}	0.10	0.35	0.35	0.34248	0.3499	0.25887
P_{W5}	0.0	0.60	0.59999	0.5999	0.5989	0.45538
P_{W11}	0.0	0.60	0.59999	0.5999	0.5999	0.29917
P_{W13}	0.0	0.60	0.59999	0.50831	0.52734	0.39942
V_{G1}	0.95	1.1	1.098741	1.055253	1.09889	0.970136
V_{G2}	0.95	1.1	1.09917	1.030293	1.0985	0.990947
V_{G5}	0.95	1.1	1.085662	1.020134	1.08124	1.018309
V_{G8}	0.95	1.1	1.092562	1.053799	1.09126	1.008344
V_{G11}	0.95	1.1	1.092776	1.027338	1.09975	1.052348
V_{G13}	0.95	1.1	1.078042	1.084105	1.09965	0.999021
Q_{10}	0.0	0.05	0.05	0.04	0.05	0.04
Q_{12}	0.0	0.05	0.05	0.05	0.05	0.05
Q_{15}	0.0	0.05	0.05	0.05	0.03	0.04
Q_{17}	0.0	0.05	0.05	0.03	0.05	0.05
Q_{20}	0.0	0.05	0.04	0.02	0.04	0.04
Q_{21}	0.0	0.05	0.05	0	0.05	0.04
Q_{23}	0.0	0.05	0.03	0.03	0.05	0.04
Q_{24}	0.0	0.05	0.05	0.04	0.05	0.04
Q_{29}	0.0	0.05	0.02	0.05	0.02	0.02
t_{11}	0.9	1.1	1.08	0.96	1.06	1.05
t_{12}	0.9	1.1	0.91	1.1	0.9	0.94
t_{15}	0.9	1.1	0.99	1.1	0.99	0.97
t_{36}	0.9	1.1	0.98	1.03	0.98	0.95
Overall Cost ($/hr)	-	-	**885.05**	898.551	890.885	991.087
Emission (ton/hr)	-	-	0.09585	**0.09438**	0.09351	0.10432
PL (MW)	-	-	2.168	3.674	**1.952**	5.573
Voltage deviation (p.u.)	-	-	1.79416	0.41083	0.58765	**0.162436**

Note: Bold values indicate the optimum results.

Table 5.3: Comparison of results for test system-X

Techniques	**Best**	**Worst**	**Average**	**SD**	**NFE**
***F_{OC}*($/hr)**					
IWO	121868.655	123178.24	122042.30	223.301	168000
IWO-STS	119528.473	120034.781	119668.627	172.523	134190
IWO-PPS	119416.747	119623.489	119541.447	56.263	128340
***E*(ton/hr)**					
IWO	7.02913	8.3678	7.38107	0.52054	151200
IWO-STS	5.12516	5.4567	5.22825	0.11102	113880
IWO-PPS	5.06469	5.0966	5.07932	0.009	108630
***P_{LOSS}*(MW)**					
IWO	88.228	95.47	90.68	2.1427	162000
IWO-STS	77.672	81.145	79.22	1.0110	129930
IWO-PPS	74.833	76.056	75.19	0.41393	122400
***VMD*(p.u.)**					
IWO	1.132308	1.17664	1.1513	0.01151	155520
IWO-STS	1.08821	1.09677	1.0909	0.00257	113220
IWO-PPS	1.008612	1.00937	1.0089	0.00024	104520

Hence, it is summarized that the IWO-PPS technique performs better as compared to

the IWO and IWO-STS techniques for large-scale optimization problems.The convergence behaviors attained with IWO, IWO-STS and IWO-PPS techniques for all the objective functions are represented by Figures 5.1, 5.2, 5.3 and 5.4, respectively. These figures demonstrate that the IWO-PPS technique exhibits better convergence criteria. The optimum values of decision variables achieved by the IWO-PPS technique for all the objectives are presented in Table 5.4.

Table 5.4: Optimum value of decision variables for test system-X

Decision variables (p.u.)	Limits		F_C ($/hr)	E(ton/hr)	P_{LOSS} (MW)	VMD (p.u.)
	min	max				
P_{T1}	0.0	1.00	0.26987	0.29987	0.31227	0.27643
P_{T4}	0.0	1.00	0.00011	0.28878	0.28839	0.001239
P_{T6}	0.0	1.00	0.00065	0.27665	0.26555	0.000234
P_{T8}	0.0	1.00	0.00041	0.23411	0.23556	0.001321
P_{T10}	1.65	5.50	3.95987	3.49987	3.72326	3.92133
P_{T15}	0.0	1.00	0.20041	0.22324	0.26549	0.22654
P_{T18}	0.0	1.00	0.11348	0.25671	0.21887	0.13231
P_{T19}	0.0	1.00	0.21269	0.12216	0.13554	0.21266
P_{T24}	0.0	1.00	0.00012	0.25443	0.28865	0.00033
P_{T25}	0.96	3.20	1.91644	1.71136	1.76654	1.61136
P_{T26}	1.242	4.14	2.83377	2.20077	2.27659	2.60086
P_{T27}	0.0	1.00	0.10601	0.27676	0.20023	0.43112
P_{T31}	0.0	1.07	0.06877	0.25687	0.28862	0.08123
P_{T32}	0.0	1.00	0.17763	0.27776	0.27765	0.12345
P_{T34}	0.0	1.00	0.00009	0.19287	0.18872	0.000531
P_{T40}	0.0	1.00	0.44657	0.34654	0.42235	0.40345
P_{T42}	0.0	1.00	0.41432	0.24434	0.31281	0.400232
P_{T46}	0.0	1.19	0.18988	0.19987	0.15009	0.16773
P_{T54}	0.0	1.48	0.47461	0.27466	0.42236	0.41223
P_{T55}	0.0	1.00	0.29994	0.25544	0.26996	0.22243
P_{T56}	0.0	1.00	0.31028	0.24988	0.32976	0.30344
P_{T59}	0.765	2.55	1.49334	1.43334	1.67543	1.51234
P_{T61}	0.78	2.60	1.45733	1.75765	1.76651	1.31123
P_{T62}	0.0	1.00	0.00038	0.14387	0.11673	0.00021
P_{T65}	1.473	4.91	3.68451	3.18445	3.39654	3.54452
P_{T66}	1.476	4.92	3.49557	3.45563	3.49879	3.41236
P_{T69}	0.0	8.052	3.56030	3.38386	1.92492	4.75942
P_{T70}	0.0	1.00	0.00029	0.23459	0.36546	0.001323
P_{T72}	0.0	1.00	0.00018	0.28998	0.21772	0.00021
P_{T73}	0.0	1.00	0.00036	0.17766	0.17765	0.00032
P_{T74}	0.0	1.00	0.15223	0.13223	0.20654	0.15677
P_{T76}	0.0	1.00	0.25563	0.22443	0.24565	0.28943
P_{T77}	0.0	1.00	0.00217	0.18877	0.19978	0.00511
P_{T80}	1.731	5.77	4.35548	4.21233	4.21223	4.2112
P_{T85}	0.0	1.00	0.00043	0.16983	0.12228	0.000243
P_{T87}	0.0	1.04	0.00472	0.18872	0.19987	0.00411
P_{T89}	2.121	7.07	5.13222	4.13222	4.07766	4.91232
P_{T90}	0.0	1.00	0.00039	0.14339	0.12231	0.000232
P_{T91}	0.0	1.00	0.00045	0.11645	0.17736	0.000266
P_{T92}	0.0	1.00	0.10077	0.14567	0.14876	0.12453
P_{T99}	0.0	1.00	0.00068	0.23568	0.13326	0.00121

Table 5.4: Optimum value of decision variables for test system-X (Continued)

Decision variables (p.u.)	Limits		F_C ($/hr)	E(ton/hr)	P_{LOSS} (MW)	VMD (p.u.)
	min	max				
P_{T100}	1.056	3.52	2.03161	2.23675	2.17755	2.11232
P_{T103}	0.0	1.40	0.39279	0.47079	0.41233	0.31223
P_{T104}	0.0	1.00	0.00007	0.13467	0.12000	0.000103
P_{T105}	0.0	1.00	0.00054	0.14454	0.09343	0.000401
P_{T107}	0.0	1.00	0.24344	0.21568	0.25522	0.19886
P_{T110}	0.0	1.00	0.09976	0.09976	0.09776	0.09776
P_{T111}	0.0	1.36	0.35875	0.40875	0.42214	0.30432
P_{T112}	0.0	1.00	0.36782	0.26782	0.32119	0.33221
P_{T113}	0.0	1.00	0.02134	0.11134	0.10265	0.02654
P_{T116}	0.0	1.00	0.00081	0.06498	0.14442	0.00051
P_{W36}	0.0	4.00	1.17635	0.17654	0.18724	1.24233
P_{W49}	0.0	6.00	1.99834	2.41232	2.35428	1.91334
V_{G1}	0.94	1.06	0.996768	0.9947907	0.990077	0.980909
V_{G4}	0.94	1.06	1.01534	1.01334	1.0171	1.0233
V_{G6}	0.94	1.06	1.01065	1.01665	1.012049	1.01153
V_{G8}	0.94	1.06	1.03098	1.020098	1.0265	1.0298
V_{G10}	0.94	1.06	1.037607	1.027506	1.022616	1.024698
V_{G12}	0.94	1.06	1.00115	1.01415	1.0108	1.00211
V_{G15}	0.94	1.06	0.98978	0.9769217	0.987134	0.994075
V_{G18}	0.94	1.06	0.994162	0.99466	0.98893	0.999157
V_{G19}	0.94	1.06	0.9915587	0.9590248	0.9450007	0.99981
V_{G24}	0.94	1.06	1.01188	1.01788	1.0222	1.0123
V_{G25}	0.94	1.06	1.024533	1.007745	1.0218	1.019197
V_{G26}	0.94	1.06	1.059965	1.0465	1.04119	1.05543
V_{G27}	0.94	1.06	1.00422	1.00122	1.000228	1.00301
V_{G31}	0.94	1.06	0.99883	0.99883	0.99875	0.98764
V_{G32}	0.94	1.06	1.00409	1.01391	1.0139	1.00298
V_{G34}	0.94	1.06	1.010773	1.012805	1.01759	1.010922
V_{G36}	0.94	1.06	1.011282	1.016768	1.021622	1.010089
V_{G40}	0.94	1.06	1.00015	1.01265	1.0122	1.00122
V_{G42}	0.94	1.06	1.00857	1.01576	1.01722	1.00856
V_{G46}	0.94	1.06	1.03665	1.01665	1.01998	1.03422
V_{G49}	0.94	1.06	1.04645	1.024402	1.0302	1.04323
V_{G54}	0.94	1.06	1.02365	1.01365	1.01886	1.02933
V_{G55}	0.94	1.06	1.018078	1.01635	1.014175	1.018868
V_{G56}	0.94	1.06	1.005077	1.012943	1.00342	1.003795
V_{G59}	0.94	1.06	1.026604	1.017977	1.018407	1.017648
V_{G61}	0.94	1.06	1.038388	1.04093	1.04013	1.0422
V_{G62}	0.94	1.06	1.043334	1.02279	1.026447	1.027739
V_{G65}	0.94	1.06	1.05989	1.034014	1.053664	1.048815
V_{G66}	0.94	1.06	1.0576	1.0476	1.037272	1.0552
V_{G69}	0.94	1.06	1.0368	1.05998	1.05991	1.03099
V_{G70}	0.94	1.06	1.02645	1.009364	1.0288	1.029091
V_{G72}	0.94	1.06	1.02398	1.01398	1.0122	1.02921
V_{G73}	0.94	1.06	1.02243	1.02243	1.0229	1.02112
V_{G74}	0.94	1.06	1.00329	1.000571	0.998737	1.000292
V_{G76}	0.94	1.06	0.986565	0.982054	0.964807	0.99861
V_{G77}	0.94	1.06	1.01552	1.023302	1.017685	1.01511
V_{G80}	0.94	1.06	1.020769	1.01569	1.008945	1.02212
V_{G85}	0.94	1.06	1.02395	1.02395	1.02001	1.03347
V_{G87}	0.94	1.06	1.04865	1.02865	1.02547	1.04221
V_{G89}	0.94	1.06	1.02098	1.01098	1.010122	1.02123
V_{G90}	0.94	1.06	1.00498	1.03498	1.0311	1.0023
V_{G91}	0.94	1.06	1.057492	1.0556	1.0511	1.0509

Table 5.4: Optimum value of decision variables for test system-X (Continued)

Decision variables (p.u.)	Limits		F_C ($/hr)	E(ton/hr)	P_{LOSS} (MW)	VMD (p.u.)
	min	max				
V_{G92}	0.94	1.06	1.009907	1.01269	1.018939	1.004317
V_{G99}	0.94	1.06	1.01112	1.02112	1.0221	1.01004
V_{G100}	0.94	1.06	1.01624	1.01624	1.01922	1.01233
V_{G103}	0.94	1.06	1.015445	0.991427	0.983524	1.01343
V_{G104}	0.94	1.06	1.001724	0.986068	0.9878402	1.001003
V_{G105}	0.94	1.06	1.005488	0.996968	0.9936318	1.003698
V_{G107}	0.94	1.06	0.98655	0.98655	0.97549	0.98334
V_{G110}	0.94	1.06	1.0134	1.020963	1.01186	1.010402
V_{G111}	0.94	1.06	1.0266	1.05996	1.01552	1.02232
V_{G112}	0.94	1.06	1.00336	1.0136	1.0202	1.00522
V_{G113}	0.94	1.06	1.00512	1.00112	1.00199	1.00501
V_{G116}	0.94	1.06	1.0545	1.0245	1.0389	1.0533
Q_{34}	0.00	0.30	0.02	0.13	0.10	0.05
Q_{44}	0.00	0.30	0.06	0.14	0.14	0.11
Q_{45}	0.00	0.30	0.22	0.15	0.20	0.18
Q_{46}	0.00	0.30	0.11	0.12	0.12	0.11
Q_{48}	0.00	0.30	0.05	0.11	0.18	0.08
Q_{74}	0.00	0.30	0.24	0.12	0.21	0.27
Q_{79}	0.00	0.30	0.24	0.16	0.15	0.19
Q_{82}	0.00	0.30	0.23	0.17	0.19	0.21
Q_{83}	0.00	0.30	0.20	0.15	0.14	0.21
Q_{105}	0.00	0.30	0.13	0.20	0.13	0.15
Q_{107}	0.00	0.30	0.02	0.12	0.12	0.11
Q_{110}	0.00	0.30	0.18	0.11	0.16	0.11
t_8	0.9	1.1	0.95	0.98	0.97	0.96
t_{32}	0.9	1.1	1.04	1.02	1.02	1.02
t_{36}	0.9	1.1	1.02	0.98	0.98	1.01
t_{51}	0.9	1.1	0.95	1.01	1.01	0.96
t_{93}	0.9	1.1	0.95	1.01	1.02	0.96
t_{95}	0.9	1.1	0.95	1.01	1.01	0.95
t_{102}	0.9	1.1	0.99	0.98	0.99	0.99
t_{107}	0.9	1.1	1.01	1.01	1.01	1.02
t_{127}	0.9	1.1	0.99	1.02	1.01	0.98
Overall Cost ($/hr)	-	-	**119416.747**	122323.123	123363.123	119856.48
Emission (ton/hr)	-	-	7.18869	**5.06469**	5.08335	6.75052
P_{LOSS}(MW)	-	-	83.148	78.383	**74.833**	85.328
Voltage deviation (p.u.)	-	-	1.02288	1.008718	1.09548	**1.008612**

Note: Bold values indicate the optimum results

5.5.2 Statistical Analysis

The rate of success of an optimization technique is verified from the robustness of the technique. To confirm the robustness of the IWO-PPS technique, the two-sample *t*-test is conducted on test system-X for the first objective function *i.e.*, minimization of overall cost with 5% significant level. The *t*-test results are presented in Table 5.5 and the statistical output of *t-calculated* is more than the critical value. This rejects the null hypothesis and it is confirmed that there is a significant difference between the means of two populations at 5% level of significance. It demonstrates the better robustness of the IWO-PPS technique over the

IWO and IWO-STS techniques.

Table 5.5: *t*-test (two tail) results for the objective minimization of overall cost for test system-X at α=0.05

Statistics/Techniques	**IWO-PPS Vs. IWO-STS**	**IWO-PPS Vs. IWO**
t-calculated	3.902	60.466
t-critical	2	2

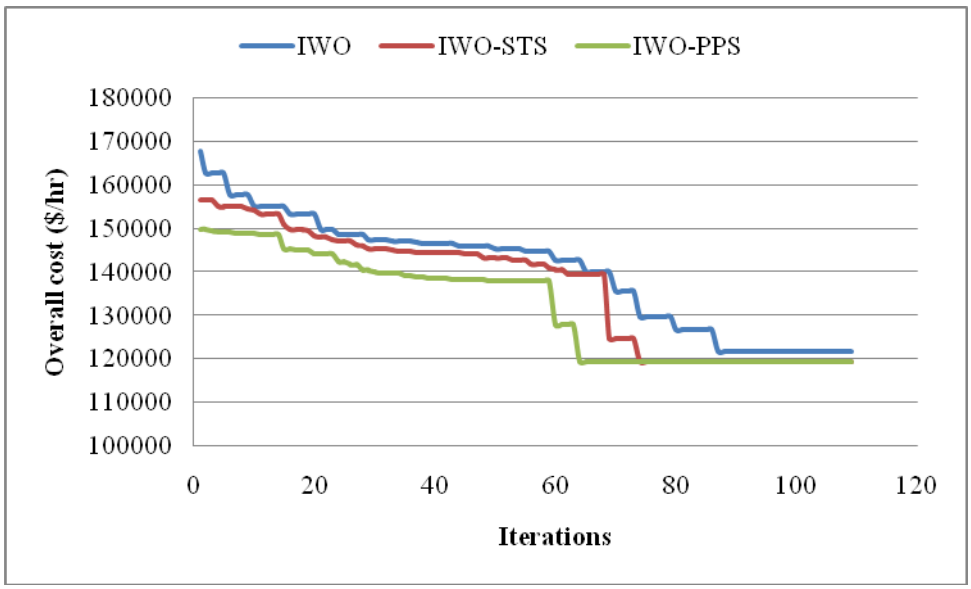

Figure 5.1: Convergence behaviors of overall cost: Test system-X

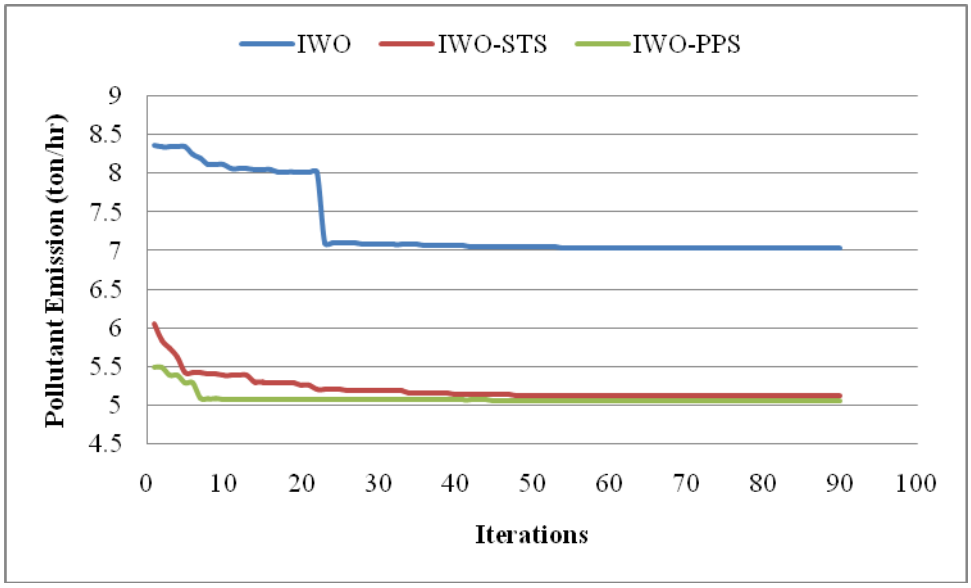

Figure 5.2: Convergence behaviors of emission pollutant: Test system-X

5.6 CONCLUSIONS

In this chapter, the IWO, IWO-STS and IWO-PPS techniques are applied for solving the OPF problem incorporating wind system. In this work, the four OPF objective functions *i.e.*, the overall cost, pollutant emission, active power losses and total voltage magnitude deviations, are

sequentially minimized. The IWO, IWO-STS and IWO-PPS techniques are tested on two standard IEEE test systems. In case of test system-IX, the IWO-PPS technique attains overall cost value as 885.05 $/hr that is better than its counterpart techniques *i.e.*, BFA and GABC. The result obtained by the IWO-PPS technique is also compared with IWO and IWO-STS techniques and found better. The pollutant emission, active power losses and total voltage magnitude deviations values attained by the IWO-PPS technique are 0.09438 ton/hr, 1.952 MW and 0.16243 p.u., respectively, which are improved results over the IWO and IWO-STS techniques.

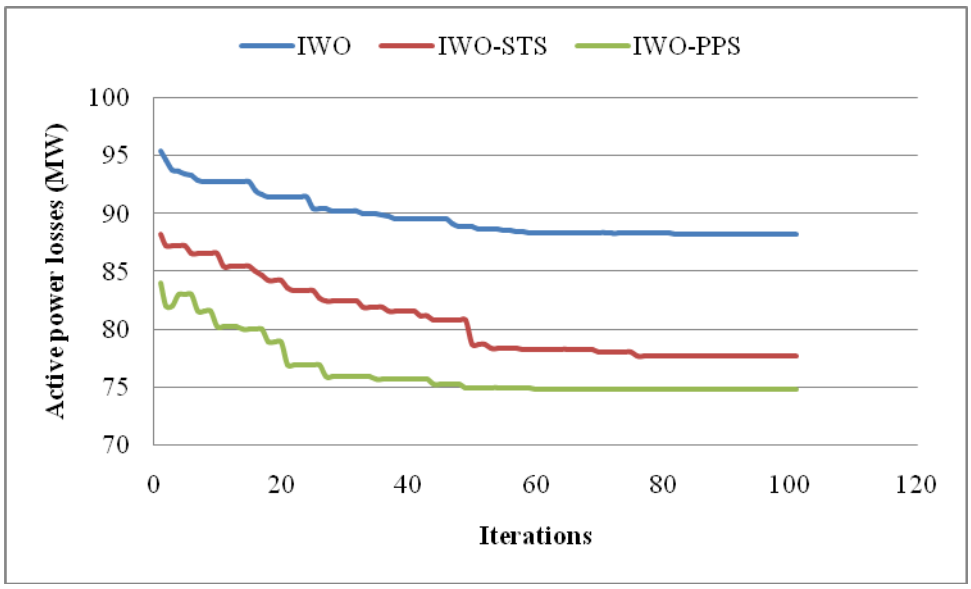

Figure 5.3: Convergence behaviors of active power losses: Test system-X

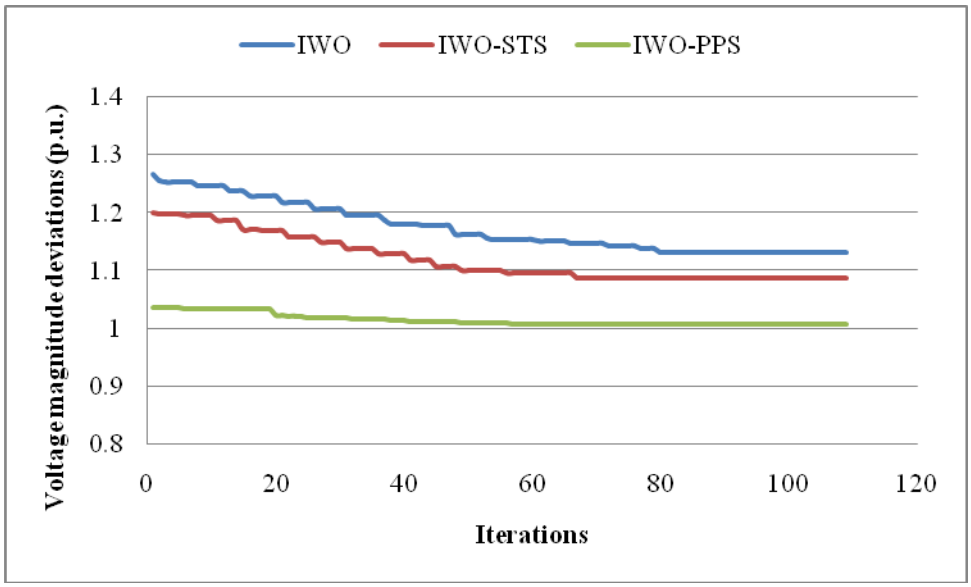

Figure 5.4: Convergence behaviors of voltage magnitude deviations: Test system-X

For test system-X, it is observed that the IWO-PPS technique is able to search high-

quality results as compared to IWO and IWO-STS techniques. The inclusion of WP in the system reduces the pollutant emission level and requirements of conventional fossil fuels that make the system cleaner and more efficient. The comparative convergence behaviors demonstrate that the IWO-PPS technique is competent in exploring a better quality solution. The robustness of the IWO-PPS technique is verified by the *t*-test.

CHAPTER-6

OPTIMAL POWER FLOW SOLUTION INCORPORATING WIND AND CHP UNITS USING TENT MAP-BASED HYBRID OPTIMIZATION TECHNIQUE

6.1 INTRODUCTION

In order to meet high power demand in an efficient and optimal manner, the penetration of *combined heat and power* (CHP) units is increasing in the power system networks. The integration of CHP units along with *wind power* (WP) units into the power flow network makes the system quite complicated. The *optimal power flow* (OPF) problem for a network consisting of CHP and WP units is a challenging task due to the interdependence of power and heat generation in the cogeneration process and the intermittent nature of wind energy sources, which may affect the voltage level of system buses. The OPF problem including wind and cogeneration system is a non-convex, nonlinear and complex optimization problem subject to a number of constraints.

In this chapter, the OPF problem is formulated for thermal, CHP and wind generation system by considering the power uncertainty of wind units as a cost factor and the chaotic Tent map-based hybrid IWO-PPS optimization technique (CIWO-PPS) and hybrid IWO-STS optimization technique (CIWO-STS) are proposed. A hybrid technique maintains the proper balance between exploration and exploitation. Further, the chaotic Tent map accelerates the convergence process. The impact of CHP and WP units is analyzed on IEEE 30-bus and IEEE 118-bus systems for solving the OPF problem.

6.2 PROBLEM FORMULATION

The main aim of the OPF problem incorporating cogeneration units and wind generators is to search the OPF solutions of different objectives *i.e.*, overall cost of the system, total emission pollutant, active power losses and voltage magnitude deviations sequentially with the satisfaction of all the system constraints.

The objective functions are formulated as under:

6.2.1 Objective Functions

The mathematical model of each objective function is presented as under:

Overall cost of system: The overall cost of the system includes fuel cost of conventional thermal units, cogeneration units, heat only units and operating cost of available WP and is given as:

$$F_{OC} = f_T + f_C + f_H + f_W \tag{6.1}$$

where f_T, f_C, f_H and f_W represent the fuel cost of conventional thermal units, cogeneration units, heat only units and operating cost of wind units, respectively.

Fuel cost of conventional thermal units: The fuel cost for the conventional thermal units is expressed as [6]:

$$f_T = \sum_{m=1}^{NG} a_m + b_m P_{Gm} + c_m P_{Gm}^2 + \left| d_m \sin\left(e_m \left(P_{Gm}^{\min} - P_{Gm}\right)\right)\right| \tag{6.2}$$

where a_m, b_m, c_m, d_m and e_m represent the coefficients of the fuel cost for the m^{th} generating unit; P_{Gm} represents the active power output of the m^{th} generating unit; and NG denotes the total number of thermal generating units.

Fuel cost of cogeneration units: The power and heat is simultaneously generated by the cogeneration units. In cogeneration units, the production of power and heat depend mutually on each other and this dependency is represented by the *feasible operation region* (FOR). The fuel cost function for the cogeneration units is represented as under [6]:

$$f_C = \sum_{l=1}^{N_C} \alpha_l + \beta_l P_{Cl} + \gamma_l P_{Cl}^2 + \lambda_l P_{Cl} H_{Cl} + \varepsilon_l H_{Cl} + \xi_l H_{Cl}^2 \tag{6.3}$$

where $\alpha_l, \beta_l, \gamma_l \lambda_l, \varepsilon_l, \xi_l$ are the fuel cost coefficients of l^{th} cogeneration unit; P_{Cl} is power generated by l^{th} cogeneration unit; H_{Cl} is heat produced by l^{th} cogeneration unit and N_C denotes the total number of cogeneration units.

Fuel cost of heat only units: The function for fuel cost of heat only units is given as under [6]:

$$f_H = \sum_{n=1}^{N_h} a_n + b_n H_{hn} + c_n H_{hn}^2 \tag{6.4}$$

where a_n, b_n, c_n represent the fuel cost coefficients of n^{th} heat only unit; H_{hn} is the heat produced by n^{th} heat only unit and N_h denotes total number of heat units.

The operating cost of wind power: Due to the intermittent availability of WP, additional cost component is being added in the system operating cost. The cost of wind system is segregated

into three components: direct cost, overestimation cost and underestimation cost. Therefore, the WP generator total operating cost is expressed as under [79]:

$$f_W = \sum_{i=1}^{N_W} \left\{ (d_i \times P_{Wi}) + d_{ri} \times E\left(P_{oe,i}\right) + d_{pi} \times E\left(P_{ue,i}\right) \right\} \tag{6.5}$$

where d_i, d_{ri}, d_{pi} are the cost coefficients of i^{th} wind generator for direct, overestimated and underestimated power, respectively; P_{Wi} is actual power of i^{th} wind generator; $E(P_{oe,i})$ and $E(P_{ue,i})$ represent the expected overestimation and underestimation power of i^{th} wind generator, respectively and N_W denotes the total number of wind generators.

The modeling of wind speed variability and details of the cost of a wind system are given in section 5.2 and subsection 5.3.1 under Chapter 5, respectively.

Total emission pollutant: The release of pollutant emission quantum by thermal units, heat only units and cogeneration units is modeled as below [182]:

$$E = \sum_{m=1}^{NG} \left(\alpha_m + \beta_m P_{Gm} + \gamma_m P_{Gm}^2 + \eta_m \exp\left(\lambda_m P_{Gm}\right) \right) + \sum_{l=1}^{N_C} \chi_l P_{Cl} + \sum_{n=1}^{N_h} \psi_n H_{hn} \tag{6.6}$$

where $\alpha_m, \beta_m, \gamma_m, \eta_m$ and λ_m represent the emission coefficients for the m^{th} generating unit; χ_l is emission coefficient of l^{th} cogeneration unit and ψ_n is emission coefficient of n^{th} heat only unit.

Active power loss: The mathematical model for transmission line active power losses is represented by Eq. (2.19) in subsection 2.3.1 under Chapter 2.

Total voltage magnitude deviations: The total voltage magnitude deviation of all the load buses with respect to $V_{reference}$ is given in subsection 4.2.1 under Chapter 4.

6.2.2 System Constraints

The following system constraints are taken for the OPF problem incorporating thermal, cogeneration and wind generating units.

Equality constraints: Equality constraints are represented by the static power flow equations and heat balance equation as below:

Static power flow equations:

$$P_{Gk} + P_{Ck} + P_{Wk} - P_{Lk} = |V_k| \sum_{l=1}^{N_{BUS}} |V_l| |Y_{kl}| \cos\left(\delta_{kl} + \theta_k - \theta_l\right) \ (k = 1,2,..., N) \tag{6.7}$$

$$Q_{gk} - Q_{Lk} = -|V_k| \sum_{l=1}^{N_{BUS}} |V_l| |Y_{kl}| \sin\left(\delta_{kl} + \theta_k - \theta_l\right) \ (k = 1,2,..., N_{PQ}) \tag{6.8}$$

where P_{Gk}, Q_{Gk} represent the active and reactive power generation available at the k^{th} bus, respectively; P_{Lk}, Q_{Lk} are the active and reactive power demand at the k^{th} bus, respectively; P_{Ck}, P_{Wk} are the active powers generated by cogeneration and wind units at the k^{th} bus, respectively; Y_{kl} and δ_{kl} represent the total admittance and admittance angle of the transmission line, which connect the k^{th} and l^{th} bus; N_{BUS}, N and N_{PQ} are the total number of buses, total system buses except slack bus and the total number of load buses, respectively.

Heat balance equation:

$$\sum_{l=1}^{N_C} H_{Cl} + \sum_{n=1}^{N_h} H_{hn} = H_D \tag{6.9}$$

where H_{hn} is the heat produced by n^{th} heat only unit. H_{Cl} is the heat produced by l^{th} cogeneration unit; H_D is the total heat demand and N_C, N_h represents the total number of cogeneration units and heat units, respectively.

Inequality constraints: The different inequality constraints for the system under consideration are listed as below [182]:

Generating Unit constraints: The lower and upper limits for generating units are given as:

$$P_{Gm}^{\min} \le P_{Gm} \le P_{Gm}^{\max} \ (m = 1,2,...,NG) \tag{6.10}$$

$$Q_{gl}^{\min} \le Q_{gl} \le Q_{gl}^{\max} \ (l = 1,2,...,Ng) \tag{6.11}$$

$$0 \le P_{Wi} \le P_{Wi}^{\max} \ (i = 1,2,...,N_W) \tag{6.12}$$

$$H_{hn}^{\min} \le H_{hn} \le H_{hn}^{\max} \ (n = 1,2,...,N_h) \tag{6.13}$$

$$P_{Cl}^{\min}(H_{Cl}) \le P_{Cl} \le P_{Cl}^{\max}(H_{Cl}) \ (l = 1,2,...,N_C) \tag{6.14}$$

$$H_{Cl}^{\min}(P_{Cl}) \le H_{Cl} \le H_{Cl}^{\max}(P_{Cl}) \ (l = 1,2,...,N_C) \tag{6.15}$$

where $P_{Gm}^{\min}$ and $P_{Gm}^{\max}$ represent the minimum and maximum active power limits for the m^{th} generating unit, respectively; $Q_{gl}^{\min}$ and $Q_{gl}^{\max}$ are the minimum and maximum reactive power limits of the l^{th} generating unit, respectively; N_g denotes total number of generating units that contains thermal units, cogeneration units and wind units; $P_{Wi}, P_{Wi}^{\max}$ represent the actual and maximum power of i^{th} wind generator, respectively; $H_{hn}^{\max}, H_{hn}^{\min}$ represent the upper, lower heat limits for the n^{th} heat only unit, respectively; $P_{Cl}^{\max}, P_{Cl}^{\min}$ represent the upper, lower power limits for the l^{th} cogeneration unit, respectively; $H_{Cl}^{\max}, H_{Cl}^{\min}$ represent the upper, lower heat limits for the l^{th} cogeneration unit, respectively; N_W, N_h and N_C denote the total number of wind units,

heat only units and cogeneration units, respectively.

The CHP units should be operated in a *feasible operation region* (FOR) along with taking care of the capacity limits. Figure 6.1 shows the typical FOR of a CHP unit. The other system constraints *i.e.*, transformer constraints, shunt compensator constraints and security constraints, are discussed in detail in subsection 2.3.2 under Chapter 2.

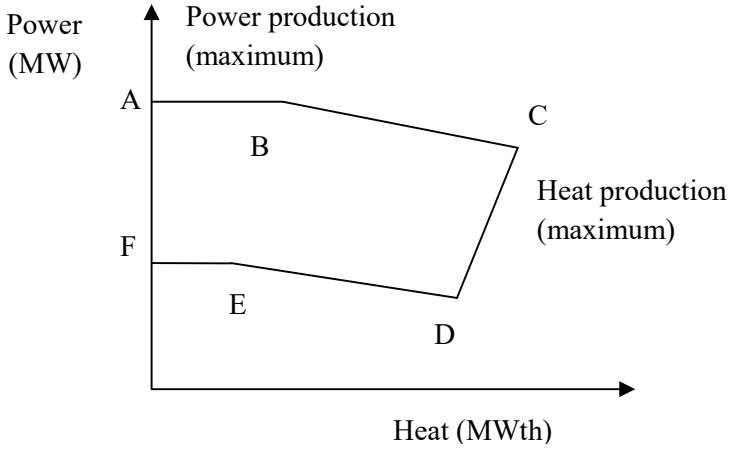

Figure 6.1: Typical FOR of a CHP

6.3 CONSTRAINTS HANDLING APPROACH

During the search process, the equality constraints (Eqs.(6.7)-(6.8)) are handled by the load flow solution. The NR method is executed to satisfy active and reactive power load flow. To satisfy heat balance equality constraint (Eq. (6.9)) and inequality constraints *i.e.*, slack real power output, voltage magnitudes of load buses, reactive powers generated by all generator units, line flows of system exterior penalty method approach is applied. In this approach, a penalty function φ_i is introduced to penalize the overall objective function by incorporating the cumulative error of all constraint violations and is given as [79]:

$$f_i = of_i + \sum_{i=1}^{ni} \varphi_i \ \ (i = 1,2,...,N_{obj}) \tag{6.16}$$

with

$$\varphi_i = \begin{cases} \psi_i \times \left(x_i - x_i^{\lim}\right)^2; & violated \\ 0; & else \end{cases} \tag{6.17}$$

where f represents overall objective function value; ni denotes the number of inequality constraints; N_{obj} are the number of objectives; φ_i represents penalty function and ψ_i represents the penalty coefficient of i^{th} inequality constraint.

***FOR constraint handling*:** The FOR constraint for CHP unit is handled as under:

- Heat is randomly generated within limits.
- Perpendicular is drawn on FOR graph from the randomly generated heat point.
- The minimum and maximum power values with respect to the random heat value are given by the intersection of perpendicular on FOR graph.
- Power is randomly generated within these minimum and maximum limits.

6.4 CHAOTIC TENT MAP

In recent past, the application of chaotic maps is getting a great attention in the optimization field. The dynamic behavior of chaotic maps helps the optimization algorithms to explore the search space more dynamically and globally. The behavior of chaotic maps is predictable only during the initial conditions, but it exhibits random behaviors afterward. The chaotic Tent map is well accepted and is employed for the randomization of algorithm parameters during the search process.

The chaotic sequence for Tent map is given as under [175]:

$$\chi_{i+1} = \begin{cases} \chi_i / 0.7; & \chi_i < 0.7 \\ 10(1-\chi_i)/3; & else \end{cases} \tag{6.18}$$

where χ_i denotes the chaotic number.

6.5 SOLUTION METHODOLOGY

For OPF problem including wind and cogeneration units, decision variables are power generated from thermal and wind generators, power and heat generation from cogeneration units, heat generation from heat only units, magnitude of voltage for all generator units, transformer tap ratios and shunt compensator VAR values. The continuous type variables are the active power of thermal and wind generators, active power and heat generation of cogeneration units and the voltage magnitude for all the power units. The transformer tap ratios and the shunt compensator device output are discrete variables. The decision variables array is given as [X] in Eq. (6.19):

$$X = \begin{matrix} P_{1,1} & \cdots & P_{1,N_T-1}, & P_{1,1} & \cdots & P_{1,N_W-1}, & P_{1,1} & \cdots & P_{1,N_C-1}, & H_{1,1} & \cdots & H_{1,N_C-1}, & H_{1,1} & \cdots & H_{1,N_h-1}, & V_{1,1} & \cdots & V_{1,N_g}, & Q_{1,1} & \cdots & Q_{1,NC}, & t_{1,1} & \cdots & t_{1,N_T} \\ \vdots & & \vdots & \vdots & & \vdots & \vdots & & \vdots & \vdots & & \vdots & \vdots & & \vdots & \vdots & & \vdots & \vdots & & \vdots & \vdots & & \vdots \\ P_{G,1} & \cdots & P_{G,N_T-1}, & P_{W,1} & \cdots & P_{W,N_W-1}, & P_{C,1} & \cdots & P_{C,N_C-1}, & H_{C,1} & \cdots & H_{C,N_C-1}, & H_{hn} & \cdots & H_{h,N_h-1}, & V_{G,1} & \cdots & V_{G,N_g}, & Q_{q,1} & \cdots & Q_{q,NC}, & t_{p,1} & \cdots & t_{p,N_T} \end{matrix} \tag{6.19}$$

where P_G is power generated by thermal generators; P_W is power generated by wind generators; P_C is power generated by cogeneration units; H_C is heat generated by cogeneration units; H_h is heat generated by heat only units; V_G is voltage magnitude for all generating units; Q_q is the output of shunt devices and t_p is transformer tap ratio.

The implementation procedure of the CIWO-PPS technique is explained as under:

Step 1: The weeds are initialized randomly within the described limits as per Eq. (2.36) and Eq. (2.37) under Chapter 2.

Step 2: For the cogeneration unit, the heat is initialized randomly within the described limits as per Eq. (2.36) and Eq. (2.37) and the power is initialized randomly within the FOR according to the generated heat.

Step 3: The values of algorithm parameters are updated during the search process using Tent map Eq. (6.18).

Step 4: The NR method is employed for solving the OPF problem including CHP and wind units for each weed.

During the search process, the equality constraints (Eqs.(6.7)-(6.8)) are satisfied by the load flow equations and the heat balance equation is satisfied by using Eq. (6.9). The error corresponding to each inequality constraint is figured out as per Eq. (6.17)

Step 5: The overall objective function is derived from Eq. (6.16).

Step 6: The weeds are arranged from the best to the worst value based on overall objective function evaluation.

Step 7: The count of new seeds is evaluated according to the best and the worst value of the overall objective function and the new seeds are generated in current search space as discussed in section 2.4 under Chapter 2.

Step 8: If IWO does not converge up to a certain level of expected result for the set iterations, then the PPS method is employed.

The NR method is applied to the solution obtained from the PPS method to compute the value of the overall objective function.

Step 9: The weed population is updated by the combined arrangement of seeds and parent weed on the basis of overall objective function evaluation values using Eq. (6.20).

$$X_{j,l} = \begin{cases} \overline{X}_{j,l}; & f\left(\overline{X}_{j,l}\right) < f\left(X_{j,l}\right) \\ X_{j,l}; & else \end{cases} (j = 1,2,...,NP; l = 1,2,...,D) \tag{6.20}$$

Step 10: Step 3 is repeated until the termination criterion is met.

The flowchart of implementation of the CIWO-PPS technique is presented in Figure 6.2.

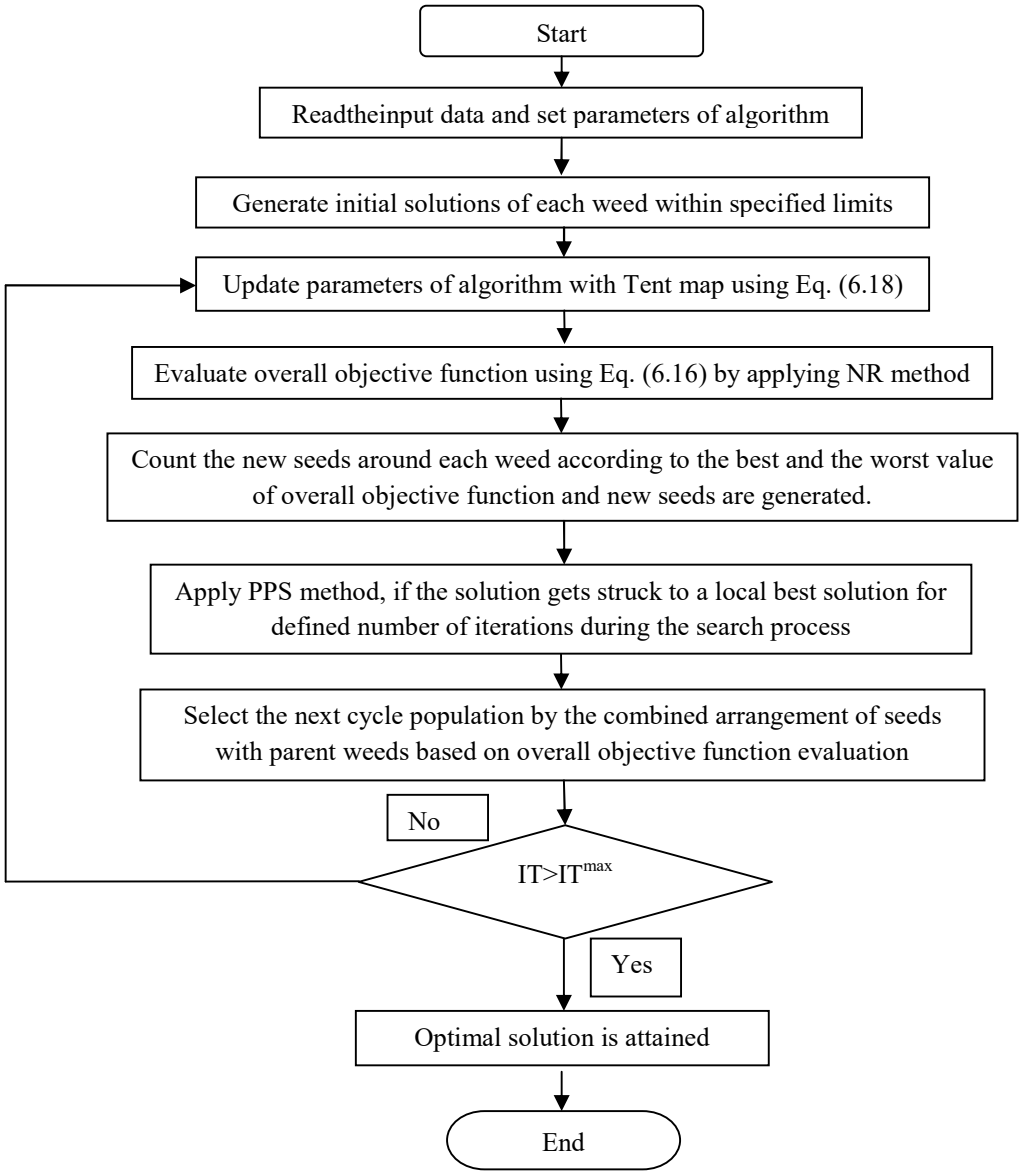

Figure 6.2: Flowchart of implementation of CIWO-PPS technique

6.6 TEST SYSTEMS AND RESULTS

In this work, three test systems are considered. Test system-VI is the standard IEEE 30-bus system [202].The test system-XI and test system-XII are modified IEEE 30-bus system and modified IEEE 118-bus system, respectively [48].The test system-VI includes 6-thermal units, 41-transmission line branches, 24-load buses, 4-transformers tap position settings, 9-shunt compensators and total power demand is 283.4 MW. The details of the test system-VI are discussed in section 4.5 under Chapter 4.

The test system-XI includes 2-thermal units, 3-cogeneration units, 1-heat unit, 1-wind unit, 41-transmission line branches, 24-load buses, 4-transformers tap position settings, 9-shunt compensators. The total demand of power is 283.4 MW and the demand of heat is 175 MWth.

The two thermal units are connected at buses 1 and 2. Three cogeneration units are connected at buses 5, 8 and 11 and the heat only unit is connected at bus 31. The wind unit is connected at bus 13.The single-line diagram of test system-XI is shown in Figure A.3.1 under Appendix-A. The input data of thermal, heat only and cogeneration units for test system-XI are given in Tables A.3.1, A.3.2 and A.3.3, respectively, under Appendix-A. The load data and transmission lines data for test system-XI are given in Tables A.1.3 and A.1.4, respectively, under Appendix-A. The data of wind units of test system-XI is presented in Table A.3.7 under Appendix-A. The test system-XII includes 46-thermal units, 6-cogeneration units, 1-heat unit, 2-wind units, 186-transmission line branches, 132-load buses, 9-transformer tap position settings, 14-shunt compensators. The heat and power demands are 950MWth and 4242.001MW, respectively. The six cogeneration units are connected at buses 12, 31, 54, 87, 103 and 111 and one heat only unit is connected at bus 119 to cater the heat demand only. The wind units are connected at buses 36 and 49. The data of heat only and cogeneration units have been taken from Ref. [6]. The single-line diagram of test system-XII is shown in Figure A.3.2 under Appendix-A. The input data of thermal, cogeneration and heat only units for test system-XII are given in Tables A.3.4, A.3.5 and A.3.6, respectively, under Appendix-A. The load data and transmission lines data for test system-XII are given in Tables A.1.11 and A.1.12, respectively, under Appendix-A. The data of wind units of test system-XII is presented in Table A.3.7 under Appendix-A.

6.6.1 Results and Discussion

The Chaotic *IWO-STS* (CIWO-STS) and CIWO-PPS techniques are applied to solve the OPF problem of cogeneration units with wind system in FORTRAN-90 command line. Thirty one trial runs have been taken to obtain the statistical results.

6.6.1.1 Test system-VI

The IWO, IWO-STS, IWO-PPS, CIWO-STS and CIWO-PPS techniques are applied to test system-VI and the obtained results (best, worst, mean and SD of results) are compared to the results of the state-of-the-art techniques and are presented in Table 6.1. The CIWO-PPS technique achieves the minimum fuel cost value of 799.551 $/hr and that is superior to the results reported by PSO [133], IPSO [133], JAYA [203], AGSO [43], SF-DE [28], AMTPG-JAYA [202], IWO, IWO-STS, IWO-PPS and CIWO-STS techniques. Further, the mean and the worst fuel cost achieved with the CIWO-PPS technique are lower side to the cost attained

with other techniques. The SD of results attained with the CIWO-PPS technique is 0.00508, which is superior to the results obtained by AMTPG-JAYA [202], IWO, IWO-STS, IWO-PPS and CIWO-STS techniques. However, the SD of the results achieved by SF-DE [28] technique is better than the CIWO-PPS technique. The NFE is computed for comparing the computational cost of the optimization techniques as CPU time is dependent on the hardware configuration of the machine, operating system *etc*. The CIWO-PPS technique needs 12.5% less NFE as compared to the CIWO-STS technique.

Table 6.1: Comparison of results for test system-VI

Techniques	Best	Worst	Average	SD	NFE
F_{OC}(\$/hr)					
PSO [133]	802.205	-	-	-	-
IPSO [133]	801.98	-	-	-	-
JAYA [203]	800.479	-	-	-	-
AGSO [43]	801.75	-	-	-	-
SF-DE [28]	800.413	800.419	800.415	0.0015	-
AMTPG-JAYA [202]	800.195	800.343	800.224	0.0063	-
IWO	816.61	817.13	816.67	0.1201	30160
IWO-STS	799.73	799.77	799.755	0.0059	28080
IWO-PPS	799.627	799.67	799.634	0.0075	27950
CIWO-STS	799.551	799.566	799.583	0.0052	26640
CIWO-PPS	799.373	799.402	799.399	0.00508	23680
E **(ton/hr)**					
TLBO [117]	0.2124	0.2156	0.2141	-	-
LTLBO [117]	0.2047	0.2104	0.2065	-	-
SF-DE [28]	0.20482	0.20482	0.20482	0	-
NISSO [130]	0.20479	-	-	-	
IWO	0.20487	0.20529	0.20493	0.0001	31200
IWO-STS	0.20475	0.20481	0.20476	0.000046	29520
IWO-PPS	0.20473	0.20479	0.20475	0.000018	28400
CIWO-STS	0.2047	0.20473	0.204799	0.000032	28800
CIWO-PPS	0.2047	0.2048	0.204751	0.000023	25600
P_{LOSS}(MW)					
PSO [82]	3.43	-	-	-	-
EP [82]	3.335	-	-	-	-
GA [82]	3.37	-	-	-	-
SF-DE [28]	3.0844	3.0857	3.0849	0.0003	-
AMTPG-JAYA [202]	3.0802	3.0937	3.0836	0.0027	-
IWO	3.17	3.254	3.184	0.0144	34320
IWO-STS	2.981	2.991	2.987	0.00259	33120
IWO-PPS	2.887	2.899	2.892	0.00249	31700
CIWO-STS	2.882	2.889	2.898	0.00234	29240
CIWO-PPS	2.8774	2.8856	2.8817	0.00172	25800
VMD **(p.u.)**					
MSCA [17]	0.1030	-	-	-	-
IWO	0.1243	0.12997	0.12876	0.00196	31800
IWO-STS	0.1019	0.1094	0.10222	0.00135	31080
IWO-PPS	0.1018	0.10198	0.10187	0.000045	30800
CIWO-STS	0.1016	0.1023	0.1039	0.00058	30400
CIWO-PPS	0.1014	0.1018	0.10158	0.000078	27200

PSO: particle swarm optimization; IPSO: improved PSO; TLBO: teaching-learning-based optimization; AGSO: adaptive group search optimization; LTLBO: levy mutation based TLBO; SF-DE: superiority of feasibly solutions-DE; MSCA: modified sine cosine algorithm; GA: genetic algorithm; EP: evolutionary programming; AMTPG-JAYA: adaptive multiple teams perturbation-guiding Jaya; NISSO: novel improved social spider optimization

The CIWO-PPS technique achieves the minimum emission pollutant value as 0.2047 ton/hr, that is superior to the results given by TLBO [117], LTLBO [117], SF-DE [28], NISSO [130], IWO, IWO-STS, IWO-PPS and CIWO-STS techniques. The mean and the worst values of the emission pollutant achieved with the CIWO-PPS technique are better than its counterpart techniques. The CIWO-PPS technique has better NFE and SD as compared to IWO, IWO-STS, IWO-PPS and CIWO-STS techniques. The active power losses results achieved by the CIWO-PPS technique have been compared to its counterpart techniques *i.e.*, GA [82], PSO [82], EP [82], SF-DE [28] and AMTPG-JAYA [202]. The CIWO-PPS technique achieves 7.05% less losses as compared to the best reported result by AMTPG-JAYA [202]. The values of the best, mean, and worst active power losses achieved by the CIWO-PPS technique are less in comparison to SF-DE [28], AMTPG-JAYA [202], IWO, IWO-STS, IWO-PPS and CIWO-STS techniques. The value of total voltage magnitude deviations achieved by the CIWO-PPS technique is 0.1014 p.u., that is 1.58% less as compared to the best result reported by the MSCA technique [17]. The values of mean and the worst voltage magnitude deviations and the SD of results achieved by the CIWO-PPS technique are superior to IWO, IWO-STS, IWO-PPS and CIWO-STS techniques. The values of the optimum decision variables obtained by the CIWO-PPS technique for minimum fuel cost, emission pollutant, active power losses and voltage magnitude deviations are presented in Table 6.2.

6.6.1.2 Test system-XI

For test system-XI, the results obtained by the CIWO-PPS technique are compared with the results of IWO-STS and CIWO-STS techniques since as per the best of author's knowledge, no published literature related to OPF problem incorporating wind and CHP units are available. The comparison of results is presented in Table 6.3 and it is observed that the CIWO-PPS technique attains the minimum overall cost as 11900.595$/hr, that is 2.346% and 0.1114% less than IWO-STS and CIWO-STS techniques, respectively. The CIWO-PPS technique is able to attain better average and the worst cost as compared to the IWO-STS and CIWO-STS techniques. The CIWO-PPS technique also achieved better SD of results than of IWO-STS and CIWO-STS techniques. The NFE for the CIWO-PPS technique is 28880 that is less in comparison to IWO-STS and CIWO-STS techniques.

In order to compare the impact of wind units instead of thermal and CHP units, the achieved result for overall system cost is compared to the result reported by Ref. [91].The result attained with the inclusion of wind generators is 14.646% less than the reported result

(13643.549 $/hr) of conventional thermal system with CHP units. Hence, it is summarized that overall system cost is reduced with the inclusion of wind generators because of the higher fuel cost of the thermal and CHP units. The value of minimum emission pollutant achieved with the CIWO-PPS technique is 0.047176ton/hr that is less than that of results obtained by IWO-STS and CIWO-STS techniques. The average and the worst values for total emission pollutants achieved with the CIWO-PPS technique are better than IWO-STS and CIWO-STS techniques.

Further, the SD of results and NFE required by the CIWO-PPS technique are superior to IWO-STS and CIWO-STS techniques. The CHP and wind energy source impact is analyzed by the comparison of obtained results with conventional OPF system emission results. The reported result for pollutant emission of the conventional thermal system is 0.2047ton/hr [117]. The total pollutant emission for the system including thermal, wind and CHP units attained by the CIWO-PPS technique, is reduced by 0.157524 ton/hr over the reported result of the conventional thermal system. Hence, it is concluded that including wind farms, CHP units and heat only units reduce pollutant emission.

Table 6.2: Optimum value of decision variables for test system-VI

Decision variables	Limits		F_{OC} ($/hr)	E (ton/hr)	P_{LOSS} (MW)	VMD (p.u)
	min	max				
P_{t1} *(MW)*	50	200	176.388	63.215	51.3446	173.484
P_{t2} *(MW)*	20	80	49.223	68.443	79.982	49.812
P_{t5} *(MW)*	15	50	21.922	49.999	49.999	23.679
P_{t8} *(MW)*	10	35	20.912	34.912	34.954	20.984
P_{t11} *(MW)*	10	30	11.611	29.999	29.999	13.236
P_{t13}*(MW)*	12	40	12.003	39.999	39.999	12.006
V_{g1} *(p.u.)*	0.95	1.1	1.09991	1.09999	1.098741	1.03114
V_{g2} *(p.u.)*	0.95	1.1	1.08834	1.09796	1.09917	1.02148
V_{g5} *(p.u.)*	0.95	1.1	1.06233	1.09953	1.080662	1.01832
V_{g8} *(p.u.)*	0.95	1.1	1.07221	1.09654	1.092562	1.00252
V_{g11} *(p.u.)*	0.95	1.1	1.09464	1.09878	1.09976	1.03464
V_{g13} *(p.u.)*	0.95	1.1	1.06432	1.05564	1.098042	1.00142
Q_{10} *(MVAr)*	0	5	5	5	5	5
Q_{12}*(MVAr)*	0	5	5	5	5	2
Q_{15}*(MVAr)*	0	5	5	5	5	4
Q_{17}*(MVAr)*	0	5	5	5	5	2
Q_{20}*(MVAr)*	0	5	5	5	4	5
Q_{21}*(MVAr)*	0	5	5	5	5	5
Q_{23}*(MVAr)*	0	5	5	5	3	5
Q_{24}*(MVAr)*	0	5	4	5	5	4
Q_{29}*(MVAr)*	0	5	2	5	2	2
t_{11}	0.9	1.1	1.01	1.01	1.08	1.05
t_{12}	0.9	1.1	1.06	1.08	0.90	0.91
t_{15}	0.9	1.1	1.03	1.02	0.99	0.96
t_{36}	0.9	1.1	0.99	1.02	0.98	0.96
Cost ($/hr)	-	-	**799.373**	945.531	967.017	804.725
Emission (ton/hr)	-	-	0.36439	**0.2047**	0.20713	0.35577
P_L(MW)	-	-	8.6589	3.1665	**2.8774**	9.8019
Voltage deviation (p.u.)	-	-	1.20324	1.44864	1.95275	**0.1014**

Note: Bold values indicate the optimum results

Table 6.3: Comparison of results for test system-XI

Techniques	Best	Worst	Average	SD	NFEs
F_{OC} **($/hr)**					
IWO-STS	12179.766	12289.39	12228.20	25.128	31920
CIWO-STS	11913.864	1195273	11932.095	6.9055	29640
CIWO-PPS	11900.595	11931.78	11919.844	6.29	28880
E **(ton/hr)**					
IWO-STS	0.049163	0.04977	0.04933	0.00014	31720
CIWO-STS	0.047962	0.048363	0.048099	0.000022	31160
CIWO-PPS	0.047176	0.047378	0.047234	0.0000178	28080
P_{LOSS}**(MW)**					
IWO-STS	5.171	6.571	5.673	0.34112	33800
CIWO-STS	4.1859	4.2742	4.203	0.01657	33120
CIWO-PPS	4.0434	4.1379	4.10592	0.01596	31680
VMD**(p.u.)**					
IWO-STS	0.3667	0.3952	0.37969	0.00797	30800
CIWO-STS	0.2887	0.2988	0.29242	0.00247	30400
CIWO-PPS	0.23233	0.24287	0.23944	0.00199	28120

For the third objective, minimization of active power loss, the losses attained by the CIWO-PPS technique are 4.0434 MW that is superior to the IWO-STS and CIWO-STS techniques. The active power losses are increased due to the generation-demand gap caused by the intermittent availability of WP. Further, the value of minimum voltage deviations achieved with the CIWO-PPS technique is 0.23233 p.u., that is superior to the IWO-STS and CIWO-STS techniques. The voltage magnitude deviation is increased as compared to the conventional thermal system due to the intermittent nature of WP availability. The values of average and worst active power losses and voltage deviations obtained by the CIWO-PPS technique are better in comparison to IWO-STS and CIWO-STS techniques. The SD and NFE for the CIWO-PPS technique are better than the IWO-STS and CIWO-STS techniques. The optimum values of decision variables attained by the CIWO-PPS technique for all the objectives are given in Table 6.4.

6.6.1.3 Test system-XII

The results obtained by the CIWO-PPS technique are compared with the results achieved by IWO-STS and CIWO-STS techniques and are presented in Table 6.5. It has been observed from Table 6.5 that for all four objectives *i.e.*, minimum overall cost of system, total emission pollutant, active power loss and magnitude of voltage deviations results obtained by CIWO-PPS technique are 0.815%, 6.49%, 3.456% and 19.16% less as compared to results attained by CIWO-STS technique, respectively. Further, it is evident from overall cost results that the CIWO-PPS technique is capable of attaining superior results with respect to the average value, worst value, SD and NFE than the IWO-STS and CIWO-STS techniques.

Table 6.4: Optimum value of decision variables for test system-XI

Decision variables	Limits		F_{OC} (\$/hr)	E(ton/hr)	P_{LOSS} (MW)	VMD (p.u.)
	min	max				
P_{t1} *(MW)*	50	200	143.133	61.667	54.737	76.571
P_{t2} *(MW)*	20	80	51.654	65.444	76.765	71.238
P_{C5} *(MW)*	15	50	19.965	39.922	39.086	29.611
P_{C8} *(MW)*	10	35	12.872	34.542	34.548	33.328
P_{C11}*(MW)*	10	30	12.322	27.665	28.866	25.543
P_{W13}*(MW)*	0	60	52.347	58.322	53.443	52.344
H_5*(MWth)*	0	55	42.995	50.866	49.665	47.544
H_8*(MWth)*	0	55	41.092	48.609	47.965	48.055
H_{11}*(MWth)*	0	55	40.966	47.402	48.025	46.543
H_{31}*(MWth)*	0	2695.2	49.947	28.123	29.345	32.858
V_{g1} *(p.u.)*	0.95	1.1	1.027987	1.02543	1.03437	1.03227
V_{g2} *(p.u.)*	0.95	1.1	1.01262	1.01662	1.03442	1.01941
V_{g5} *(p.u.)*	0.95	1.1	1.02531	1.04517	1.04007	1.02222
V_{g8} *(p.u.)*	0.95	1.1	0.995456	1.03764	1.03997	1.03009
V_{g11}*(p.u.)*	0.95	1.1	0.999872	0.996654	1.044554	1.02465
V_{g13}*(p.u.)*	0.95	1.1	1.03023	1.043323	0.99923	1.023876
Q_{10}*(MVAr)*	0	5	1	3	3	1
Q_{12}*(MVAr)*	0	5	5	5	4	2
Q_{15}*(MVAr)*	0	5	5	5	4	2
Q_{17}*(MVAr)*	0	5	5	5	5	3
Q_{20}*(MVAr)*	0	5	5	5	5	4
Q_{21}*(MVAr)*	0	5	5	5	5	5
Q_{23}*(MVAr)*	0	5	4	4	4	4
Q_{24}*(MVAr)*	0	5	5	5	5	5
Q_{29}*(MVAr)*	0	5	5	1	5	4
t_{11}	0.9	1.1	0.97	1.02	1.09	1.02
t_{12}	0.9	1.1	1.03	0.95	0.94	0.97
t_{15}	0.9	1.1	1.06	1.06	1.01	0.96
t_{36}	0.9	1.1	0.97	1.01	1.01	0.98
Overall Cost (\$/hr)	-	-	**11900.595**	14073.305	14176.978	13597.443
Emission pollutant (ton/hr)	-	-	0.118588	**0.047176**	0.049835	0.054776
P_L *(MW)*	-	-	8.896	4.162	**4.0434**	5.2322
Voltage deviation (p.u.)	-	-	0.30278	0.32393	0.28018	**0.23233**

Note: Bold values indicate the optimum results.

Table 6.5: Comparison of results for test system-XII

Techniques	**best**	**Worst**	**Average**	**SD**	**NFEs**
***F_{OC}*(\$/hr)**					
IWO-STS	138602.48	138718.29	138666.95	30.445	170100
CIWO-STS	137861.54	137938.24	137893.16	16.958	132060
CIWO-PPS	136746.93	136809.56	136792.704	16.761	127800
***E*(ton/hr)**					
IWO-STS	3.5746	3.6212	3.5875	0.01685	153360
CIWO-STS	3.4406	3.4621	3.4497	0.00512	111690
CIWO-PPS	3.2309	3.2477	3.2378	0.00441	102930
***P_{LOSS}*(MW)**					
IWO-STS	69.616	70.35	69.81	0.21138	164160
CIWO-STS	67.504	67.943	67.76	0.11213	129600
CIWO-PPS	65.249	65.543	65.37	0.08102	116640
***VMD* (p.u.)**					
IWO-STS	1.01599	1.01956	1.01748	0.00081	157680
CIWO-STS	0.994977	0.995745	0.995213	0.000185	113880
CIWO-PPS	0.83496	0.83578	0.83518	0.00016	109500

Hence, it is summarized that the CIWO-PPS technique performs better as compared to the IWO-STS and CIWO-STS techniques for large-scale optimization problems.The convergence behaviors attained with IWO-STS, CIWO-STS and CIWO-PPS techniques for all objective functions are represented by Figures 6.3, 6.4, 6.5 and 6.6, respectively. These figures demonstrate that the CIWO-PPS approach exhibits better convergence criteria. The optimum values of decision variables achieved by the CIWO-PPS technique for all the objectives are presented in Table 6.6.

Table 6.6: Optimum value of decision variables for test system-XII

Decision variables	Limits		F_{OC} ($/hr)	E (ton/hr)	P_{LOSS} (MW)	VMD (p.u.)
	min	max				
P_{t1} *(MW)*	0	100	44.123	48.762	35.221	34.123
P_{t4} *(MW)*	0	100	40.321	41.144	41.145	41.323
P_{t6} *(MW)*	0	100	49.354	48.874	49.978	50.333
P_{t8} *(MW)*	0	100	3.11	3.22	3.29	3.03
P_{t10}*(MW)*	165	550	171.429	170.988	178.984	179.422
P_{t15}*(MW)*	0	100	44.7650	46.5540	44.5180	44.4440
P_{t18}*(MW)*	0	100	58.7570	55.6650	58.5550	58.7750
P_{t19}*(MW)*	0	100	23.9540	23.5540	23.2130	23.0990
P_{t24}*(MW)*	0	100	0.0021	0.0022	0.0029	0.0023
P_{t25}*(MW)*	96	320	206.433	212.333	197.873	197.559
P_{t26}*(MW)*	124.2	414	89.976	88.877	89.876	89.964
P_{t27}*(MW)*	0	100	61.032	60.372	60.779	61.948
P_{t32}*(MW)*	0	100	48.765	49.876	46.762	46.255
P_{t34}*(MW)*	0	100	38.9220	39.8870	38.9930	38.9390
P_{t40}*(MW)*	0	100	39.3450	38.8770	36.5540	36.0750
P_{t42}*(MW)*	0	100	3.143	3.234	3.065	3.154
P_{t46}*(MW)*	0	119	18.943	19.988	18.977	18.926
P_{t55}*(MW)*	0	100	54.065	53.444	53.466	54.567
P_{t56}*(MW)*	0	100	0.001	0.003	0.001	0.002
P_{t59}*(MW)*	76.5	255	157.6650	156.5540	157.6550	159.3230
P_{t61}*(MW)*	78	260	88.7640	87.8870	87.8320	88.8660
P_{t62}*(MW)*	0	100	0.0650	0.0670	0.0630	0.0680
P_{t65}*(MW)*	147.3	491	311.665	310.988	252.882	353.855
P_{t66}*(MW)*	147.6	492	253.324	251.233	245.637	348.554
P_{t69}*(MW)*	0	805.2	201.935	221.93	312.151	150.402
P_{t70}*(MW)*	0	100	28.876	29.787	29.044	29.039
P_{t72}*(MW)*	0	100	2.4120	2.4540	2.4110	2.4850
P_{t73}*(MW)*	0	100	0.0800	0.0650	0.0601	0.0800
P_{t74}*(MW)*	0	100	23.4660	22.3440	22.4450	23.4660
P_{t76}*(MW)*	0	100	0.092	0.091	0.089	0.091
P_{t77}*(MW)*	0	100	0.134	0.132	0.165	0.164
P_{t80}*(MW)*	173.1	577	325.24	301.334	343.543	344.829
P_{t85}*(MW)*	0	100	13.097	14.335	13.997	13.237
P_{t89}*(MW)*	212.1	707	410.998	412.345	412.522	411.923
P_{t90}*(MW)*	0	100	1.9990	1.8770	1.8660	1.9990
P_{t91}*(MW)*	0	100	0.0020	0.0010	0.0020	0.0010
P_{t92}*(MW)*	0	100	0.0010	0.0030	0.0010	0.0020
P_{t99}*(MW)*	0	100	107.654	109.887	108.776	108.926
P_{t100}*(MW)*	105.6	352	221.465	223.444	203.487	201.684
P_{t104}*(MW)*	0	100	0.002	0.001	0.001	0.002
P_{t105}*(MW)*	0	100	10.4530	11.2340	11.0320	10.0691

Table 6.6: Optimum value of decision variables for test system-XII (Continued)

Decision variables	Limits		F_{OC} ($/hr)	E (ton/hr)	P_{LOSS} (MW)	VMD (p.u.)
	min	max				
P_{t107}(MW)	0	100	11.3550	12.3450	11.2330	11.3610
P_{t110}(MW)	0	100	5.6580	5.8450	5.4550	5.6580
P_{t112}(MW)	0	100	0.0010	0.0010	0.0030	0.0010
P_{t113}(MW)	0	100	28.7760	27.6650	27.0210	27.7850
P_{t116}(MW)	0	100	0.002	0.001	0.002	0.002
P_{W36}(MW)	0	400	369.832	255.554	175.484	167.983
P_{W49}(MW)	0	600	395.544	319.875	418.665	388.694
P_{C12}(MW)	0	185	110.628	111.237	94.557	93.222
P_{C31}(MW)	0	107	68.088	67.669	53.269	52.655
P_{C54}(MW)	0	148	84.206	82.776	83.445	84.255
P_{C87}(MW)	0	104	73.004	72.344	52.355	53.534
P_{C103}(MW)	0	140	98.324	97.665	97.983	98.322
P_{C111}(MW)	0	136	99.133	98.876	97.863	96.551
H_{12}(MWth)	0	180	120.564	109.412	91.253	110.455
H_{31}(MWth)	0	135.6	96.122	81.182	70.826	84.128
H_{54}(MWth)	0	180	106.321	101.362	92.625	106.356
H_{87}(MWth)	0	180	103.025	81.281	75.814	83.258
H_{103}(MWth)	0	135.6	114.421	104.206	92.643	114.216
H_{111}(MWth)	0	180	112.344	102.381	93.188	112.388
H_{119}(MWth)	0	2695.2	297.203	370.176	433.651	339.199
V_{g1} (p.u.)	0.94	1.06	0.981132	0.991118	0.99821	0.981132
V_{g4} (p.u.)	0.94	1.06	1.00031	1.00121	1.00116	1.00031
V_{g6} (p.u.)	0.94	1.06	1.00462	1.00407	1.00472	1.00462
V_{g8} (p.u.)	0.94	1.06	0.990401	0.98871	0.98772	0.98401
V_{g10}(p.u.)	0.94	1.06	1.00392	1.00387	1.00372	1.00392
V_{g12}(p.u.)	0.94	1.06	1.00508	1.00491	1.00487	1.00508
V_{g15}(p.u.)	0.94	1.06	1.00112	1.00104	1.00112	1.00112
V_{g18}(p.u.)	0.94	1.06	1.00355	1.00322	1.00317	1.00355
V_{g19}(p.u.)	0.94	1.06	1.000021	1.00012	1.00013	1.000021
V_{g24}(p.u.)	0.94	1.06	1.00522	1.00533	1.00512	1.00522
V_{g25}(p.u.)	0.94	1.06	1.01982	1.01889	1.01792	1.01982
V_{g26}(p.u.)	0.94	1.06	1.01132	1.01301	1.02313	1.01132
V_{g27}(p.u.)	0.94	1.06	0.98123	0.98002	0.98012	0.98123
V_{g31}(p.u.)	0.94	1.06	0.978543	0.974343	0.99545	0.978543
V_{g32}(p.u.)	0.94	1.06	0.987112	0.987221	0.987123	0.987112
V_{g34}(p.u.)	0.94	1.06	1.01554	1.01422	1.01427	1.01554
V_{g36}(p.u.)	0.94	1.06	1.00515	1.00551	1.00513	1.01515
V_{g40}(p.u.)	0.94	1.06	1.01954	1.01856	1.00824	1.01954
V_{g42}(p.u.)	0.94	1.06	0.98761	0.98654	0.98615	0.98761
V_{g46}(p.u.)	0.94	1.06	1.0381	1.0312	1.0123	1.0381
V_{g49}(p.u.)	0.94	1.06	1.01564	1.01621	1.01613	1.01564
V_{g54}(p.u.)	0.94	1.06	1.00003	1.00011	1.00018	1.00003
V_{g55}(p.u.)	0.94	1.06	0.985832	0.98435	0.98452	0.985832
V_{g56}(p.u.)	0.94	1.06	0.982321	0.98203	0.99219	0.982321
V_{g59}(p.u.)	0.94	1.06	1.0214	1.0211	1.0101	1.0214
V_{g61}(p.u.)	0.94	1.06	1.03722	1.03675	1.03532	1.03722
V_{g62}(p.u.)	0.94	1.06	1.0311	1.0312	1.0325	1.0211
V_{g65}(p.u.)	0.94	1.06	1.01345	1.01234	1.01241	1.01345
V_{g66}(p.u.)	0.94	1.06	1.0382	1.0354	1.03422	1.0382
V_{g69}(p.u.)	0.94	1.06	1.01392	1.01278	1.01138	1.01392
V_{g70}(p.u.)	0.94	1.06	0.983124	0.98443	0.98354	0.983124
V_{g72}(p.u.)	0.94	1.06	0.98922	0.988721	0.98732	0.98922
V_{g73}(p.u.)	0.94	1.06	0.98711	0.98654	0.96874	0.98711
V_{g74}(p.u.)	0.94	1.06	0.962223	0.96287	0.96732	0.96222

Table 6.6: Optimum value of decision variables for test system-XII (Continued)

Decision variables	Limits		F_{OC} ($/hr)	E (ton/hr)	P_{LOSS} (MW)	VMD (p.u.)
	min	max				
V_{g76}(p.u.)	0.94	1.06	0.95112	0.95221	0.95122	0.95112
V_{g77}(p.u.)	0.94	1.06	1.00412	1.00402	1.00414	1.00412
V_{g80}(p.u.)	0.94	1.06	1.01211	1.01212	1.00221	1.01211
V_{g85}(p.u.)	0.94	1.06	0.994123	0.993213	0.99211	0.994123
V_{g87}(p.u.)	0.94	1.06	0.99799	0.99654	0.99123	0.99799
V_{g89}(p.u.)	0.94	1.06	1.03555	1.03435	1.01023	1.01555
V_{g90}(p.u.)	0.94	1.06	1.00413	1.00343	1.00331	1.00413
V_{g91}(p.u.)	0.94	1.06	1.0402	1.0421	1.00141	1.0202
V_{g92}(p.u.)	0.94	1.06	1.00461	1.00412	1.00132	1.00461
V_{g99}(p.u.)	0.94	1.06	1.0222	1.0202	1.0111	1.0222
V_{g100}(p.u.)	0.94	1.06	1.03012	1.0312	1.0121	1.01012
V_{g103}(p.u.)	0.94	1.06	1.01582	1.01521	1.01511	1.01582
V_{g104}(p.u.)	0.94	1.06	1.01033	1.0111	1.0132	1.01033
V_{g105}(p.u.)	0.94	1.06	1.03922	1.03223	1.01211	1.03932
V_{g107}(p.u.)	0.94	1.06	1.01132	1.01122	1.0212	1.01132
V_{g110}(p.u.)	0.94	1.06	1.01122	1.01112	1.03211	1.01122
V_{g111}(p.u.)	0.94	1.06	1.01653	1.01434	1.04427	1.01653
V_{g112}(p.u.)	0.94	1.06	1.02833	1.02763	1.00634	1.02833
V_{g113}(p.u.)	0.94	1.06	1.01482	1.01476	1.00816	1.014822
V_{g116}(p.u.)	0.94	1.06	1.00511	1.00432	1.00842	1.00511
Q_5(MVAr)	0	30	1	3	2	1
Q_{34}(MVAr)	0	30	17	16	15	17
Q_{37}(MVAr)	0	30	15	16	17	16
Q_{44}(MVAr)	0	30	4	3	3	4
Q_{45}(MVAr)	0	30	9	7	8	9
Q_{46}(MVAr)	0	30	16	16	17	18
Q_{48}(MVAr)	0	30	13	14	14	14
Q_{74}(MVAr)	0	30	10	10	10	11
Q_{79}(MVAr)	0	30	18	18	17	16
Q_{82}(MVAr)	0	30	2	3	3	2
Q_{83}(MVAr)	0	30	9	9	9	9
Q_{105}(MVAr)	0	30	16	16	16	16
Q_{107}(MVAr)	0	30	7	7	6	7
Q_{110}(MVAr)	0	30	3	3	3	3
t_8	0.9	1.1	0.95	0.94	0.95	0.95
t_{32}	0.9	1.1	1.01	1.02	1.02	1.03
t_{36}	0.9	1.1	1.01	1.01	0.99	1.01
t_{51}	0.9	1.1	0.95	0.94	0.99	0.95
t_{93}	0.9	1.1	0.95	0.95	0.97	0.95
t_{95}	0.9	1.1	0.95	0.94	0.92	0.95
t_{102}	0.9	1.1	0.99	0.99	0.99	0.99
t_{107}	0.9	1.1	1.01	1.01	0.94	1.01
t_{127}	0.9	1.1	0.99	0.98	0.99	0.99
Overall Cost ($/hr)	-	-	**136746.93**	137311.63	136838.97	137693.54
Emission pollutant (ton/hr)	-	-	3.23647	**3.2308**	4.4442	3.5071
P_L *(MW)*	-	-	81.687	76.419	**65.249**	71.868
Voltage deviation (p.u.)	-	-	0.86390	0.83621	0.83860	**0.83496**

Note: Bold values indicate the optimum results.

6.6.2 Statistical Analysis

The success rate of an optimization technique is confirmed by its robustness. The two-sample

t-test is performed to verify the robustness of test system-XII for the first objective function *i.e.*, minimization of overall cost with 5% significant level. Table 6.7 represents the *t*-test results and it is observed that the statistical output of *t-calculated* is more than the critical value. This rejects the null hypothesis and confirms the significant difference between the means of two populations at 5% level of significance. It is ascertained that the CIWO-PPS technique exhibits better robustness than the CIWO-STS and IWO-STS techniques.

Table 6.7: *t*-test (two tail) results for objective minimization of overall cost for test system-XII at α=0.05

Statistics/Techniques	**CIWO-PPS Vs. CIWO-STS**	**CIWO-PPS Vs. IWO-STS**
t-calculated	256.972	300.265
t-critical	2	2

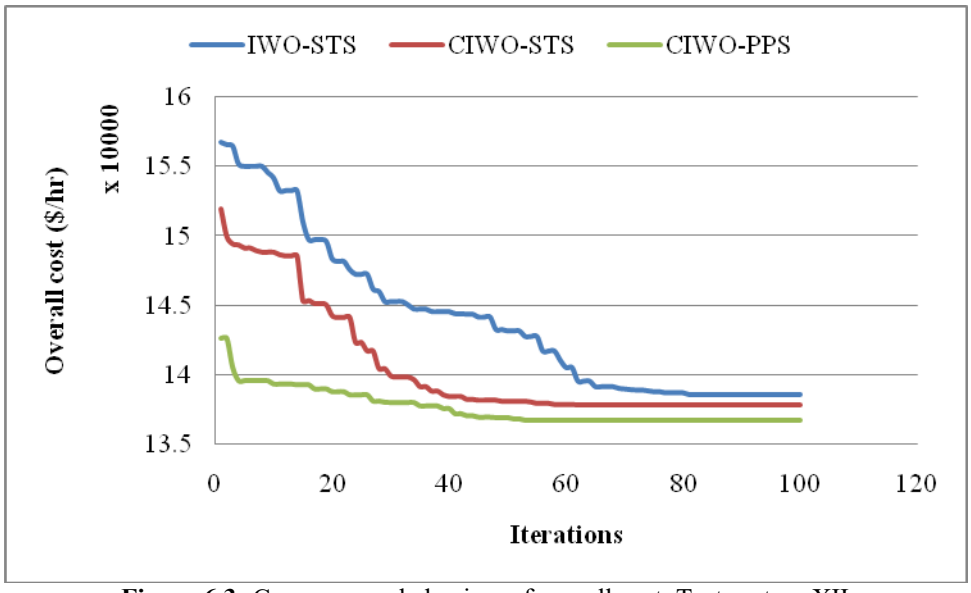

Figure 6.3: Convergence behaviors of overall cost: Test system-XII

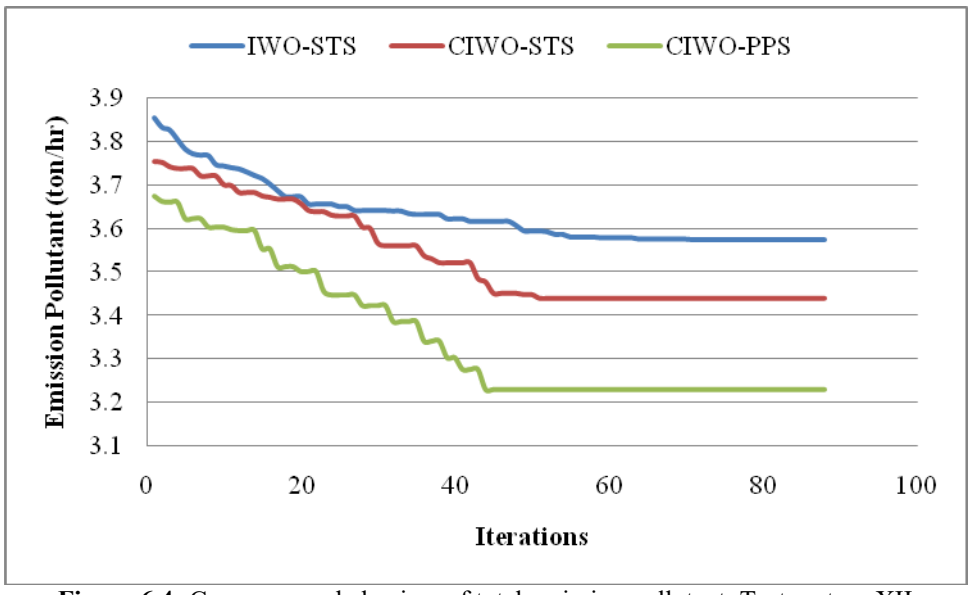

Figure 6.4: Convergence behaviors of total emission pollutant: Test system-XII

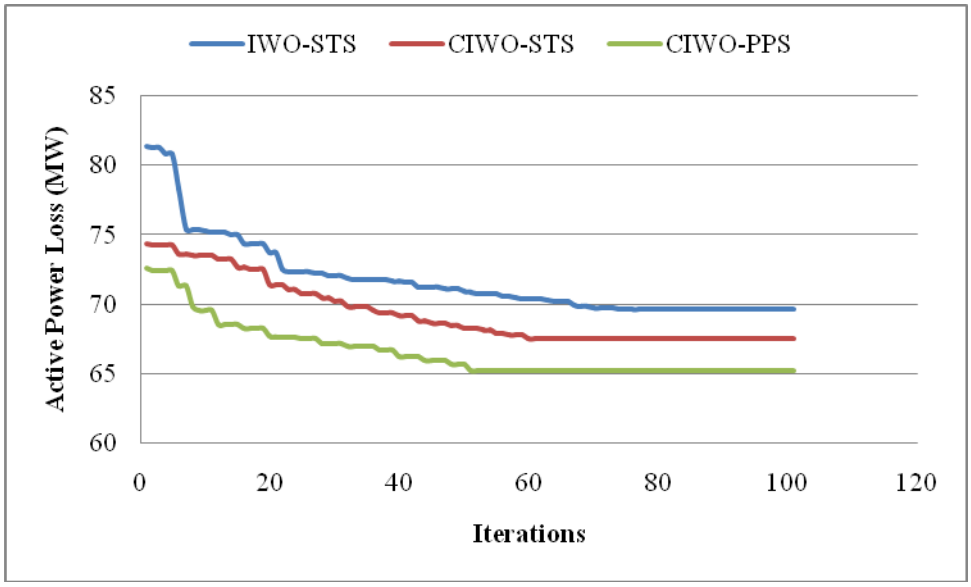

Figure 6.5: Convergence behaviors of active power losses: Test system-XII

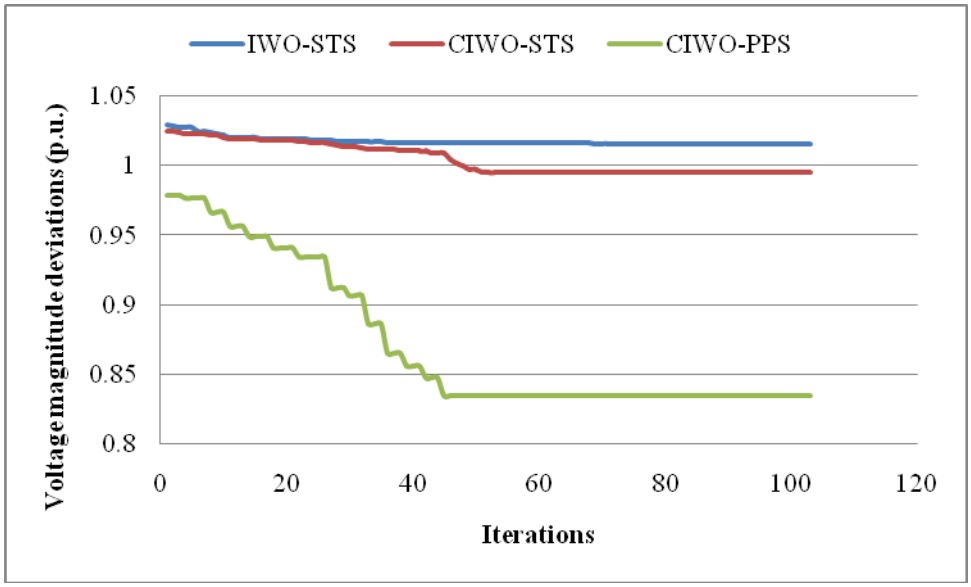

Figure 6.6: Convergence behaviors of voltage magnitude deviations: Test system-XII

6.7 CONCLUSIONS

In this chapter, a chaotic Tent map-based hybrid optimization technique is proposed for solving the OPF problem incorporating wind and cogeneration system. The hybrid optimization technique integrates the IWO technique and PPS method to obtain the global optimum solution. The chaotic Tent map is introduced into the hybrid optimization technique to improve the opportunity of finding the solutions nearer to the global best and accelerating the speed of convergence. In this work, the four OPF objective functions *i.e.*, overall cost, total emission pollutant, active power losses, total voltage magnitude deviations, are sequentially minimized. The proposed techniques are tested on three standard IEEE test systems. In the case of test

system-VI, the CIWO-PPS technique attains a fuel cost value as 799.373$/hr that is better than its counterpart techniques and CIWO-STS technique. The pollutant emission, active power losses and total voltage magnitude deviations values attained by the CIWO-PPS technique are 0.2047 ton/hr, 2.8774 MW and 0.1014p.u., respectively, which show improved results over the well-established techniques and CIWO-STS technique. For test system-XI, the CIWO-PPS technique attains an overall cost value as 11900.595 $/hr that is 0.1114% less in comparison to the CIWO-STS technique. The total pollutant emission, active power losses and total voltage magnitude deviations values attained by the CIWO-PPS technique are 0.046909 ton/hr, 4.0434MW and 0.23233p.u., respectively showing enhancement over the results attained with the CIWO-STS technique. For test system-XII, it has been found that the CIWO-PPS technique is able to search high-quality results as compared to CIWO-STS technique. The results show that the overall system cost is reduced with the inclusion of wind units because of the higher fuel cost of the thermal and cogeneration units. The inclusion of WP and CHP units reduces the pollutant emission level and requirement of conventional fossil fuels. The comparative convergence behaviors demonstrate that the CIWO-PPS technique is competent in exploring better quality solutions. The robustness of the CIWO-PPS technique is verified by the *t*-test.

CHAPTER 7

CONCLUSIONS AND FUTURE SCOPE OF WORK

7.1 INTRODUCTION

This chapter presents significant contributions of the thesis along with a brief description of the future scope of research work.

7.2 SIGNIFICANT CONTRIBUTIONS

This section summarizes the important contributions as presented below:

1. An *optimal power flow* (OPF) problem is formulated with defined objectives and constraints. The OPF problem is solved by the proposed integrated optimization technique. The proposed technique integrates the *invasive weed optimization* (IWO) technique with the *Powell pattern search* (PPS) method. The IWO technique is taken as a global search technique and the PPS method has been explored as a local search technique. The IWO technique explores the search area effectively and the PPS method is applied to exploit the best result obtained by the IWO technique. The integrated IWO-PPS optimization technique requires less *number of function evaluations* (NFE) as it is capable of keeping a fine balance between exploration and exploitation search.
2. The IWO-PPS technique is applied to solve the OPF problem formulated by incorporating the FACTS devices in the power system. The efficacy of the IWO-PPS technique is tested on standard test systems with and without FACTS devices by undertaking fuel cost, pollutant emission, active power loss and total voltage magnitude deviations as objective functions. The attained results by the IWO-PPS technique are found better as compared to the other state-of-art algorithms. The comparative convergence characteristics illustrate that the IWO-PPS technique is able to search high-quality solutions with the same NFE. The *t*-test has been successfully tested on test systems of OPF problem and demonstrated that the IWO-PPS technique is more robust as compared to other state-of-the-art algorithms.
3. The OPF problem with defined objectives has been considered as a *multi-objective optimal power flow* (MO-OPF) problem due to the contradictory nature of the

objectives. The IWO-PPS technique is applied to solve the MO-OPF problem. Being indistinct, the conflicting objectives have been characterized by their membership functions employing fuzzy theory and these are further utilized for the implementation of the satisficing function. To search the best non-dominated solution of MO problem, a non-interactive approach has been explored. The IWO-PPS technique has been tested on three test systems of MO-OPF problem with FACT devices. The cardinal priority ranking attained by the IWO-PPS technique for all the cases is better than its counterpart techniques. Further, the ability of the IWO-PPS technique to search high-quality solutions is confirmed by the comparative convergence characteristics. The robustness of the IWO-PPS technique is also examined by applying the *t*-test and found satisfactory.

4. The hybrid technique that integrates IWO with *space transformation search* (STS) techniques has also been applied to solve the OPF problem. The IWO-STS technique simultaneously evaluates the solution in current and transformed search area. This feature enhances the possibility of finding the solutions nearer to the global optimum and accelerates the convergence speed. The results obtained by the IWO-STS technique are compared with the results reported by its counterpart techniques and found better. The comparative convergence characteristics show that the IWO-STS technique is capable of searching better quality solutions.
5. The IWO, IWO-STS and IWO-PPS techniques are applied for solving the OPF problem incorporating wind system. The IWO, IWO-STS and IWO-PPS techniques are tested on two standard IEEE test systems and the results obtained by the IWO-PPS technique are better than its counterpart techniques. The result obtained by the IWO-PPS technique is also compared with IWO and IWO-STS techniques and it is observed that the IWO-PPS technique is able to search high-quality results as compared to IWO and IWO-STS techniques. It has been observed that the inclusion of WP generators has reduced the emission level as compared to conventional thermal systems. The comparative convergence behaviors demonstrate that the IWO-PPS technique is competent in exploring better quality solutions. The robustness of the IWO-PPS technique is verified by the *t*-test.
6. The OPF problem is formulated by including the thermal, *combined heat and power* (CHP) and wind generation system and considering the power uncertainty of wind units as a cost factor. A chaotic Tent map-based hybrid optimization technique, integrating IWO and PPS (CIWO-PPS), is proposed. The introduction of a chaotic Tent map

improves the opportunity of finding the solutions nearer to the global best and accelerates the speed of convergence.

7. The *chaotic IWO-STS* (CIWO-STS) and CIWO-PPS techniques are applied to solve the OPF problem incorporating CHP and WP units. The efficacy of the CIWO-PPS technique is tested on three standard IEEE test systems and the results obtained by the CIWO-PPS technique are found better than other well-established techniques. The results obtained by the CIWO-PPS technique are also compared with IWO-STS, IWO-PPS and CIWO-STS techniques and it has been found that the CIWO-PPS technique is able to search high-quality results as compared to IWO-STS, IWO-PPS and CIWO-STS techniques. The overall system cost is reduced with the inclusion of wind generators because of the higher fuel cost of the thermal and cogeneration units. The total pollutant emission attained by the CIWO-PPS technique is better than the reported result of the conventional thermal system. Hence, it is summarized that overall system cost and pollutant emission are reduced with the inclusion of wind and CHP units. The comparative convergence behaviors demonstrate that the CIWO-PPS technique is competent in exploring a better quality solution. The robustness of the CIWO-PPS technique is verified by the *t*-test.

7.3 FUTURE SCOPE OF WORK

All research fields have possible future scope as there is no endpoint of research. This section highlights some possible future research directions as under:

- The search field of hybrid optimization techniques is an open research area. The advanced optimization techniques have a great scope for searching the optimum solution of the OPF problem with the least computational effort.
- The formulation of the OPF problem with network security constraints of power system incorporating the load and wind power uncertainties.
- The subject OPF problem with wind and CHP units has been considered as a single-objective problem and it may be extended as a multi-objective problem.
- Extending the OPF problem under consideration by including distributed generation sources.
- Inclusion of probabilistic nature of contingency in the OPF problem formulation.
- The OPF problem may be formulated by including hydro, thermal and wind generation systems.

- Extend the subject OPF problem to a dynamic OPF problem.
- Formulate the OPF problem including the voltage and transient stability of the system.
- Formulate the OPF problem taking the effect of Microgrid with tie line switching.

REFERENCES

[1] **Abaci, K., and Yamacli, V. (2017).** Optimal reactive-power dispatch using differential search algorithm, *Electrical Engineering*, vol. 99(1), pp. 213–225.

[2] **Abdel-Moamen, M.A., and Padhy, N.P. (2006).** Optimal power flow model with TCSC for practical power networks, *International Journal of Power and Energy Systems*, vol. 26(1), pp. 58-65.

[3] **Abido, M.A. (2002).** Optimal power flow using particle swarm optimization, *International Journal of Electrical Power and Energy Systems*, vol. 24(7), pp. 563–571.

[4] **Abou El Ela, A.A., Abido, M.A., and Spea, S.R. (2011).** Differential evolution algorithm for optimal reactive power dispatch, *Electric Power Systems Research*, vol. 81(2), pp. 458-464.

[5] **Adhvaryyu, P.K., and Adhvaryyu, S. (2020).** Static optimal load flow of combined heat and power system with valve point effect and prohibited operating zones using krill herd algorithm, *Energy Systems*. DOI: 10.1007/s12667-020-00378-9.

[6] **Adhvaryyu, P.K., Chattopadhyay, P.K., and Bhattacharjya, A. (2017).** Dynamic optimal power flow of combined heat and power system with valve point effect using krill herd algorithm, *Energy*, vol. 127, pp. 756-767.

[7] **Aeidapu, M., and Sandhu, K.S. (2018).** Optimal sizing of a grid-connected PV/wind/battery system using particle swarm optimization, *Iranian Journal of Science and Technology-Transactions of Electrical Engineering*, vol. 43, pp. 107-121.

[8] **Agarwal, A., and Sandhu, K.S. (2016).** Energy scheduling for grid connected wind farm systems, *Annual IEEE India Conference (INDICON)*, New Delhi, India.

[9] **Ahmadi, M., Mojallali, H., and Izadi-zamanabadi, R. (2012).** State estimation of nonlinear stochastic systems using a novel meta-heuristic particle filter, *Swarm and Evolutionary Computation*, vol. 4, pp. 44–53.

[10] **Ai, Q., and Gu, C. (2009).** Economic operation of wind farm integrated system considering voltage stability, *Renewable Energy*, vol. 34, pp. 608-614.

[11] **Akbari, E., Ghasemi, M., Gil, M., Rahimnejad, A., and Gadsden, S.A. (2021).** Optimal power flow via teaching-learning-studying-based optimization algorithm, *Electric Power Components and Systems*. DOI: 10.1080/15325008.2021.1971331.

[12] **Albatsh, F.M., Mekhilef, S., Ahmad, S., Mokhlis, H., and Hassan, M.A. (2015).** Enhancing power transfer capability through flexible AC transmission system devices: a review, *Frontiers of Information Technology and Electronic Engineering*, vol. 16(8), pp.

658-678.

[13] **Anand, H., Narang, N., and Dhillon, J. S. (2018).** Unit commitment considering dual-mode combined heat and power generating units using integrated optimization technique, *Energy Conversion and Management*, vol. 171, pp. 984–1001.

[14] **Arabali, A., Ghofrani, M., and Etezadi-Amoli, M. (2013).** Cost analysis of a power system using probabilistic optimal power flow with energy storage integration and wind generation, *International Journal of Electrical Power and Energy Systems,* vol. 53, pp. 832–841.

[15] **Arora, J.S., Elwakeil, O.A., and Chahande, A.I. (1995).** Global optimization methods for engineering applications: a review, *Structural Optimization*, vol. 9, pp. 137–159.

[16] **Attarha, A., Amjady, N., and Conejo, A.J. (2018).** Adaptive robust AC optimal power flow considering load and wind power uncertainties, *International Journal of Electrical Power and Energy Systems*, vol. 96, pp. 132–142.

[17] **Attia, A.F., El-Sehiemy, R.A., and Hasanien, H.M. (2018).** Optimal power flow solution in power systems using a novel Sine-Cosine algorithm, *International Journal of Electrical Power and Energy Systems,* vol. 99, pp. 331–343.

[18] **Awad, N.H., Ali, M.Z., Mallipeddi, R., and Suganthan, P.N. (2019).** An efficient differential evolution algorithm for stochastic OPF based active-reactive power dispatch problem considering renewable generators, *Applied Soft Computing*, vol. 76, pp. 445-458.

[19] **Baghernejad, A., and Anvari-Moghaddam, A. (2021).**Exergoeconomic and environmental analysis and multi-objective optimization of a new regenerative gas turbine combined cycle, *Applied Sciences*, vol. 11(23), pp. 1-29.

[20] **Bahmani-Firouzi, B., Farjah, E., and Seifi, A. (2013).** A new algorithm for combined heat and power dynamic economic dispatch considering valve-point effects, *Energy*, vol. 52, pp. 320-332.

[21] **Bansal, J.C., Sharma, H., Jadon, S.S., and Clerc, M. (2014).**Spider monkey optimization algorithm for numerical optimization, *Memetic Computing*, vol.6, pp. 31-47.

[22] **Barisal, A.K., and Prusty, R.C. (2015).** Large scale economic dispatch of power systems using oppositional invasive weed optimization. *Applied Soft Computing*,vol. 29, pp. 122–137.

[23] **Basu, M. (2008).** Optimal power flow with FACTS devices using differential evolution, *International Journal of Electrical Power and Energy Systems*, vol. 30, pp.150–156.

[24] **Basu, M. (2011).** Multi-objective optimal power flow with FACTS devices, *Energy Conversion and Management*, vol. 52(2), pp. 903–910.

[25] **Basu, M. (2016).**Group Search Optimization for Solution of Different Optimal Power Flow Problems, *Electric Power Components and Systems*, vol. 44(6), pp. 606-615.

[26] **Bhamidi, L., and Shanmugavelu, S. (2019).** Multi-objective Harmony Search Algorithm for Dynamic Optimal Power Flow with Demand Side, *Electric Power Components and Systems*, vol. 47(8), pp. 692-702.

[27] **Bhattacharya, A., and Roy, P.K. (2012).** Solution of multi-objective optimal power flow using gravitational search algorithm, *IET Generation Transmission and Distribution*, vol. 6(8), pp. 751–763.

[28] **Biswas, P.P., Suganthan, P.N., Mallipeddi, R., and Amaratunga, G.A.J. (2018).** Optimal power flow solutions using differential evolution algorithm integrated with effective constraint handling techniques, *Engineering Applications of Artificial Intelligence*, vol. 68, pp. 81–100.

[29] **Biswas, P.P., Suganthan, P.N., Mallipeddi, R., and Amaratunga, G.A.J. (2019).** Multi-objective optimal power flow solutions using a constraint handling technique of evolutionary algorithms, *Soft Computing*, vol. 24, pp. 2999-3023.

[30] **Bouchekara, H.R.E.H., Abido, M.A., and Boucherma, M. (2014).** Optimal power flow using Teaching-Learning-Based Optimization technique, *Electric Power Systems Research*, vol. 114, pp. 49–59.

[31] **Bouchekara, H.R.E.H., Chaib, A.E., Abido, M.A., and El-Sehiemy, R.A. (2016).** Optimal power flow using an Improved Colliding Bodies Optimization, *Applied Soft Computing*, vol. 42, pp. 119-131.

[32] **Carpentier, J. (1979).** Optimal power flows, *International Journal of Electrical Power and Energy Systems*, vol. 1(1), pp. 3-15.

[33] **Carvalho, L., Leite da Silva, A.M., and Miranda, V. (2018).** Security-constrained optimal power flow via cross entropy method, *IEEE Transactions on Power Systems*, vol. 33, pp. 6621-6629.

[34] **Chang, Y., Lee, T., Chen, C., and Jan, R. (2014).** Optimal power flow of a wind-thermal generation system, *International Journal of Electrical Power and Energy Systems*, vol. 55, pp. 312–320.

[35] **Chaohua, D., Weirong, C., Yunfang, Z., and Xuexia, Z. (2009).** Seeker optimization algorithm for optimal reactive power dispatch, *IEEE Transactions on Power Systems*, vol. 24(3), pp. 1218-1231.

[36] **Chen, G., Liu, L., Zhang, Z., and Huang, S. (2017).** Optimal reactive power dispatch by improved GSA- based algorithm with the novel strategies to handle constraints, *Applied Soft Computing*, vol. 50, pp. 58-70.

[37] **Chen, G., Yi, X., Zhang, Z., and Wang, H. (2018).** Applications of multi-objective dimension-based firefly algorithm to optimize the power losses, emission, and cost in power systems, *Applied Soft Computing*, vol. 68, pp. 322–342.

[38] **Chen, G., Qian, J., Zhang, Z., and Li S. (2020).** Application of modified pigeon-inspired optimization algorithm and constraint-objective sorting rule on multi-objective optimal power flow problem, *Applied Soft Computing.*DOI: 10.1016/j.asoc.2020.106321

[39] **Civicioglu, P. (2013[1]).** Artificial cooperative search algorithm for numerical optimization problems, *Information Sciences*, vol. 229, pp. 58-76.

[40] **Civicioglu, P. (2013[2]).** Backtracking search optimization algorithm for numerical optimization problems, *Applied Mathematics and Computation*, vol. 219, pp. 8121-8144.

[41] **Cui, Y., Geng, Z., Han, Y., and Zhu, Q. (2017).** Review: Multi-objective optimization methods and application in energy saving, *Energy*, vol. 125, pp. 681-704.

[42] **Dai, C., Chen, W., Zhu, Y., Jiang, Z., and You, Z. (2011).** Seeker optimization algorithm for tuning the structure and parameters of neural networks, *Neurocomputing*, vol. 74(6), 876-883.

[43] **Daryani, N., Hagh M.T., and Teimourzadeh, S. (2016).** Adaptive group search optimization algorithm for multi-objective optimal power flow problem, *Applied Soft Computing*, vol. 38, pp. 1012-1024.

[44] **Daqaq, F., Ouassaid, M., and Ellaia, R. (2021).** A new meta-heuristic programming for multi-objective optimal power flow, *Electrical Engineering*, vol. 103, pp. 1217-1237.

[45] **Deb, K. (2004).** Optimization for engineering design: Algorithms and Examples, PHI Learning Pvt. Ltd.

[46] **Denny, E., and O' Malley, M. (2006).** Wind generation, power system operation, and emission reduction, *IEEE Transactions on Power Systems*, vol. 21(1), pp. 341-347.

[47] **Dutta, S., Mukhopadhyay, P., Roy, P.K., and Nandi, D. (2016).** Unified power flow controller based reactive power dispatch using oppositional krill herd algorithm, *International Journal of Electrical Power and Energy Systems*, vol. 80, pp. 10-25.

[48] **Elattar, E. E., and Elsayed, S. K. (2019).** Modified JAYA algorithm for optimal power flow incorporating renewable energy sources considering the cost, emission, power loss

and voltage profile improvement, *Energy*, vol. 178, pp. 598–609.

[49] **El-Fergany, A.A., and Hasanien, H.M. (2018[1]).** Single and multi-objective optimal power flow using grey wolf optimizer and differential evolution algorithms, *Electric Power Components and Systems*, vol. 43(13), pp. 1548-1559.

[50] **El-Fergany, A.A., and Hasanien, H.M. (2018[2]).** Tree-seed algorithm for solving optimal power flow problem in large-scale power systems incorporating validations and comparisons, *Applied Soft Computing*, vol. 64, pp. 307–316.

[51] **El-Sattar, S.A., Kamel, S., Ebeed, M., and Jurado, F. (2021).** An improved version of salp swarm algorithm for solving optimal power flow problem, *Soft Computing*, vol. 25, pp. 4027–4052.

[52] **El-Sehiemy, R.A., Selim, F., Bentouati, B., and Abido, M.A. (2020).** A novel multi-objective hybrid particle swarm and salp optimization algorithm for technical-economical-environmental operation in power systems, *Energy*. DOI: 10.1016/j.energy.2019.116817

[53] **Essiet, I.O., and Sun, Y. (2020).**Tracking variable fitness landscape in dynamic multi-objective optimization using adaptive mutation and crossover operators, *IEEE Access*, vol. 8, pp. 188927-188937.

[54] **Ettappan, M., Vimala, V., Ramesh, S., and Kesavan, V.T. (2020).** Optimal reactive power dispatch for real power loss minimization and voltage stability enhancement using artificial bee colony algorithm, *Microprocessors and Microsystems*.DOI: 10.1016/j.micpro.2020.103035.

[55] **Evangeline, S.I., and Rathika, P. (2022).** Wind farm incorporated optimal power flow solutions through multi-objective horse herd optimization with a novel constraint handling technique, *Expert Systems with Applications*, vol. 194, DOI:10.1016/j.eswa.2022.116544.

[56] **Fahd, G., and Sheble, G.B. (1992).** Optimal power flow emulation of interchange brokerage systems using linear programming, *IEEE Transactions on Power Systems*, vol. 7 (2), pp. 497-504.

[57] **Fang, T., and Lahdelma, R. (2016).** Optimization of combined heat and power production with heat storage based on sliding time window method, *Applied Energy*, vol. 162, pp. 723-732.

[58] **Gandomi, A.H., and Kashani, A.R. (2018).** Construction cost minimization of shallow foundation using recent swarm intelligence techniques, *IEEE Transactions on Industrial Informatics*, vol. 14(3), pp. 1099-1106.

[59] **Ghasemi, M., Ghavidel, S., Ghanbarian, M.M., and Habibi, A. (2014[1]).** A new hybrid algorithm for optimal reactive power dispatch problem with discrete and continuous control variables, *Applied Soft Computing*, vol. 22, pp. 126-140.

[60] **Ghasemi, M., Ghavidel, S., Rahmani, S., Roosta, A., and Falah, H. (2014[2]).** A novel hybrid algorithm of imperialist competitive algorithm and teaching learning algorithm for optimal power flow problem with non-smooth cost functions, *Engineering Applications of Artificial Intelligence*, vol. 29, pp. 54-69.

[61] **Gil, E., and Aravena, I. (2014).** Evaluating the capacity value of wind power considering transmission and operational constraints, *Energy Conversion and Management*, vol.78, pp. 948-955.

[62] **Gilvaei, M.N., Jafari, H., Ghadi, M.J., and Li, L. (2020).** A novel hybrid optimization approach for reactive power dispatch problem considering voltage stability index, *Engineering Applications of Artificial Intelligence*. DOI: 10.1016/j.engappai.2020.103963.

[63] **Gnanadass, R., Venkatesh, P., and Padhy, N.P. (2004).** Evolutionary programming based optimal power flow for units with non-smooth fuel cost functions, *Electric Power Components and Systems*, vol. 33(3), pp. 349-361.

[64] **Granville, S. (1994).** Optimal reactive power dispatch through interior point methods, *IEEE Transactions on Power Systems*, vol. 9(1), pp. 136–146.

[65] **Gupta, S., Kumar, N., Srivastava, L., Malik, H., Anvari-Moghaddam, A., and Marquez, F.P.G. (2021).**A robust optimization approach for optimal power flow solutions using Rao algorithms, *Energies*, vol 14(17), pp. 1-28.

[66] **Harman, M., and McMinn, P. (2010).** A theoretical and empirical study of search-based testing: local, global and Hybrid search, *IEEE Transactions on Software Engineering*, vol. 36(2), pp. 226–247.

[67] **Hatamlou, A., Javidy, B., and Mirjalili, S. (2015).** Ions motion algorithm for solving optimization problems, *Applied Soft Computing*, vol. 32, pp. 72-79.

[68] **Heidari, A.A., Abbaspour, R.A., and Jordehi, A.R. (2017).** Gaussian bare-bones water cycle algorithm for optimal reactive power dispatch in electrical power systems, *Applied Soft Computing*, vol. 57, pp. 657–671.

[69] **Hetzer, J., Yu, D.C., and Bhattarai, K. (2008).** An economic dispatch model incorporating wind power,*IEEE Transactions on Energy Conversion*, vol. 23(2), pp. 603–611.

[70] **Hmida, J. B., Chambers, T., and Lee, J. (2019).** Solving constrained optimal power

flow with renewables using hybrid modified imperialist competitive algorithm and sequential quadratic programming, *Electric Power Systems Research*.DOI:10.1016/j.epsr.2019.105989.

[71] **Hughes, A., Sun, D.I., Ashley, B., Brewer, B., and Tinney, W.F. (1984).** Optimal power flow by Newton approach, *IEEE Transactions on Power Apparatus and Systems*, vol. 103(10), pp. 2864–2880.

[72] **Jabr, R.A., and Pal, B.C. (2009).** Intermittent wind generation in optimal power flow dispatching, *IET Generation Transmission and Distribution*, vol. 3(1), pp. 66-74.

[73] **Jabr, R.A., Džafić, I., and Pal, B.C. (2015).** Robust optimization of storage investment on transmission networks, *IEEE Transactions on Power Systems*,vol. 30(1), pp. 531-539.

[74] **Jadhav, H.T., and Bamane, P.D. (2016).** Temperature dependent optimal power flow using g-best guided artificial bee colony algorithm, *International Journal of Electrical Power and Energy Systems*, vol. 77, pp. 77–90.

[75] **Jain, T., Singh, S.N., and Srivastava, S.C. (2009).** Dynamic ATC enhancement through optimal placement of FACTS controllers, *Electric Power Systems Research*, vol. 79(11), pp. 1473-1482.

[76] **Jain, T., Singh, S.N., and Srivastava, S.C. (2011).**Fast static available transfer capability determination using radial basis function neural network, *Applied Soft Computing*, vol. 11(2), pp. 2756-2764.

[77] **Jamian, J.J., Abdullah, M.N., Mokhlis, H.B., Mustafa, M.W., and Bakar, A.H.A. (2014).** Global particle swarm optimization for high dimension numerical functions analysis, *Journal of Applied Mathematics*, pp.1-14.

[78] **Jayabarathi, T., Yazdani A., Ramesh, V., and Raghunathan, T. (2014).** Combined heat and power economic dispatch problem using the invasive weed optimization algorithm, *Frontiers in Energy*, vol. 8(1), pp. 25-30.

[79] **Jiang, S., Ji, Z., and Wang, Y. (2015).** A novel gravitational acceleration enhanced particle swarm optimization algorithm for wind-thermal economic emission dispatch problem considering wind power availability, *International Journal of Electrical Power and Energy Systems*, vol. 73, pp. 1035–1050.

[80] **Jiang, Q., Geng, G., Guo, C., and Cao, Y. (2010).** An Efficient Implementation of Automatic Differentiation in Interior Point Optimal Power Flow. *IEEE Transactions on Power Systems*, vol. 25(1), pp.147–155.

[81] **Jordehi, A.R. (2016).** Optimal allocation of FACTS devices for static security

enhancement in power systems via imperialistic competitive algorithm, *Applied Soft Computing*, vol. 48, pp. 317–328.

[82] **Kahourzade, S., Mahmoudi, A., and Mokhlis, H. B. (2015).** A comparative study of multi-objective optimal power flow based on particle swarm, evolutionary programming and genetic algorithm, *Electrical Engineering*, vol. 97, pp. 1–12.

[83] **Kahraman, H.T., Akbel, M., and Duman S. (2022).**Optimization of optimal power flow problem using multi-objective manta ray foraging optimizer, *Applied Soft Computing*, vol. 116, DOI: 10.1016/j.asoc.2021.108334.

[84] **Karimkashi, S., and Kishk, A.A. (2010).** Invasive weed optimization and its features in electromagnetics, *IEEE Transactions on Antennas and Propagation*, vol. 58(4), pp. 1269–1278.

[85] **Kaya, C.Y., and Maurer, H. (2014).** A numerical method for nonconvex multi-objective optimal control problems, *Computational Optimization and Applications*, vol. 57, pp. 685–702.

[86] **Keirstead, J., Samsatli, N., Shah, N., and Weber, C. (2012).** The impact of CHP (combined heat and power) planning restrictions on the efficiency of urban energy systems, *Energy*, vol. 41(1), pp. 93-103.

[87] **Kennedy, J., and Eberhart, R. (1995).** Particle swarm optimization, *Proc IEEE International Conference on Neural Networks*, Perth, WA, Australia, vol. 4, pp. 1942–1948.

[88] **Khan, Z.A., Zafar, A., Javaid, S., Aslam, S., Rahim, M.H., and Javaid, N. (2019).** Hybrid meta-heuristic optimization based home energy management system in smart grid, *Journal of Ambient Intelligence and Humanized Computing*, vol. 10, pp. 4837-4853.

[89] **Khorsandi, A., Alimardani, A., Vahidi, B., and Hosseinian, S.H. (2010).** Hybrid shuffled frog leaping algorithm and Nelder-Mead simplex search for optimal reactive power dispatch, *IET Generation Transmission and Distribution*, vol. 5(2), pp. 249-256.

[90] **Krishnanand, K.N., and Ghose, D. (2009).** Glowworm swarm optimization for simultaneous capture of multiple local optima of multimodal functions, *Swarm Intelligence*, vol. 3, pp. 87-124.

[91] **Kumar, P., and Shreya, A. (2020).** Static optimal load flow of combined heat and power system with valve point effect and prohibited operating zones using Krill Herd algorithm, *Energy Systems*, vol. 12, pp. 133-156.

[92] **Lee, K.Y., Park, Y.M., and Ortiz, J.L. (1985).** A united approach to optimal real and

reactive power dispatch, *IEEE Transactions on Power Apparatus and Systems*, vol. 5(5), pp. 42–43.

[93] **Li, C., Luo, G., Qin, K., and Li, C. (2017).** An image encryption scheme based on chaotic tent map, *Nonlinear Dynamics*, vol. 87, pp. 127-133.

[94] **Li, S., Gong, W., Wang, L., Yan, X., and Hu, C. (2020).** Optimal power flow by meansof improved adaptive differential evolution, *Energy*. DOI: 10.1016/j.energy.2020.117314.

[95] **Liang, R.H., Wang, J.C., Chen, Y.T., and Tseng, W.T. (2015).** An enhanced firefly algorithm to multi-objective optimal active/reactive power dispatch with uncertainties consideration, *International Journal of Electrical Power and Energy Systems*, vol. 64, pp. 1088-1097.

[96] **Liu, C., Shahidehpour, M., Li, Z., and Fotuhi-Firuzabad, M. (2009).** Component and mode models for the short term scheduling of combined cycle units, *IEEE Transactions on Power Systems*, vol. 24(2), pp. 976-990.

[97] **Liu, X., and Xu, W. (2010).** Minimum emission dispatch constrained by stochastic wind power availability and cost,*IEEE Transactions on Power Systems*, vol. 25(3), pp. 1705–1713.

[98] **Liu, Y., Cetenovic, D., Li, H., Gryazina, E., and Terzija, V. (2022).** An optimized multi-objective reactive power dispatch strategy based on improved genetic algorithm for wind power integrated systems,*International Journal of Electrical Power and Energy Systems*, vol. 136, DOI: 10.1016/j.ijepes.2021.107764.

[99] **Lu, L., Anderson-cook, C.M., and Robinson, V. (2012).** A case study to demonstrate a Pareto Frontier for selecting a best response surface design while simultaneously optimizing multiple criteria, *Applied Stochastic Models in Business and Industry*, vol.28(3), pp. 85–96.

[100] **Mahdad, B. (2020).** Improvement optimal power flow solution considering SVC and TCSC controllers using new partitioned ant lion algorithm, *Electrical Engineering*, vol. 102, pp. 2655–2672.

[101] **Man-Im, A., Ongsakul, W., Singh, J. G., and Madhu, M. N. (2019).** Multi-objective optimal power flow considering wind power cost functions using enhanced PSO with chaotic mutation and stochastic weights, *Electrical Engineering*, vol. 101(3), pp. 699–718.

[102] **Marcelino, C., Almeida, P., Wanner, E., Baumann, M., Weil, M., Carvalho, L., and Miranda, V. (2018).** Solving security constrained optimal power flow problems: a

hybrid evolutionary approach, *Applied Intelligence*, vol. 48, pp. 3672-3690.

[103] **Marler, R.T., and Arora, J.S. (2004).** Survey of multi-objective optimization methods for engineering, *Structural and Multidisciplinary Optimization*, vol. 26, pp. 369-395.

[104] **Medina, M.A., Das, S., Coello, C.A., and Ramirez, J.M. (2014).** Engineering Applications of Artificial Intelligence Decomposition-based modern metaheuristic algorithms for multi-objective optimal power flow-A comparative study. *Engineering Applications of Artificial Intelligence*, vol. 32, pp. 10-20.

[105] **Mehrabian, A.R., and Lucas, C. (2006).** A novel numerical optimization algorithm inspired from weed colonization, *Ecological Informatics*, vol. 1(4),pp. 355–366.

[106] **Mei, S.R., Sulaiman, H.M., Mustaffa, Z., and Daniyal, H. (2017).** Optimal reactive power dispatch solution by loss minimization using moth-flame optimization technique, *Applied Soft Computing*, vol. 59, pp. 210-222.

[107] **Meng, A.B., Chen, Y.C., Yin, H., and Chen, S. (2014).** Crisscross optimization algorithm and its application, *Knowledge-Based Systems*, vol. 67, pp. 218-229.

[108] **Miranda, V., and Hang, P.S. (2005).** Economic dispatch model with fuzzy wind constraints and attitudes of dispatchers, *IEEE Transactions on Power Systems*, vol. 20(4), pp. 2143–2145.

[109] **Mirjalili, S. (2015[1]).** Moth-flame optimization algorithm: A novel nature-inspired heuristic paradigm, *Knowledge-Based Systems*, vol. 89, pp. 228-249.

[110] **Mirjalili, S. (2015[2]).** The ant lion optimizer, *Advances in Engineering Software*, vol. 83, pp. 80-98.

[111] **Mirjalili, S., and Lewis, A. (2016).** The whale optimization algorithm, *Advances in Engineering Software*, vol. 95, pp. 51-67.

[112] **Mirjalili, S., Saremi, S., Mirjalili S.M., and Coelho, L.S. (2016).** Multi-objective grey wolf optimizer: A novel algorithm for multi-criterion optimization, *Expert Systems with Applications*, vol. 47, pp. 106-119.

[113] **Mishra, S., Mishra, Y., and Vignesh, S. (2011).** Security constrained economic dispatch considering wind energy conversion systems, *IEEE Power and Energy Society General Meeting*, Detroit, MI, USA.

[114] **Mohamed, A.A.A., Mohamed, Y.S., El-Gaafary, A.A.M., and Hemeida, A.M. (2017).** Optimal power flow using moth swarm algorithm, *Electric Power Systems Research*, vol. 142, pp. 190-206.

[115] **Mohseni-Bonab, S.M., Rabiee, A., and Mohammadi-Ivatloo, B. (2016[1]).** Voltage stability constrained multi-objective optimal reactive power dispatch under load and

wind power uncertainties: A stochastic approach, *Renewable Energy*, vol. 85, pp. 598–609.

[116] **Mohseni-Bonab, S.M., Rabiee, A., Mohammadi-Ivatloo, B., Jalilzadeh, S., and Nojavan, S. (2016[2]).** A two-point estimate method for uncertainty modeling in multi-objective optimal reactive power dispatch problem, *International Journal of Electrical Power and Energy Systems*, vol. 75, pp. 194–204.

[117] **Mojtaba, A. E. G., Sahand, G., and Mohsen G. (2015).** An improved teaching–learning-based optimization algorithm using Levy mutation strategy for non-smooth optimal power flow, *International Journal of Electrical Power and Energy Systems*, vol. 65, pp. 375–384.

[118] **Momoh, J.A., El-Hawary, M.E., and Adapa, R. (1999).** A review of selected optimal power flow literature to 1993 part I & II, *IEEE Transactions on Power Systems*, vol. 14(1), pp. 96-111.

[119] **Moradi, M., Abdi, H., Lumbreras, S., Ramos, A. G., and Karimi, S. (2016).** Transmission expansion planning in the presence of wind farms with a mixed AC and DC power flow model using an imperialist competitive algorithm, *Electric Power Systems Research*, vol. 140, pp. 493-506.

[120] **Mouassa, S., Althobaiti, A., Jurado, F., and Ghoneim, S.S.M, (2022).** Novel design of slim mould optimizer for the solution of optimal power flow problems incorporating intermittent sources: A case study of Algerian electricity grid, *IEEE Access*, vol.10, pp. 22646-22661.

[121] **Mukherjee, V., and Mukherjee, A. (2016[1]).** Solution of optimal power flow with FACTS devices using a novel oppositional krill herd algorithm, *International Journal of Electrical Power and Energy Systems*, vol.78, pp. 700–714.

[122] **Mukherjee, V., and Mukherjee, A. (2016[2]).** Chaos embedded krill herd algorithm for optimal VAR dispatch problem of power system, *International Journal of Electrical Power and Energy Systems*, vol. 82, pp. 37-48.

[123] **Naderi, E., Pourakbari-Kasmaei, M., Cerna, F.V., and Lehtonen, M. (2021).** A novel hybrid self-adaptive heuristic algorithm to handle single and multi-objective optimal power flow problems, *International Journal of Electrical Power & Energy Systems*, vol. 125. DOI: 10.1016/j.ijepes.2020.106492.

[124] **Nagib, M.M., Othman, M.M., Naiem, A.A., and Hegazy, Y.G. (2016).** Invasive weed optimization algorithm for solving economic load dispatch,*IEEE 16th International Conference on Environment and Electrical Engineering*, Florence, Italy.

[125] **Naidu, K., Mokhlis, H., and Bakar, A.H.A. (2014).**Multiobjective optimization using weighted sum artificial bee colony algorithm for load frequency control, *International Journal of Electrical Power and Energy Systems*, vol. 55, pp. 657-667.

[126] **Naidu, Y. R., and Ojha, A. K. (2018).** Solving Multiobjective Optimization Problems Using Hybrid Cooperative Invasive Weed Optimization With Multiple Populations, *IEEE Transactions on Systems, Man, and Cybernetics Systems*, vol. 48(6), pp. 821–832.

[127] **Narang, N., Dhillon, J.S., and Kothari, D.P. (2012).** Multiobjective fixed head hydrothermal scheduling using integrated predator-prey optimization and Powell search method, *Energy*, vol. 47(1), pp. 237–252.

[128] **Narang, N., Dhillon, J.S., and Kothari, D.P. (2014).** Weight pattern evaluation for multiobjective hydrothermal generation scheduling using hybrid search technique, *International Journal of Electrical Power and Energy Systems*, vol. 62, pp. 665–678.

[129] **Nayak, M.R., Krishnanand, K.R., and Rout, P.K. (2011).** Optimal reactive power dispatch based on adaptive invasive weed optimization algorithm, *International Conference on Energy, Automation and Signal, Bhubaneswar, India*.

[130] **Nguyen, T.T. (2019).** A high performance social spider optimization algorithm for optimal power flow solution with single objective optimization, *Energy*, vol. 171, pp. 218–240.

[131] **Niknam, T., Azizipanah-Abarghooee, R., Roosta, A., and Amiri, B. (2012[1]).** A new multi-objective reserve constrained combined heat and power dynamic economic emission dispatch, *Energy*, vol. 42(1), pp. 530-545.

[132] **Niknam, T., Azizipanah-Abarghooee, R., and Rasoul-Narimani, M. (2012[2]).** Reserve constrained dynamic optimal power flow subject to valve-point effects, prohibited zones and multi-fuel constraints, *Energy*, vol. 47(1), pp. 451-464.

[133] **Niknam, T., Narimani, M., Aghaei, J., and Azizipanah-Abarghooee, R. (2012[3]).** Improved particle swarm optimization for multi-objective optimal power flow considering the cost, loss, emission and voltage stability index, *IET Generation Transmission and Distribution*, vol. 6(6), pp. 515–527.

[134] **Noman, N., and Iba, H. (2008).** Accelerating differential evolution using an adaptive local search, *IEEE Transactions on Neural Networks*, vol. 12(1), pp. 107-125.

[135] **Ongsakul, W., and Bhasaputra, P. (2002).** Optimal power flow with FACTS devices by hybrid TS/SA approach, *International Journal of Electrical Power and Energy Systems*, vol. 24(10), pp. 851-857.

[136] **Packiasudha, M., Suja, S., and Jerome, J. (2017).** A new Cumulative Gravitational

Search algorithm for optimal placement of FACT device to minimize system loss in the deregulated electrical power environment, *International Journal of Electrical Power and Energy Systems*, vol. 84, pp. 34–46.

[137] **Padhy, N.P., and Abdel-Moamen, M.A. (2005).** Power flow control and solutions with multiple and muti-type FACTS devices, *Electric Power Systems Research*, vol.74, pp. 341-351.

[138] **Paliwal, N.K., Singh, N.K., and Singh, A.K. (2016).** Optimal power flow in grid connected microgrid using artificial bee colony algorithm,*IEEE Region 10 Conference (TENCON)*, Singapore.

[139] **Panda, A. and Tripathy, M., (2014).** Optimal power flow solution of wind integrated power system using modified bacteria foraging algorithm, *International Journal of Electrical Power and Energy Systems*, vol. 54, pp. 306-314.

[140] **Perveen, R., Kishor, N., and Mohanty, S.R. (2014).** Off-shore wind farm development:present status and challenges, *Renewable and Sustainable Energy Reviews*, vol. 29, pp. 780-792.

[141] **Polprasert, J., Ongsakul, W., and Dieu, V.N. (2016).** Optimal reactive power dispatch using improved pseudo-gradient search particle swarm optimization, *Electric Power Components and Systems*, vol. 44(5), pp. 518-532.

[142] **Prasad, D., and Mukherjee, V. (2016).** A novel symbiotic organisms search algorithm for optimal power flow of power system with FACTS devices, *Engineering Science and Technology, an International Journal*, vol. 19(1), pp. 79–89.

[143] **Pulluri, H., Naresh R., and Sharma V. (2016).** A solution network based on stud krill herd algorithm for optimal power flow problems, *Soft Computing*, vol. 22(1), pp. 159–176.

[144] **Pulluri, H., Naresh, R., and Sharma, V. (2017).** An enhanced self-adaptive differential evolution based solution methodology for multiobjective optimal power flow, *Applied Soft Computing*, vol. 54,pp. 229–245.

[145] **Quan, H., Lv, J., Guo, J., and Jhang, W. (2022).** Investigation of Spatial correlation on optimal power flow with high penetration of wind power: A comparative study, *Applied Energy*, vol. 316, DOI:10.1016/j.apenergy.2022.119034.

[146] **Rafique, S., Nizami, M.S.H., Irshad, U.B., Hossain, M.J., and Mukhopadhyay S.C. (2022).** A two-stage multi-objective stochastic optimization strategy to minimize cost for electric bus depot operators, *Journal of Cleaner Production*, vol 332, DOI:10.1016/j.jclepro.2021.129856.

[147] **Rahmani, S., and Amjady, N. (2017).** A new optimal power flow approach for wind energy integrated power systems, *Energy*, vol. 134, pp. 349–359.

[148] **Rajan, A., and Malakar, T. (2015).** Optimal reactive power dispatch using hybrid Nelder-Mead simplex based firefly algorithm, *International Journal of Electrical Power and Energy Systems*, vol. 66, pp. 9-24.

[149] **Ramos, J.L.M., Exposito, A.G., and Quintana, V.H. (2005).** Transmission power loss reduction by interior-point methods implementation issues and practical experience, *IEE Proceedings- Generation, Transmission and Distribution*, vol. 152(1), pp. 90-98.

[150] **Rao, S.S. (1996).** Engineering optimization: theory and practice, 3rd edition, John Wiley & Sons, New York.

[151] **Rao, B.S., and Vaisakh, K. (2014).** Multi-objective adaptive clonal selection algorithm for solving optimal power flow considering multi-type FACTS devices and load uncertainty, *Applied Soft Computing*, vol. 23, pp. 286–297.

[152] **Rashedi, E., Nezamabadi-Pour, H., and Saryazdi, S. (2009).** GSA: A gravitational search algorithm, *Information Sciences*, vol 179(13), pp. 2232-2248.

[153] **Reid, G.F., and Hasdorff, L. (1973).** Economic dispatch using quadratic programming, *IEEE Transactions on Power Apparatus and Systems*, vol 92(6), pp. 2015-2023.

[154] **Roberge, V., Tarbouchi, M., and Okou, F. (2016).** Optimal power flow based on parallel metaheuristics for graphics processing units, *Electric Power Systems Research*, vol. 140, pp. 344-353.

[155] **Rong, A., Hakonen, H., and Lahdelma, R. (2009).** A dynamic regrouping based sequential dynamic programming algorithm for unit commitment of combined heat and power systems, *Energy Conversion and Management*, vol.50(4), pp. 1108-1115.

[156] **Roy, R., and Jadhav, H.T. (2015).** Optimal power flow solution of power system incorporating stochastic wind power using Gbest guided artificial bee colony algorithm, *International Journal of Electrical Power and Energy Systems*, vol. 64, pp. 562–578.

[157] **Roy, S., Islam, S.M., Das, S., and Ghosh, S. (2013).** Multimodal optimization by artificial weed colonies enhanced with localized group search optimizers, *Applied Soft Computing*, vol. 13(1), pp. 27–46.

[158] **Saber, A.Y., and Alshareef, A.M. (2008).** Scalable unit commitment by memory-bounded ant colony optimization with A^* local search, *International Journal of Electrical Power & Energy Systems*, vol. 30(6-7), pp. 403-414.

[159] **Saha, A., Bhattacharya, A., Das, P., and Chakraborty A. K. (2020).** HSOS: a novel hybrid algorithm for solving the transient-stability-constrained OPF problem, *Soft*

Computing, vol. 24(4), pp. 7481-7510.

[160] **Saini, A., and Saraswat, A. (2013).** Multi-objective reactive power market clearing in competitive electricity market using HFMOEA, *Applied Soft Computing*, vol. 13(4), pp. 2087-2103.

[161] **Sakr, W.S., El-Sehiemy, R.A., and Azmy, A.M. (2017).** Adaptive differential evolution algorithm for efficient reactive power management, *Applied Soft Computing*, vol. 53(1), pp. 336-351.

[162] **Sanjay, R., Jayabarathi, T., Raghunathan, T., Ramesh, V., and Mithulananthan, N. (2017).** Optimal allocation of distributed generation using hybrid grey wolf optimizer, *IEEE Access*, vol. 5, pp. 14807-14818.

[163] **Saravanan, B., Vasudevan, E.R., and Kothari, D.P. (2014).** Unit commitment problem solution using invasive weed optimization algorithm, *International Journal of Electrical Power and Energy Systems*, vol. 55, pp. 21–28.

[164] **Shaheen, A.M., El-Sehiemy, R.A., and Farrag, S. M. (2016).** Solving multi-objective optimal power flow problem via forced initialized differential evolution algorithm, *IET Generation Transmission and Distribution*, vol. 10 (7), pp. 1634–1647.

[165] **Shaheen, A.M., El-Sehiemy, R.A., Hasanien, H.M., and Ginidi, A. R. (2022).**An improved heap optimization algorithm for efficient energy management based optimal power flow model, *Energy*, vol. 250, DOI:10.1016/j.energy.2022.123795.

[166] **Shargh, S., Khorshid, B., Seyedi, H. and Abapour, M. (2016).** Probabilistic multi-objective optimal power flow considering correlated wind power and load uncertainties, *Renewable Energy*, vol. 94, pp. 10–21.

[167] **Sharifzadeh, H., Amjady, N., and Zareipour, H. (2017).** Multi-period stochastic security-constrained OPF considering the uncertainty sources of wind power, load demand and equipment unavailability, *Electric Power Systems Research*, vol. 146, pp. 33–42.

[168] **Shaw, B., Mukherjee, V., and Ghoshal, S.P. (2014).** Solution of reactive power dispatch of power systems by an opposition-based gravitational search algorithm, *International Journal of Electrical Power and Energy Systems*, vol. 55, pp. 29-40.

[169] **Shilaja, C., and Arunprasath, T. (2019).** Optimal power flow using moth swarm algorithm with gravitational search algorithm considering wind power, *Future Generation Computer Systems*, vol. 98(1), pp. 708-715.

[170] **Shirazi, A., Naja, B., Aminyavari, M., Rinaldi, F., and Taylor, R.A. (2014).** Thermal - economic - environmental analysis and multi-objective optimization of an ice thermal

energy storage system for gas turbine cycle inlet air cooling, *Energy*, vol. 69, pp. 212–226.

[171] **Shojaei, A.H., Ghadimi, A.A., Miveh, M.R., Ahmadi, A., and Gandoman, F.H. (2021).**Multiobjective reactive power planning considering the uncertainties of wind farms and loads using information gap decision theory, *Renewable Energy*, vol. 163, pp. 1427-1443.

[172] **Shukla, P.K., and Deb, K. (2007).** On finding multiple Pareto-optimal solutions using classical and evolutionary generating methods, *European Journal of Operational Research,* vol. 181(3), pp.1630–1652.

[173] **Singh, L., Dhillon, J.S., and Chauhan, R.C. (2006).** Evaluation of Best Weight Pattern for Multiple Criteria Load Dispatch, *Electric Power Components and Systems*, vol. 34(1), pp. 21–35.

[174] **Singh, N.J., Dhillon, J.S., and Kothari, D.P. (2018).** Non-interactive approach to solve multi-objective thermal power dispatch problem using composite search algorithm, *Applied Soft Computing*, vol. 65, pp. 644–658.

[175] **Singh, N.J., Dhillon, J.S., and Kothari, D.P. (2017).** Multi-objective thermal power load dispatch using chaotic differential evolutionary algorithm and Powell's method, *Soft Computing,* vol. 22(4), pp. 2159-2174.

[176] **Singh, R.P., Mukherjee, V., and Ghoshal, S.P. (2015).** Particle swarm optimization with an aging leader and challengers algorithm for optimal power flow problem with FACTS devices, *International Journal of Electrical Power and Energy Systems*, vol. 64, pp.1185–1196.

[177] **Sodhi, R., Srivastava, S.C., and Singh, S.N. (2011).** Multi-criteria decision making approach for multi-stage optimal placement of phasor measurement units, *IET Generation, Transmission and Distribution*, vol. 5(2), pp. 181-190.

[178] **Souza *et al.* (2022).**A gradient-based approach for solving the stochastic optimal power flow problem with wind power generation, *Electric Power Systems Research*, vol. 209, DOI: 10.1016/j.epsr.2022.108038.

[179] **Srilakshmi, K., Babu, P.R., and Aravindhababu, P. (2020).** An enhanced most valuable player algorithm based optimal power flow using Broyden's method, *Sustainable Energy Technologies and Assessments*, DOI: 10.1016/j.seta.2020.100801.

[180] **Sulaiman, M.H., and Mustaffa, Z. (2020).** Optimal power flow incorporating stochastic wind and solar generation by metaheuristic optimizers,*Microsystem Technologies*, DOI: 10.1007/s00542-020-05046-7.

[181] **Sulaiman, M.H., Mustaffa, Z., Daniyal, H., Mohamed, M.R., and Aliman, O. (2015).** Solving optimal reactive power planning problem utilizing nature inspired computing techniques, *ARPNJournal of Engineering and Applied Sciences*, vol. 10(21), pp. 9779-9785.

[182] **Sun, J., Deng, J. and Li, Y. (2020).** Indicator & crowding distance-based evolutionary algorithm for combined heat and power economic emission dispatch, *Applied Soft Computing*, DOI:10.1016/j.asoc.2020.106158.

[183] **Taha, I.B.M., and Elattar, E.E. (2018).** Optimal reactive power resources sizing for power system operations enhancement based on improved grey wolf optimizer, *IET Generation, Transmission and Distribution*, vol. 12(14), pp. 3421-3434.

[184] **Taher M.A., Jurado, F., Kamel, S., and Ebeed, M. (2019).** Modified grasshopper optimization framework for optimal power solution, *Electrical Engineering*, vol. 101, pp. 121-148.

[185] **Talukdar, S.N., Giras, T.C., and Kalyan, V.K. (1983).** Decompositions for optimal power flows, *IEEE Transactions on Power Apparatus and Systems*, vol. 102 (12), pp. 3877–3884.

[186] **Tamura, K., and Yasuda, K. (2011).** Primary study of spiral dynamics inspired optimization, *IEEJ Transactions on Electrical and Electronic Engineering*, vol. 6(S1), pp. 98-100.

[187] **Tayarani, N.M.H., and Akbarzadeh-T, M.R. (2008).** Magnetic optimization algorithms a new synthesis, *In: Proceedings of IEEE Congress on Evolutionary Computation*, Hong Kong, China, pp. 2664-2669.

[188] **Teeparthi, K., and Kumar, D.M.V. (2016).** Security-constrained optimal power flow with wind and thermal power generators using fuzzy adaptive artificial physics optimization algorithm, *Neural Computing and Applications*, vol. 29(3), pp. 855-871.

[189] **Teeparthi, K., and Kumar, D.M.V. (2017).** Multi-objective hybrid PSO-APO algorithm based security constrained optimal power flow with wind and thermal generators, *Engineering Science and Technology, an International Journal*, vol. 20(2), pp. 411-426.

[190] **Thangaraj, R., Pant, M., Chelliah, T.R., and Abraham, A. (2012).** Opposition based chaotic differential evolution algorithm for solving global optimization problems, *In: Fourth world congress on nature and biologically inspired computing*, Mexico City, Mexico, pp. 1-7.

[191] **Thapar, S., Sharma, S., and Verma, A. (2018).** Key determinants of wind energy

growth in India: Analysis of policy and non-policy factors, *Energy Policy*, vol. 122, pp. 622-638.

[192] **Tinney, W.F., and Domell, H.W. (1968).** Optimal power flow solutions, *IEEE Transactions on Power Apparatus and Systems*, vol. 87(10), pp.1866–1876.

[193] **Tizhoosh, H. R. (2005).** Opposition-based learning: A new scheme for machine intelligence, *International Conference on Computational Intelligence for Modelling, Control and Automation*, Vienna, Austria, vol. 1, pp. 695–701.

[194] **Tripathy M., and Mishra, S. (2007).** Bacteria foraging-based solution to optimize both real power loss and voltage stability limit, *IEEE Transactions on Power Systems*, vol. 22(1), pp. 240-248.

[195] **Vaisakh, K., Srinivas, L.R., and Meah, K. (2013).** Genetic evolving ant direction particle swarm optimization algorithm for optimal power flow with non-smooth cost functions and statistical analysis, *Applied Soft Computing*, vol. 13(12), pp. 4579-4593.

[196] **Varadarajan, M., and Swarup, K.S. (2008).** Differential evolution approach for optimal reactive power dispatch, *Applied Soft Computing*, vol. 8(4), pp.1549-1561.

[197] **Verma, A., Krishan, R., and Mishra, S. (2018).** A novel PV inverter control for maximization of wind power penetration, *IEEE Transactions of Industry Applications*, vol. 54(6), pp. 6364-6373.

[198] **Vlachogiannis, J.G., and Lee, K.Y. (2006).** A comparative study of particle swarm optimization for optimal steady state performance of power systems, *IEEE Transactions on Power Systems*, vol. 21(4), pp.1718-1728.

[199] **Wang, H., Wu, Z., Liu, Y., Wang, J., Jiang, D., and Chen, L. (2009).** Space transformation search: A new evolutionary technique, *ACM/SIGEVOSummit on Genetic and Evolutionary Computation, Shanghai, China*, pp. 537–544.

[200] **Wang, H., Wu, Z., Rahnamayan, S., liu, Y., and Ventresca, M. (2011).** Enhancing particle swarm optimization using generalized opposition-based learning, *Information Sciences*, vol. 181(20), pp. 4699–4714.

[201] **Wang, H., Chen, G., Yi, X., and Zhang, Z. (2018).** Applications of multi-objective dimension-based firefly algorithm to optimize the power losses, emission, and cost in power systems, *Applied Soft Computing*, vol. 68, pp. 322-342.

[202] **Warid, W. (2020).** Optimal power flow using the AMTPG-Jaya algorithm, *Applied Soft Computing*, DOI:10.1016/j.asoc.2020.106252.

[203] **Warid, W., Hizam, W., Mariun, N., and Abdul-Wahab, N. I. (2016).** Optimal power flow using the Jaya algorithm, *Energies*, vol. 9(9), DOI:10.3390/en9090678.

[204] **Wei, W., Zhou, J., Chen, F., and Yuan, H. (2016).** Constrained differential evolution using generalized opposition-based learning, *Soft Computing*, vol. 20(11), pp. 4413–4437.

[205] **Wolpert, D., and Macready, W. (1997).** No free lunch theorems for optimization, *IEEE Transactions on Evolutionary Computation*, vol. 1(1), pp. 67–82.

[206] **Wu, Q.H., Zheng, J.H., Chen, J.J., and Jing, Z.X. (2015).** Multi-objective optimization and decision making for power dispatch of a large-scale integrated energy system with distributed DHCs embedded, *Applied Energy*, vol. 154, pp. 369-379.

[207] **Xia, S., Ding, Z., Shahidehpour, M., Chan, K.W., Bu, S., and Li, G. (2021).**Transient stability-constrained optimal power flow calculation with extremely unstable conditions using energy sensitivity method, *IEEE Transactions on Power Systems*, vol. 36(1), pp. 355-365.

[208] **Xia, X., Xu, Y., Dong Z.Y., Zhang, Y., and Liu, J. (2020).** Multi-objective coordinated dispatch of high wind-penetrated power systems against transient instability, *IET Generation, Transmission and Distribution*, vol. 14(19), pp. 4079-4088.

[209] **Xiang, Y., and Zhou, Y. (2015).** A dynamic multi-colony artificial bee colony algorithm for multi-objective optimization, *Applied Soft Computing*, vol. 35(1), pp.766–785.

[210] **Xu, K., Zhou, J., Zhang, Y., and Gu, R. (2012).** Differential evolution based on e-domination and orthogonal design method for power environmentally-friendly dispatch, *Expert Systems with Applications*, vol. 39, pp. 3956–3963.

[211] **Yang, X.S. (2011).** Bat algorithm for multi-objective optimization, *International Journal of Bio-Inspired Computation*, vol. 3(5), pp. 267-274.

[212] **Yang, X.S. (2020).** Nature-inspired optimization algorithms: Challenges and open problems, *Journal of Computational Science*, vol. 46, DOI: 10.1016/j.jocs.2020.101104.

[213] **Yu, K., Wang, X., and Wang, Z. (2015).** Self-adaptive multi-objective teaching-learning-based optimization and its application in ethylene cracking furnace operation optimization, *Chemometrics and Intelligent Laboratory Systems*, vol. 146, pp. 198-210.

[214] **Zhang, J., Tang, Q., Li, P., Deng, D., and Chen, Y. (2016).** A modified MOEA/D approach to the solution of multi-objective optimal power flow problem, *Applied Soft Computing*, vol. 47, pp. 494–514.

[215] **Zhang, J., Zhu, X., and Li, P. (2020).** MOEA/D with many-stage dynamical resource allocation strategy to solution of many-objective OPF problems, *International Journal of Electrical Power and Energy Systems*, vol. 120,DOI: 10.1016/j.ijepes.2020.106050.

[216] **Zhang, H. *et al.* (2019).** Coordination of generation, transmission and reactive power sources expansion planning with high penetration of wind power, *International Journal of Electrical Power and Energy Systems*, vol. 108: pp. 191–203.

[217] **Zhang, X., Rehtanz, C., and Pal, B. (2006).** Flexible AC Transmission Systems: Modelling and Control, Berlin:Springer.

[218] **Zheng, J.H., Chen, J.J., Wu, Q.H., and Jing, Z.X. (2015).** Multi-objective optimization and decision making for power dispatch of a large-scale integrated energy system with distributed DHCs embedded, *Applied Energy*, vol. 154, pp. 369–379.

[219] **Zhihuan, L., Yinhong, L., and Xianzhong, D. (2010).** Non-dominated sorting genetic algorithm-II for robust multi-objective optimal reactive power dispatch, *IET Generation, Transmission and Distribution*, vol. 4(9), pp. 1000-1008.

APPENDIX-A

TEST SYSTEMS

A.1 TEST SYSTEMSOF OPTIMAL POWER FLOW

The four test systems of the OPF problem have been undertaken in Chapter 2. The test system-I and test system-II are the standard IEEE 30-bus and IEEE 57-bus systems without FACTS devices. The test system-III and IV are modified IEEE 30-bus and modified IEEE 57-bus systems including FACTS devices. These test systems are used to confirm the usefulness of the optimization techniques. The input data for test system-I has been referred from Ref. [196]. The input data of thermal generating limits, generator cost and emission coefficients, load data and transmission lines data for test system-I are provided in Tables A.1.1, A.1.2, A.1.3 and A.1.4, respectively. The input data for test system-II is referred from Ref. [33,106]. The input data of generating units, load data and transmission lines data for test system-II are provided in Tables A.1.5, A.1.6 and A.1.7, respectively. The single-line diagram of test system-I and II are shown in Figures A.1.1 and A.1.2, respectively.

Table A.1.1: Generator input data for test system-I, III, V and VI

Bus No.	Generator Limits			
	P_{Gm}^{min}(MW)	P_{Gm}^{max}(MW)	Q_{Gm}^{min}(MVAr)	Q_{Gm}^{max}(MVAr)
1	50	200	-20	200
2	20	80	-20	100
5	15	50	-15	80
8	10	35	-15	60
11	10	30	-10	50
13	12	40	-15	60

Table A.1.2: Generator cost and emission coefficients for test system-I, V and VI

Bus No.	Cost Coefficient					Emission Coefficient				
	a_m ($/ hr)	b_m ($/ MWhr)	c_m ($/ MW^2hr)	d_m ($/ hr)	e_m (rad/ MW)	α_mx 10^{-2} (ton/hr)	β_mx 10^{-4} (ton/hr)	γ_m x 10^{-6} (ton/ MW^2hr)	η_m (ton/ hr)	λ_m x 10^{-2} (1/MW)
1	0	2.00	0.00375	0	0	4.091	-5.554	6.490	2.0E-4	2.857
2	0	1.75	0.01750	0	0	2.543	-6.047	5.638	5.0E-4	3.333
5	0	1.00	0.06250	0	0	4.258	-5.094	4.586	1.0E-6	8.000
8	0	3.25	0.00834	0	0	5.326	-3.550	3.380	2.0E-3	2.000
11	0	3.00	0.025	0	0	4.258	-5.094	4.586	1.0E-6	8.000
13	0	3.00	0.025	0	0	6.131	-5.555	5.151	1.0E-5	6.667

The input data for test system-III and IV is referred from Ref. [24,121]. The generator cost and emission coefficient for test system-III are provided in Table A.1.8. The input data of

generating units, load data and transmission lines data for test system-III are the same as the test system-I provided in Tables A.1.1, A.1.3 and A.1.4, respectively. The input data of generating units for test system-IV is given in Table A.1.9. The load data and transmission lines data for test system-IV are the same as test system-II provided in Tables A.1.6 and A.1.7, respectively.

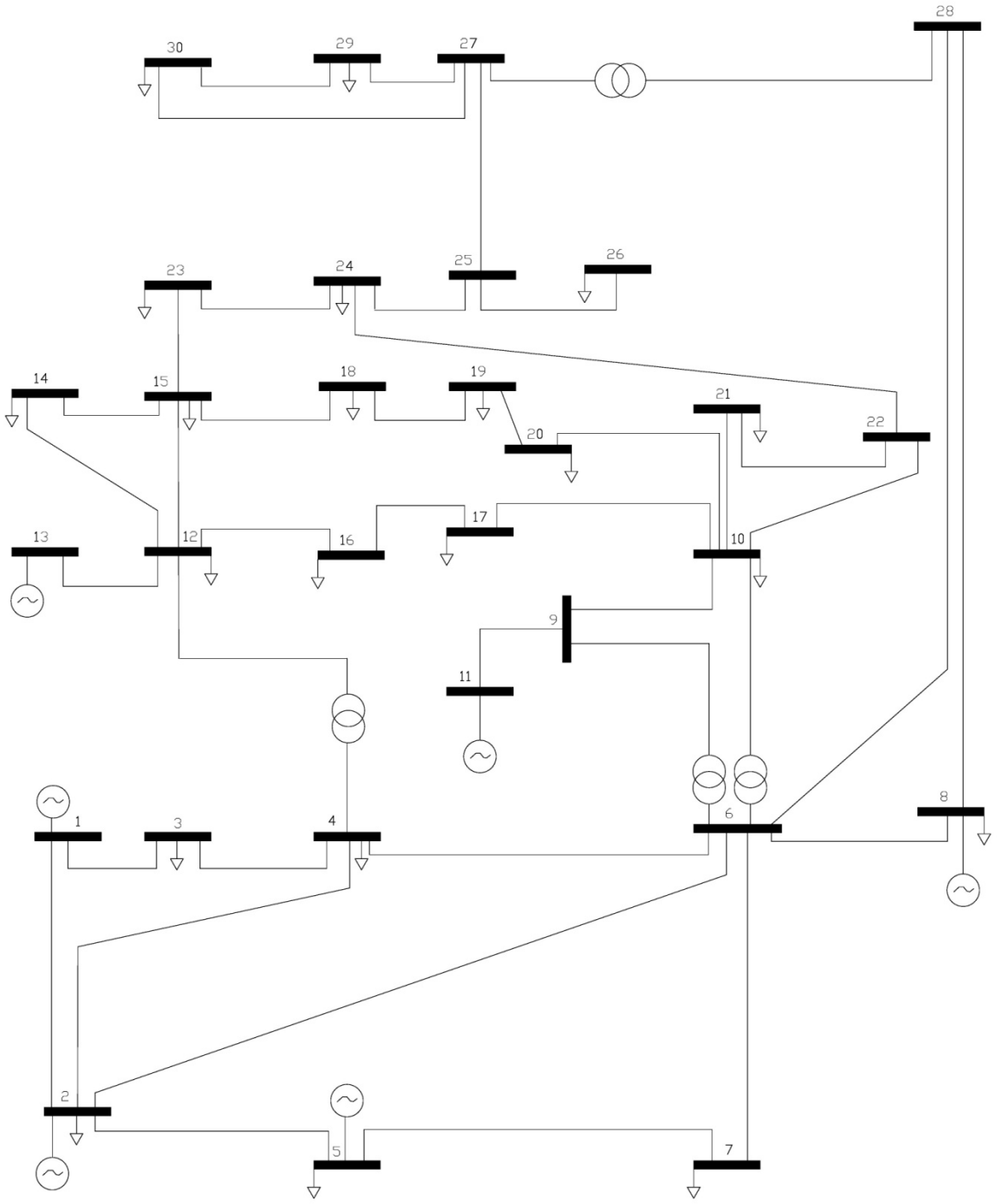

Figure A.1.1: Single-line diagram of IEEE 30-bus system (Test system-I)

Table A.1.3: Load input data for test system-I, III, V, VI, IX and XI

Bus No.	Load		Bus No.	Load	
	P(p.u.)	Q(p.u.)		P(p.u.)	Q(p.u.)
1	0.000	0.000	16	0.035	0.018
2	0.217	0.127	17	0.090	0.058
3	0.024	0.012	18	0.032	0.009
4	0.076	0.016	19	0.095	0.034
5	0.942	0.190	20	0.022	0.007
6	0.000	0.000	21	0.175	0.112
7	0.228	0.109	22	0.000	0.000
8	0.300	0.300	23	0.032	0.016
9	0.000	0.000	24	0.087	0.067
10	0.058	0.020	25	0.000	0.000
11	0.000	0.000	26	0.035	0.023
12	0.112	0.075	27	0.000	0.000
13	0.000	0.000	28	0.000	0.000
14	0.062	0.016	29	0.024	0.009
15	0.082	0.025	30	0.106	0.019

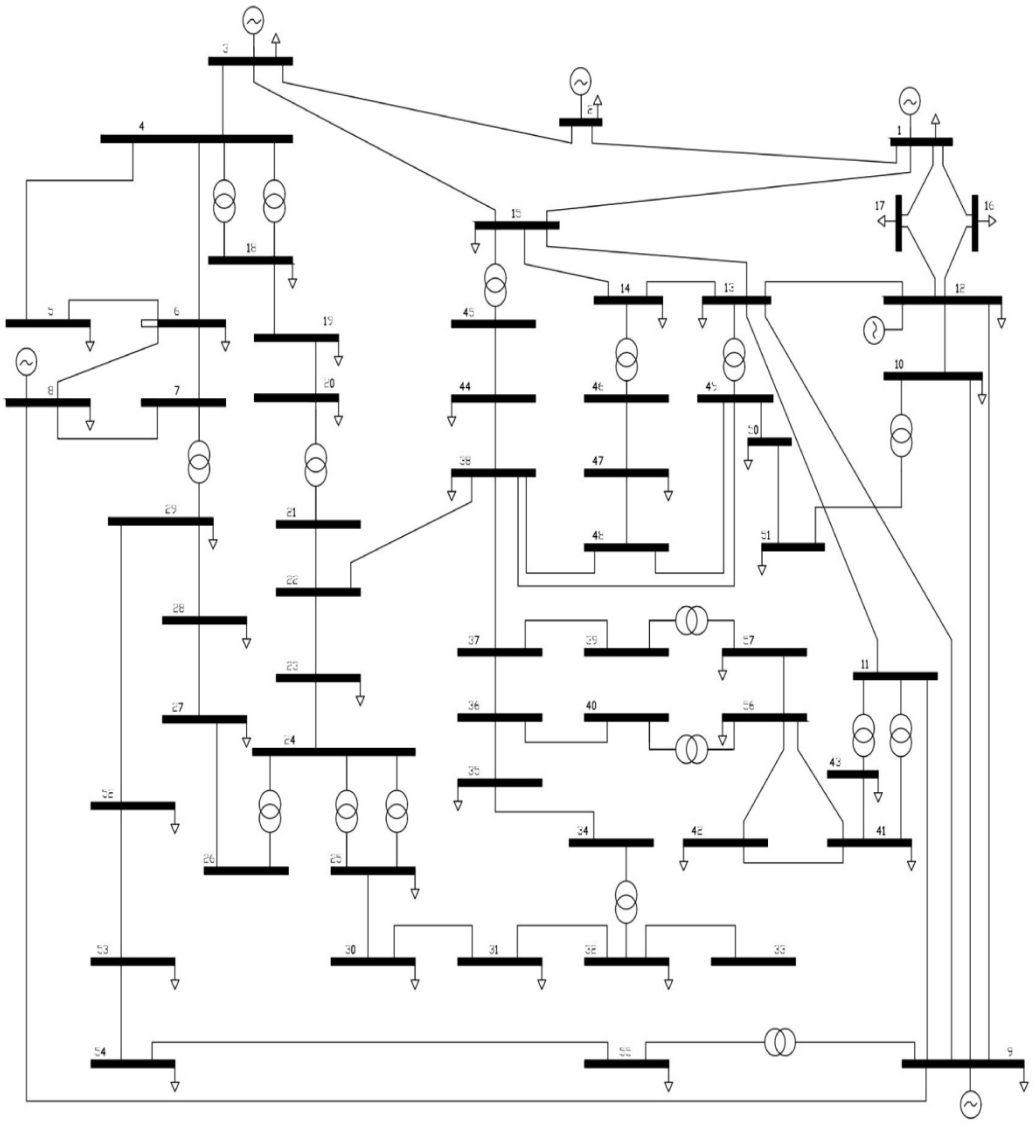

Figure A.1.2: Single-line diagram of IEEE 57-bus system (Test system-II)

Table A.1.4: Transmission line input data for test system-I, III, V, VI, IX and XI

Line No.	From Bus No.	To Bus No.	Line impedance			T_{min}	T_{max}
			R(p.u.)	X(p.u.)	½ B (p.u.)		
1	1	2	0.0192	0.0575	0.0264	-	-
2	1	3	0.0452	0.1852	0.0204	-	-
3	2	4	0.0570	0.1737	0.0184	-	-
4	3	4	0.0132	0.0379	0.0042	-	-
5	2	5	0.0472	0.1983	0.0209	-	-
6	2	6	0.0581	0.1763	0.0187	-	-
7	4	6	0.0119	0.0414	0.0045	-	-
8	5	7	0.0460	0.1160	0.0102	-	-
9	6	7	0.0267	0.0820	0.0085	-	-
10	6	8	0.0120	0.0420	0.0045	-	-
11	6	9	0.0000	0.2080	0	0.9	1.1
12	6	10	0.0000	0.5560	0	0.9	1.1
13	9	11	0.0000	0.2080	0	-	-
14	9	10	0.0000	0.1100	0	-	-
15	4	12	0.0000	0.2560	0	0.9	1.1
16	12	13	0.0000	0.1400	0	-	-
17	12	14	0.1231	0.2559	0	-	-
18	12	15	0.0662	0.1304	0	-	-
19	12	16	0.0945	0.1987	0	-	-
20	14	15	0.2210	0.1997	0	-	-
21	16	17	0.0824	0.1932	0	-	-
22	15	18	0.1070	0.2185	0	-	-
23	18	19	0.0639	0.1292	0	-	-
24	19	20	0.0340	0.0680	0	-	-
25	10	20	0.0936	0.2090	0	-	-
26	10	17	0.0324	0.0845	0	-	-
27	10	21	0.0348	0.0749	0	-	-
28	10	22	0.0727	0.1499	0	-	-
29	21	22	0.0116	0.0236	0	-	-
30	15	23	0.1000	0.2020	0	-	-
31	22	24	0.1150	0.1790	0	-	-
32	23	24	0.1320	0.2700	0	-	-
33	24	25	0.1885	0.3292	0	-	-
34	25	26	0.2544	0.3800	0	-	-
35	25	27	0.1093	0.2087	0	-	-
36	28	27	0.0000	0.3960	0	0.9	1.1
37	27	29	0.2198	0.4153	0	-	-
38	27	30	0.3202	0.6027	0	-	-
39	29	30	0.2399	0.4533	0	-	-
40	8	28	0.6360	0.2000	0.0214	-	-
41	6	28	0.0169	0.0599	0.0650	-	-

Table A.1.5: Generator input data for test system-II and VII

Bus No.	Generator Limits				Cost Coefficient		
	P_{Gm}^{min} (MW)	P_{Gm}^{max} (MW)	Q_{Gm}^{min} (MVAr)	Q_{Gm}^{max} (MVAr)	a_m (\$/hr)	b_m (\$/MWhr)	c_m (\$/MW^{2}hr)
1	0	575.88	-140	200	0	20	0.0775795
2	0	150	-17	50	0	0	0
3	42	140	-10	60	0	20	0.25
6	0	150	-8	25	0	0	0
8	165	550	-140	200	0	20	0.022222
9	0	150	-3	9	0	0	0
12	123	410	-150	155	0	20	0.0322581

Table A.1.5: Generator input data for test system-II and VII (Continued)

Bus No.	Emission Coefficient				
	α_m (ton/hr)	β_m (ton/hr)	γ_m (ton/MW^{2}hr)	η_m (ton/hr)	λ_m (1/MW)
1	0.04	-0.05	0.04	4	0.4
2	0.04	-0.05	0.04	4	0.4
3	0.04	-0.05	0.04	4	0.4
6	0.04	-0.05	0.04	4	0.4
8	0.04	-0.05	0.04	4	0.4
9	0.04	-0.05	0.04	4	0.4
12	0.04	-0.05	0.04	4	0.4

Table A.1.6: Load input data for test system-II, IV and VII

Bus No.	Load		Bus No.	Load	
	P(p.u.)	Q(p.u.)		P(p.u.)	Q(p.u.)
1	0.550	0.170	30	0.036	0.018
2	0.030	0.880	31	0.058	0.029
3	0.410	0.210	32	0.016	0.008
4	0.000	0.000	33	0.038	0.019
5	0.130	0.040	34	0.000	0.000
6	0.750	0.020	35	0.060	0.030
7	0.000	0.000	36	0.000	0.000
8	1.500	0.220	37	0.000	0.000
9	1.210	0.260	38	0.140	0.070
10	0.050	0.020	39	0.000	0.000
11	0.000	0.000	40	0.000	0.000
12	3.770	0.240	41	0.063	0.030
13	0.180	0.023	42	0.071	0.044
14	0.105	0.053	43	0.020	0.010
15	0.220	0.050	44	0.120	0.018
16	0.430	0.030	45	0.000	0.000
17	0.420	0.080	46	0.000	0.000
18	0.272	0.098	47	0.297	0.116
19	0.033	0.006	48	0.000	0.000
20	0.023	0.010	49	0.180	0.085
21	0.000	0.000	50	0.210	0.105
22	0.000	0.000	51	0.180	0.053
23	0.063	0.021	52	0.049	0.022
24	0.000	0.000	53	0.200	0.100
25	0.063	0.032	54	0.041	0.014
26	0.000	0.000	55	0.068	0.034
27	0.093	0.005	56	0.076	0.022
28	0.046	0.023	57	0.067	0.020
29	0.170	0.026			

Test system-V consisting of IEEE 30-bus system has been undertaken in Chapter-3. The system data is taken from Ref. [92].The input data of generating units, generator cost and emission coefficients, load data and transmission lines data for test system-V are the same as test system-I provided in Tables A.1.1, A.1.2, A.1.3 and A.1.4, respectively. The three OPF test systems have been undertaken in Chapter-4. The test system-VI, VII and VIII are IEEE 30-bus system, IEEE 57-bus and IEEE 118-bus system, respectively. The system data for test system-VI and VII has been taken from Ref. [144].

Figure A.1.3: Single-line diagram of IEEE 118-bus system (Test system-XIII)

The input data of generating units, generator cost and emission coefficients, load data and transmission lines data for test system-VI are the same as test system-I provided in Tables A.1.1, A.1.2, A.1.3 and A.1.4, respectively. The input data of generating units, load data and transmission lines data for test system-VII are the same as test system-II provided in Tables A.1.5, A.1.6 and A.1.7, respectively. The system data for test system-VIII has been taken from

Ref. [202]. The input data of generating units, load data and transmission lines data for test system-VIII are provided in the Tables A.1.10, A.1.11 and A.1.12, respectively. The single-line diagram of test system-VIII is shown in Figure A.1.3.

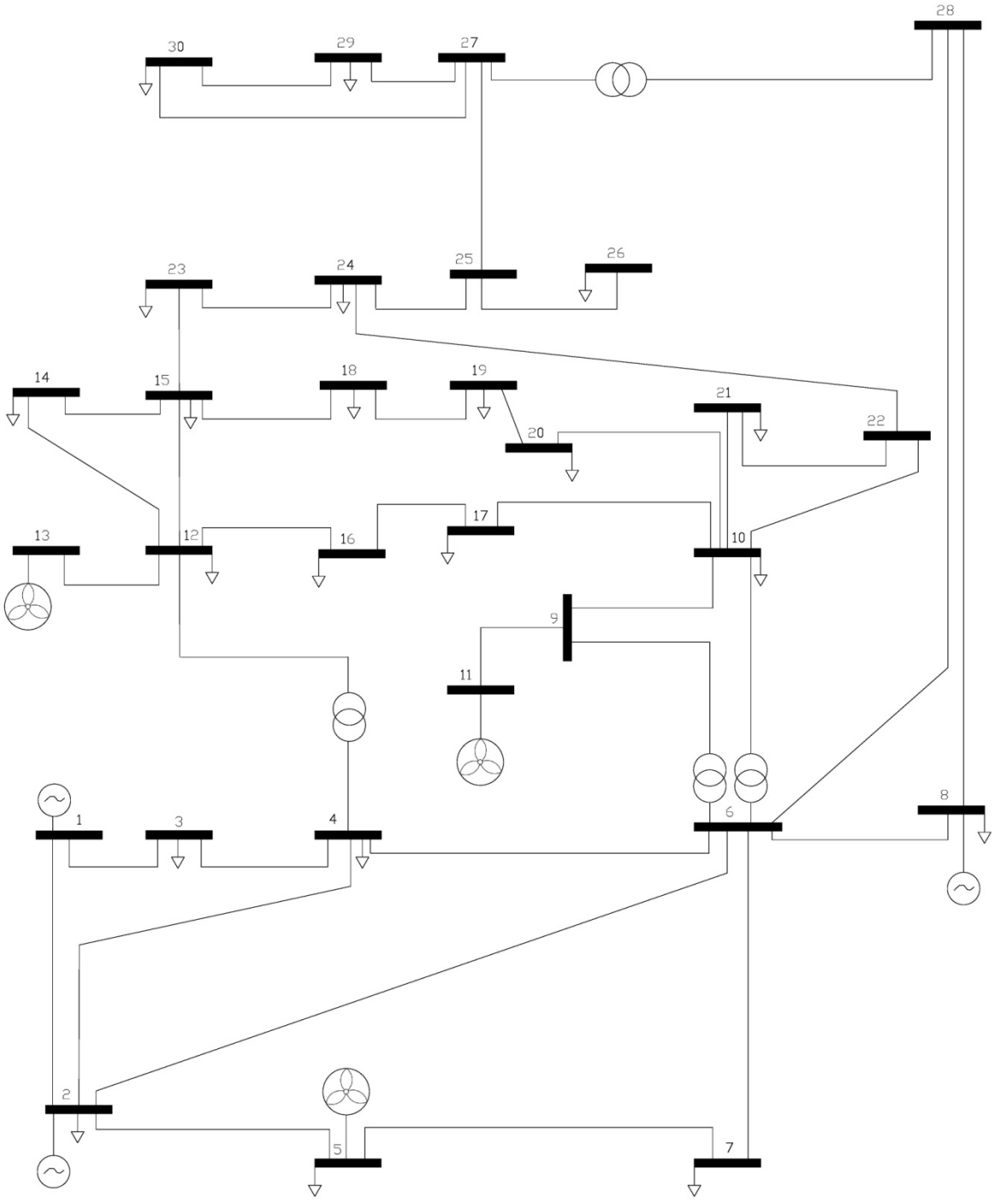

Figure A.2.1: Single-line diagram of modified IEEE 30-bus system (Test system-IX)

Table A.1.7: Transmission line input data for test system-II, IV and VII

Line No.	From Bus No.	To Bus No.	Line impedance			T_{min}	T_{max}
			R(p.u.)	X(p.u.)	1/2B (p.u.)		
1	1	2	0.0083	0.0280	0.1290	-	-
2	2	3	0.0298	0.0850	0.0818	-	-

Table A.1.7: Transmission line input data for test system-II, IV and VII (Continued)

Line No.	From Bus No.	To Bus No.	Line impedance			T_{min}	T_{max}
			R(p.u.)	X(p.u.)	1/2B (p.u.)		
3	3	4	0.0112	0.0366	0.0380	-	-
4	4	5	0.0625	0.1320	0.0258	-	-
5	4	6	0.0430	0.1480	0.0348	-	-
6	6	7	0.0200	0.1020	0.0276	-	-
7	6	8	0.0339	0.1730	0.0470	-	-
8	8	9	0.0099	0.0505	0.0548	-	-
9	9	10	0.0369	0.1679	0.0440	-	-
10	9	11	0.0258	0.0848	0.0218	-	-
11	9	12	0.0648	0.2950	0.0772	-	-
12	9	13	0.0481	0.1580	0.0406	-	-
13	13	14	0.0132	0.0434	0.0110	-	-
14	13	15	0.0269	0.0869	0.0230	-	-
15	1	15	0.0178	0.0910	0.0988	-	-
16	1	16	0.0454	0.2060	0.0546	-	-
17	1	17	0.0238	0.1080	0.0286	-	-
18	3	15	0.0162	0.0530	0.0544	-	-
19	4	18	0.0	0.5550	0.0	0.9	1.1
20	4	18	0.0	0.4300	0.0	0.9	1.1
21	5	6	0.0302	0.0641	0.0124	-	-
22	7	8	0.0139	0.0712	0.0194	-	-
23	10	12	0.0277	0.1262	0.0328	-	-
24	11	13	0.0223	0.0732	0.0188	-	-
25	12	13	0.0178	0.0580	0.0604	-	-
26	12	16	0.0180	0.0813	0.0216	-	-
27	12	17	0.0397	0.1790	0.0476	-	-
28	14	15	0.0171	0.0547	0.0148	-	-
29	18	19	0.4610	0.6850	0.0	-	-
30	19	20	0.2830	0.4340	0.0	-	-
31	21	20	0.0	0.7767	0.0	0.9	1.1
32	21	22	0.0736	0.1170	0.0	-	-
33	22	23	0.0099	0.0152	0.0	-	-
34	23	24	0.1660	0.2560	0.0084	-	-
35	24	25	0.0	1.1820	0.0	-	-
36	24	25	0.0	1.2300	0.0	-	-
37	24	26	0.0	0.0473	0.0	0.9	1.1
38	26	27	0.1650	0.2540	0.0	-	-
39	27	28	0.0618	0.0954	0.0	-	-
40	28	29	0.0418	0.0587	0.0	-	-
41	7	29	0.0	0.0648	0.0	0.9	1.1
42	25	30	0.1350	0.2020	0.0	-	-
43	30	31	0.3260	0.4970	0.0	-	-
44	31	32	0.5070	0.7550	0.0	-	-
45	32	33	0.0392	0.0360	0.0	-	-
46	34	32	0.0	0.9530	0.0	0.9	1.1
47	34	35	0.0520	0.0780	0.0032	-	-
48	35	36	0.0430	0.0537	0.0016	-	-
49	36	37	0.0290	0.0366	0.0	-	-
50	37	38	0.0651	0.1009	0.0020	-	-
51	37	39	0.0239	0.0379	0.0	-	-
52	36	40	0.0300	0.0466	0.0	-	-
53	22	38	0.0192	0.0295	0.0	-	-
54	11	41	0.0	0.7490	0.0	0.9	1.1
55	41	42	0.2070	0.3520	0.0	-	-
56	41	43	0.0	0.4120	0.0	-	-
57	38	44	0.0289	0.0585	0.0020	-	-

Table A.1.7: Transmission line input data for test system-II, IV and VII (Continued)

Line No.	From Bus No.	To Bus No.	Line impedance			T_{min}	T_{max}
			R(p.u.)	X(p.u.)	1/2B (p.u.)		
58	15	45	0.0	0.1042	0.0	0.9	1.1
59	14	46	0.0	0.0735	0.0	0.9	1.1
60	46	47	0.0230	0.0680	0.0032	-	-
61	47	48	0.0182	0.0233	0.0	-	-
62	48	49	0.0834	0.1290	0.0048	-	-
63	49	50	0.0801	0.1280	0.0	-	-
64	50	51	0.1386	0.2200	0.0	-	-
65	10	51	0.0	0.0712	0.0	0.9	1.1
66	13	49	0.0	0.1910	0.0	0.9	1.1
67	29	52	0.1442	0.1870	0.0	-	-
68	52	53	0.0762	0.0984	0.0	-	-
69	53	54	0.1878	0.2320	0.0	-	-
70	54	55	0.1732	0.2265	0.0	-	-
71	11	43	0.0	0.1530	0.0	0.9	1.1
72	44	45	0.0624	0.1242	0.0040	-	-
73	40	56	0.0	1.1950	0.0	0.9	1.1
74	56	41	0.5530	0.5490	0.0	-	-
75	56	42	0.2125	0.3540	0.0	-	-
76	39	57	0.0	1.3550	0.0	0.9	1.1
77	57	56	0.1740	0.2600	0.0	-	-
78	38	49	0.1150	0.1770	0.0030	-	-
79	38	48	0.0312	0.0482	0.0	-	-
80	9	55	0.0	0.1205	0.0	0.9	1.1

Table A.1.8: Generator cost and emission coefficients for test system-III

Bus No.	Cost Coefficient					Emission Coefficient				
	a_m ($/hr)	b_m ($/MWhr)	c_m ($/MW^{2}hr)	d_m ($/hr)	e_m (rad/MW)	α_mx10^{-2} (ton/hr)	β_mx10^{-4} (ton/hr)	γ_mx10^{-6} (ton/MW^{2}hr)	η_m (ton/hr)	λ_mx10^{-2} (1/MW)
1	0	2.00	0.00375	18.0	0.0370	4.091	-5.554	6.490	2.0E-4	2.857
2	0	1.75	0.01750	16.0	0.0380	2.543	-6.047	5.638	5.0E-4	3.333
5	0	1.00	0.06250	14.0	0.0400	4.258	-5.094	4.586	1.0E-6	8.000
8	0	3.25	0.00834	12.0	0.0450	5.326	-3.550	3.380	2.0E-3	2.000
11	0	3.00	0.025	13.0	0.0420	4.258	-5.094	4.586	1.0E-6	8.000
13	0	3.00	0.025	13.5	0.0410	6.131	-5.555	5.151	1.0E-5	6.667

Table A.1.9: Generator input data for test system-IV

Bus No.	Generator Limits			
	P_{Gm}^{min}(MW)	P_{Gm}^{max}(MW)	Q_{Gm}^{min}(MVAr)	Q_{Gm}^{max}(MVAr)
1	0	600	-140	200
2	0	500	-17	50
3	0	500	-10	60
6	0	500	-8	25
8	0	650	-140	200
9	0	500	-3	9
12	0	500	-150	155

Table A.1.9: Generator input data for test system-IV (continued)

Bus No.	Cost Coefficient					Emission Coefficient				
	a_m ($/hr)	b_m ($/MWhr)	c_m ($/MW^{2}hr)	d_m ($/hr)	e_m (rad/MW)	α_mx10^{-2} (ton/hr)	β_m x10^{-4} (ton/hr)	γ_mx10^{-6} (ton/MW^{2}hr)	η_m (ton/hr)	λ_m x10^{-3} (1/MW)
1	0	2.00	0.00375	18.00	0.0370	4.091	-5.554	6.490	2.0E-4	2.857
2	0	1.75	0.01750	16.00	0.0380	2.543	-6.047	5.638	5.0E-4	3.333

Table A.1.9: Generator input data for test system-IV (continued)

Bus No.	Cost Coefficient					Emission Coefficient				
	a_m ($/hr)	b_m ($/MWhr)	c_m ($/MW^{2}hr)	d_m ($/hr)	e_m (rad/MW)	α_mx10^{-2} (ton/hr)	β_m x10^{-4} (ton/hr)	γ_m x10^{-6} (ton/MW^{2}hr)	η_m (ton/hr)	λ_m x10^{-3} (1/MW)
3	0	3.00	0.02500	13.50	0.0410	6.131	-5.555	5.151	1.0E-5	6.667
6	0	2.00	0.00375	18.00	0.0370	3.491	-5.754	6.390	3.0E-4	2.657
8	0	1.00	0.06250	14.00	0.0400	4.258	-5.094	4.586	1.0E-6	8.000
9	0	1.75	0.01950	15.00	0.0390	2.754	-5.847	5.238	4.0E-4	2.875
12	0	3.25	0.00834	12.00	0.0450	5.326	-3.555	3.380	2.0E-3	2.000

Table A.1.10: Generator input data for test system-VIII, X

Bus No.	Generator Limits				Cost Coefficient		
	P_{Gm}^{min} (MW)	P_{Gm}^{max} (MW)	Q_{Gm}^{min} (MVAr)	Q_{Gm}^{max} (MVAr)	a_m ($/hr)	b_m ($/MWhr)	c_m ($/MW^{2}hr)
1	0	100	-5	15	0	40	0.01
4	0	100	-300	300	0	40	0.01
6	0	100	-13	50	0	40	0.01
8	0	100	-300	300	0	40	0.01
10	165	550	-147	200	0	20	0.022222
12	55.5	185	-35	120	0	20	0.117647
15	0	100	-10	30	0	40	0.01
18	0	100	-16	50	0	40	0.01
19	0	100	-8	24	0	40	0.01
24	0	100	-300	300	0	40	0.01
25	96	320	-47	140	0	20	0.0454545
26	124.2	414	-1000	1000	0	20	0.0318471
27	0	100	-300	300	0	40	0.01
31	0	107	-300	300	0	20	0.142857
32	0	100	-14	42	0	40	0.01
34	0	100	-8	24	0	40	0.01
36	0	100	-8	24	0	40	0.01
40	0	100	-300	300	0	40	0.01
42	0	100	-300	300	0	40	0.01
46	0	119	-100	100	0	20	0.0526316
49	91.2	304	-85	210	0	20	0.0490196
54	0	148	-300	200	0	20	0.0208333
55	0	100	-8	23	0	40	0.01
56	0	100	-8	15	0	40	0.01
59	76.5	255	-60	180	0	20	0.0645161
61	78	260	-100	300	0	20	0.0625
62	0	100	-20	20	0	40	0.01
65	147.3	491	-67	200	0	20	0.0255754
66	147.6	492	-67	200	0	20	0.0255102
69	0	805.2	-300	300	0	20	0.0193648
70	0	100	-10	32	0	40	0.01
72	0	100	-100	100	0	40	0.01
73	0	100	-100	100	0	40	0.01
74	0	100	-6	9	0	40	0.01
76	0	100	-8	23	0	40	0.01
77	0	100	-20	70	0	40	0.01
80	173.1	577	-165	280	0	20	0.0209644
85	0	100	-8	23	0	40	0.01
87	0	104	-100	1000	0	20	0.025
89	212.1	707	-210	300	0	20	0.0164745
90	0	100	-300	300	0	40	0.01
91	0	100	-100	100	0	40	0.01

Table A.1.10: Generator input data for test system-VIII, X (Continued)

Bus No.	Generator Limits				Cost Coefficient		
	P_{Gm}^{min} (MW)	P_{Gm}^{max} (MW)	Q_{Gm}^{min} (MVAr)	Q_{Gm}^{max} (MVAr)	a_m ($/hr)	b_m ($/MWhr)	c_m ($/MW^{2}hr)
92	0	100	-3	9	0	40	0.01
99	0	100	-100	100	0	40	0.01
100	105.6	352	-50	155	0	20	0.0396825
103	0	140	-15	40	0	20	0.025
104	0	100	-8	23	0	40	0.01
105	0	100	-8	23	0	40	0.01
107	0	100	-200	200	0	40	0.01
110	0	100	-8	23	0	40	0.01
111	0	136	-100	1000	0	20	0.0277778
112	0	100	-100	1000	0	40	0.01
113	0	100	-100	200	0	40	0.01
116	0	100	-1000	1000	0	40	0.01

Table A.1.10: Generator input data for test system-VIII, X (Continued)

Bus No.	Emission Coefficient				
	α_mx10^{-2} (ton/hr)	β_mx10^{-4} (ton/hr)	γ_mx10^{-6} (ton/MW^{2}hr)	η_mx10^{-5} (ton/hr)	λ_mx10^{-2} (1/MW)
1	6.0	-5.0	4.0	2.0	0.5
4	6.0	-6.0	3.0	5.0	1.5
6	4.0	-5.0	4.0	1.0	1.0
8	3.5	-3.0	3.5	2.0	0.5
10	4.5	-5.0	5.0	4.0	2.0
12	5.0	-4.0	4.5	1.0	2.0
15	5.0	-5.0	6.0	1.0	1.5
18	6.0	-5.0	4.0	2.0	0.5
19	6.0	-6.0	3.0	5.0	1.5
24	4.0	-5.0	4.0	1.0	1.0
25	3.5	-3.0	3.5	2.0	0.5
26	4.5	-5.0	5.0	4.0	2.0
27	5.0	-4.0	4.5	1.0	2.0
31	5.0	-5.0	6.0	1.0	1.5
32	6.0	-5.0	4.0	2.0	0.5
34	6.0	-6.0	3.0	5.0	1.5
36	4.0	-5.0	4.0	1.0	1.0
40	3.5	-3.0	3.5	2.0	0.5
42	4.5	-5.0	5.0	4.0	2.0
46	5.0	-4.0	4.5	1.0	2.0
49	5.0	-5.0	6.0	1.0	1.5
54	6.0	-5.0	4.0	2.0	0.5
55	6.0	-6.0	3.0	5.0	1.5
56	4.0	-5.0	4.0	1.0	1.0
59	3.5	-3.0	3.5	2.0	0.5
61	4.5	-5.0	5.0	4.0	2.0
62	5.0	-4.0	4.5	1.0	2.0
65	5.0	-5.0	6.0	1.0	1.5
66	6.0	-5.0	4.0	2.0	0.5
69	6.0	-6.0	3.0	5.0	1.5
70	4.0	-5.0	4.0	1.0	1.0
72	3.5	-3.0	3.5	2.0	0.5
73	4.5	-5.0	5.0	4.0	2.0
74	5.0	-4.0	4.5	1.0	2.0
76	5.0	-5.0	6.0	1.0	1.5
77	6.0	-5.0	4.0	2.0	0.5

Table A.1.10: Generator input data for test system-VIII, X (Continued)

Bus No.	Emission Coefficient				
	α_mx10^{-2} (ton/hr)	β_m x10^{-4} (ton/hr)	γ_m x10^{-6} (ton/MW^{2}hr)	η_mx10^{-5} (ton/hr)	λ_mx10^{-2} (1/MW)
80	6.0	-6.0	3.0	5.0	1.5
85	4.0	-5.0	4.0	1.0	1.0
87	3.5	-3.0	3.5	2.0	0.5
89	4.5	-5.0	5.0	4.0	2.0
90	5.0	-4.0	4.5	1.0	2.0
91	5.0	-5.0	6.0	1.0	1.5
92	6.0	-5.0	4.0	2.0	0.5
99	6.0	-6.0	3.0	5.0	1.5
100	4.0	-5.0	4.0	1.0	1.0
103	3.5	-3.0	3.5	2.0	0.5
104	4.5	-5.0	5.0	4.0	2.0
105	5.0	-4.0	4.5	1.0	2.0
107	5.0	-5.0	6.0	1.0	1.5
110	6.0	-5.0	4.0	2.0	0.5
111	6.0	-6.0	3.0	5.0	1.5
112	4.0	-5.0	4.0	1.0	1.0
113	3.5	-3.0	3.5	2.0	0.5
116	4.5	-5.0	5.0	4.0	2.0

Table A.1.11: Load input data for test system-XIII, X and XII

Bus No.	Load		Bus No.	Load	
	P(p.u.)	Q(p.u.)		P(p.u.)	Q(p.u.)
1	0.51	0.27	60	0.78	0.03
2	0.20	0.09	61	0.00	0.00
3	0.39	0.10	62	0.77	0.14
4	0.39	0.12	63	0.00	0.00
5	0.00	0.00	64	0.00	0.00
6	0.52	0.22	65	0.00	0.00
7	0.19	0.02	66	0.39	0.18
8	0.28	0.00	67	0.28	0.07
9	0.00	0.00	68	0.00	0.00
10	0.00	0.00	69	0.00	0.00
11	0.70	0.23	70	0.66	0.20
12	0.47	0.10	71	0.00	0.00
13	0.34	0.16	72	0.12	0.00
14	0.14	0.01	73	0.06	0.00
15	0.90	0.30	74	0.68	0.27
16	0.25	0.10	75	0.47	0.11
17	0.11	0.03	76	0.68	0.36
18	0.60	0.34	77	0.61	0.28
19	0.45	0.25	78	0.71	0.26
20	0.18	0.03	79	0.39	0.32
21	0.14	0.08	80	1.30	0.26
22	0.10	0.05	81	0.00	0.00
23	0.07	0.03	82	0.54	0.27
24	0.13	0.00	83	0.20	0.10
25	0.00	0.00	84	0.11	0.07
26	0.00	0.00	85	0.24	0.15
27	0.71	0.13	86	0.21	0.10
28	0.17	0.07	87	0.00	0.00
29	0.24	0.04	88	0.48	0.10
30	0.00	0.00	89	0.00	0.00
31	0.43	0.27	90	1.63	0.42

Table A.1.11: Load input data for test system-XIII, X and XII (Continued)

Bus No.	Load		Bus No.	Load	
	P(p.u.)	Q(p.u.)		P(p.u.)	Q(p.u.)
32	0.59	0.23	91	0.10	0.00
33	0.23	0.09	92	0.65	0.10
34	0.59	0.26	93	0.12	0.07
35	0.33	0.09	94	0.30	0.16
36	0.31	0.17	95	0.42	0.31
37	0.00	0.00	96	0.38	0.15
38	0.00	0.00	97	0.15	0.09
39	0.27	0.11	98	0.34	0.08
40	0.66	0.23	99	0.42	0.00
41	0.37	0.10	100	0.37	0.18
42	0.96	0.23	101	0.22	0.15
43	0.18	0.07	102	0.05	0.03
44	0.16	0.08	103	0.23	0.16
45	0.53	0.22	104	0.38	0.25
46	0.28	0.10	105	0.31	0.26
47	0.34	0.01	106	0.43	0.16
48	0.20	0.11	107	0.50	0.12
49	0.87	0.30	108	0.02	0.01
50	0.17	0.04	109	0.08	0.03
51	0.17	0.08	110	0.39	0.30
52	0.18	0.05	111	0.00	0.00
53	0.23	0.11	112	0.68	0.13
54	1.13	0.32	113	0.06	0.00
55	0.63	0.22	114	0.08	0.03
56	0.84	0.18	115	0.22	0.07
57	0.12	0.03	116	1.84	0.00
58	0.12	0.03	117	0.20	0.08
59	2.77	1.13	118	0.33	0.15

A.2 TEST SYSTEMS OFOPTIMAL POWER FLOW PROBLEM INCLUDING WIND UNITS

The two test systems of the OPF problem including wind units have been undertaken in Chapter-5. The test system-IX and test system-X are modified IEEE 30-bus system and modified IEEE 118-bus system, respectively. A detailed description of test system-IX is given in Ref. [101]. The input data of thermal generators for test system-IX is given in Table A.2.1. The load data and transmission lines data for test system-IX are the same as test system-I provided in Tables A.1.3 and A.1.4, respectively.

The system data of test system-X is taken from Ref. [48]. The input data of generating units, load data and transmission lines data for test system-X are the same as test system-VIII provided in Tables A.1.10, A.1.11 and A.1.12, respectively. The wind generator data for test system-IX and X is given in Table A.2.2.The single-line diagram of test system-IX and X is shown in Figures A.2.1 and A.2.2, respectively.

Figure A.2.2: Single-line diagram of modified IEEE 118-bus system (Test system-X)

Table A.1.12: Transmission line input data for test system-VIII, X and XII

Line No.	From Bus No.	To Bus No.	Line impedance			T_{min}	T_{max}
			R(p.u.)	X(p.u.)	1/2B (p.u.)		
1	1	2	0.0303	0.0999	0.0254	-	-
2	1	3	0.0129	0.0424	0.01082	-	-
3	4	5	0.00176	0.00798	0.0021	-	-
4	3	5	0.0241	0.108	0.0284	-	-
5	5	6	0.0119	0.054	0.01426	-	-

Table A.1.12: Transmission line input data for test system-VIII, X and XII (Continued)

Line No.	From Bus No.	To Bus No.	Line impedance			T_{min}	T_{max}
			R(p.u.)	X(p.u.)	1/2B (p.u.)		
6	6	7	0.00459	0.0208	0.0055	-	-
7	8	9	0.00244	0.0305	1.162	-	-
8	8	5	0.000	0.0267	0.000	0.9	1.1
9	9	10	0.00258	0.0322	1.23	-	-
10	4	11	0.0209	0.0688	0.01748	-	-
11	5	11	0.0203	0.0682	0.01738	-	-
12	11	12	0.00595	0.0196	0.00502	-	-
13	2	12	0.0187	0.0616	0.01572	-	-
14	3	12	0.0484	0.16	0.0406	-	-
15	7	12	0.00862	0.034	0.00874	-	-
16	11	13	0.02225	0.0731	0.01876	-	-
17	12	14	0.0215	0.0707	0.01816	-	-
18	13	15	0.0744	0.2444	0.06268	-	-
19	14	15	0.0595	0.195	0.0502	-	-
20	12	16	0.0212	0.0834	0.0214	-	-
21	15	17	0.0132	0.0437	0.0444	-	-
22	16	17	0.0454	0.1801	0.0466	-	-
23	17	18	0.0123	0.0505	0.01298	-	-
24	18	19	0.01119	0.0493	0.01142	-	-
25	19	20	0.0252	0.117	0.0298	-	-
26	15	19	0.012	0.0394	0.0101	-	-
27	20	21	0.0183	0.0849	0.0216	-	-
28	21	22	0.0209	0.097	0.0246	-	-
29	22	23	0.0342	0.159	0.0404	-	-
30	23	24	0.0135	0.0492	0.0498	-	-
31	23	25	0.0156	0.08	0.0864	-	-
32	26	25	0.000	0.0382	0.000	0.9	1.1
33	25	27	0.0318	0.163	0.1764	-	-
34	27	28	0.01913	0.0855	0.0216	-	-
35	28	29	0.0237	0.0943	0.0238	-	-
36	30	17	0.000	0.0388	0.000	0.9	1.1
37	8	30	0.00431	0.0504	0.514	-	-
38	26	30	0.00799	0.086	0.908	-	-
39	17	31	0.0474	0.1563	0.0399	-	-
40	29	31	0.0108	0.0331	0.0083	-	-
41	23	32	0.0317	0.1153	0.1173	-	-
42	31	32	0.0298	0.0985	0.0251	-	-
43	27	32	0.0229	0.0755	0.01926	-	-
44	15	33	0.038	0.1244	0.03194	-	-
45	19	34	0.0752	0.247	0.0632	-	-
46	35	36	0.00224	0.0102	0.00268	-	-
47	35	37	0.011	0.0497	0.01318	-	-
48	33	37	0.0415	0.142	0.0366	-	-
49	34	36	0.00871	0.0268	0.00568	-	-
50	34	37	0.00256	0.0094	0.00984	-	-
51	38	37	0.000	0.0375	0.000	0.9	1.1
52	37	39	0.0321	0.106	0.027	-	-
53	37	40	0.0593	0.168	0.042	-	-
54	30	38	0.00464	0.054	0.422	-	-
55	39	40	0.0184	0.0605	0.01552	-	-
56	40	41	0.0145	0.0487	0.01222	-	-
57	40	42	0.0555	0.183	0.0466	-	-
58	41	42	0.041	0.135	0.0344	-	-
59	43	44	0.0608	0.2454	0.06068	-	-
60	34	43	0.0413	0.1681	0.04226	-	-

Table A.1.12: Transmission line input data for test system-VIII, X and XII (Continued)

Line No.	From Bus No.	To Bus No.	Line impedance			T_{min}	T_{max}
			R(p.u.)	X(p.u.)	1/2B (p.u.)		
61	44	45	0.0224	0.0901	0.0224	-	-
62	45	46	0.04	0.1356	0.0332	-	-
63	46	47	0.038	0.127	0.0316	-	-
64	46	48	0.0601	0.189	0.0472	-	-
65	47	49	0.0191	0.0625	0.01604	-	-
66	42	49	0.0715	0.323	0.086	-	-
67	42	49	0.0715	0.323	0.086	-	-
68	45	49	0.0684	0.186	0.0444	-	-
69	48	49	0.0179	0.0505	0.01258	-	-
70	49	50	0.0267	0.0752	0.01874	-	-
71	49	51	0.0486	0.137	0.0342	-	-
72	51	52	0.0203	0.0588	0.01396	-	-
73	52	53	0.0405	0.1635	0.04058	-	-
74	53	54	0.0263	0.122	0.031	-	-
75	49	54	0.073	0.289	0.0738	-	-
76	49	54	0.0869	0.291	0.073	-	-
77	54	55	0.0169	0.0707	0.0202	-	-
78	54	56	0.00275	0.00955	0.00732	-	-
79	55	56	0.00488	0.0151	0.00374	-	-
80	56	57	0.0343	0.0966	0.0242	-	-
81	50	57	0.0474	0.134	0.0332	-	-
82	56	58	0.0343	0.0966	0.0242	-	-
83	51	58	0.0255	0.0719	0.01788	-	-
84	54	59	0.0503	0.2293	0.0598	-	-
85	56	59	0.0825	0.251	0.0569	-	-
86	56	59	0.0803	0.239	0.0536	-	-
87	55	59	0.04739	0.2158	0.05646	-	-
88	59	60	0.0317	0.145	0.0376	-	-
89	59	61	0.0328	0.15	0.0388	-	-
90	60	61	0.00264	0.0135	0.01456	-	-
91	60	62	0.0123	0.0561	0.01468	-	-
92	61	62	0.00824	0.0376	0.0098	-	-
93	63	59	0.000	0.0386	0.000	0.9	1.1
94	63	64	0.00172	0.02	0.216	-	-
95	64	61	0.000	0.0268	0.000	0.9	1.1
96	38	65	0.00901	0.0986	1.046	-	-
97	64	65	0.00269	0.0302	0.38	-	-
98	49	66	0.018	0.0919	0.0248	-	-
99	49	66	0.018	0.0919	0.0248	-	-
100	62	66	0.0482	0.218	0.0578	-	-
101	62	67	0.0258	0.117	0.031	-	-
102	65	66	0.000	0.037	0.000	0.9	1.1
103	66	67	0.0224	0.1015	0.02682	-	-
104	65	68	0.00138	0.016	0.638	-	-
105	47	69	0.0844	0.2778	0.07092	-	-
106	49	69	0.0985	0.324	0.0828	-	-
107	68	69	0.000	0.037	0.000	0.9	1.1
108	69	70	0.03	0.127	0.122	-	-
109	24	70	0.00221	0.4115	0.10198	-	-
110	70	71	0.00882	0.0355	0.00878	-	-
111	24	72	0.0488	0.196	0.0488	-	-
112	71	72	0.0446	0.18	0.04444	-	-
113	71	73	0.00866	0.0454	0.01178	-	-
114	70	74	0.0401	0.1323	0.03368	-	-
115	70	75	0.0428	0.141	0.036	-	-

Table A.1.12: Transmission line input data for test system-VIII, X and XII (Continued)

Line No.	From Bus No.	To Bus No.	Line impedance			T_{min}	T_{max}
			R(p.u.)	X(p.u.)	1/2B (p.u.)		
116	69	75	0.0405	0.122	0.124	-	-
117	74	75	0.0123	0.0406	0.01034	-	-
118	76	77	0.0444	0.148	0.0368	-	-
119	69	77	0.0309	0.101	0.1038	-	-
120	75	77	0.0601	0.1999	0.04978	-	-
121	77	78	0.00376	0.0124	0.01264	-	-
122	78	79	0.00546	0.0244	0.00648	-	-
123	77	80	0.017	0.0485	0.0472	-	-
124	77	80	0.0294	0.105	0.0228	-	-
125	79	80	0.0156	0.0704	0.0187	-	-
126	68	81	0.00175	0.0202	0.808	-	-
127	81	80	0.000	0.037	0.000	0.9	1.1
128	77	82	0.0298	0.0853	0.08174	-	-
129	82	83	0.0112	0.03665	0.03796	-	-
130	83	84	0.0625	0.132	0.0258	-	-
131	83	85	0.043	0.148	0.0348	-	-
132	84	85	0.0302	0.0641	0.01234	-	-
133	85	86	0.035	0.123	0.0276	-	-
134	86	87	0.02828	0.2074	0.0445	-	-
135	85	88	0.02	0.102	0.0276	-	-
136	85	89	0.0239	0.173	0.047	-	-
137	88	89	0.0139	0.0712	0.01934	-	-
138	89	90	0.0518	0.188	0.0528	-	-
139	89	90	0.0238	0.0997	0.106	-	-
140	90	91	0.0254	0.0836	0.0214	-	-
141	89	92	0.0099	0.0505	0.0548	-	-
142	89	92	0.0393	0.1581	0.0414	-	-
143	91	92	0.0387	0.1272	0.03268	-	-
144	92	93	0.0258	0.0848	0.0218	-	-
145	92	94	0.0481	0.158	0.0406	-	-
146	93	94	0.0223	0.0732	0.01876	-	-
147	94	95	0.0132	0.0434	0.0111	-	-
148	80	96	0.0356	0.182	0.0494	-	-
149	82	96	0.0162	0.053	0.0544	-	-
150	94	96	0.0269	0.0869	0.023	-	-
151	80	97	0.0183	0.0934	0.0254	-	-
152	80	98	0.0238	0.108	0.0286	-	-
153	80	99	0.0454	0.206	0.0546	-	-
154	92	100	0.0648	0.295	0.0472	-	-
155	94	100	0.0178	0.058	0.0604	-	-
156	95	96	0.0171	0.0547	0.01474	-	-
157	96	97	0.0173	0.0885	0.024	-	-
158	98	100	0.0397	0.179	0.0476	-	-
159	99	100	0.018	0.0813	0.0216	-	-
160	100	101	0.0277	0.1262	0.0328	-	-
161	92	102	0.0123	0.0559	0.01464	-	-
162	101	102	0.0246	0.112	0.0294	-	-
163	100	103	0.016	0.0525	0.0536	-	-
164	100	104	0.0451	0.204	0.0541	-	-
165	103	104	0.0466	0.1584	0.0407	-	-
166	103	105	0.0535	0.1625	0.0408	-	-
167	100	106	0.0605	0.229	0.062	-	-
168	104	105	0.00994	0.0378	0.00986	-	-
169	105	106	0.014	0.0547	0.01434	-	-
170	105	107	0.053	0.183	0.0472	-	-

Table A.1.12: Transmission line input data for test system-VIII, X and XII (Continued)

Line No.	From Bus No.	To Bus No.	Line impedance			T_{min}	T_{max}
			R(p.u.)	X(p.u.)	1/2B (p.u.)		
171	105	108	0.0261	0.0703	0.01844	-	-
172	106	107	0.053	0.183	0.0472	-	-
173	108	109	0.0105	0.0288	0.0076	-	-
174	103	110	0.03906	0.1813	0.0461	-	-
175	109	110	0.0278	0.0762	0.0202	-	-
176	110	111	0.022	0.0755	0.02	-	-
177	110	112	0.0247	0.064	0.062	-	-
178	17	113	0.00913	0.0301	0.00768	-	-
179	32	113	0.0615	0.203	0.0518	-	-
180	32	114	0.0135	0.0612	0.01628	-	-
181	27	115	0.0164	0.0741	0.01972	-	-
182	114	115	0.0023	0.0104	0.00276	-	-
183	68	116	0.00034	0.00405	0.164	-	-
184	12	117	0.0329	0.14	0.0358	-	-
185	75	118	0.0145	0.0481	0.01198	-	-
186	76	118	0.0164	0.0544	0.01356	-	-

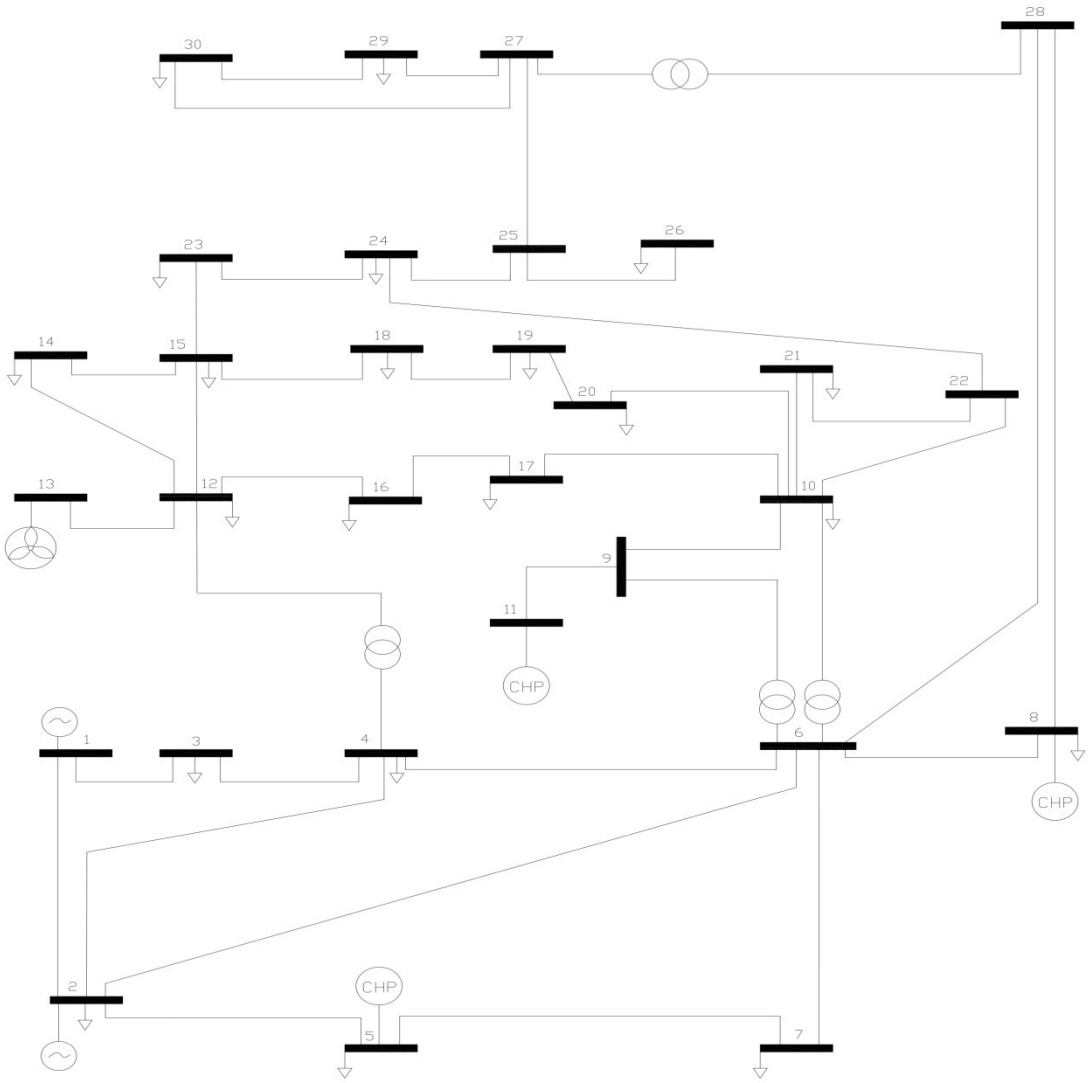

Figure A.3.1: Single-line diagram of modified IEEE 30-bus system (Test system-XI)

Table A.2.1: Input data of thermal generators for test system-IX

Bus No.	Generator Limits		Cost Coefficient			Emission Coefficient				
	P_{Gm}^{min} (MW)	P_{Gm}^{max} (MW)	a_m ($/ hr)	b_m ($/ MWhr)	c_m ($/ MW^2hr)	α_mx10^{-2} (ton/ hr)	β_mx10^{-4} (ton/ hr)	γ_m x10^{-6} (ton/ MW^2hr)	η_m (ton/ hr)	λ_m x10^{-2} (1/MW)
1	50	200	0	2.5	0.00975	4.091	-5.554	6.490	2.0E-4	2.857
2	20	80	0	3.25	0.00675	2.543	-6.047	5.638	5.0E-4	3.333
8	10	35	0	2.75	0.00934	5.326	-3.550	3.380	2.0E-3	2.000

Figure A.3.2: Single-line diagram of modified IEEE 118-bus system (Test system-XII)

Table A.2.2: Wind generator data for test system-IX and X

Bus No.	c_i	k_i	$v_{IN,i}$(m/s)	$v_{R,i}$(m/s)	$v_{o,i}$(m/s)	$P_{R,i}$(MW)	d_i($/MW)	d_{ri}($/MW)	d_{pi}($/MW)
Test system-IX									
5	15	1	3	12	30	60	1.75	3	1.5
11	15	2	3	12	30	60	2.00	3	1.5
13	25	2	3	12	30	60	2.25	3	1.5
Test system-X									
36	10	2	3	12	30	400	1.3	4.0	1.0
49	9	2	3	12	30	600	1.6	3.0	1.5

A.3 TEST SYSTEMS OF OPTIMAL POWER FLOW PROBLEM INTEGRATED WITH WIND AND CHP UNITS

The two test systems of the OPF problem including CHP and wind units have been undertaken in Chapter-6. The test system-XI and test system-XII are modified IEEE 30-bus system and modified IEEE 118-bus system, respectively. The system data for test system-XI and XII has been taken from [48].The input data of thermal, heat only and cogeneration units for test system-XI are provided in Tables A.3.1, A.3.2 and A.3.3, respectively. The load data and transmission lines data for test system-XI are the same as test system-I provided in Tables A.1.3 and A.1.4, respectively. The input data of thermal, cogeneration and heat only units for test system-XII are provided in Tables A.3.4, A.3.5 and A.3.6, respectively.

Table A.3.1: Input data of thermal units for test system-XI

Bus No.	Generator Limits		Cost Coefficient				
	P_{Gm}^{min} (MW)	P_{Gm}^{max} (MW)	a_m ($/hr)	b_m ($/MWhr)	c_m ($/MW^{2}hr)	d_m ($/hr)	e_m (rad/MW)
1	50	200	0	2.0	0.00375	18	0.037
2	20	80	0	1.75	0.00175	16	0.038

Table A.3.1: Input data of thermal units for test system-XI (Continued)

Bus No.	Emission Coefficient				
	α_mx10^{-2}(ton/hr)	β_mx10^{-4}(ton/hr)	γ_m x10^{-6} (ton/MW^{2}hr)	η_mx10^{-4}(ton/hr)	λ_m(1/MW)
1	4.09	-5.55	6.49	2.0	2.86E-2
2	2.54	-6.04	5.63	5.0	3.33E-3

Table A.3.2: Input dataof heat only units for test system-XI

Unit	Cost Coefficient			Emission Coefficient	Generator Limits	
	a_n	b_n	c_n	ψ_n	H_{hn}^{min}(MWTh)	H_{hn}^{max}(MWTh)
Heat only unit	950	2.0109	0.038	1.7E-6	0	2695.2

Table A.3.3: Input data of cogeneration units for test system-XI

Bus No.	Cost Coefficient						Emission Coefficient	Generator Limits	
	α_l	β_l	γ_l	λ_l	ε_l	ξ_l	χ_l	P_{Cl}^{min} (MW)	P_{Cl}^{max} (MW)
5	2650	34.5	0.1035	2.203	0.025	0.051	2.2E-6	15	50
8	2650	34.5	0.1035	2.203	0.025	0.051	2.2E-6	10	35
11	2650	34.5	0.1035	2.203	0.025	0.051	2.2E-6	10	30

Table A.3.4: Input data of thermal units for test system-XII

Bus No.	Generator Limits		Cost Coefficient			Emission Coefficient				
	P_{Gm}^{min} (MW)	P_{Gm}^{max} (MW)	a_m ($/ hr)	b_m ($/ MWhr)	c_m ($/ MW^2hr)	α_mx10^{-2} (ton/ hr)	β_m x10^{-4} (ton/ hr)	γ_m x10^{-6} (ton/ MW^2hr)	η_m (ton/ hr)	λ_mx10^{-3} (1/MW)
1	0	100	0	40	0.01	2.54	-6.04	5.638	5.0E-4	3.33
4	0	100	0	40	0.01	2.54	-6.04	5.638	5.0E-4	3.33
6	0	100	0	40	0.01	2.54	-6.04	5.638	5.0E-4	3.33
8	0	100	0	40	0.01	2.54	-6.04	5.638	5.0E-4	3.33
10	165	550	0	20	0.022222	4.25	-5.09	4.59	1.0E-6	8.0
15	0	100	0	40	0.01	2.54	-6.04	5.638	5.0E-4	3.33
18	0	100	0	40	0.01	2.54	-6.04	5.638	5.0E-4	3.33
19	0	100	0	40	0.01	2.54	-6.04	5.638	5.0E-4	3.33
24	0	100	0	40	0.01	2.54	-6.04	5.638	5.0E-4	3.33
25	96	320	0	20	0.0454545	5.33	-3.55	3.38	2.0E-3	2.0
26	124.2	414	0	20	0.0318471	4.25	-5.09	4.59	1.0E-6	8.0
27	0	100	0	40	0.01	2.54	-6.04	5.638	5.0E-4	3.33
32	0	100	0	40	0.01	2.54	-6.04	5.638	5.0E-4	3.33
34	0	100	0	40	0.01	2.54	-6.04	5.638	5.0E-4	3.33
40	0	100	0	40	0.01	2.54	-6.04	5.638	5.0E-4	3.33
42	0	100	0	40	0.01	2.54	-6.04	5.638	5.0E-4	3.33
46	0	119	0	20	0.0526316	6.13	-5.55	5.15	1.0E-5	6.67
55	0	100	0	40	0.01	2.54	-6.04	5.638	5.0E-4	3.33
56	0	100	0	40	0.01	2.54	-6.04	5.638	5.0E-4	3.33
59	76.5	255	0	20	0.0645161	5.33	-3.55	3.38	2.0E-3	2.0
61	78	260	0	20	0.0625	5.33	-3.55	3.38	2.0E-3	2.0
62	0	100	0	40	0.01	2.54	-6.04	5.638	5.0E-4	3.33
65	147.3	491	0	20	0.0255754	4.25	-5.09	4.59	1.0E-6	8.0
66	147.6	492	0	20	0.0255102	4.25	-5.09	4.59	1.0E-6	8.0
69	0	805.2	0	20	0.0193648	4.09	-5.55	6.49	2.0E-4	2.86
70	0	100	0	40	0.01	2.54	-6.04	5.638	5.0E-4	3.33
72	0	100	0	40	0.01	2.54	-6.04	5.638	5.0E-4	3.33
73	0	100	0	40	0.01	2.54	-6.04	5.638	5.0E-4	3.33
74	0	100	0	40	0.01	2.54	-6.04	5.638	5.0E-4	3.33
76	0	100	0	40	0.01	2.54	-6.04	5.638	5.0E-4	3.33
77	0	100	0	40	0.01	2.54	-6.04	5.638	5.0E-4	3.33
80	173.1	577	0	20	0.0209644	4.25	-5.09	4.59	1.0E-6	8.0
85	0	100	0	40	0.01	2.54	-6.04	5.638	5.0E-4	3.33
89	212.1	707	0	20	0.0164745	4.09	-5.55	6.49	2.0E-4	2.86
90	0	100	0	40	0.01	2.54	-6.04	5.638	5.0E-4	3.33
91	0	100	0	40	0.01	2.54	-6.04	5.638	5.0E-4	3.33
92	0	100	0	40	0.01	2.54	-6.04	5.638	5.0E-4	3.33
99	0	100	0	40	0.01	2.54	-6.04	5.638	5.0E-4	3.33
100	105.6	352	0	20	0.0396825	5.33	-3.55	3.38	2.0E-3	2.0
104	0	100	0	40	0.01	2.54	-6.04	5.638	5.0E-4	3.33
105	0	100	0	40	0.01	2.54	-6.04	5.638	5.0E-4	3.33
107	0	100	0	40	0.01	2.54	-6.04	5.638	5.0E-4	3.33
110	0	100	0	40	0.01	2.54	-6.04	5.638	5.0E-4	3.33
112	0	100	0	40	0.01	2.54	-6.04	5.638	5.0E-4	3.33
113	0	100	0	40	0.01	2.54	-6.04	5.638	5.0E-4	3.33
116	0	100	0	40	0.01	2.54	-6.04	5.638	5.0E-4	3.33

The load data and transmission lines data for test system-XII are same as test system-VIII provided in the Tables A.1.11 and A.1.12, respectively. The wind generator data for test system-XI and XII is given in the Table A.3.7.The single-line diagram of test system-XI and XII is shown in Figures A.3.1 and A.3.2, respectively.

Table A.3.5: Input data of cogeneration units for test system-XII

Bus No.	Cost Coefficient						Emission Coefficient	Generator Limits	
	α_l	β_l	γ_l	λ_l	ε_l	ξ_l	χ_l	P_{Cl}^{min} (MW)	P_{Cl}^{max} (MW)
12	2650	14.5	0.0345	4.2	0.03	0.031	2.2E-6	0	185
31	1250	36	0.0435	0.6	0.027	0.011	2.2E-6	0	107
54	2650	14.5	0.0345	4.2	0.03	0.031	2.2E-6	0	148
87	1250	36	0.0435	0.6	0.027	0.011	2.2E-6	0	104
103	2650	14.5	0.0345	4.2	0.03	0.031	2.2E-6	0	140
111	2650	14.5	0.0345	4.2	0.03	0.031	2.2E-6	0	136

Table A.3.6: Input data of heat only units for test system-XII

Unit	Cost Coefficient	Emission Coefficient	Generator Limits	
	c_n	ψ_n	H_{hn}^{min}(MWTh)	H_{hn}^{max}(MWTh)
Heat only unit	23.4	1.7E-6	0	2695.2

Table A.3.7: Wind generator data for test system-XI and XII

Bus No.	c_i	k_i	$v_{IN,i}$(m/s)	$v_{R,i}$(m/s)	$v_{o,i}$(m/s)	$P_{R,i}$(MW)	d_i($/MW)	d_{ri}($/MW)	d_{pi}($/MW)
Test system-XI									
13	10	2	3	12	30	60	1.3	4.0	1.0
Test system-XII									
36	10	2	3	12	30	400	1.3	4.0	1.0
49	9	2	3	12	30	600	1.6	3.0	1.5

CURRICULUM VITAE OF AUTHOR

MANDEEP KAUR

Father's Name: S. TEJ BAHADUR SINGH

DOB: 25/03/1986

E-mail:mandeep_longia25@yahoo.co.in,mandeep_kaur@thapar.edu

Academic Qualification:

Qualification	Trade / Branch	College / University	Division / Percentage	Year of Passing
M-Tech	Power Engineering	BBSBEC, FGS	67.91%	2011
B-Tech	Electrical Engineering	BBSBEC, FGS	74.62%	2007
Class 12th	Non-Medical (PSEB)	DAV Public Sr. Sec. school	74.89%	2003
Class 10th	Science (PSEB)	Govt. Sen. Sec. school	78.78%	2001

SCI Journal

[1] M. Kaur and N. Narang, "An integrated optimization technique for optimal power flow solution" *Soft Computing*, vol. 24, pp. 10865-10882, 2020.

[2] M. Kaur and N. Narang, "Non-interactive approach to solve multi-objective optimal power flow problem" *Electrical Engineering*, vol. 103, pp. 167-182, 2021.

[3] M. Kaur and N. Narang, "Optimal Power Flow Solution using Space Transformational Invasive Weed Optimization Algorithm" *Iranian Journal of Science and Technology, Transactions of Electrical Engineering*. DOI:10.1007/s40998-023-00592-y